

# Synthesis of Heterocycles using Visible Light Photoredox Catalysis

**Dissertation**

Zur Erlangung des Doktorgrades der Naturwissenschaften

(Dr. rer. nat)

an der Fakultät für Chemie und Pharmazie

der Universität Regensburg



vorgelegt von

**Amrita Das**

aus

Kolkata, West Bengal (Indien)

**2018**



The experimental part of this work was carried out between September 2014 and March 2018 under the supervision of Prof. Dr. Burkhard König at the Institute of Organic Chemistry, University of Regensburg.

The Ph.D. thesis was submitted on: 12.05.2018

The colloquium took place on: 20.07.2018

|                     |                                 |                           |
|---------------------|---------------------------------|---------------------------|
| Board of examiners: | Prof. Dr. Hubert Motschmann     | (chair)                   |
|                     | Prof. Dr. Burkhard König        | (1 <sup>st</sup> referee) |
|                     | Prof. Dr. Julia Rehbein         | (2 <sup>nd</sup> referee) |
|                     | Prof. Dr. Frank-Michael Matysik | (examiner)                |





*Dedicated*  
*to*  
*My Family*  
*and*  
*my teacher Dr. Chandan Saha*

*"Chance favors the prepared mind"*

*- Louis Pasteur*



# Table of Contents

## 1. Transition Metal- and Photoredox- Catalyzed Valorization of Lignin

|   |          |
|---|----------|
| <b>Subunits .....</b>   | <b>1</b> |
| 1.1 Introduction .....  | 3        |
| 1.2 Transition metal catalyzed reduction of C-O bonds in lignin and lignin model systems .... | 4        |
| 1.3 Visible light mediated reduction of C-O bonds in lignin and lignin model systems.....     | 7        |
| 1.4 Transition metal catalyzed oxidation of C-O bonds in lignin and lignin model systems .... | 8        |
| 1.5 Visible light mediated oxidation of C-O bonds in lignin and lignin model systems.....     | 11       |
| 1.6 Redox-neutral conversion of lignin .....  | 17       |
| 1.7 Conclusion, challenges and outlook.....   | 18       |
| 1.8 Experimental section .....  | 20       |
| 1.8.1 Materials and methods .....   | 20       |
| 1.8.2 Photocatalytic oxidation of the lignin model compounds.....                             | 21       |
| 1.8.3 Cyclic voltammetry measurements of compounds 1-5.....                                   | 28       |
| 1.8.4 Synthesis of the lignin model compounds .....   | 32       |
| 1.8.5 <sup>1</sup> H- and <sup>13</sup> C NMR spectra of synthesized compounds .....          | 35       |
| 1.9 References .....  | 39       |

## 2. Synthesis of Pyrrolo[1,2-a]quinolines and Ullazines by Visible Light Mediated One- and Two Fold Annulation of N-Arylpyrroles with Arylalkynes ....

|  |    |
|--|----|
| 2.1 Introduction .....   | 46 |
| 2.2 Results and discussions .....  | 47 |
| 2.3 Conclusion.....  | 53 |
| 2.4 Experimental section .....   | 54 |
| 2.4.1 Materials and methods .....  | 54 |
| 2.4.2 Synthesis of starting materials.....   | 55 |
| 2.4.3 General procedure for C-H arylation followed by intramolecular cyclization reactions ..... | 58 |
| 2.4.4 Glass microreactors and irradiation setup used for photocatalysis.....                     | 58 |

|  |            |
|--|------------|
| 2.4.5 Absorption spectra of Rh-6G and Rh-6G <sup>-</sup> .....   | 59         |
| 2.4.6 <sup>1</sup> H- and <sup>13</sup> C NMR spectra of synthesized compounds.....  | 71         |
| 2.5 References .....   | 89         |
| <b>3. Synthesis of Aryl Sulfides via Radical-Radical Cross Coupling of Electron Rich Arenes using Visible Light Photoredox Catalysis .....</b> | <b>93</b>  |
| 3.1 Introduction.....  | 96         |
| 3.2 Results and discussions .....  | 98         |
| 3.3. Conclusion.....   | 104        |
| 3.4. X-ray crystallographic data .....   | 104        |
| 3.5 Experimental section .....   | 105        |
| 3.5.1 Materials and methods .....  | 105        |
| 3.5.2 Optimization of the reactions and control experiments.....   | 106        |
| 3.5.3 General procedure for C–H sulfenylation.....   | 109        |
| 3.5.4 Crystallographic Data.....   | 116        |
| 3.5.5 <sup>1</sup> H- and <sup>13</sup> C NMR spectra of synthesized compounds.....  | 118        |
| 3.4 References .....   | 131        |
| <b>4. Photochemical versus Photocatalytic Oxidation of Benzyl alcohols – A Comparison .....</b>  | <b>135</b> |
| 4.1 Introduction.....  | 137        |
| 4.2 Quantum Yield of MBA Photo-oxidation in MeOH.....  | 138        |
| 4.3 Photocatalyzed oxidation of lignin substructure - benzylic alcohols .....  | 142        |
| 4.4 Conclusion.....  | 147        |
| 4.5 Experimental section .....   | 148        |
| 4.5.1 Materials and methods .....  | 148        |
| 4.5.2 Gas Chromatographic traces for different concentrations of MBA and MBAlD in MeOH .....   | 149        |
| 4.5.3 Synthesis of the 1,3 diols.....  | 151        |
| 4.5.4 <sup>1</sup> H- and <sup>13</sup> C NMR spectra of synthesized compounds .....   | 153        |
| 4.6 References .....   | 156        |

|  |            |
|--|------------|
| <b>5. Attempts Towards the Photochemical Generation of Amidinyl Radicals and Syntheses of Oxadiazole and Quinazolinone Derivatives .....</b> | <b>157</b> |
| 5.1 Introduction .....   | 159        |
| 5.2 Results and discussions .....  | 162        |
| 5.2.1 Generation of amidinyl radical from benzamidine.....   | 162        |
| 5.2.2 Generation of amidinyl radicals from sulfonyl amidoximes.....  | 163        |
| 5.2.3 Synthesis of N-aryl sulfoxynylamidines .....   | 170        |
| 5.2.4 Towards the formation of EDA compexes .....  | 171        |
| 5.2.5 Generation of amidinyl radicals from N-phenylsulfonyl benzimidamide.....   | 174        |
| 5.2.6 Generation of amidinyl radicals from a different class of benzamides and synthesis of quinazolinone derivatives .....                  | 176        |
| 5.2.7 Plausible mechanism for the formation of quinazolinone derivative .....  | 183        |
| 5.3 Conclusion.....  | 183        |
| 5.4 Attempts towards the syntheses of oxadiazoles using visible light photoredox catalysis   | 184        |
| 5.4.1 Introduction .....   | 184        |
| 5.4.2 Results and discussions .....  | 186        |
| 5.5 Conclusion.....  | 196        |
| 5.6 Experimental section .....   | 197        |
| 5.6.1 Materials and methods .....  | 197        |
| 5.6.2 General procedures .....   | 198        |
| 5.7 References .....   | 237        |
| <b>6. Summary.....</b>   | <b>239</b> |
| <b>7. Zusammenfassung.....</b>   | <b>243</b> |
| <b>8. Abbreviations .....</b>  | <b>247</b> |
| <b>9. Acknowledgements .....</b>   | <b>253</b> |
| <b>10. Curriculum Vitae .....</b>  | <b>257</b> |



# *Chapter 1*

## *1. Transition Metal- and Photoredox- Catalyzed Valorization of Lignin Subunits*





## 1.1 Introduction

Lignocellulose is an integral component of plant cell walls and is considered as the largest renewable feedstock with an aromatic backbone. Lignin forms a matrix that surrounds cellulose in woody cells protecting the cellulose and hemicellulose, thereby, preventing the plant from microbial depolymerization. Lignin represents 30% of the non-fossil organic carbon on earth. The primary structure of lignin is a randomly cross-linked polymer of phenyl propane units joined by many different linkages. The most common precursors are the three monolignol monomers, all of which are methoxylated to various degrees: coumaryl alcohol, coniferyl alcohol and sinapyl alcohol (**Figure 1**). These are incorporated into lignin in the form of phenyl propanoids. The structure, composition and abundant availability of lignin are reasons why this biopolymer is considered as a very important renewable resource for chemical and energy industry. However, degradation of lignin by controlled depolymerization to fine chemicals is very challenging due to its highly complex rigid, irregular and cross-linked structure. Therefore, many elegant protocols to deconstruct the lignin polymer were investigated. The strategies can be categorized into three groups: reductive, oxidative and redox-neutral conversions. However, a reliable and efficient procedure for lignin degradation has not been developed so far. In this chapter, we will discuss the three types of lignin depolymerization and compare methods based on transition metal catalysis with photoredox catalysis. The respective advantages and disadvantages of the two complementary approaches will be discussed.

---

**This chapter is a review article, prepared for submission to a journal:**

A. Das, B. König; manuscript in progress.

A.D. performed the experimental work on photodegradation and wrote the manuscript. Tim den Hartog synthesized the compounds. BK supervised the project and is the corresponding author.

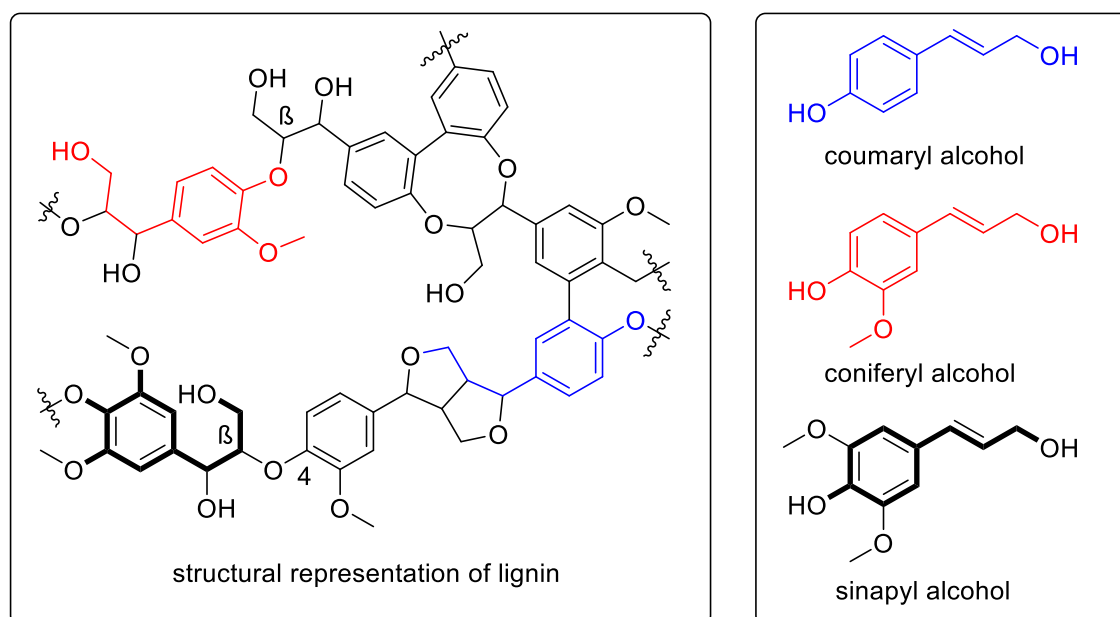


**Figure 1:** Schematic representation of a lignin polymer

## 1.2 Transition metal catalyzed reduction of C-O bonds in lignin and lignin model systems

Since 1930, scientists were interested to find out what happens when a biomass isolated from tree sawdust is subjected to hydrogenation. The goal was to determine how much hydrogen lignin could absorb and what are the final products after hydrogenation. There can be two fates to lignin degradation: (a) **hydrogenolysis**, where lignin is converted into oxygenated aromatics and (b) **hydrogenation**, where the lignin is over-reduced to form cyclohexyl ether products. It was found that the key challenge for lignin valorization is the selective hydrogenolysis over hydrogenation. Therefore, it was crucial to develop different methods for selective hydrogenolysis of lignin and lignin model systems.

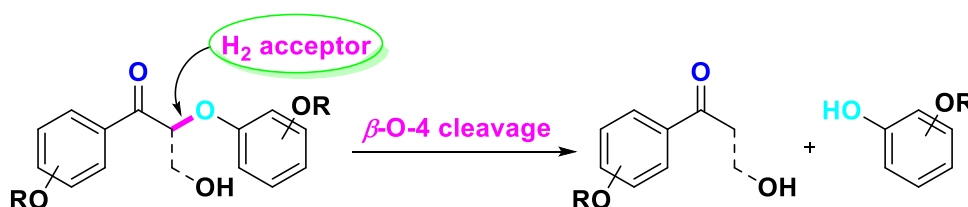
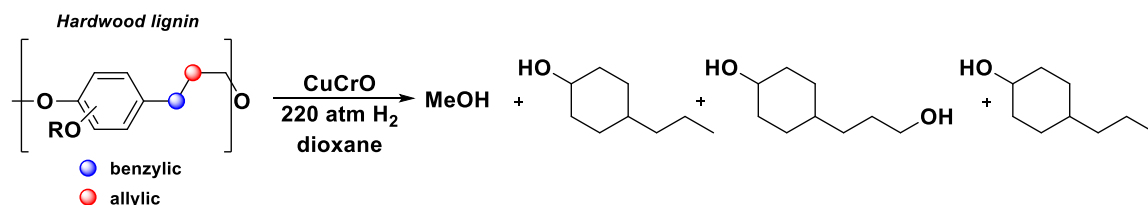


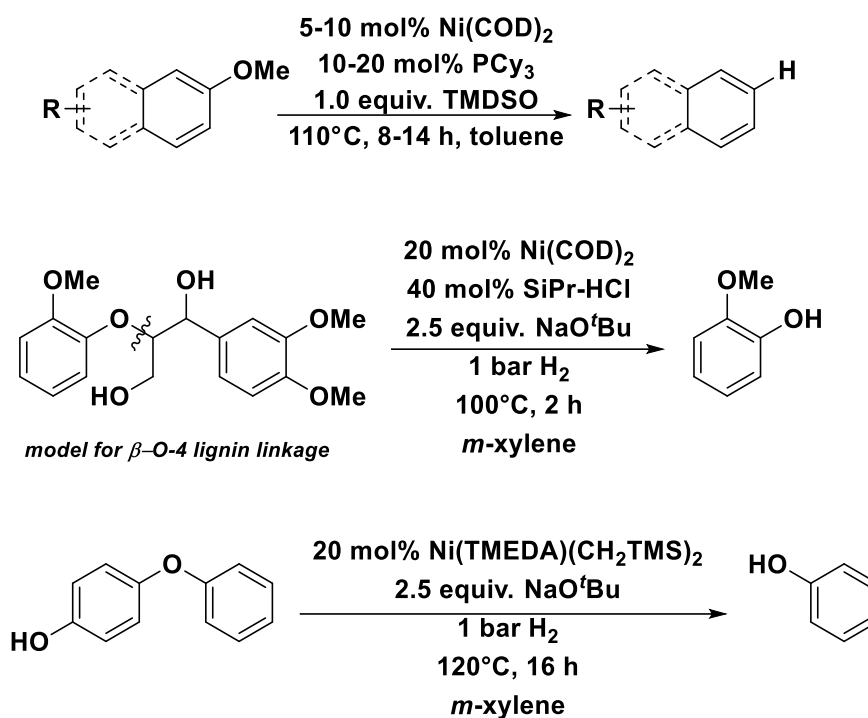
**Figure 2:** Working principle for reduction of C-O bonds in lignin.

Back in the year 1938, Adkins and co-workers used a copper-chromium oxide catalyst (Cu-Cr-O) to reduce hardwood lignin.<sup>[1]</sup> Although the selectivity of hydrogenolysis was not observed with this method, it represented the highest recoveries of lignin depolymerization products (**Scheme 1**).



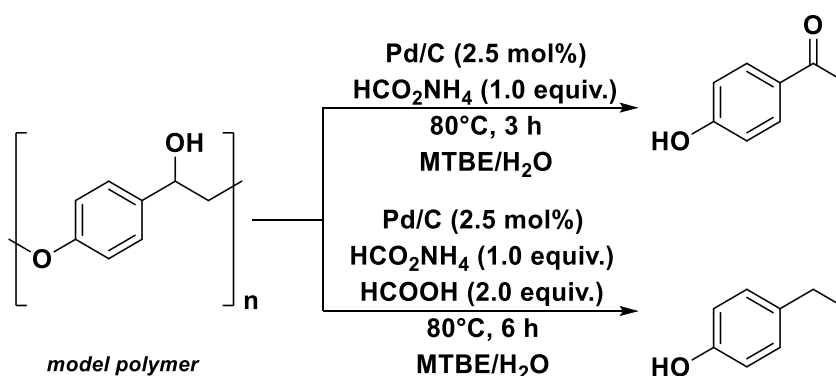
**Scheme 1:** Isolation and confirmation of phenyl propanoid structures in lignin.

About ten years later, Hibbert and co-workers used Raney-Ni to reduce maple woodmeal.<sup>[2]</sup> Recently, there has been a lot of progress in transition metal catalyzed reactions.<sup>[3-5]</sup> In the case of lignin depolymerization, the arene C-O bonds are activated by a Pd or Ni catalyst. Wenkert and co-workers first reported the oxidative insertion of Ni into a C-O bond using  $\text{Ni}(\text{PCy}_3)\text{Cl}_2$  as a precatalyst.<sup>[6]</sup> Followed by the work of Wenkert, several methods for C-O bond reduction<sup>[7-9]</sup> of different aryl ether moieties in lignin model compounds were developed (**Scheme 2**). Also, a variety of heterogeneous nickel catalysts have been developed for selective hydrogenolysis in the  $\alpha$ -O-4 and  $\beta$ -O-4 model lignin systems. In a few cases, the catalysts gave selective hydrogenolysis over hydrogenation. These results showed that different catalysts led to different selectivities on different lignin monomers. Therefore, controlled depolymerization with selectivity was difficult to achieve.



**Scheme 2:** Nickel catalyzed hydrogenolysis of aryl ethers.

Samee and co-workers further demonstrated that the reduction of  $\beta$ -O-4 lignin model systems is also possible using Pd/C and transfer hydrogenation.<sup>[10-12]</sup> A variety of transition metals were screened such as Rh/C, Ir/C, Ni/C, Re/C, out of which Pd/C was found to be the unique reducing agent for  $\beta$ -O-4 lignin models. Also, addition of a stoichiometric equivalent of amine *e.g.*, ammonia, ethyl amine, allylamine directed the selectivity towards  $\beta$ -O-4 cleavage rather than the disproportionation reaction. In addition, formic acid was found to facilitate the reduction as compared to  $\text{H}_2$ . A few examples of palladium catalyzed reductive C-O bond cleavage are shown in **Scheme 3**.



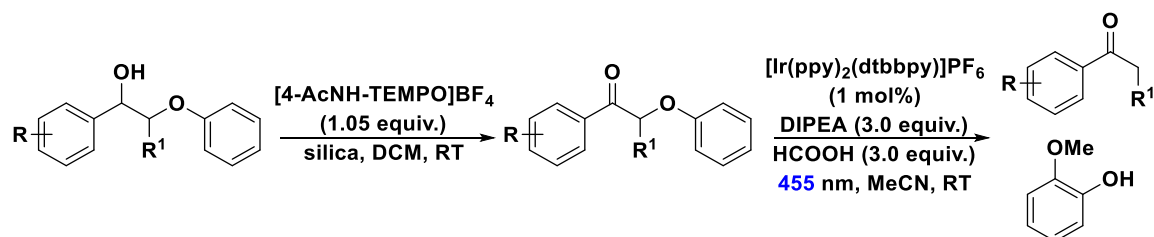
**Scheme 3:** Depolymerization of lignin model polymer by Pd/C.

While Ni and Pd are the most investigated catalysts for lignin degradation, other metal complexes such as  $\text{TiCp}_2(\text{BTSMA})$  complex,<sup>[13]</sup>  $\text{TiCp}_2(\text{OTf})_2$ ,<sup>[13]</sup>  $\text{Fe}(\text{acac})_3$ ,<sup>[14]</sup> and dihydroiridium complexes<sup>[15]</sup> were also tested for  $\beta$ -O-4 bond fragmentation of lignin. Ligand selection also proved to play a crucial role in selecting an effective catalyst for these transformations. The formation of innumerable side products, poisoning of the catalysts and small turnover numbers in many cases led to the development of alternative catalytic systems.

### 1.3 Visible light mediated reduction of C-O bonds in lignin and lignin model systems

In the previous section, we reviewed transition metal catalyzed lignin valorization methods. All these methods typically require elevated temperatures and functional groups such as free phenols and  $\gamma$ -alcohols are not tolerated, which may result in poor selectivity of the desired products. Therefore, it was necessary to develop a room temperature lignin degradation strategy that could address the above issues. Recently, organic transformations utilizing visible light photoredox catalysis have received significant attention. A fascinating feature of photoredox catalysis is the ability of the photocatalyst to engage in both oxidative and reductive chemistry from its excited state.<sup>[16-18]</sup> Photocatalytic methods are preferred over transition metal catalyzed methods, because (a) the reaction could be carried out at room temperature, is compatible with various solvents including water, (b) it avoids the use of stoichiometric oxidants and additives unlike in transition metal catalyzed processes and (c) photoredox catalysis occurs *via* outer sphere electron transfer process, which avoids the detrimental ligation issues. Thus, visible light mediated photoredox catalysis is an attractive method for lignin depolymerization. The cleavage of C-O bonds using visible light photoredox catalysis has been reported by Hasegawa,<sup>[19]</sup> Ollivier,<sup>[20]</sup> and Stephenson.<sup>[21]</sup> Among different kinds of C-O bonds in lignin,  $\beta$ -O-4 linkage comprises of >50% of all the linkages found in lignocellulose. DFT studies have also shown that upon oxidation of  $\alpha$  and  $\gamma$  carbon atoms of lignin, the C-O bond of  $\beta$ -O-4 linkage weakens significantly ( $\sim$  by 10 kcal/mol), hence is easy to cleave.<sup>[22]</sup> Based on these reports, Nguyen and co-workers first reported a photochemical strategy for lignin degradation at room temperature.<sup>[23]</sup> As shown in **Scheme 4**, in the first step a benzylic oxidation on lignin models was performed using  $[\text{4-AcNH-TEMPO}]\text{BF}_4$  (Bobbitt's salt) and then, the  $\text{C}\alpha\text{-O}$  bond was cleaved

photochemically using  $[\text{Ir}(\text{ppy})_2(\text{dtbbpy})]\text{PF}_6$  as the photocatalyst along with DIPEA and formic acid as additives at room temperature under 455 nm light irradiation. The oxidized products were obtained in very good yields. The reductive cleavage was performed in flow, which resulted in higher efficiency of the reaction in less time. This method was further extended to the reduction of  $\alpha$ -keto ethers, amines and sulfides. The reaction conditions are mild and several functional groups are tolerated well.



**Scheme 4:** Visible light mediated two step redox-neutral lignin degradation strategy.

In this photocatalytic method, the oxidation of the benzylic alcohol using Bobbitt's salt prior to the  $\beta$ -O-4 bond cleavage allowed for greater selectivity and control of bond cleavage, which is an improvement that could address many challenges towards a chemoselective depolymerization of lignin under mild reaction conditions. However, from an economic point of view, this two-step oxidation-reduction process still generates stoichiometric waste and currently, work is in progress to solve this problem.

## 1.4 Transition metal catalyzed oxidation of C-O bonds in lignin and lignin model systems

Another approach for lignin valorization that has been widely developed is the oxidative conversion. It has been found that, several species of white-rot fungus (*e.g.*, *Phanerochaete chrysosporium*) are capable of degrading lignin through the lignin peroxidase (LiP), which is excreted by the fungi.<sup>[24-25]</sup> Followed by the discovery of LiP, other oxidative enzymes such as manganese peroxidase (MnP), phenol oxidase and laccase, were also discovered. All these enzymes are involved in a single electron oxidation reaction<sup>[26]</sup> of the aromatic nucleus present in the lignin, generating an arene radical cation which can either undergo  $\alpha$ - $\beta$  cleavage resulting in the break in the polymeric backbone to form the corresponding

aldehyde or can undergo  $\beta$ -O-4 fragmentation to yield  $\beta$ -hydroxyketone as shown in Scheme 5.

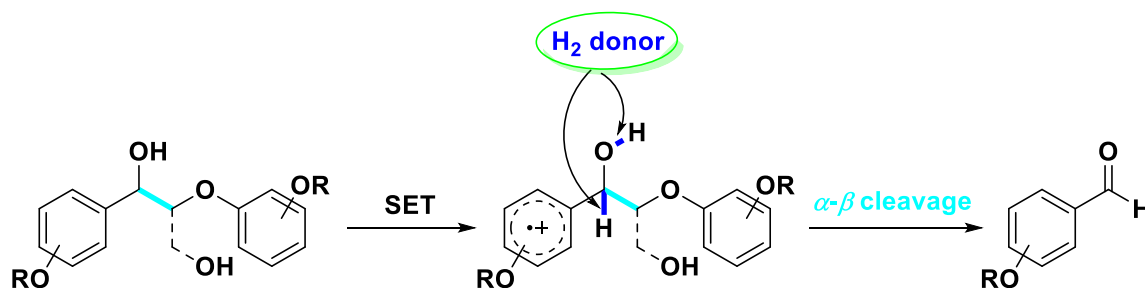
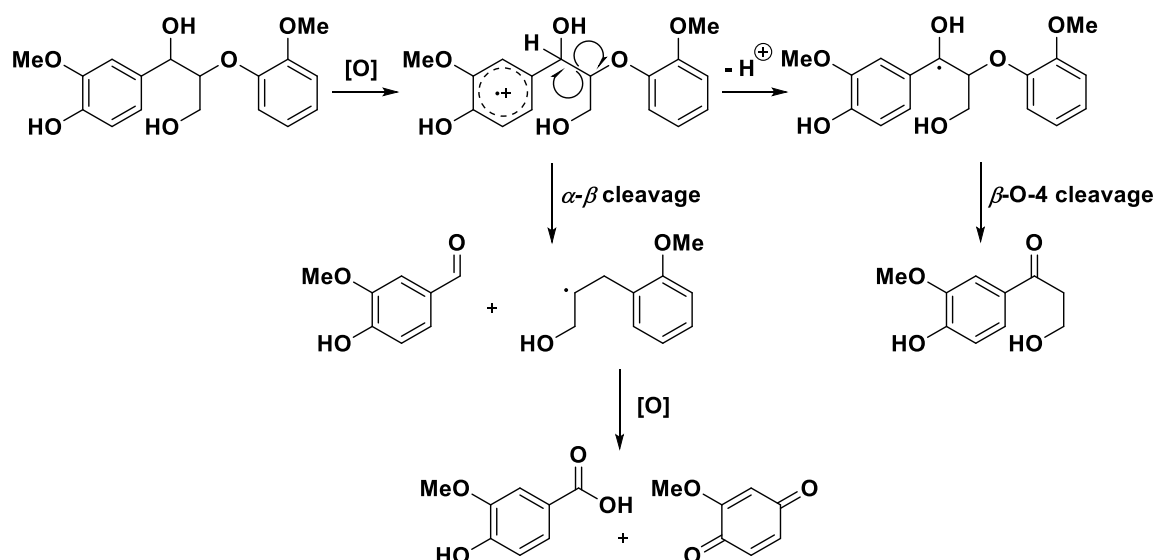
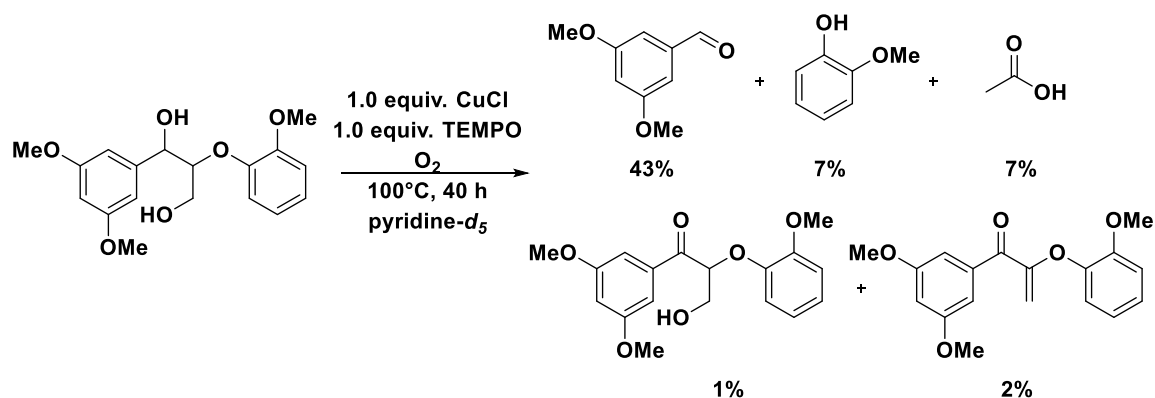


**Figure 3:** Working principle for oxidative conversion of lignin.

However, the overall delignification process is very slow and takes months. Another drawback of enzyme-catalyzed oxidation is that they are very substrate specific. However, the study on enzyme-catalyzed oxidation by microbes contributes to understand the metabolism of these organisms and can lead to the development of effective microbial methods for the deconstruction of lignin. In the later studies, several biomimetic catalysts based on iron,<sup>[27]</sup> cobalt,<sup>[28]</sup> manganese<sup>[29]</sup> and vanadium complexes<sup>[30]</sup> were developed for oxidative fragmentation of lignin. All the catalysts are also involved in single electron oxidation of the arene. The scope of these catalysts will not be described in this chapter. Based on the concept of single electron transfer (SET) mechanism, *N*-oxyl based oxidants *e.g.*, TEMPO-mediated oxidation protocols have been developed. These protocols are coupled with O<sub>2</sub> since it is an abundant, inexpensive and environmentally friendly terminal oxidant. Originally, a Cu/TEMPO system was investigated by Hanson and co-workers on complex lignin systems (**Scheme 6**).<sup>[31]</sup> Copper was believed to activate O<sub>2</sub>, and copper and TEMPO helped in the oxidation of the alcohol to afford the aldehyde. Several copper salts were investigated on different kinds of complex lignin models, but they showed very different selectivities, which was quite challenging to rationalize.



**Scheme 5:** Depolymerization of lignin by enzymes.



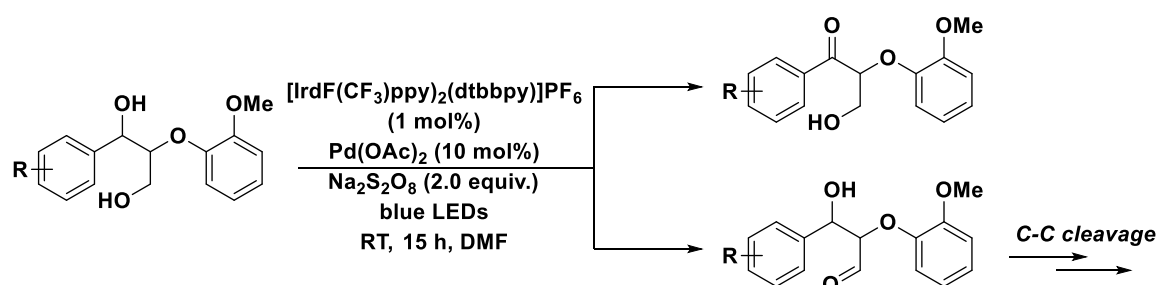
**Scheme 6:** Stoichiometric oxidation of lignin model system using  $\text{CuCl}/\text{TEMPO}$ .

However, in all the cases, the selectivity for oxidation relies on the choice of model substrates taken into consideration. A very little change in the structure or the catalytic system could result in a big change in the product composition. Under oxidative condition, the formed radicals can lead to partial re-polymerization and form complex molecules. In addition, at very high temperature, significant amounts of gases and side products prevent the formation of monomeric aromatic hydrocarbons.



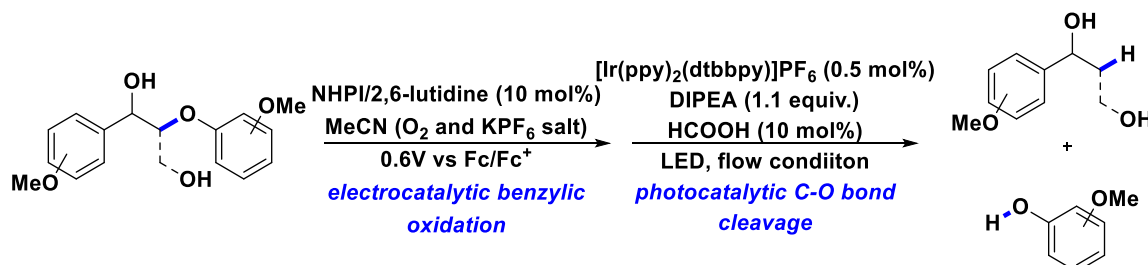
## 1.5 Visible light mediated oxidation of C-O bonds in lignin and lignin model systems

As described in **Section 1.3**, Nguyen *et. al.*, reported a lignin degradation strategy where, in the first step the benzylic position of the lignin model compound is oxidized using Bobbitt's salt [4-AcNH-TEMPO]BF<sub>4</sub>, followed by a chemoselective photocatalytic reductive C-O bond cleavage. Later, the same group reported a photocatalytic method for the oxidation of benzylic alcohol to activate the lignin systems.<sup>[32]</sup> The photocatalyst used in this case was [Ir(dF(CF<sub>3</sub>)ppy)<sub>2</sub>(dtbbpy)]PF<sub>6</sub> in combination with Pd(OAc)<sub>2</sub> and stoichiometric amount of Na<sub>2</sub>S<sub>2</sub>O<sub>8</sub> under visible light irradiation (**Scheme 7**).



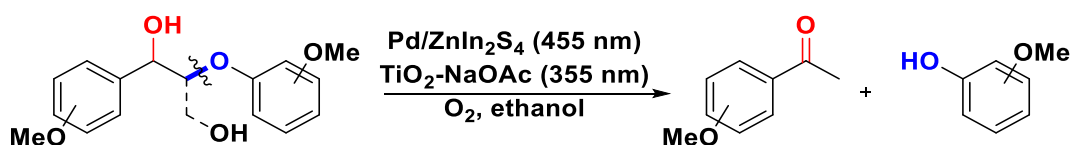
**Scheme 7:** Chemoselective oxidation of lignin models by merging photoredox and Pd catalysis.

They also combined electrocatalysis and photoredox catalysis in flow to achieve a highly selective fragmentation of the  $\beta$ -O-4 linkage of lignin model substrates in a two-step one-pot process at ambient temperature (**Scheme 8**).<sup>[33]</sup>



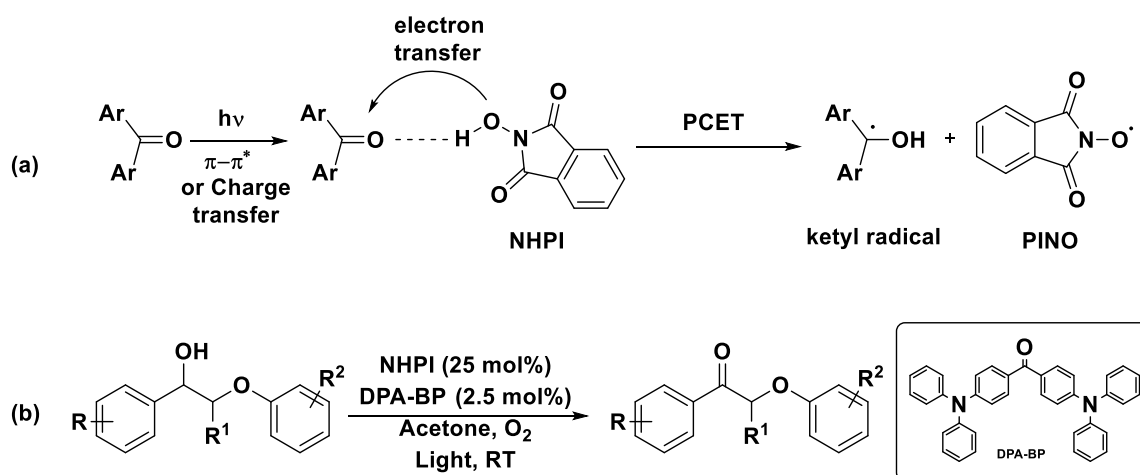
**Scheme 8:** One-pot electrocatalytic oxidation and photocatalyzed reductive cleavage.

The TEMPO mediated oxidation protocol can lead to the formation of stoichiometric waste. To overcome this problem, Wang and coworkers developed a one-step tandem photocatalytic oxidation-hydrogenolysis method using a dual light wavelength switching strategy for oxidation of the  $\alpha$ -OH followed by cleavage of  $\beta$ -O-4 linkage in lignin. (**Scheme 9**).<sup>[34]</sup> They employed a Pd/ZnIn<sub>2</sub>S<sub>4</sub> catalyst for aerobic oxidation of the benzylic alcohol under 455 nm LED, and then, a heterogeneous catalytic TiO<sub>2</sub>-NaOAc system to cleave C-O bonds by switching the light to 365 nm. Experimental evidence showed that Ti<sup>3+</sup> formed in situ activated the C-O bond, which is subsequently cleaved. This method is catalytic and provides a selective oxidation and hydrogenolysis method, which would be useful to convert highly functionalized lignin substructures in a chemoselective fashion under mild reaction conditions.



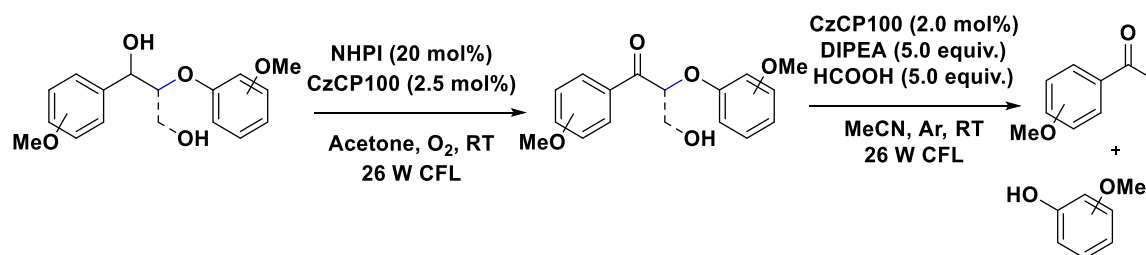
**Scheme 9:** Photocatalytic oxidation-hydrogenolysis strategy.

The group of Zhang has reported a metal free DPA-BP/NHPI/O<sub>2</sub> based photocatalytic system for aerobic oxidation of lignin  $\beta$ -O-4 models.<sup>[35]</sup> They used a donor-substituted aromatic ketone such as benzophenone (BP) to activate *N*-hydroxyphthalimide (NHPI) via a proton-coupled electron transfer (PCET) process under irradiation with a household fluorescent lamp (**Scheme 10**). The resulting short-lived phthalimide-*N*-oxyl radical (PINO) formed upon irradiation is further utilized for the selective oxidation of lignin model compounds under O<sub>2</sub>. The hydrogen bonding interaction between the aromatic ketone and *N*-hydroxyphthalimide facilitates the formation of PINO radical via photoinduced PCET process. A very fast reaction rate is achieved by this mechanism, because both electron and proton are transferred in a single step, resulting in a decreased activation barrier.



**Scheme 10:** (a) PCET from NHPI to an aromatic ketone. (b) Aerobic oxidation of lignin using DPA-BP/NHPI/O<sub>2</sub> system.

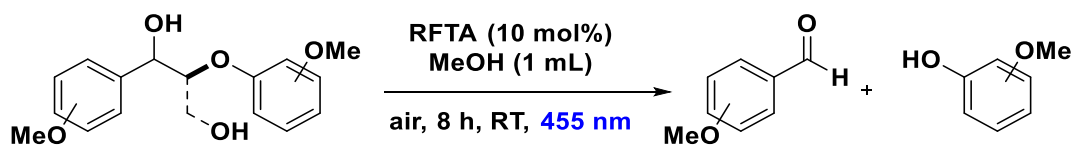
Luo *et. al.* synthesized a series of porous organic polymers (POPs) called carbazolic copolymers (CzCPs) that exhibit a wide range of redox potentials that are comparable to common transition metal complexes.<sup>[36]</sup> They used these polymers in the stepwise photocatalytic oxidation and cleavage of lignin  $\beta$ -O-4 models. CzCPs have excellent chemical stability and exhibit high recyclability acting as a promising metal free heterogeneous photocatalytic system replacing expensive transition metals. (**Scheme 11**). The reaction occurs at room temperature and shows excellent selectivity.



**Scheme 11:** Carbazolic porous organic framework for photocatalytic conversion of lignin models.

We could also show that the  $\beta$ -O-4 linkage of lignin model compounds can be cleaved aerobically under visible light irradiation using the organic dye riboflavin tetraacetate

(RFTA). We tested our reaction on five different lignin model compounds (**Scheme 12**) with 10 mol% RFTA in 1 mL CD<sub>3</sub>OD under visible light irradiation (455 nm) under air.

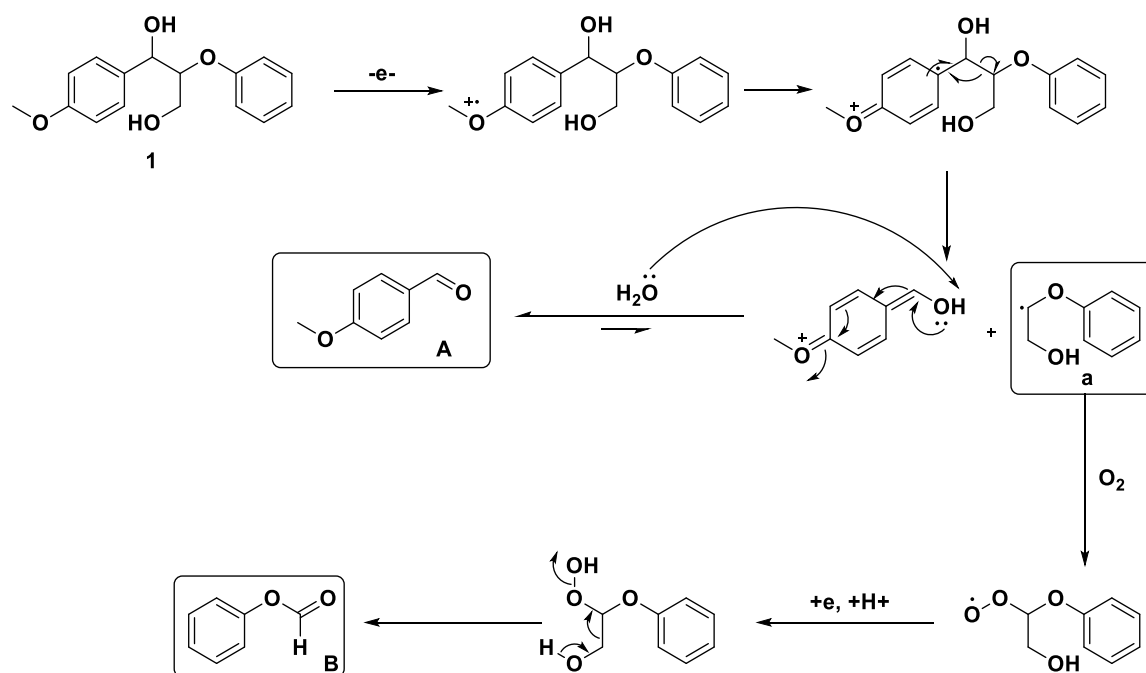


**Scheme 12:** Our photocatalytic approach for oxidation of lignin model substrate

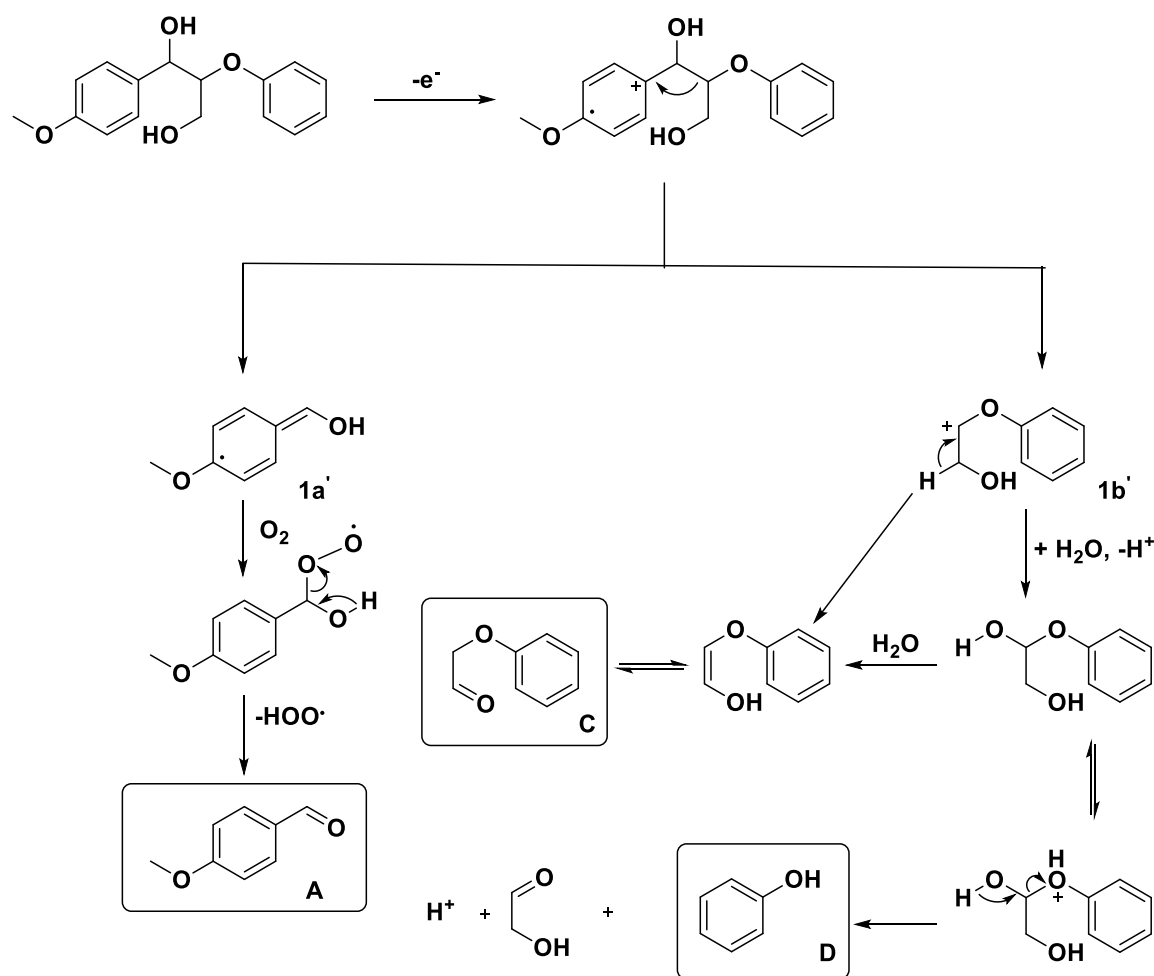
The model substrates behaved differently when subjected to the same reaction conditions. We did not only see the oxidation of the benzylic alcohol, but in addition, the C $_{\alpha}$ -C $_{\beta}$  bond breaks oxidatively yielding the corresponding aldehyde. Since the reaction is performed in methanol as solvent, the acetal of the aldehyde is formed. By introducing more methoxy groups on both aromatic rings, the rate of formation of the aldehyde decreases. Lim and co-workers reported the effect of alkoxy groups on the lignin  $\beta$ -O-4 model compounds and their efficiency towards C-C bond cleavage.<sup>[37]</sup> They investigated a series of differently substituted lignin models and based on the product distribution, quantum efficiencies, catalytic rate constants and DFT studies they concluded that less methoxy-substituted derivatives are cleaved more easily than the derivatives bearing more methoxy groups. These observations are in accordance to our experimental data (see the experimental part, **Table 1** and **2**). When the solvent was changed to a CH<sub>3</sub>CN: H<sub>2</sub>O (1:1) mixture, the reactions proceeded very slowly and long reaction times were required. When the compounds were irradiated for 18 hours, only the aldehydes could be isolated along with the starting materials. Other fractions remained unidentified. The C<sub>1</sub>-C<sub>2</sub> oxidative bond cleavage starts with the formation of a radical cation intermediate arising by SET from the arene to the excited state of the photocatalyst.

Based on these above observations, we proposed a mechanism for the oxidative degradation of lignin, which is in accordance with the SET oxidative pathway that takes place with lignin peroxidase (LiP).<sup>[38]</sup> After SET from the arene to the photocatalyst, the  $\beta$ -O-4 linkage can be cleaved by two different ways, either homolytically (**Scheme 13**) or heterolytically (**Scheme 14**). The C $_{\alpha}$ -C $_{\beta}$  bond from the radical cation of **1** can cleave homolytically to form the corresponding aldehyde **A** after tautomerization and an oxy-substituted radical (**a**), which undergoes oxidation followed by hydrolysis to form the ester **B**.

Our model compounds can also undergo heterolytic cleavage leading to the formation of a cation, which is thermodynamically<sup>[39]</sup> more favourable than the formation of the homolytic cleavage product (**Scheme 14**). The intermediate **1a'** can decompose by coupling with another peroxy radical to form an unstable tetroxide intermediate, which can further decompose to form the aldehyde **A**. The intermediate **1b'**, an oxy-substituted cation, can hydrolyze in different ways to form the fragments **C** and **D**.



**Scheme 13:** Proposed mechanism for the homolytic cleavage of lignin model compounds.



**Scheme 14:** Proposed mechanism for the heterolytic cleavage of lignin model compounds.

The discussed studies show that good progress was made towards the selective oxidation of lignin models using visible light photoredox catalysis. Although some issues remain, the oxidation under ambient temperature was achieved avoiding the formation of side reactions. With the recent progress in heterogeneous catalysis, the generation of stoichiometric waste may be avoided. Recent developments of metal free heterogeneous photocatalysts also contributed improving the lignin oxidation methods. However, until now, these methods have not been applied to the real lignin biopolymer or on larger scale.

## 1.6 Redox-neutral conversion of lignin

The third strategy for valorization of lignin would be the most atom-economical redox-neutral pathway. In this approach, the reductive equivalents generated from the initial oxidation step would be used to reductively cleave the  $\beta$ -O-4 bond of the oxidized lignin derivative (**Fig 4**).<sup>[40]</sup>

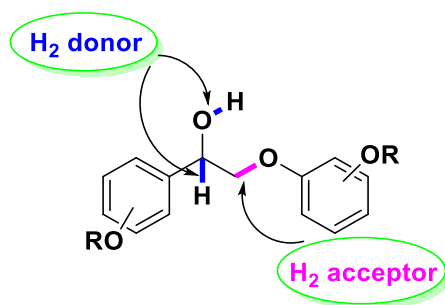
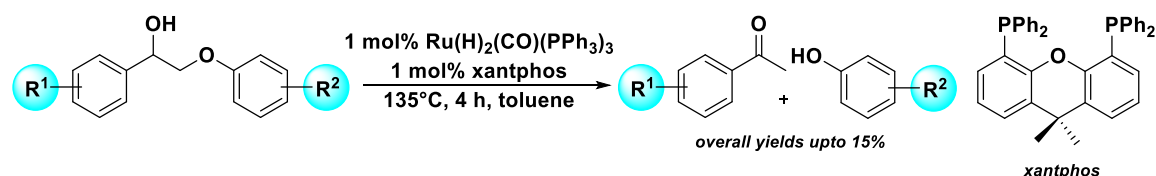
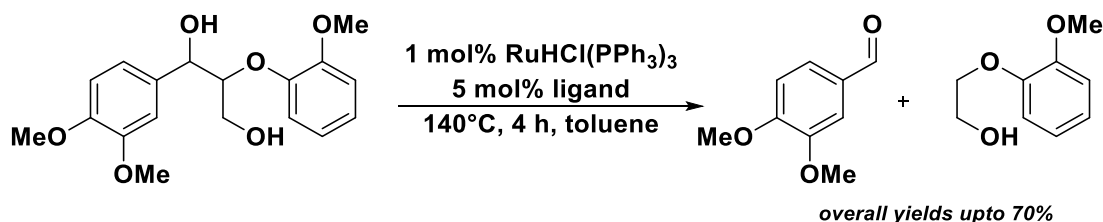


**Figure 4:** Working principle for redox-neutral conversion of lignin.

This would help to carry out the overall depolymerization process in one pot without the use of stoichiometric additives. The initial studies from Ellman, Bergman and co-workers showed that a ruthenium catalyst, produced *in situ* from  $\text{Ru}(\text{H})_2(\text{CO})(\text{PPh}_3)_3$  in combination with xantphos ((9,9-dimethyl-9*H*-xanthene-4,5-diyl)bis(diphenylphosphane)) can affect the tandem catalytic dehydrogenation and C-O bond cleavage in a single step without any external additives (**Scheme 15**).<sup>[41]</sup> Initial experiments showed that this catalytic system works well on simple arylethanol systems. However, the incorporation of a  $\gamma$ -OH functionality completely inhibited the hydrogenolysis process. The inclusion of a  $\gamma$ -OH group resulted in the deactivation of Ru/xantphos system by irreversible formation of Ru complexes, which could be isolated. These observations led to the development of new catalytic methods. Leitner and Klankermayer reported a more active Ru-based complex for redox-neutral  $\beta$ -O-4 bond cleavage in lignin model compounds.<sup>[42,43]</sup> They synthesized a Ru precursor  $[\text{Ru}(\text{cod})(\text{methallyl})_2]$  (cod = 1,5-cyclooctadiene; methallyl =  $\eta^3\text{-C}_4\text{H}_7$ ), which, in combination with a tripodal phosphine based ligand, acts as a highly active catalytic system, effectively performing a redox-neutral C-C bond cleavage on  $\gamma$ -OH containing lignin model substrates (**Scheme 16**).



**Scheme 15:** Tandem dehydrogenation/hydrogenolysis of  $\beta$ -O-4 bond in lignin models



**Scheme 16:** Selective C-C bond cleavage using  $\text{RuHCl}(\text{PPh}_3)_3$  precursor.

## 1.7 Conclusion, challenges and outlook

Depolymerization of lignin as a strategy to produce high value arenes has attracted the attention of the scientific community in the recent years. In this chapter, we highlighted some important methodologies for the valorization of lignin model compounds under oxidative, reductive and redox-neutral conditions comparing transition metal catalyzed and photoredox catalyzed methods. However, several challenges remain. In explorative laboratory research, catalytic methods are developed for the degradation of lignin model substrates. However, these methods are often ineffective when it comes to valorization of lignin polymers (*e.g.*, softwood, hardwood *etc.*) at industrial scale. Therefore, efficient catalytic methods for lignin depolymerization are required that are cost effective, produce products that are easily separable and that can be implemented on larger scale. During the initial studies of lignin valorization under reductive conditions, the first challenge was to overcome hydrogenolysis over hydrogenation. Over the years, with the development of various metal catalysts it was possible to achieve selective hydrogenolysis of lignin subunits to cleave  $\beta$ -O-4 linkages. However, the catalysts designed for this selective transformations showed very different selectivities on different lignin monomers, which are difficult to rationalize. The transition metal catalysts also required very high temperatures that led to the degradation and poisoning of the catalyst and resulted in



uncontrolled depolymerization of lignin along with unwanted side products. These limitations of the reductive lignin valorization method, which also requires high temperatures and sometimes high pressure, led to the continuous development of new catalytic systems. In this respect, visible light mediated photoredox catalysis can provide a new avenue to selectively convert lignocellulosic biomass into fine chemicals under mild conditions. Since, photochemical reactions occur under mild conditions compared to thermal processes, the bonds can be cleaved more selectively and side reactions may be minimized. A new strategy developed is the selective oxidation of the benzylic alcohol of lignin prior to the photocatalytic cleavage of  $\beta$ -O-4 linkages. Although, a room temperature method was developed, this process still generates stoichiometric waste, which is not acceptable from an economic point of view. Still the most common way to degrade lignin is via oxidation, but this method yields reactive radical species generated upon oxidation of aromatic rings. The selectivity is difficult to control. In this regard, methods using a concerted oxygen transfer to avoid the extensive formation of free radicals may be beneficial. Photoredox methods are not effective in dark solutions, and a stepwise addition of the lignin polymer would be advisable. The development of a continuous flow process may overcome several of the current challenges towards the utilization of lignin in chemical synthesis.

## 1.8 Experimental section

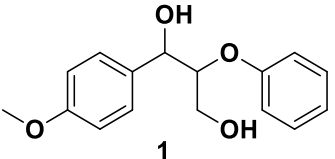
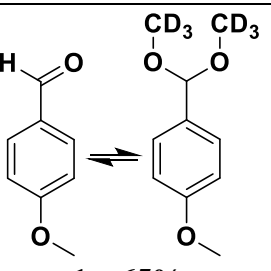
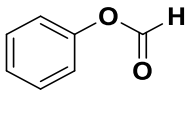
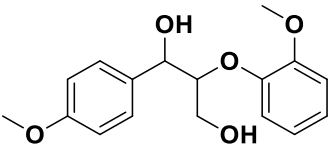
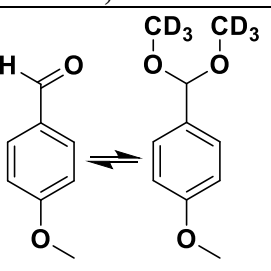
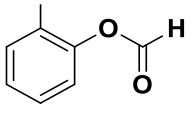
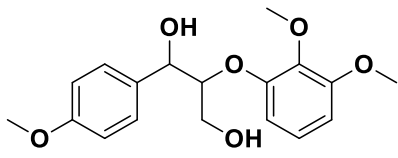
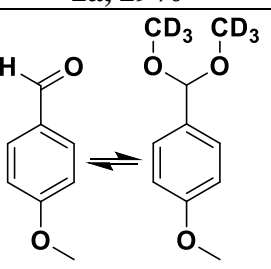
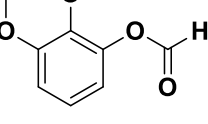
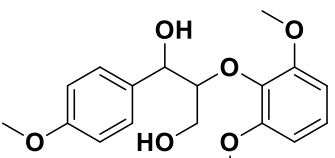
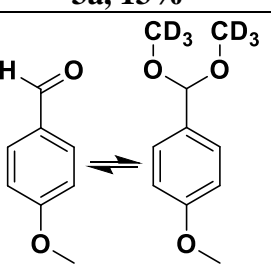
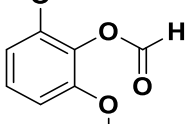
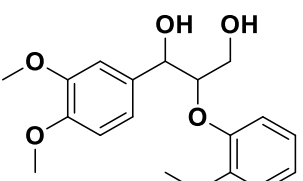
### 1.8.1 Materials and methods

The lignin model substrates were synthesized according to the literature procedures.<sup>[44-46]</sup> The photocatalyst riboflavin tetraacetate (RFTA) was synthesized according to the literature procedure.<sup>[47]</sup> Thin-layer chromatography was performed using silica gel plates 60 F254: Visualization was accomplished with short wavelength UV light (254 nm). Standard flash chromatography was performed on an Isolera™ Spektra Systems automated with high performance flash purification system using silica gel of particle size 40–63  $\mu\text{m}$  or a reverse column (specification: Biotage SNAP KP-C18-HS-12g). Preparative high-pressure liquid chromatography (HPLC) was performed using a C18 reverse column and water/acetonitrile mixtures with a UV detector.  $^1\text{H}$  and  $^{13}\text{C}$  NMR spectra were recorded on Bruker Avance spectrometers (300 MHz and 75 MHz or 400 MHz and 101 MHz) in  $\text{CDCl}_3$  and  $\text{MeOH-}d_4$  solution with internal solvent signal as reference (7.26 and 77.26, 3.31, 4.78 and 49.15 respectively). Proton NMR data are reported as follows: chemical shift (ppm), multiplicity (s = singlet, d = doublet, t = triplet, q = quartet, quint = quintet, sext = sextet, hept = heptet, dd = doublet of doublets, ddd = doublet of doublets of doublets, td = triplet of doublets, qd = quartet of doublets, m = multiplet, br. s. = broad singlet), coupling constants (Hz) and numbers of protons. Data for  $^{13}\text{C}$  NMR are reported in terms of chemical shift and no special nomenclature is used for equivalent carbons. High resolution mass spectra (HRMS) were obtained from the central analytic mass spectrometry facilities of the Faculty of Chemistry and Pharmacy, Regensburg University and are reported according to the IUPAC recommendations 2013. Quantification of oxidation products was performed by  $^1\text{H}$  and  $^{13}\text{C}$  NMR analysis using internal standards. Electrochemical studies were carried out under argon atmosphere. The measurements were performed in acetonitrile (MeCN) containing 0.1 M tetra-*n*-butylammonium tetrafluoroborate using ferrocene/ferrocenium ( $\text{Fc}/\text{Fc}^+$ ) as an internal reference. A glassy carbon electrode (working electrode), platinum wire (counter electrode), and silver wire (quasi-reference electrode) were employed. Spectroelectrochemical studies were carried out in an optically transparent thin layer electrochemical cell (OTTLE). Photooxidation reactions were performed with 455 nm LEDs (OSRAM Oslon SSL 80 royal-blue LEDs ( $\lambda = 455 \text{ nm} (\pm 15 \text{ nm})$ ), 3.5 V, 700 mA).

## 1.8.2 Photocatalytic oxidation of the lignin model compounds

Table 1:

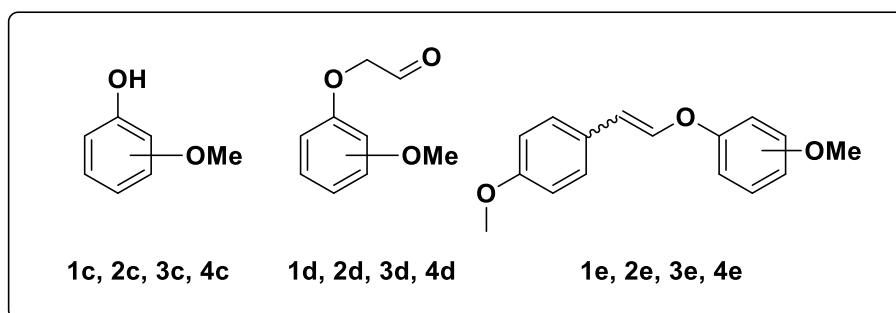
Benzylic oxidation and C $\alpha$ -C $\beta$  bond cleavage of model compounds (reaction in CD<sub>3</sub>OD):

| Substrate  | Products <sup>a</sup>  |  | Recovered starting material |
|--|--|--|-----------------------------|
|  <p>1</p>   |  <p>1a, 65%</p>   |  <p>1b, 15%</p>  | 54%                         |
|  <p>2</p>  |  <p>2a, 29%</p>  |  <p>2b, 4%</p>  | 35%                         |
|  <p>3</p> |  <p>3a, 13%</p> |  <p>3b, 1%</p> | 51%                         |
|  <p>4</p> |  <p>4a, 26%</p> |  <p>4b, 6%</p> | 26%                         |
|  <p>5</p> | <p>Very difficult to predict the NMR.<br/>Degradation of the starting material is observed.</p>    |  |                             |

The reactions were performed with 0.1 mmol of substrate, CD<sub>3</sub>OD (1 mL), 10 mol% RFTA under blue light irradiation (455 nm) in air for 8 hours.

<sup>a</sup>the yields were calculated by <sup>1</sup>H NMR (300 MHz) using 1,3,5-trimethoxybenzene as an internal standard.

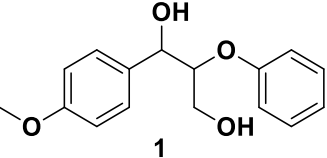
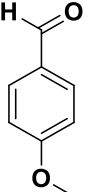
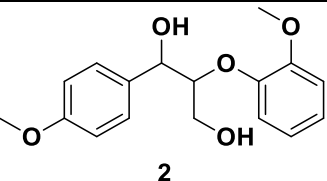
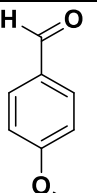
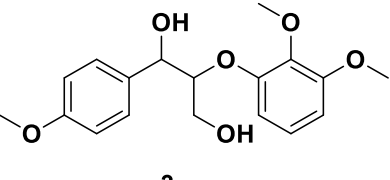
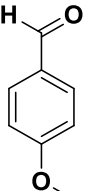
The other fragments obtained from the oxidation of compounds **1-4** were confirmed by GC-MS analysis. However, we were not able to quantify these fragments (**Figure 5**).



**Figure 5:** Fragments obtained from oxidation of compounds **1-4**.

**Table 2:**

**Benzylic oxidation of model substrates in CH<sub>3</sub>CN: H<sub>2</sub>O (1:1):**

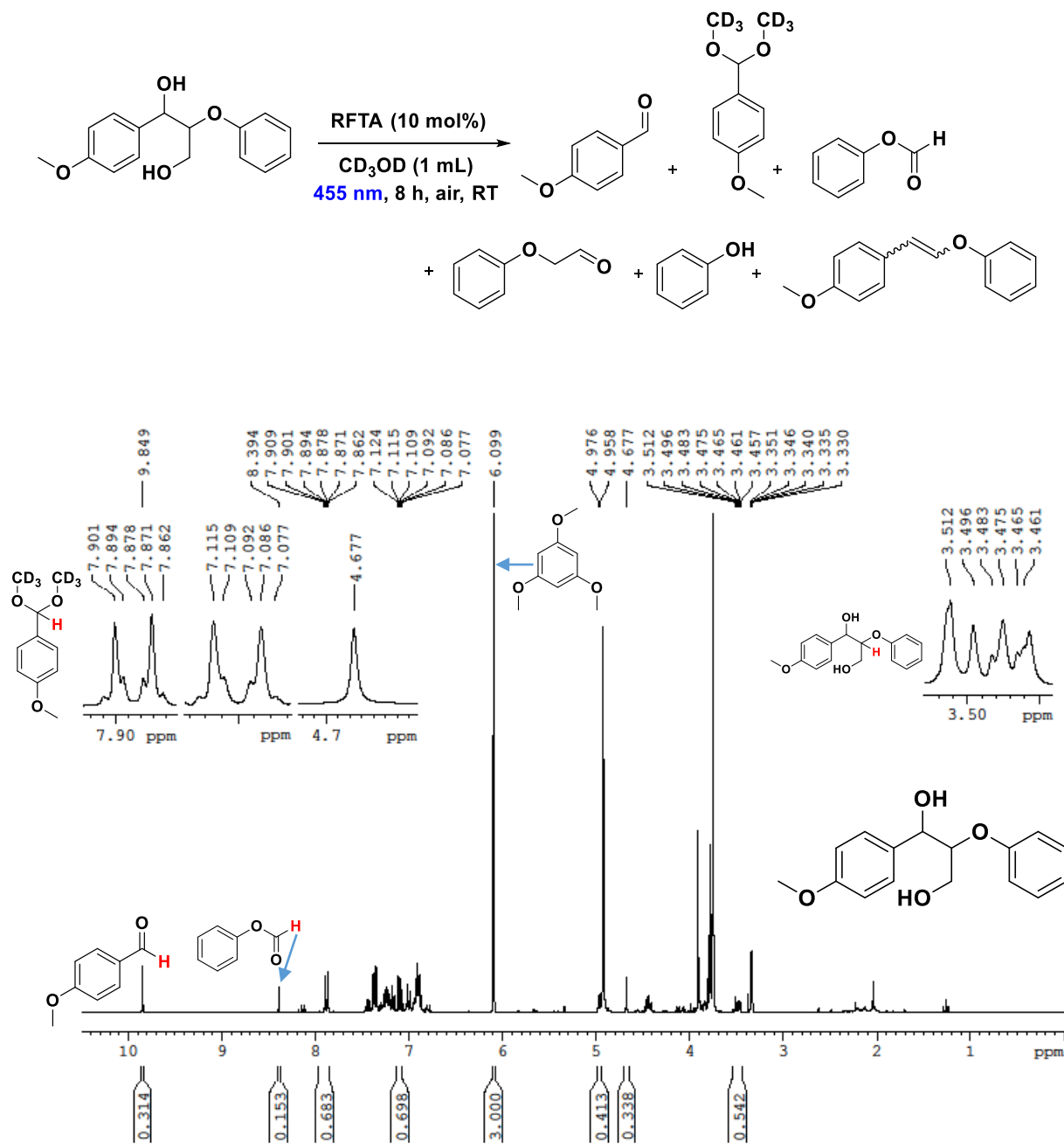
| Substrate  | Product   | Yield <sup>b</sup> (%) | Recovered starting material (%) |
|--|---|------------------------|---------------------------------|
| <br>1 |  | 55                     | 29                              |
| <br>2 |  | 40                     | 30                              |
| <br>3 |  | 30                     | 57                              |

|  |  |                  |                  |
|--|--|------------------|------------------|
| <p>Chemical structure of 4,4'-dimethoxy-2,2'-bis(hydroxymethyl)-1,1'-bi-2-naphthol (4). It consists of two naphthalene units linked at their 1-positions. Each naphthalene unit has a methoxy group at the 4-position and a hydroxymethyl group at the 2-position.</p> | <p>Chemical structure of 4-methoxybenzaldehyde, showing a benzene ring with a methoxy group at the para position and an aldehyde group at the other para position.</p> | <p><b>15</b></p> | <p><b>31</b></p> |
|--|--|------------------|------------------|

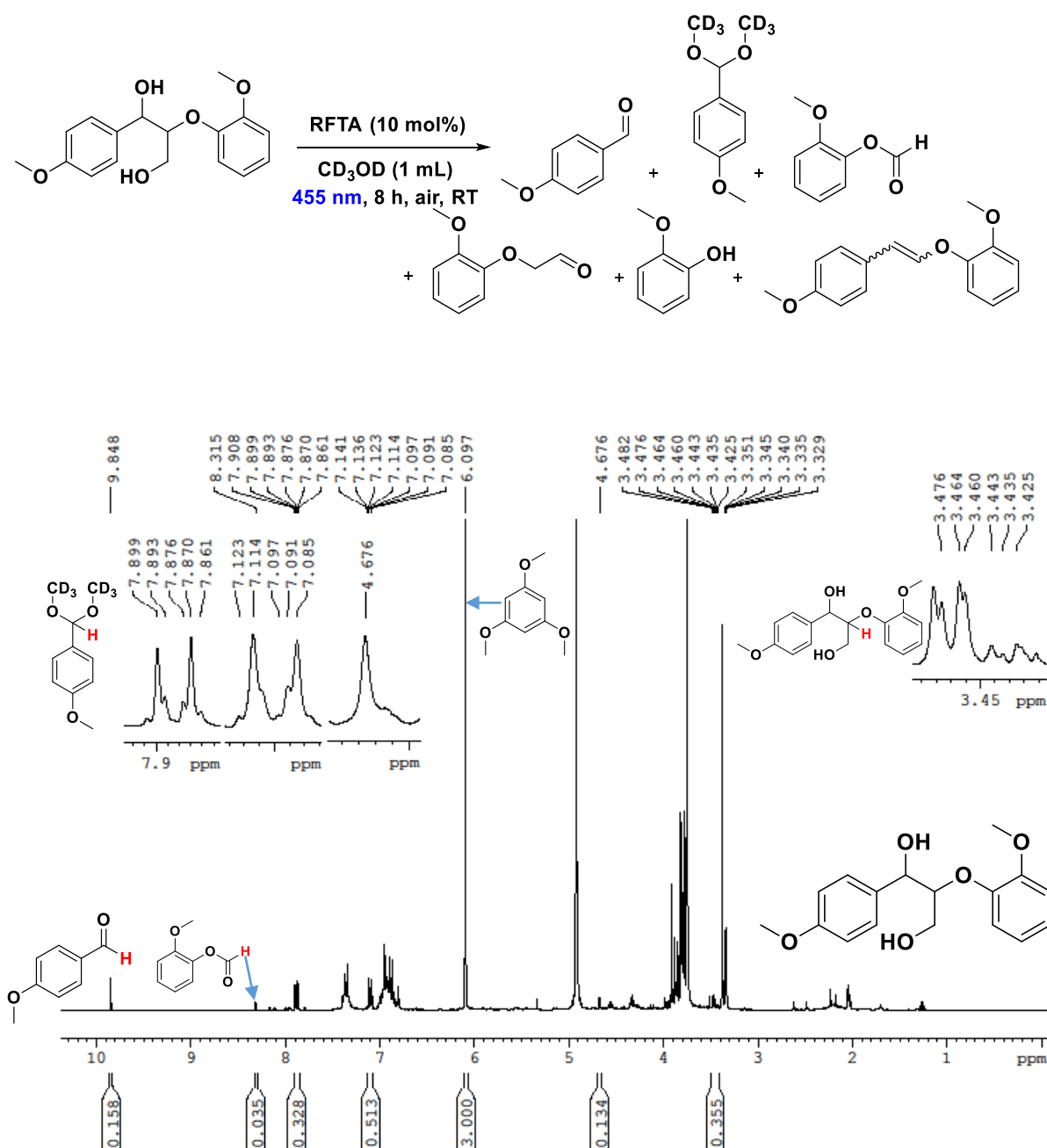
The reactions were performed with 0.1 mmol of substrate, CH<sub>3</sub>CN: H<sub>2</sub>O (1:1) (1 mL), 10 mol% RFTA under blue light irradiation (455 nm) in air for 18 hours.

<sup>b</sup> yields were determined by column chromatography over silica gel.

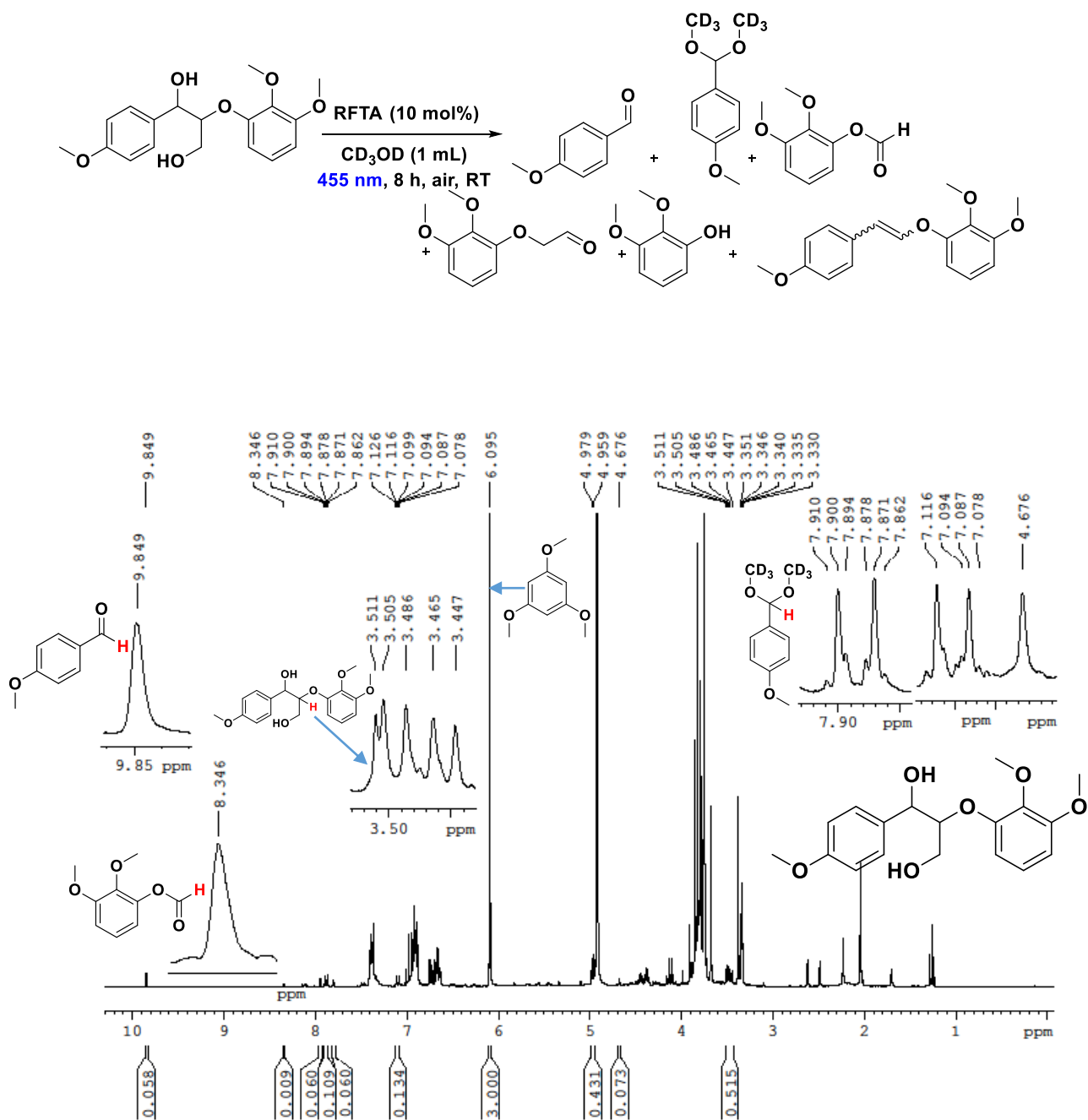
# Photocatalytic conversion of 1-(4-methoxyphenyl)-2-phenoxypropane-1,3-diol (1) to different fragments



Photocatalytic conversion of 2-(2-methoxyphenoxy)-1-(4-methoxyphenyl)propane-1,3-diol (2) to different fragments

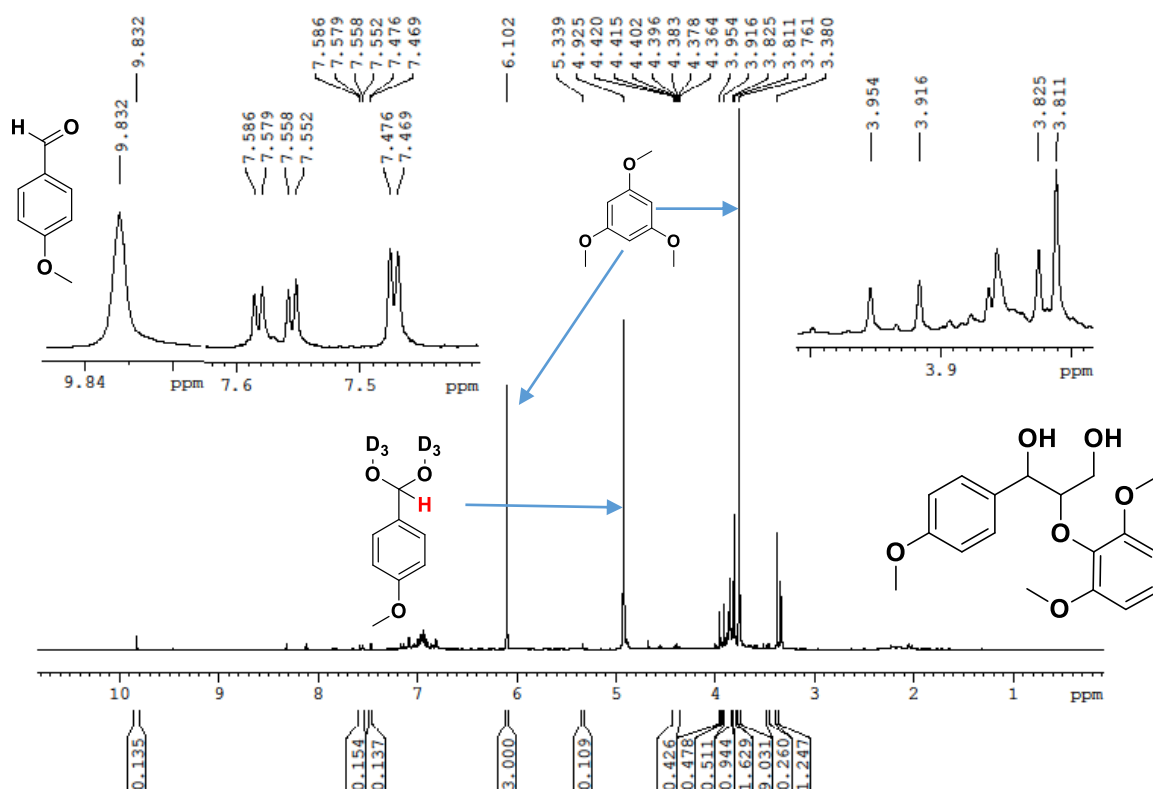
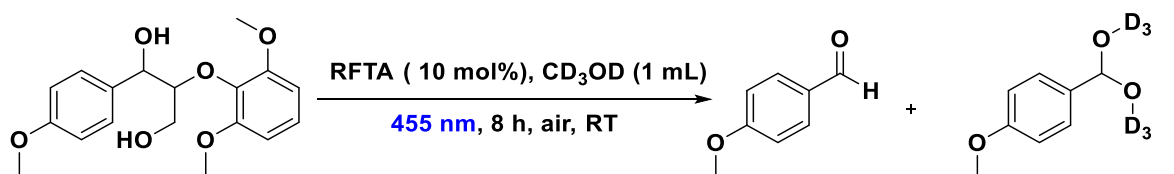


# Photocatalytic conversion of 2-(2,3-dimethoxyphenoxy)-1-(4-methoxyphenyl)propane-1,3-diol (3) to different fragments





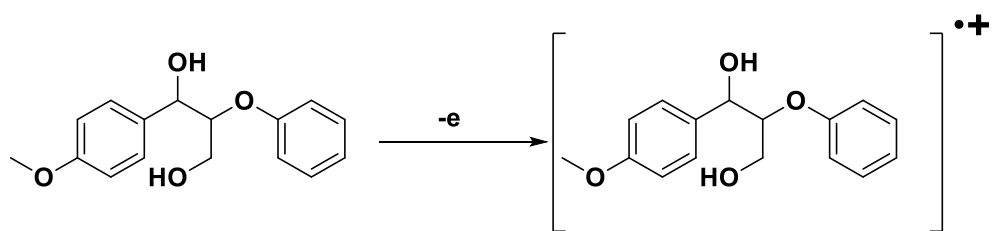
Photocatalytic conversion of 2-(2,6-dimethoxyphenoxy)-1-(4-methoxyphenyl)propane-1,3-diol (4) to 4-methoxybenzaldehyde



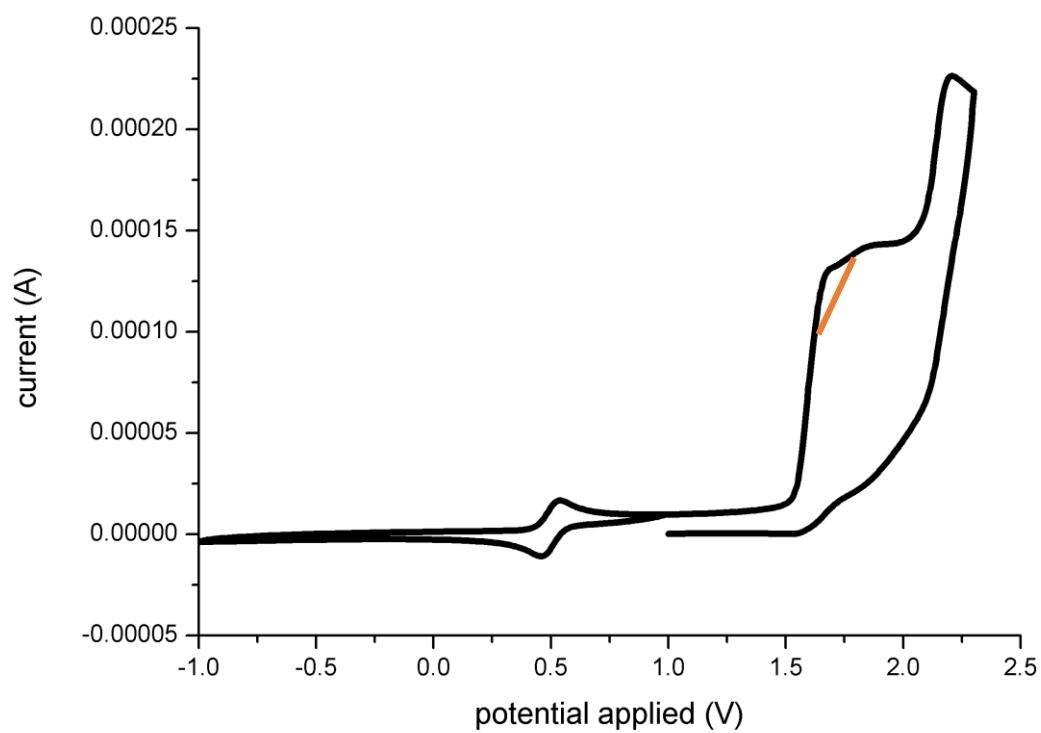
26% of the aldehyde and the corresponding acetal in total are in equilibrium with each other.

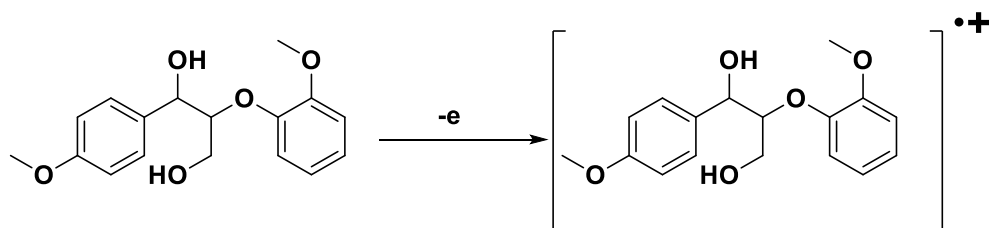
Rest is the starting material.

## 1.8.3 Cyclic voltammetry measurements of compounds 1-5

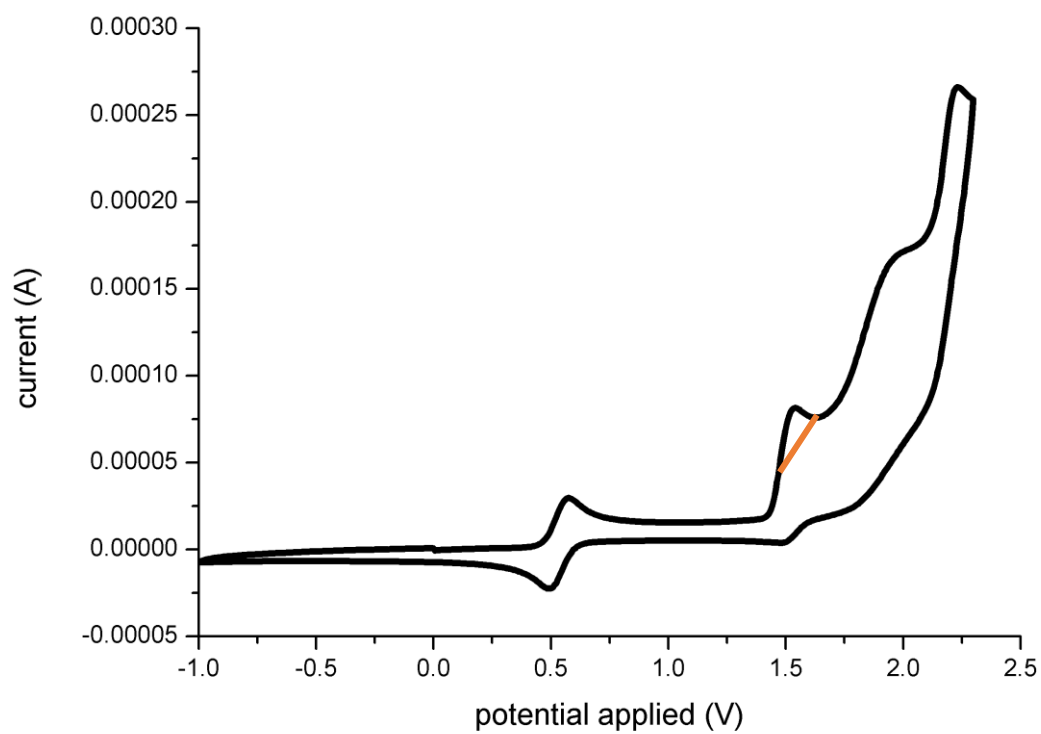


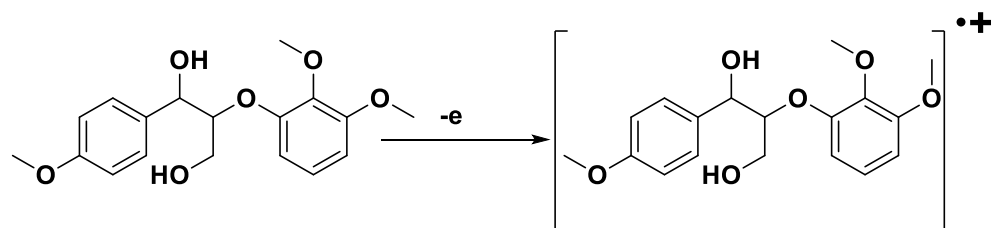
$E^0 = 1.56 \text{ V vs SCE}$



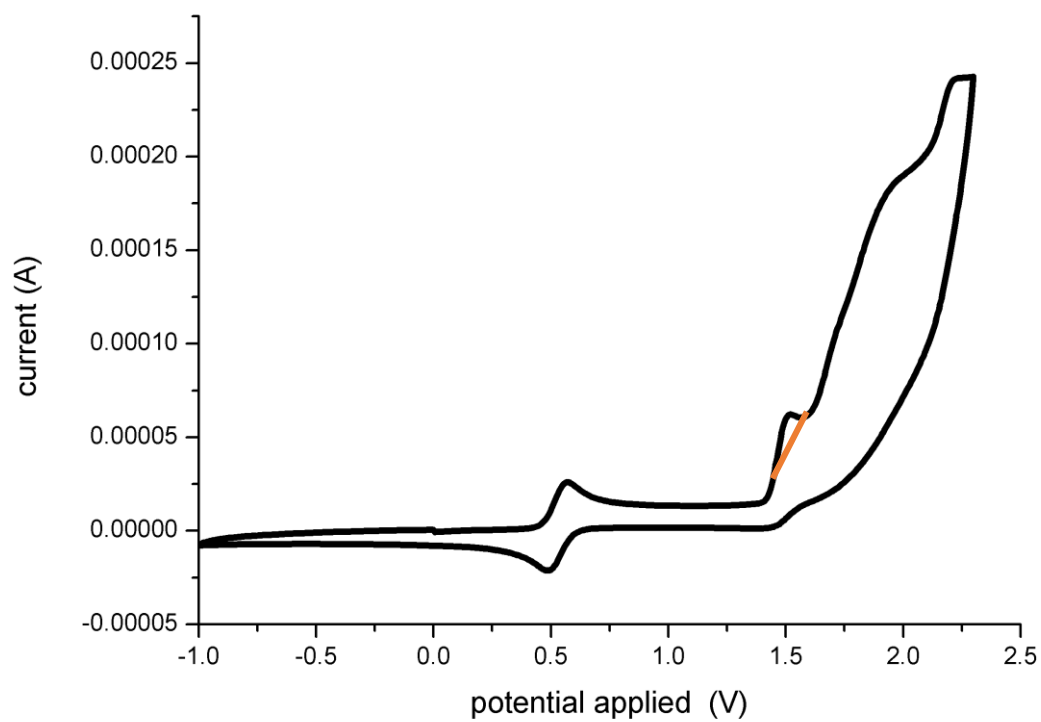


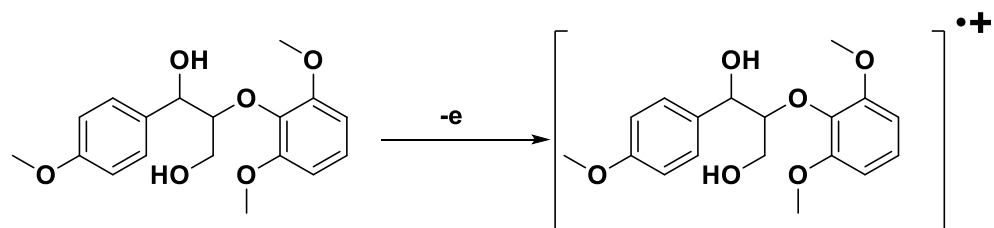
$E^0 = 1.37 \text{ V vs SCE}$



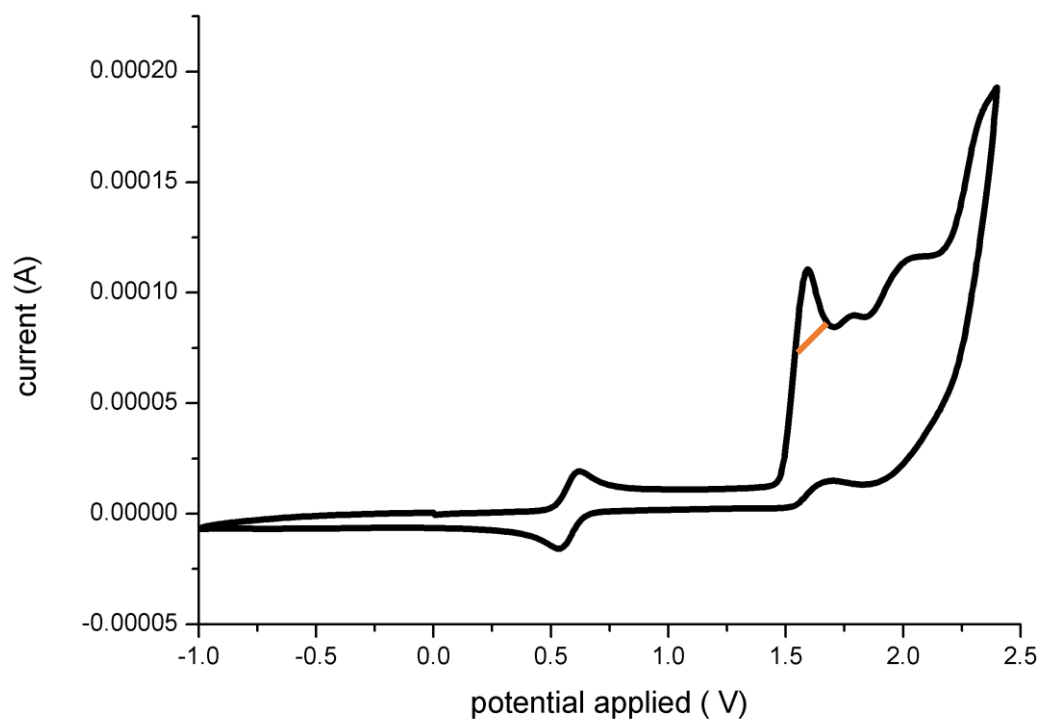


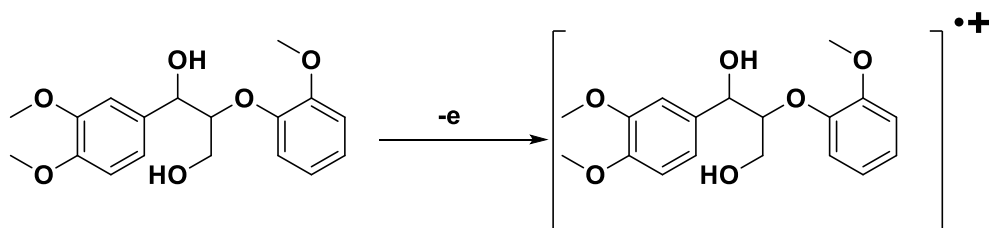
$E^0 = 1.39 \text{ V vs SCE}$



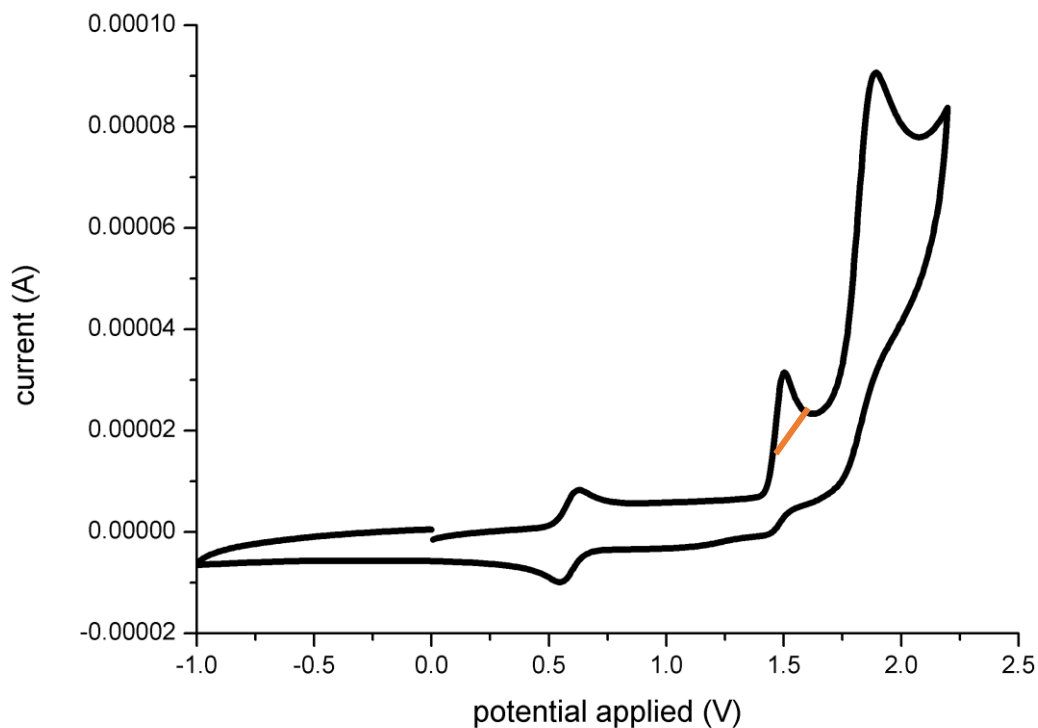


$E^0 = 1.4 \text{ V vs SCE}$



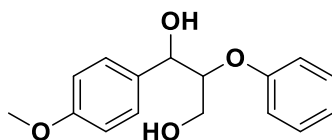


$E^0 = 1.3 \text{ V vs SCE}$



#### 1.8.4 Synthesis of the lignin model compounds

##### Synthesis of 1-(4-methoxyphenyl)-2-phenoxypropane-1,3-diol (1)<sup>[44]</sup>



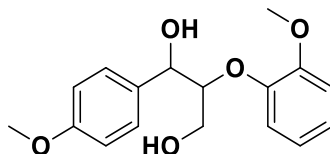
The compound was synthesized according to the literature procedure. The compound was obtained as a 3:1 mixture of diastereomers as a white sticky solid.

$^1\text{H NMR}$  (400 MHz,  $\text{CDCl}_3$ , ppm):  $\delta$  7.28-7.13 (m, 5.6H), 6.91-6.76 (m, 6.6H), 4.93 (d,  $J = 4 \text{ Hz}$ , 0.3H), 4.89 (d,  $J = 5.2 \text{ Hz}$ , 1H), 4.31-4.27 (m, 1.3 H), 3.83 (dd,  $J = 12 \text{ Hz}$ , 4.4 Hz,

0.3H), 3.75 (dd,  $J = 12$  Hz, 4 Hz, 0.3H), 3.85 (s, 3.3H), 3.84 (s, 1H), 3.44 (dd,  $J = 12.4$ Hz, 4 Hz, 1.6 Hz).

$^{13}\text{C}$  NMR (101 MHz,  $\text{CDCl}_3$ , ppm):  $\delta$  159.7, 159.5, 158.2, 157.8, 132.6, 131.8, 129.9, 129.8, 128.3, 127.6, 122.2, 122.0, 116.8, 116.7, 114.2, 114.1, 83.3, 82.0, 74.0, 73.8, 61.5, 61.2, 55.5.

**Synthesis of 2-(2-methoxyphenoxy)-1-(4-methoxyphenyl)propane-1,3-diol (2)<sup>[45]</sup>**

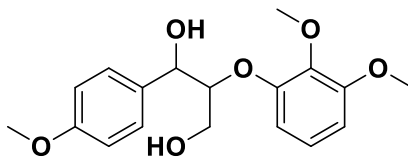


The compound is synthesized according to the literature procedure. The compound was obtained as a 1.68:1 mixture of diastereomers as a sticky oil.

$^1\text{H}$  NMR (400 MHz,  $\text{CDCl}_3$ , ppm):  $\delta$  7.37-7.33 (m, 1H), 7.32-7.28 (m, 2H), 7.13-7.10 (m, 0.5H), 7.07-7.01 (m, 1.5H), 6.94-6.85 (m, 7.2H), 4.99-4.97 (m, 1.5H), 4.16-4.12 (m, 1H), 4.03 (q,  $J = 3.6$  Hz, 0.6H), 3.91 (d,  $J = 5.8$  Hz, 0.5H), 3.88 (s, 1.8H), 3.87 (s, 0.3H), 3.85 (s, 3H), 3.79-3.78 (m, 4.5H), 3.65 (dd,  $J = 12.1$  Hz, 3.3 Hz, 1H), 3.60 (dd,  $J = 12.4$  Hz, 3.3 Hz, 0.6H), 3.44 (dd,  $J = 12.5$  Hz, 4 Hz, 0.6H).

$^{13}\text{C}$  NMR (101 MHz,  $\text{CDCl}_3$ , ppm):  $\delta$  159.6, 159.2, 151.7, 151.4, 147.8, 147.1, 132.3, 131.9, 128.5, 127.5, 124.3, 124.2, 121.8, 121.7, 121.1, 121.0, 114.1, 114.0, 112.3, 112.3, 89.6, 87.4, 73.8, 72.8, 61.1, 60.0, 56.0, 55.4.

**Synthesis of 2-(2,3-dimethoxyphenoxy)-1-(4-methoxyphenyl)propane-1,3-diol (3)<sup>[46]</sup>**



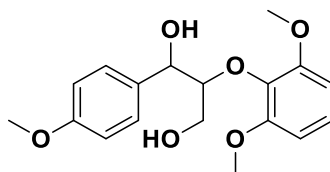
The compound is synthesized according to the literature procedure. The compound was obtained as a 1.58:1 mixture of diastereomers as a sticky oil.

$^1\text{H}$  NMR (400 MHz,  $\text{CDCl}_3$ , ppm):  $\delta$  7.25-7.15 (m, 3.5H), 6.90-6.47 (m, 8.3H), 5.18 (bs, 0.6H), 4.89-4.87 (m, 1.5H), 4.09 (q,  $J = 4.8$  Hz, 0.6H), 4.03-3.99 (m, 0.4H), 3.95 (q,  $J = 3.8$  Hz, 1H), 3.82-3.67 (m, 15.3H), 3.57 (dd,  $J = 12.2$  Hz, 3.4 Hz, 0.7H), 3.46 (dd,  $J = 12.5$  Hz, 3.2 Hz, 1H), 3.32 (dd,  $J = 12.5$  Hz, 4 Hz, 1H).

**$^{13}\text{C}$  NMR** (101 MHz,  $\text{CDCl}_3$ , ppm):  $\delta$  159.6, 159.2, 153.8, 153.8, 152.3, 151.6, 141.0, 132.6, 132.0, 128.7, 128.4, 127.5, 124.6, 124.4, 114.1, 113.9, 113.2, 112.6, 107.6, 107.3, 88.9, 86.0, 73.9, 73.2, 61.7, 61.6, 61.1, 61.0, 56.1, 55.4.

**HRMS**  $[\text{M}+\text{NH}_4]^+$   $\text{C}_{18}\text{H}_{22}\text{O}_6$  calculated 352.1755 found 352.1761.

**Synthesis of 2-(2,6-dimethoxyphenoxy)-1-(4-methoxyphenyl)propane-1,3-diol (4).**<sup>[46]</sup>



The compound is synthesized according to the literature procedure. The compound was obtained as a 1:0.5 mixture of diastereomers as a sticky oil.

**$^1\text{H}$  NMR** (400 MHz,  $\text{CDCl}_3$ , ppm):  $\delta$  7.40-7.36 (m, 2H), 7.28-7.25 (m, 0.4H), 7.08-7.03 (m, 1.4H), 6.89-6.85 (m, 3H), 6.64-6.62 (m, 3H), 5.07 (d,  $J = 8.8$  Hz, 1H), 5.02 (d,  $J = 3.6$  Hz, 0.5H), 4.15 (q,  $J = 3$  Hz, 0.5H), 4.12-4.08 (m, 0.3H), 3.92-3.89 (m, 10H), 3.87 (s, 3H), 3.79 (s, 2.7H), 3.78 (s, 1.7H), 3.55 (dd,  $J = 12.2$  Hz, 2.7 Hz, 1H), 3.49 (dd,  $J = 12$  Hz, 2.7 Hz, 0.6H), 3.29-3.26 (m, 1.2H).

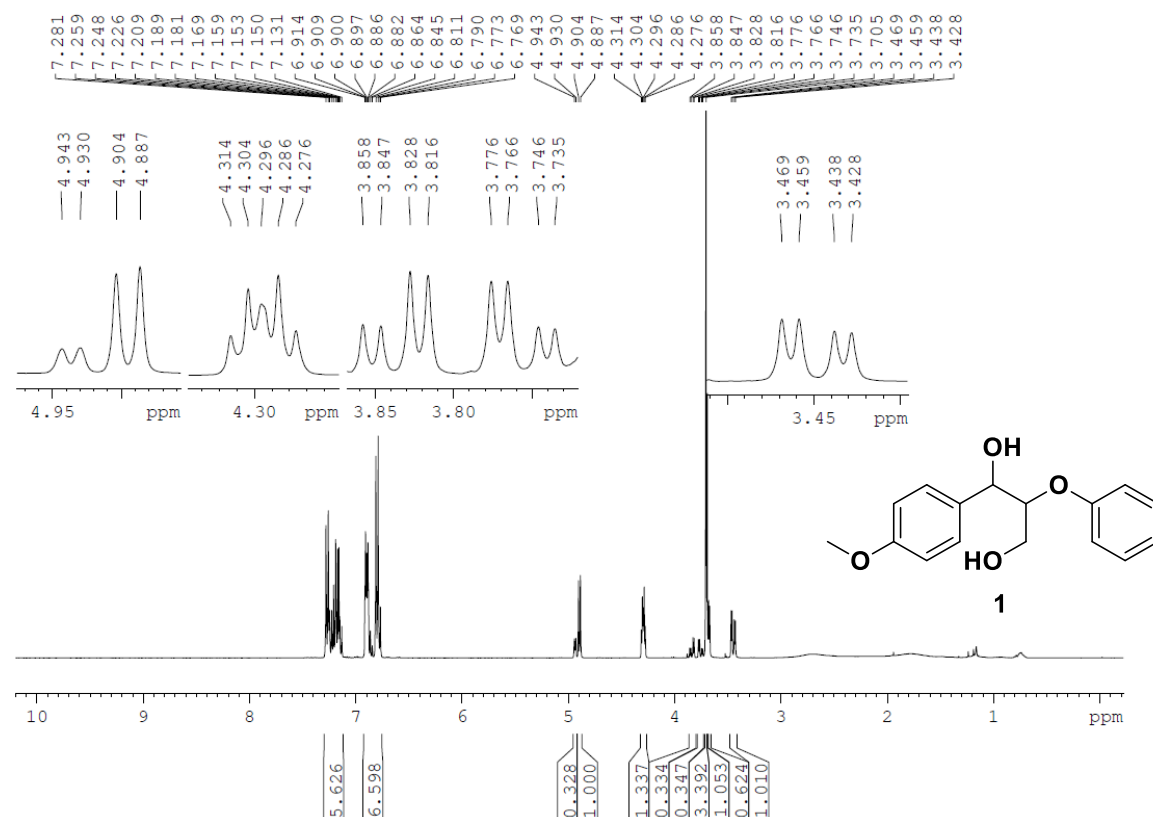
**$^{13}\text{C}$  NMR** (101 MHz,  $\text{CDCl}_3$ , ppm):  $\delta$  159.5, 159.0, 153.7, 153.4, 135.5, 135.1, 132.4, 131.7, 128.7, 127.2, 124.6, 124.6, 114.0, 113.9, 105.5, 89.2, 87.1, 73.9, 72.6, 60.7, 60.6, 56.3, 55.4.

**HRMS**  $[\text{M}+\text{Na}]^+$   $\text{C}_{18}\text{H}_{22}\text{O}_6$  calculated 357.1309 found 357.1311.

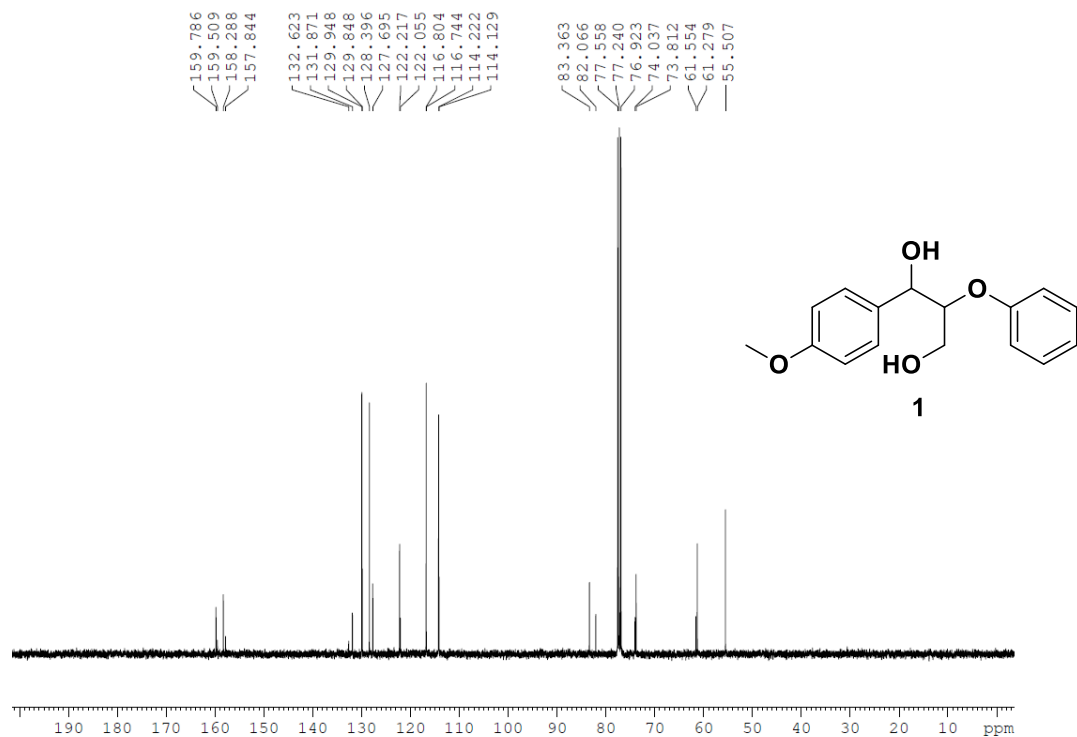


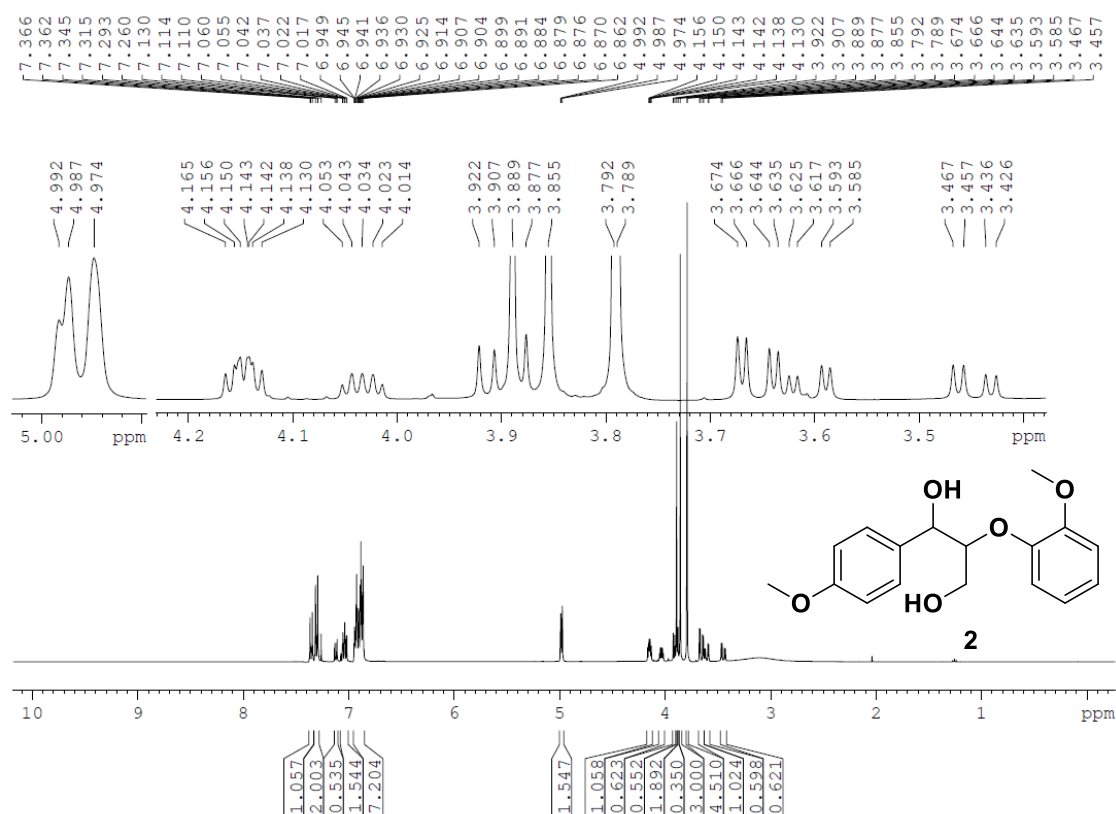
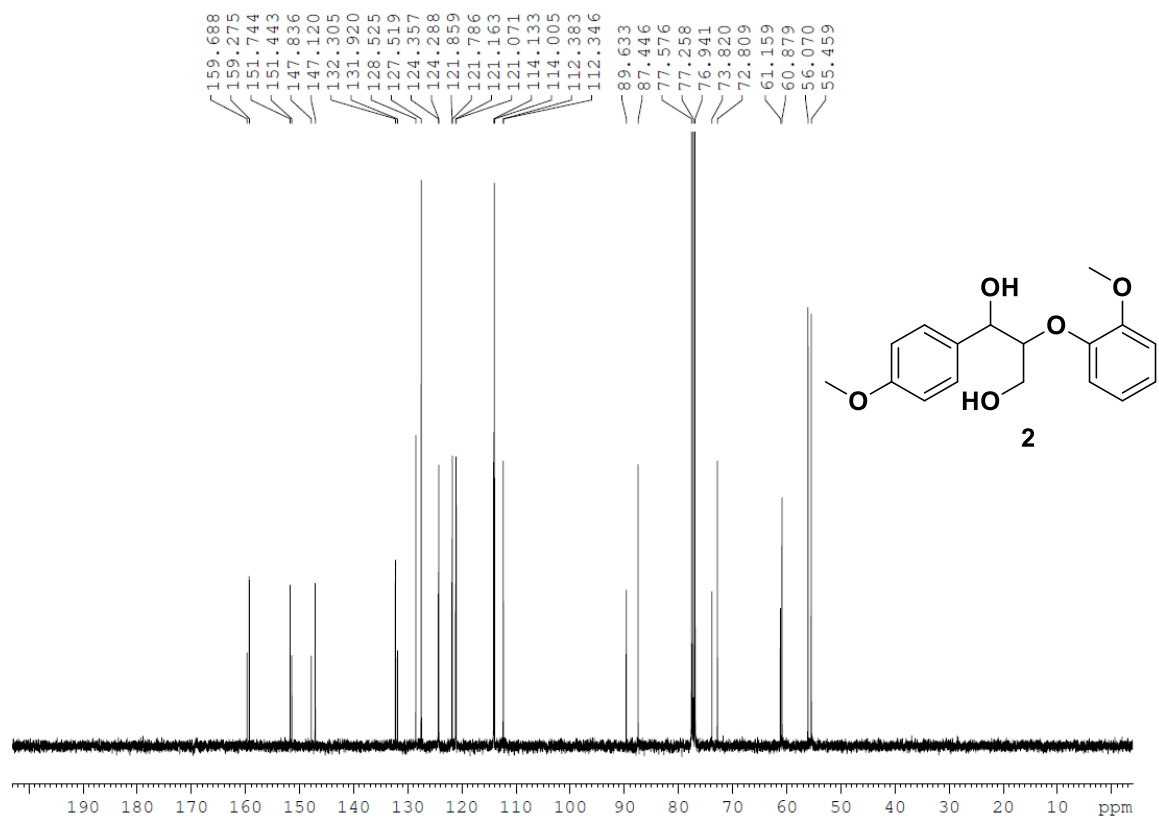
## 1.8.5 $^1\text{H}$ - and $^{13}\text{C}$ NMR spectra of synthesized compounds

### $^1\text{H}$ spectra of compound 1 ( $\text{CDCl}_3$ , 400 MHz)

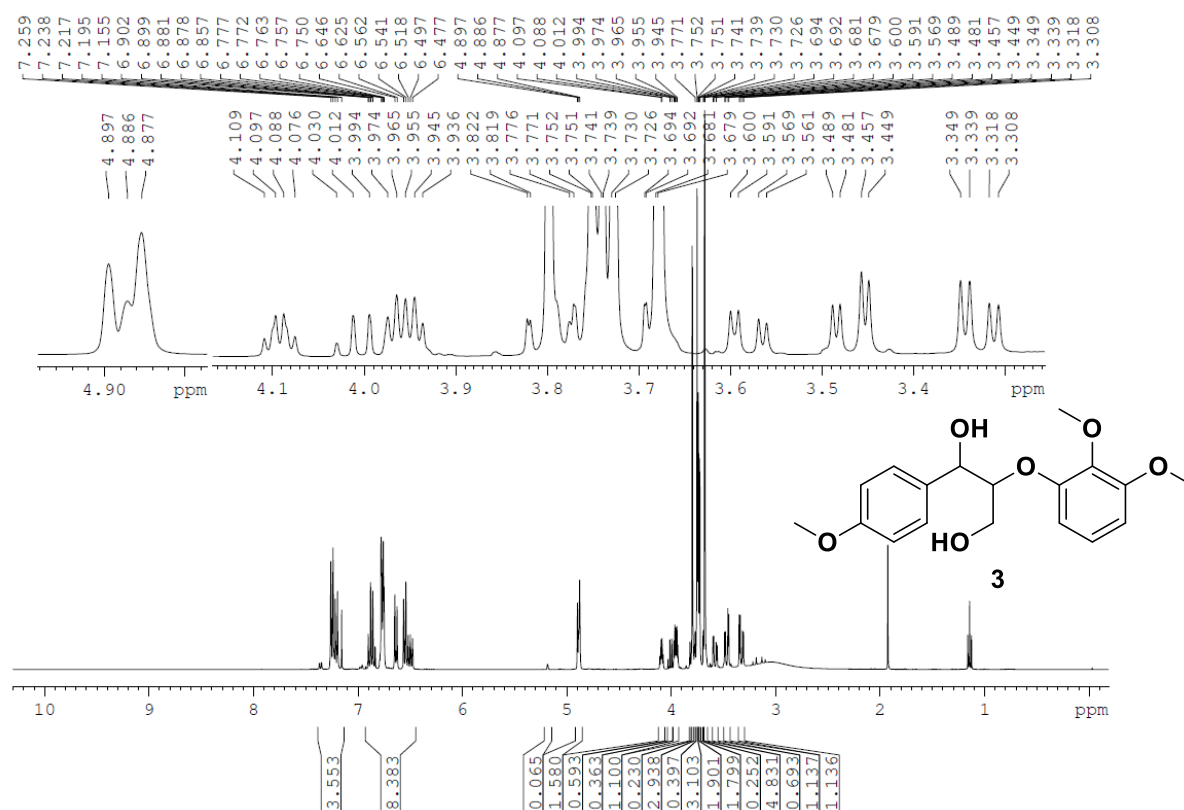


### $^{13}\text{C}$ spectra of compound 1 ( $\text{CDCl}_3$ , 101 MHz)

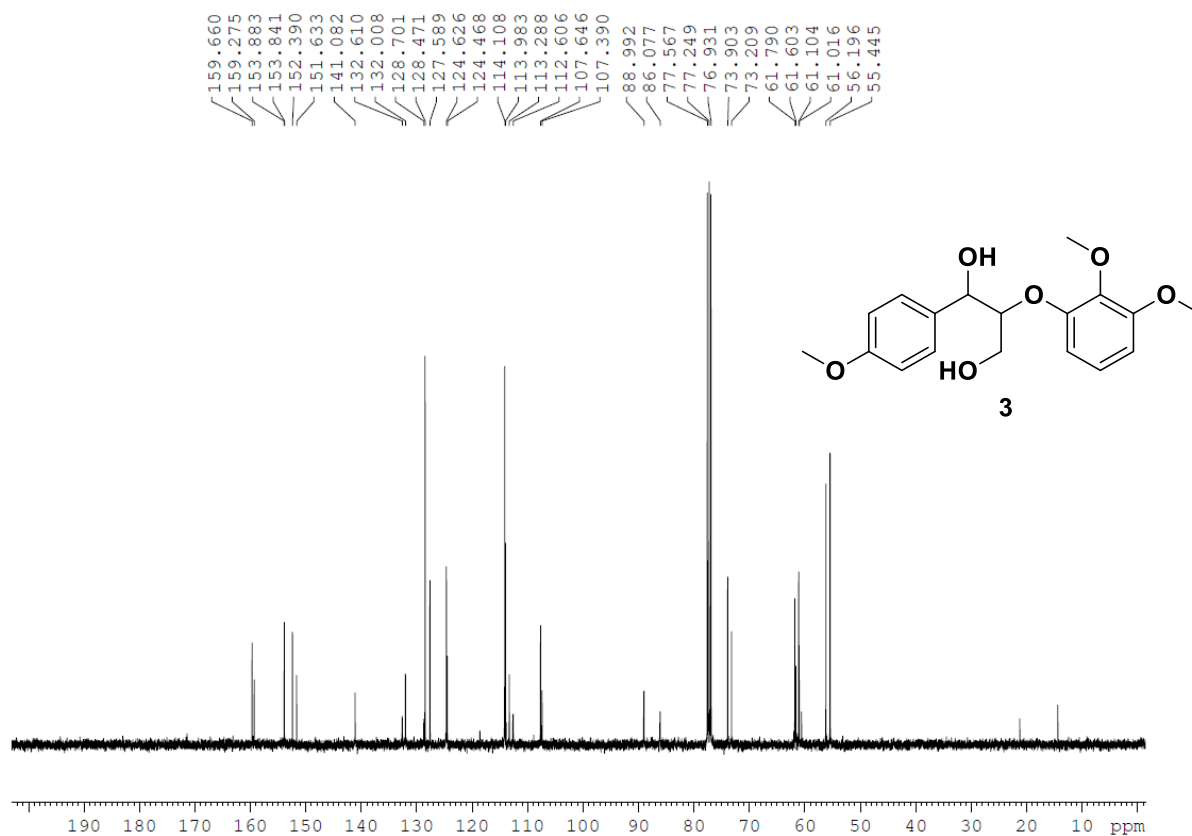


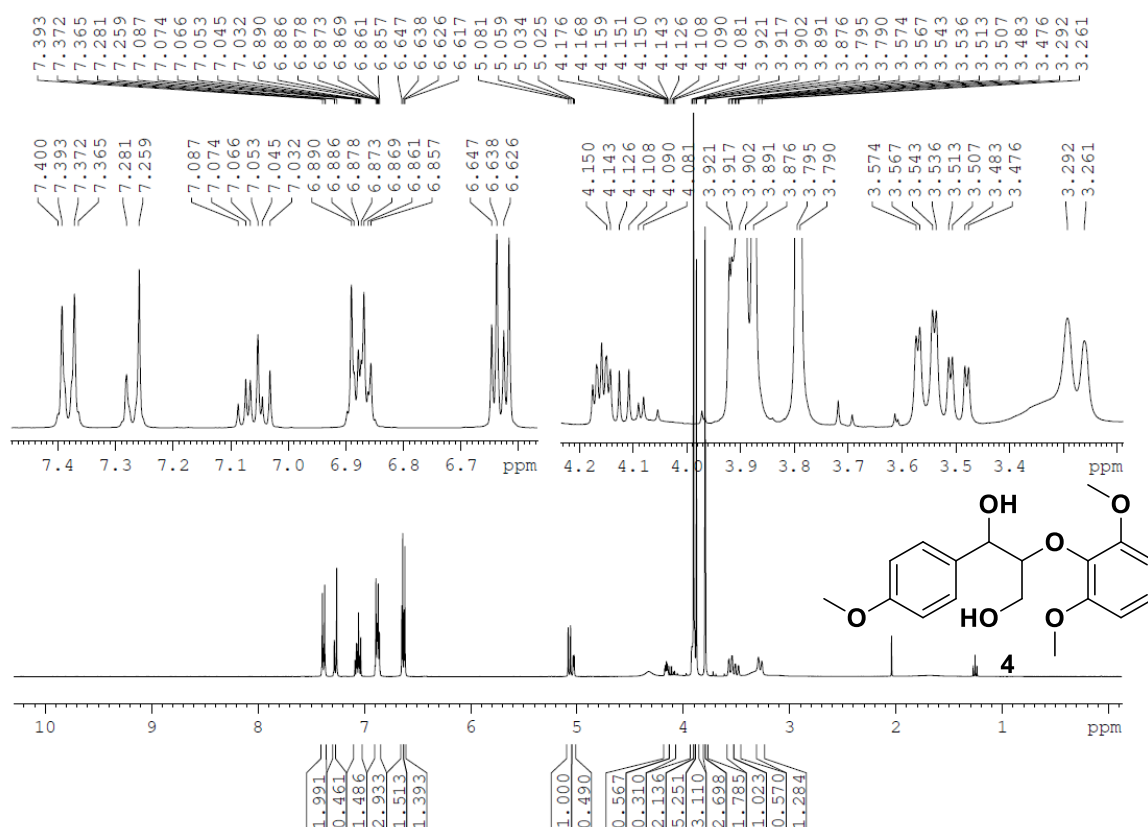
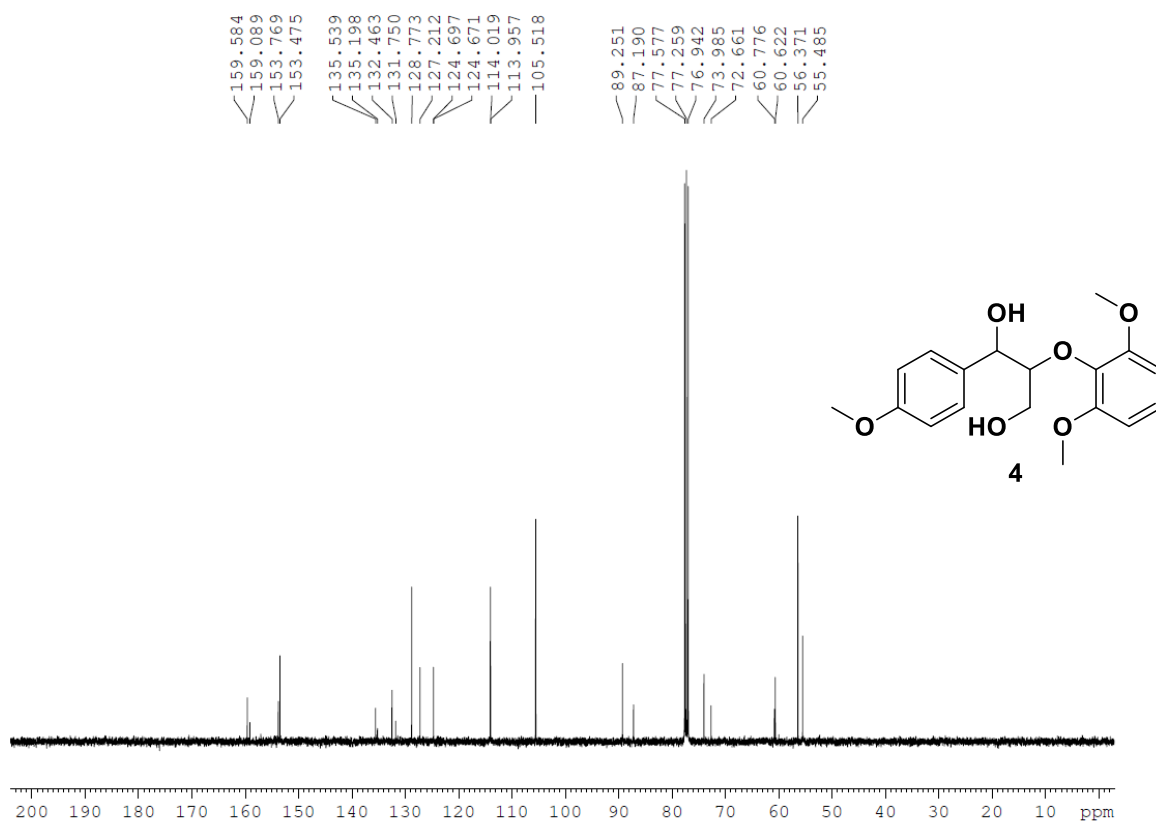
**$^1\text{H}$  spectra of compound 2 ( $\text{CDCl}_3$ , 400 MHz)** **$^{13}\text{C}$  spectra of compound 2 ( $\text{CDCl}_3$ , 101 MHz)**

**<sup>1</sup>H spectra of compound 3 (CDCl<sub>3</sub>, 400 MHz)**



**<sup>13</sup>C spectra of compound 3 (CDCl<sub>3</sub>, 101 MHz)**



**$^1\text{H}$  spectra of compound 4 ( $\text{CDCl}_3$ , 400 MHz)** **$^{13}\text{C}$  spectra of compound 4 ( $\text{CDCl}_3$ , 101 MHz)**

## 1.9 References

1. E. E. Harris, J. Dianni, H. Adkins, *J. Am. Chem. Soc.* **1938**, *60*, 1467–1470.
2. C. P. Brewer, L. M. Cooke, H. Hibbert, *J. Am. Chem. Soc.* **1948**, *70*, 57–59.
3. J. Cornella, C. Zarate, R. Martin, *Chem. Soc. Rev.* **2014**, *43*, 8081–8097.
4. M. Tobisu, N. Chatani, *Acc. Chem. Res.* **2015**, *48*, 1717–1726.
5. E. Geist, A. Kirschning, T. Schmidt, *Nat. Prod. Rep.* **2014**, *31*, 441–448.
6. E. Wenkert, E. L. Michelotti, C. S. Swindell, *J. Am. Chem. Soc.* **1979**, *101*, 2246–2247.
7. P. Álvarez-Bercedo, R. Martin, *J. Am. Chem. Soc.* **2010**, *132*, 17352–17353.
8. A. G. Sergeev, J. F. Hartwig, *Science*. **2011**, *332*, 439–443.
9. A. G. Sergeev, J. D. Webb, J. F. Hartwig, *J. Am. Chem. Soc.* **2012**, *134*, 20226–20229.
10. S. Sawadjoon, A. Lundstedt, J. S. M. Samec, *ACS Catal.* **2013**, *3*, 635–642.
11. M. V. Galkin, S. Sawadjoon, V. Rohde, M. Dawange, J. S. M. Samec, *ChemCatChem*. **2014**, *6*, 179–184.
12. M. V. Galkin, J. S. M. Samec, *ChemSusChem*. **2014**, *7*, 2154–2158.
13. A. N. Desnoyer, B. Fartel, K. C. MacLeod, B. O. Patrick, K. M. Smith, *Organometallics*. **2012**, *31*, 7625–7628.
14. Y. Ren, M. Yan, J. Wang, Z. C. Zhang, K. Yao, *Angew. Chem. Int. Ed.* **2013**, *52*, 12674–12678.
15. S. Kusumoto, K. Nozaki, *Nat. Commun.* **2015**, *6*, 6296–6302.
16. C. K. Prier, D. A. Rankic, D. W. C. MacMillan, *Chem. Rev.* **2013**, *113*, 5322–5363.
17. J. M. R. Narayanam, C. R. J. Stephenson, *Chem. Soc. Rev.* **2011**, *40*, 102–113.
18. K. Kalyanasundaram, *Coord. Chem. Rev.* **1982**, *46*, 159–244.
19. E. Hasegawa, S. Takizawa, T. Seida, A. Yamaguchi, N. Yamaguchi, N. Chiba, T. Takahashi, H. Ikeda, K. Akiyama, *Tetrahedron*. **2006**, *62*, 6581–6588.
20. M. –L. Larraufie, R. Pellet, L. Fensterbank, J. –P. Goddard, E. Lacote, M. Malacria, C. Ollivier, *Angew. Chem. Int. Ed.* **2011**, *50*, 4463–4466.
21. J. W. Tucker, J. M. R. Narayanam, P. S. Shah, C. R. J. Stephenson, *Chem. Commun.* **2011**, *47*, 5040–5042.
22. S. Kim, S. C. Chmely, M. R. Nimlos, Y. J. Bomble, T. D. Foust, R. S. Paton, G. T. Beckham, *J. Phys. Chem. Lett.* **2011**, *2*, 2846–2852.

23. J. D. Nguyen, B. S. Matsuura, C. R. J. Stephenson, *J. Am. Chem. Soc.* **2014**, *136*, 1281-1221
24. M. Tien, T. K. Kirk, *Proc. Natl. Acad. Sci. U. S. A.*, **1984**, *81*, 2280–2284.
25. 113 M. Kuwahara, J. K. Glenn, M. A. Morgan, M. H. Gold, *FEBS Lett.* **1984**, *169*, 247–250.
26. R. Have, P. J. M. Teunissen, *Chem. Rev.* **2001**, *101*, 3297-3413.
27. T. Habe, M. Shimada, T. Okamoto, B. Panijpan, T. Higuchi, *J. Chem. Soc. Chem. Commun.* **1985**, 1323–1324.
28. C. Zhu, W. Ding, T. Shen, C. Tang, C. Sun, S. Xu, Y. Chen, J. Wu, H. Ying, *ChemSusChem*. **2015**, *8*, 1768–1778
29. G. Labat, B. Meunier, *J. Org. Chem.* **1989**, *54*, 5008–5011.
30. S. K. Hanson, R. T. Baker, J. C. Gordon, B. L. Scott, D. L. Thorn, *Inorg. Chem.* **2010**, *49*, 5611–5618.
31. B. Sedai, C. Díaz-Urrutia, R. T. Baker, R. Wu, L. A. Silks, S. K. Hanson, *ACS Catal.* **2011**, *1*, 794–804.
32. M. D. Kärkäs, I. Bosque, B. S. Matsuura, C. R. J. Stephenson, *Org. Lett.* **2016**, *18*, 5166-5169.
33. I. Bosque, G. Magallanes, M. Rigoulet, M. D. Kärkäs, C. R. J. Stephenson, *ACS Cent. Sci.* **2017**, *3*, 621-628.
34. N. Luo, M. Wang, H. Li, J. Zhang, H. Liu, F. Wang, *ACS Catal.* **2016**, *6*, 7716-7721.
35. J. Luo, J. Zhang, *J. Org. Chem.* **2016**, *81*, 9131-9137.
36. J. Luo, X. Zhang, J. Lu, J. Zhang, *ACS Catal.* **2017**, *7*, 5062-5070.
37. S. H. Lim, K. Nahm, C. S. Ra, D. W. Cho, U. C. Yoon, J. A. Latham, D. D.-Mario, P. S. Mariano, *J. Org. Chem.* **2013**, *78*, 9431-9443.
38. R. T. Have, P. J. M. Teunissen, *Chem. Rev.* **2001**, *101*, 3397-3413.
39. N. L. Bauld, *Radicals, ion radicals, and triplets: the spin-bearing intermediates of organic chemistry*, Wiley-VCH: New York, **1997**.
40. M. D. Kärkäs, B. S. Matsuura, T. M. Monos, G. Magallanes, C. R. J. Stephenson, *Org. Biomol. Chem.* **2016**, *14*, 1853.
41. J. M. Nichols, L. M. Bishop, R. G. Bergman, J. A. Ellman, *J. Am. Chem. Soc.* **2010**, *132*, 12554–12555.
42. T. vom Stein, T. Weigand, C. Merkens, J. Klankermayer, W. Leitner, *ChemCatChem*. **2013**, *5*, 439–441.

43. T. vom Stein, T. den Hartog, J. Buendia, S. Stoychev, J. Mottweiler, C. Bolm, J. Klankermayer, W. Leitner, *Angew. Chem. Int. Ed.* **2015**, *54*, 5859–5863.
44. N. D. Patil, N. Yan, *Tetrahedron Lett.* **2016**, *57*, 3024-3028.
45. J. Luo, X. Zhang, J. Lu, J. Zhang, *ACS Catal.* **2017**, *7*, 5062-5070.
46. M. J. Kurth, L. A. A. Randall, C. Chen, C. Melander, R. B. Miller, K. McAlister, G. Reitz, R. Kang, T. Nakatsu, C. Green, *J. Org. Chem.* **1994**, *59*, 5862-5864.
47. A. Barthel, L. Trieschmann, D. Ströhl, R. Kluge, G. Böhm, R. Csuk, *Arch. Pharm.* **2009**, *342*, 445-452.





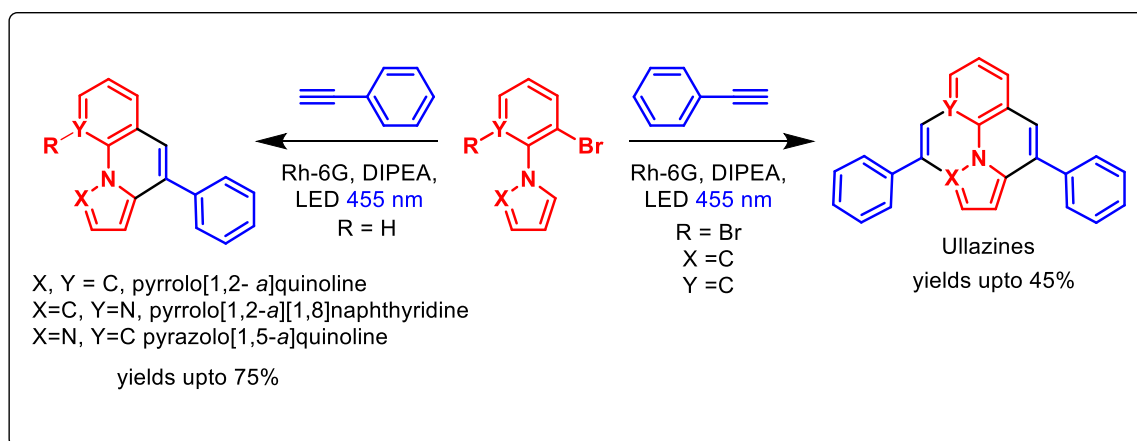
# *Chapter 2*

## *2. Synthesis of Pyrrolo[1,2-a]quinolines and Ullazines by Visible Light Mediated One- and Two Fold Annulation of N-Arylpyrroles with Arylalkynes*



## Abstract

1-(2-Bromophenyl)-1*H*-pyrrole and 1-(2,6-dibromophenyl)-1*H*-pyrrole react in the presence of catalytic amounts of rhodamine 6G (Rh-6G) and *N,N*-diisopropylethylamine (DIPEA) under blue light irradiation with aromatic alkynes and subsequently cyclize intramolecularly to form pyrrolo[1,2-*a*]quinoline and ullazines. The reactions proceed at room temperature, avoid transition metal catalysts, and provide the target compounds in one pot in moderate to good yields. Mechanistic investigations suggest that the photo excited Rh-6G is reduced by DIPEA to form the corresponding radical anion Rh-6G<sup>•-</sup>, which is again excited by 455 nm light. The excited radical anion of Rh-6G donates an electron to the aryl bromide giving an aryl radical that is trapped by aromatic alkynes. The intermediate vinyl radical cyclizes intramolecularly and yields the product after rearomatization.



### This chapter has been published:

A. Das, I. Ghosh, B. König, *Chem. Commun.* **2016**, 52, 8695-8698.

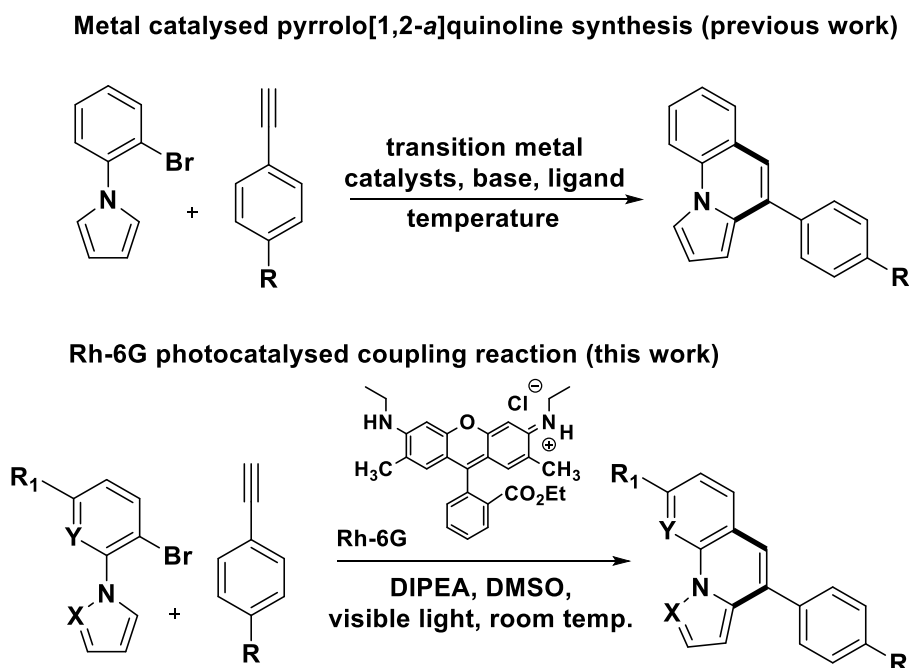
Author contribution: A.D. performed the experiments and wrote the manuscript. I.G. performed the spectroscopic measurements. B.K. supervised the project and is the corresponding author.

## 2.1 Introduction

Fused nitrogen containing heterocycles are structural elements of biologically active natural products<sup>[1]</sup> or active pharmaceutical ingredients (APIs) and find applications in organic materials.<sup>[2]</sup> Among them, pyrrolo[1,2-*a*]quinolines, pyrazolo[1,5-*a*]quinolines, and ullazines are of particular importance. Some of their derivatives show antitumor,<sup>[3]</sup> antibacterial<sup>[4]</sup> or antimicrobial<sup>[5]</sup> activities; they activate caspases or induce apoptosis<sup>[6]</sup> and are used as organic semiconductors,<sup>[7]</sup> in host-guest chemistry<sup>[8,9]</sup> or as liquid crystals.<sup>[10,11]</sup> Also, the pyrazolo derivatives, *e.g.*; 4-phenylpyrazolo[1,5-*a*]quinoline show anti reproductive utility.<sup>[12]</sup> Ullazines have found applications in optoelectronics, as organic sensitizer for solar-cell and show very good electron transport properties.<sup>[13]</sup> Several methods for the synthesis of fused nitrogen-containing heterocycles have been reported; many apply direct arylation reactions. These include palladium-catalyzed reactions,<sup>[14–17]</sup> 1,2-alkyl migration,<sup>[18]</sup> DDQ-mediated intramolecular cyclizations,<sup>[19]</sup> flash vacuum pyrolysis,<sup>[20]</sup> photosubstitution reactions,<sup>[21]</sup> and alkyne-carbonyl metathesis.<sup>[22]</sup> Lautens *et al.* reported a palladium catalyzed direct arylation of geminal dibromo-olefins with a boronic acid *via* tandem Suzuki–Miyura coupling reaction.<sup>[23]</sup> Larock *et al.* reported a copper catalyzed tandem synthetic methodology for the synthesis of pyrrolo- and indolo[2,1-*a*]isoquinolines.<sup>[24]</sup> Recently, Baxendale *et al.* developed a method for the synthesis of pyrrolo[1,2-*a*]quinolines based on an allene cascade reaction in batch and flow mode.<sup>[25]</sup> Miura *et al.* described the coupling of phenylazoles with internal alkynes in the presence of a rhodium catalyst and a copper oxidant.<sup>[26]</sup> Also, the same group reported the formation of indolo[1,2-*a*][1,8]naphthyridines by rhodium catalyzed dehydrogenative coupling *via* rollover cyclometallation.<sup>[27]</sup> Dumitrescu *et al.* developed the synthesis of pyrrolo[2,1-*a*]isoquinolines by multicomponent 1,3-dipolar cycloaddition.<sup>[28]</sup> However, all the current synthetic methods require base, specific ligands, high temperature and transition metal catalysts, multi-step processes, and in some cases both cyclized and non-cyclized products are formed, which are difficult to separate. Transition metal free visible light photoredox catalysis is an attractive mild, selective and efficient alternative for the synthesis of pyrrolo[1,2-*a*]quinolines, pyrazolo[1,5-*a*]quinolines, and ullazines by one and two fold annulation of *N*-aryl pyrroles/pyrazoles with aryl alkynes. We report here a one-step visible light mediated metal free direct arylation of 1-(2-bromophenyl)-1*H*-pyrrole, 1-(2-bromophenyl)-1*H*-pyrazole, 3-bromo-2-(1*H*-pyrrol-1-yl)pyridine and 1-(2,6-

***Synthesis of Pyrrolo[1,2-*a*]quinolines and Ullazines by Visible Light Mediated One- and Two Fold Annulation of *N*-arylpyrroles with Arylalkynes***

dibromophenyl)-1*H*-pyrrole with simple aromatic alkynes providing pyrrolo[1,2-*a*]quinolines, pyrazolo[1,5-*a*]quinolines, pyrrolo[1,2-*a*][1,8]naphthyridine and ullazine compounds, respectively. This method utilizes blue light, the organic dye rhodamine 6G (Rh-6G) as photocatalyst and *N,N*-diisopropylethylamine (DIPEA) as electron donor (Scheme 1).



**Scheme 1:** Pyrrolo[1,2-*a*]quinoline syntheses.

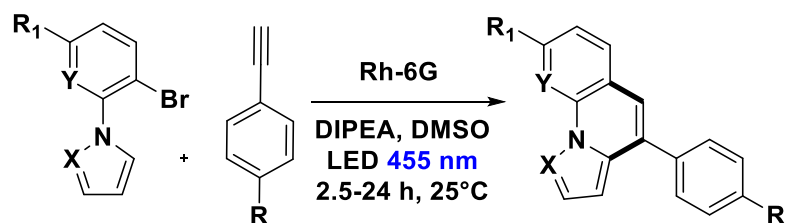
## 2.2 Results and discussions

First, the annulation reaction of aryl halide (**1a**) with aryl alkyne (**2a**) (Entry 1) in the presence of Rh-6G (10 mol%) as the photocatalyst in DMSO at 25 °C under visible light irradiation (blue LEDs:  $\lambda_{\text{max}} = 455 \pm 15$  nm) was investigated. Under the reaction conditions Rh-6G photo-bleaches and 20 mol% catalyst loading was required. The annulated pyrrolo[1,2-*a*]quinoline (**3a**) was obtained in 60% yield in 24 hours. This synthetic approach uses the high reduction power of the excited stable radical anion Rh-6G<sup>•-</sup> [29,30] obtained upon photoirradiation of the xanthene dye under nitrogen with visible light in the presence of *N,N*-diisopropylethylamine (DIPEA). Our photocatalytic method allows the activation of electron rich heteroarenes with a redox potential up to *ca.* -2.4 V *vs.* SCE,

which is not accessible using common photocatalysts,<sup>[31,32]</sup> for C–C bond formation. The synthesis of fused heterocycles combines an intermolecular radical addition to alkynes with an intramolecular cyclization reaction. To improve the efficiency of this method, the reaction conditions were optimized trying various solvents, electron donors, varying the amount of catalyst and of the starting materials. DMSO was found to be the best solvent for the photoreaction using 0.07 mol L<sup>-1</sup> substrate concentrations, 20 equiv. of the alkyne and 2.2 equiv. of DIPEA. Notably, excess amount of alkynes (unreacted alkynes were recovered during isolation) were used to avoid the dehalogenated by-product<sup>[30,33]</sup> formed upon hydrogen atom abstraction of the generated aryl radical from the radical cation of DIPEA or from the solvent.<sup>[34,35]</sup> The cyclized product was obtained in good yield with 20 mol% of the photocatalyst. We used a thin layer (1.0 mm) glass reactor with 1.5 mL volume to have an optimal exposure of the reaction mixture for irradiation (for details see experimental section). Control reactions confirmed that light, the photocatalyst, and an electron donor are needed for the reaction to occur. Having identified the optimized reaction conditions, we examined the scope of the reaction with substituted aryl halides and alkynes. The products were obtained in moderate to good yields (**Table 1**). It is observed that the reaction is much faster with neutral and electron rich alkynes, and comparatively slower in the presence of electron withdrawing alkynes. The products (Entries 5–13) in **Table 1** were obtained in shorter time, but the reaction stops before full conversion. Adding one extra nitrogen to the system increases the redox potential of the aryl halide, hence, slows down the reaction. 1-(2-Bromophenyl)-1*H*-pyrazole (**1d**) has a redox potential of ~ -2.4 V vs. SCE (**Table 1**, entries 14 and 15) and 3-bromo-2-(1*H*-pyrrol-1-yl)pyridine (**1e**) has a redox potential of ~ -2.1 V vs. SCE (**Table 1**, entries 16 and 17). The observed low yields may be attributed to the slow reaction rates owing to the high reduction potentials of the substrates<sup>[36]</sup> representing the limit of the photocatalyst scope, or due to the competing light absorption (i.e., the inner filter effect) of the colored products with the catalyst and/or its radical anion (**Figure 2**). In addition, trace amount of dehalogenated starting material was isolated as by-product.<sup>[34,35]</sup>

*Synthesis of Pyrrolo[1,2-a]quinolines and Ullazines by Visible Light Mediated One- and Two Fold Annulation of N-arylpyrroles with Arylalkynes*

**Table 1.** Synthesis of Pyrrolo[1,2-a]quinoline



| Entry | Aryl Bromide <sup>a</sup> | R <sub>1</sub>    | Alkyne <sup>a</sup> | R                | Product   | Yield <sup>b,c</sup> |
|-------|---------------------------|-------------------|---------------------|------------------|-----------|----------------------|
| 1     | <b>1a<sup>d</sup></b>     | H                 | <b>2a</b>           | H                | <b>3a</b> | 60                   |
| 2     | <b>1a<sup>d</sup></b>     | H                 | <b>2b</b>           | CH <sub>3</sub>  | <b>3b</b> | 51                   |
| 3     | <b>1a<sup>d</sup></b>     | H                 | <b>2c</b>           | OCH <sub>3</sub> | <b>3c</b> | 50                   |
| 4     | <b>1a<sup>d</sup></b>     | H                 | <b>2d</b>           | F                | <b>3d</b> | 48                   |
| 5     | <b>1b<sup>d</sup></b>     | COCH <sub>3</sub> | <b>2a</b>           | H                | <b>3e</b> | 56                   |
| 6     | <b>1b<sup>d</sup></b>     | COCH <sub>3</sub> | <b>2b</b>           | CH <sub>3</sub>  | <b>3f</b> | 54                   |
| 7     | <b>1b<sup>d</sup></b>     | COCH <sub>3</sub> | <b>2c</b>           | OCH <sub>3</sub> | <b>3g</b> | 75                   |
| 8     | <b>1b<sup>d</sup></b>     | COCH <sub>3</sub> | <b>2d</b>           | F                | <b>3h</b> | 50                   |
| 9     | <b>1b<sup>d</sup></b>     | COCH <sub>3</sub> | <b>2e</b>           | Cl               | <b>3i</b> | 50                   |
| 10    | <b>1c<sup>d</sup></b>     | CF <sub>3</sub>   | <b>2a</b>           | H                | <b>3j</b> | 52                   |
| 11    | <b>1c<sup>d</sup></b>     | CF <sub>3</sub>   | <b>2b</b>           | CH <sub>3</sub>  | <b>3k</b> | 56                   |
| 12    | <b>1c<sup>d</sup></b>     | CF <sub>3</sub>   | <b>2c</b>           | OCH <sub>3</sub> | <b>3l</b> | 41                   |
| 13    | <b>1c<sup>d</sup></b>     | CF <sub>3</sub>   | <b>2d</b>           | F                | <b>3m</b> | 41                   |
| 14    | <b>1d<sup>e</sup></b>     | H                 | <b>2a</b>           | H                | <b>3n</b> | 39                   |
| 15    | <b>1d<sup>e</sup></b>     | H                 | <b>2c</b>           | OCH <sub>3</sub> | <b>3o</b> | 35                   |
| 16    | <b>1e<sup>f</sup></b>     | H                 | <b>2a</b>           | H                | <b>3p</b> | 49                   |
| 17    | <b>1e<sup>f</sup></b>     | H                 | <b>2b</b>           | CH <sub>3</sub>  | <b>3q</b> | 50                   |

<sup>a</sup> The reaction was performed with **1(a-e)** (0.1 mmol), **2(a-d)** (20 equiv.), DIPEA (2.2 equiv.), and Rh-6G (20 mol%) in 1.5 mL of DMSO. <sup>b</sup> Isolated yields after purification by flash column chromatography using silica gel. <sup>c</sup> for the reaction times see experimental section. <sup>e</sup> X = N, Y = C (Entries 14 and 15) and <sup>f</sup> X = C, Y = N (Entries 16 and 17).

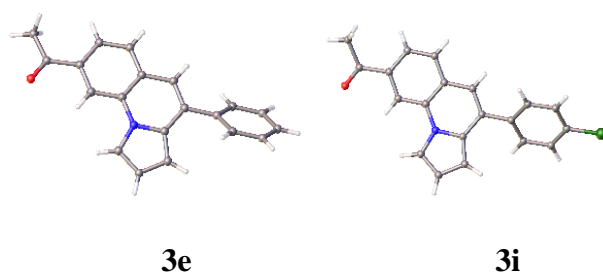
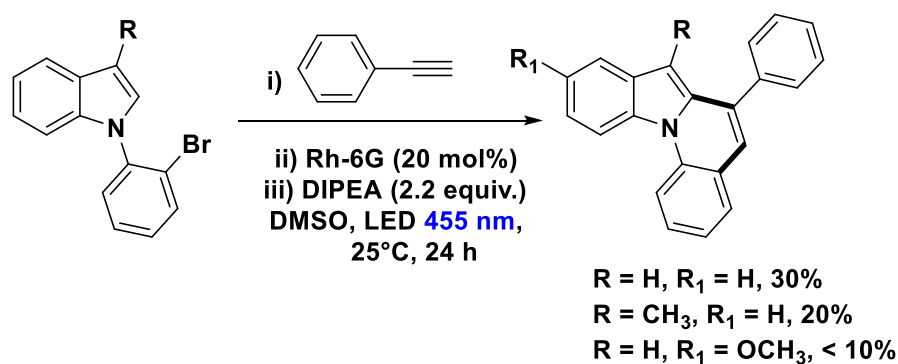


**Figure 1:** Crystal structures of compounds **3e** and **3i**.

Extending the scope of the reaction by replacing the pyrrole moiety by indole resulted in low yields for the transformation. A likely rational for the lower reactivity and yields of indoles in the cyclization reaction is the enforced unfavorable substitution at the 2-position (**Scheme 2**).<sup>[37]</sup>



**Scheme 2:** Indolo[1,2-*a*]quinoline syntheses.

Next, we explored the photocatalytic synthesis of ullazines. First derivatives of these class of compounds were prepared in 1983 by Balli *et. al.*<sup>[38]</sup> in 9 steps with very poor yields.

Takahasi's route<sup>[39]</sup> showed no regioselectivity and required harsh conditions. Grätzel's synthesis<sup>[40]</sup> uses InCl<sub>3</sub> and requires four steps. The photoredox reaction yields ullazines in



one pot. Using the optimized reaction condition, the annulation reaction was carried out between the dibromo compound **1f** and aryl alkynes. The results are summarized in **Table 2**. The observed low yields are due to the extremely high reduction potentials of quinoline intermediates and intensively colored products that inhibit the reaction by competing in absorption with the catalyst and/or its radical anion (see **Fig. 2**). Although not quantified, most of the unreacted starting materials could be recovered during the purification process.

**Table 2.** Synthesis of ullazines

| Entry | Substrate | Alkyne           | R  | Product | Yield <sup>a</sup> |
|-------|-----------|------------------|----|---------|--------------------|
| 1     | 1f        | H                | 2a | 3r      | 45                 |
| 2     | 1f        | CH <sub>3</sub>  | 2b | 3s      | 30                 |
| 3     | 1f        | OCH <sub>3</sub> | 2c | 3t      | 30                 |

The reaction was performed with **1f** (0.1 mmol), **2(a-c)** (20 equiv.), DIPEA (2.2 equiv.), and Rh-6G (20 equiv.) in 1.5 mL of DMSO. <sup>a</sup> Isolated yields after purification by flash column chromatography using silica gel.

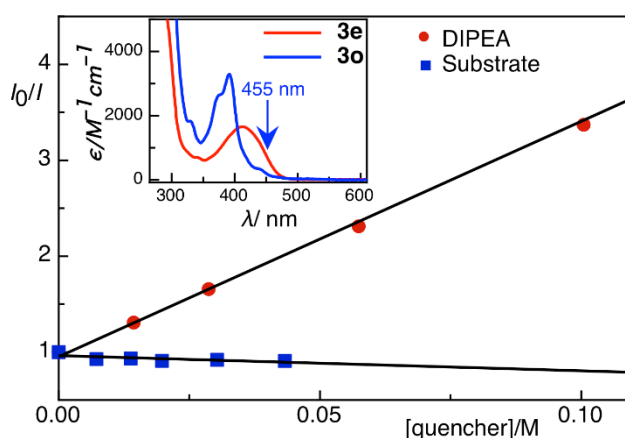
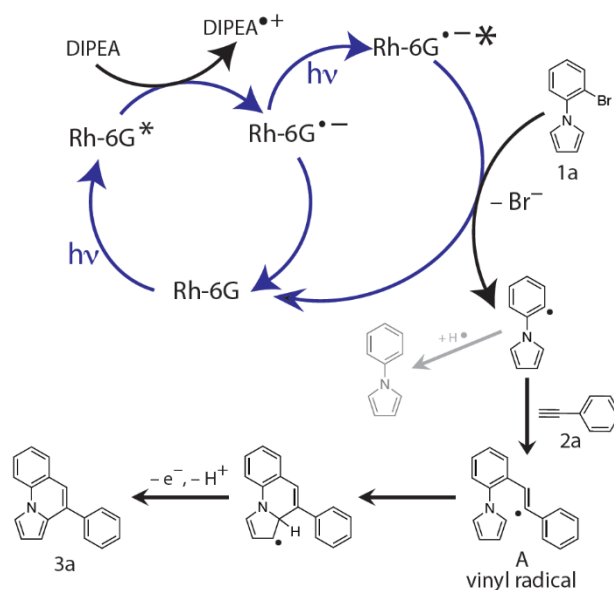


**Figure 2:** Stern-Volmer quenching plot of Rh-6G in the presence of DIPEA and **1b** (test substrate). In the inset, absorption spectra of compounds **3e**, and **3o** are shown.

Based on previous results,<sup>[30]</sup> spectroscopic investigations, and our experimental observations we propose the following mechanism (**Scheme 3**) for the cyclization reaction. Upon photoexcitation with blue light ( $\lambda_{\text{max}} = 455 \text{ nm}$ ),<sup>[41]</sup> Rh-6G is photoreduced in the presence of DIPEA to the stable radical anion Rh-6G $^{\bullet-}$ , which is again excited by blue light and transfers an electron to the *N*-aryl bromide **1a** forming Ar-Br $^{\bullet-}$  while regenerating the neutral Rh-6G. While the radical anion of rhodamine 6G (Rh-6G $^{\bullet-}$ ) can also be generated with green light, the blue light excitation is required to photoexcite it again. Using blue light for both steps simplifies the experimental set up. The reduction potential of Rh-6G $^{\bullet-}$  (*ca.* -1.0 V) is not sufficient to reduce the *N*-aryl bromide substrates investigated here. Fragmentation of the radical anion Ar-Br $^{\bullet-}$  generates the aryl radical, which reacts intermolecularly with the alkyne **2a** to form the vinyl radical **A**. This vinyl radical cyclizes intramolecularly giving the annulated product **3a** after oxidation and rearomatization. The formation of the dehalogenated product is due to hydrogen atom abstraction by the intermediate aryl radical either from the radical cation of DIPEA or from the solvent



**Scheme 3:** Proposed reaction mechanism.

## **2.3 Conclusion**

In conclusion, the first photocatalytic synthesis of pyrrolo[1,2-*a*]quinolines and ullazines was accomplished starting from *N*-aryl halides and aryl alkynes. This method provides in a single step mild and efficient access to different types of substituted pyrrolo[1,2-*a*]quinolines, pyrazolo[1,5-*a*]quinolines, pyrrolo[1,2-*a*][1,8]naphthyridine and ullazines avoiding transition metal catalysts, bases, ligands, and high temperature.

## 2.4 Experimental section

### 2.4.1 Materials and methods

Solvents and reagents were obtained from commercial sources and used without further purification. Spectroscopic grade DMF and DMSO were dried with 3 Å molecular sieves. Rhodamine 6G (**Rh-6G**) (dye content ~ 95%) was purchased from Sigma Aldrich. Proton NMR spectra were recorded on a Bruker Avance 300 MHz spectrometer and 600 MHz spectrometer in CDCl<sub>3</sub> solution with internal solvent signal peak at 7.26 ppm. Carbon NMR were recorded at 75 MHz spectrometer and 151 MHz spectrometer in CDCl<sub>3</sub> solution and referenced to the internal solvent signal at 77.26 ppm. Proton NMR data are reported as follows: chemical shift (ppm), multiplicity (s = singlet, d = doublet, t = triplet, q = quartet, quint = quintet, dd = doublet of doublets, ddd = doublet of doublet of doublets, td = triplet of doublets, qd = quartet of doublets, m = multiplet, br. s. = broad singlet), and coupling constants (Hz). High resolution mass spectra (HRMS) were obtained from the central analytic mass spectrometry facilities of the Faculty of Chemistry and Pharmacy, Regensburg University and are reported according to the IUPAC recommendations 2013. All reactions were monitored by thin-layer chromatography using Merck silica gel plates 60 F254; visualization was accomplished with short wave length UV light (254 nm). UV–Vis and fluorescence measurements were performed with Varian Cary 50 UV/Vis spectrophotometer and FluoroMax-4 spectrofluorometer, respectively. Electrochemical studies were carried out under argon atmosphere. The measurements were performed in acetonitrile (CH<sub>3</sub>CN) containing 0.1 M tetra-n-butylammonium tetrafluoroborate using ferrocene/ferrocenium (Fc/Fc<sup>+</sup>) as an internal reference. A glassy carbon electrode (working electrode), platinum wire (counter electrode), and silver wire (quasi-reference electrode) were employed. Spectroelectrochemical studies were carried out in an optically transparent thin layer electrochemical cell (OTTLE). Standard flash chromatography was performed using silica gel of particle size 40–63 µm. Photoreduction and annulation reactions were performed with 455 nm LEDs (OSRAM Oslon SSL 80 royal-blue LEDs ( $\lambda$  = 455 nm ( $\pm$  15 nm), 3.5 V, 700 mA).

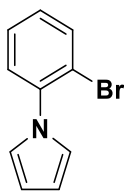
## 2.4.2 Synthesis of starting materials

### Procedure for the synthesis of N-Aryl Pyrroles

N-Aryl Pyrroles **1(a-c, e and f)** were prepared by Paal-Knorr synthesis from the respective aniline, according to the procedure reported by Lee *et. al.*<sup>[42]</sup>

**General Method:** A solution of aniline (1.0 equiv.) and acetic acid (0.07 mL/mmol aniline) in DCE (1.86 mL/mmol aniline) and water (1.12 mL/mmol aniline) was heated to 80° C. 2,5- Dimethoxytetrahydrofuran (1.05 equiv.) was then added in one portion and the heating continued at 80° C overnight. Once cooled, the layers were separated and the aqueous layer was extracted with DCM. The combined organic layers were then dried (MgSO<sub>4</sub>), filtered, and the solvent was removed in vacuo to yield the crude pyrrole.

### Synthesis of 1-(2-Bromo-phenyl)-1H-pyrrole (1a)



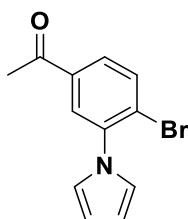
Synthesized according to the general procedure using 2-bromo-aniline (1.0 g, 4.5 mmol). Purified by flash column chromatography (hexane: ethyl acetate, 10:1) to yield the title compound as a colourless oil (0.64 g, 75%).

<sup>1</sup>H NMR (CDCl<sub>3</sub>, 300 MHz, ppm): δ 7.70 (dd, *J* = 8.1 Hz, *J* = 1.2 Hz, 1H), 7.4-7.31 (m, 2H), 7.25-7.20 (m, 1H), 6.88 (t, *J* = 2.1 Hz, 2H), 6.34 (t, *J* = 2.1 Hz, 2H).

<sup>13</sup>C NMR (CDCl<sub>3</sub>, 75 MHz, ppm): δ 140.4, 133.8, 128.8, 128.3, 128.1, 122.2, 119.9, 109.2.

HRMS [*M*+*H*]<sup>+</sup> C<sub>10</sub>H<sub>9</sub>BrN calculated 221.9913 was found 221.9919, spectral data are consistent with those reported in the literature.<sup>[43]</sup>

### Synthesis of 1-(4-bromo-3-(1H-pyrrol-1-yl)phenyl)ethan-1-one (1b)



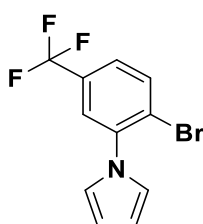
Synthesized according to the general procedure using 2-bromo-aniline (1.0 g, 4.6 mmol). Purified by flash column chromatography (hexane: ethyl acetate, 6:4) to yield the compound as a white solid (1.04 g, 85%).

**<sup>1</sup>H NMR** (CDCl<sub>3</sub>, 300 MHz, ppm): δ 7.89 (t, *J* = 1.2 Hz, 1H), 7.80 (m, 2H), 6.90 (t, *J* = 2.2 Hz, 2H), 6.37 (t, *J* = 2.1 Hz, 2H), 2.61 (s, 3H).

**<sup>13</sup>C NMR** (CDCl<sub>3</sub>, 75 MHz, ppm): δ 196.4, 140.9, 137.2, 134.4, 128.2, 128.0, 125.6, 122.3, 109.9, 26.8.

**HRMS** [*M*<sup>+</sup>] C<sub>12</sub>H<sub>10</sub>BrNO calculated 262.9940 found 262.9937.

### Synthesis of 1-(2-bromo-5-(trifluoromethyl)phenyl)-1*H*-pyrrole (1c)



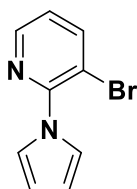
Synthesized according to the general procedure using 2-bromo-aniline (1.0 g, 4.1 mmol). Purified by flash column chromatography (hexane: ethyl acetate, 1:9) to yield the desired compound as a colourless oil (0.96 g, 80%).

**<sup>1</sup>H NMR** (CDCl<sub>3</sub>, 300 MHz, ppm): δ 7.84 (d, *J* = 8.3 Hz, 1H), 7.6 (s, 1H), 7.49 (s, 1H), 6.94 (t, *J* = 1.8 Hz, 2H), 6.41 (t, *J* = 1.8 Hz, 2H).

**<sup>13</sup>C NMR** (CDCl<sub>3</sub>, 75 MHz, ppm): δ 141.1, 134.8, 131.7, 131.3, 130.8, 130.4, 125.5, 125.4, 125.4, 125.3, 125.2, 123.9, 122.3, 110.2.

**HRMS** [*M*<sup>+</sup>] C<sub>11</sub>H<sub>7</sub>NF<sub>3</sub>Br calculated 288.9704 found 288.9703.

### Synthesis of 3-bromo-2-(1*H*-pyrrol-1-yl)pyridine (1e)



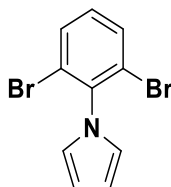
Synthesized according to the general procedure using 2-bromo-aminopyridine (1.0 g, 5.7 mmol). Purified by flash column chromatography (hexane: ethyl acetate, 1:9) to yield the desired compound as a colorless solid (0.65 g, 51%).

**<sup>1</sup>H NMR** (CDCl<sub>3</sub>, 300 MHz, ppm): δ 8.44 (dd, *J* = 4.6, 1.6 Hz, 1H), 8.0 (dd, *J* = 7.9, 1.6 Hz, 1H), 7.29 (t, *J* = 2.2 Hz, 2H), 7.1 (dd, *J* = 7.9, 4.6 Hz, 1H), 6.36 (t, *J* = 2.2 Hz, 2H).

**<sup>13</sup>C NMR** (CDCl<sub>3</sub>, 75 MHz, ppm): δ 150.1, 147.6, 143.7, 122.7, 121.5, 112.5, 110.2.

**HRMS** [*M*<sup>+</sup>] C<sub>9</sub>H<sub>7</sub>N<sub>2</sub>Br calculated 221.97871 found 221.97878.

**Synthesis of 1-(2,6-dibromophenyl)-1*H*-pyrrole (1f)**

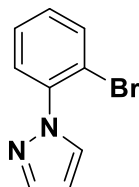


Synthesized according to the general procedure using 2,6-dibromo-aniline (1.0 g, 3.3 mmol). Purified by flash column chromatography (hexane: ethyl acetate, 8:2) to yield the desired compound as white solid (1.01 g, 84%).

**<sup>1</sup>H NMR** (CDCl<sub>3</sub>, 300 MHz, ppm): δ 7.67 (s, 1H), 7.64 (s, 1H), 7.20 – 7.11 (m, 1H), 7.84 – 6.25 (m, 8H), 6.69 (t, *J* = 2.1 Hz, 2H), 6.40 (t, *J* = 2.1 Hz, 2H).

**<sup>13</sup>C NMR** (CDCl<sub>3</sub>, 75 MHz, ppm): δ 139.8, 132.4, 130.6, 124.31, 121.5, 109.3. data identical to those reported.<sup>[44]</sup>

**Synthesis of 1-(2-bromophenyl)-1*H*-pyrazole (1d)**



A round bottomed flask was charged with pyrazole (14.6 mmol), 2-bromo-fluorobenzene (5.1 g, 29.3 mmol, 2.0 equiv.) and K<sub>3</sub>PO<sub>4</sub> (15.5 g, 73.4 mmol, 5.0 equiv.) in DMF (140 mL) and refluxed under nitrogen for 24hrs. After the reaction, the mixture was cooled to room temperature. It was mixed with H<sub>2</sub>O and the organic layer was extracted with ethyl acetate. The solvent was removed and the crude product was purified by flash column chromatography on silica gel using (hexane: ethyl acetate, 1:9) to yield the desired compound as colorless liquid in 83% yield.

**<sup>1</sup>H NMR** (CDCl<sub>3</sub>, 300 MHz, ppm): δ 7.81 (d, *J* = 2.3 Hz, 1H), 7.75 (d, *J* = 1.6 Hz, 1H), 7.70 (dd, *J* = 7.9, 1.4 Hz, 1H), 7.52 (dd, *J* = 7.9, 1.7 Hz, 1H), 7.42 (ddd, *J* = 7.9, 7.4, 1.4 Hz, 1H), 7.28 (ddd, *J* = 8.0, 7.4, 1.7 Hz, 1H), 6.47 (t, *J* = 2.1 Hz, 1H).

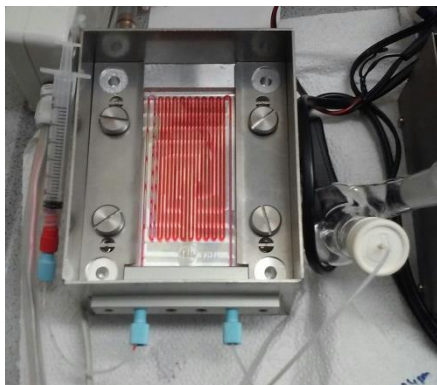
**<sup>13</sup>C NMR** (CDCl<sub>3</sub>, 75 MHz, ppm): δ 140.8, 139.9, 133.8, 131.3, 129.6, 128.3, 128.2, 118.6, 106.5, data are identical to those reported in literature.<sup>[45]</sup>

### 2.4.3 General procedure for C–H arylation followed by intramolecular cyclization reactions

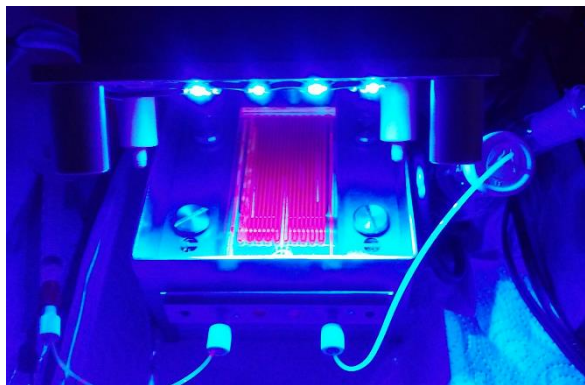
In a 5 mL snap vial with magnetic stirring bar the aryl halide (0.1 mmol, 1.0 equiv.), the corresponding alkyne (20.0 equiv.) and Rh-6G (0.01 mmol, 0.2 equiv.) were added and the mixture was degassed by “pump-freeze-thaw” cycles ( $\times 3$ ) via a syringe needle. DIPEA (2.2 equiv.) and dry DMSO (total volume of the solution 1.5 mL), were added under  $N_2$  and the resulting mixture was again degassed twice by syringe needle. This reaction mixture was transferred into a microreactor (capacity 1.7 mL) and irradiated with blue light (455 nm) under nitrogen at 25°C. The reaction progress was monitored by GC analysis. After 2.5 h to 24 hours of irradiation, the reaction mixture was transferred to separating funnel, diluted with ethyl acetate and washed with 15 mL of water. The aqueous layer was washed three times ( $3 \times 15$  mL) with ethyl acetate. The combined organic phases were dried over  $MgSO_4$ , filtered and concentrated in vacuum. Purification of the crude product was achieved by flash column chromatography using petrol ether/ethyl acetate as eluent.

### 2.4.4 Glass microreactors and irradiation setup used for photocatalysis

The reaction mixture (1.5 mL) was injected by syringe into the glass microreactor (LTF,  $11 \times 5.7$  cm  $\times$  1.7 mL internal volume, 0.3 mL volume of the reactor tubing) previously flushed with nitrogen. The flow reactor was cooled down to 20°C with a custom-made aluminum cooling block placed opposite to LEDs with a mirror to minimize loss of the light.



(a)



(b)



**Figure 3:** (a) Glass microreactor with suspension of reaction mixture (no flow method). (b) irradiation setup for the reaction in microreactor with 455 nm blue LED.

#### 2.4.5 Absorption spectra of Rh-6G and Rh-6G<sup>•−</sup>

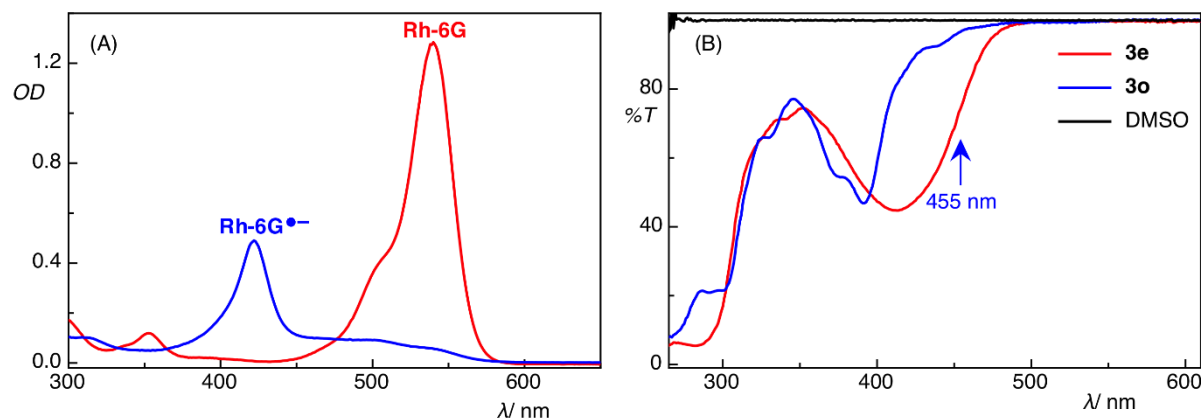
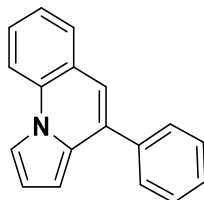


**Figure 4:** (A) Absorption spectra of Rh-6G and Rh-6G<sup>•−</sup>, (generated electrochemically). (B) Transmittance spectra of compound **3e** and **3o** in DMSO.

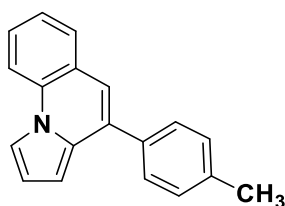
#### 4-Phenylpyrrolo[1,2-a]quinoline (**3a**)<sup>[46]</sup>



The compound was prepared according to the general procedure using 22.2 mg of 1-(2-bromophenyl)-1*H*-pyrrole, 9.5 mg of Rh-6G, 219.6  $\mu$ L of phenylacetylene, 38.3  $\mu$ L of DIPEA and 1.5 mL dry DMSO. The reaction mixture was irradiated for 24 hours under N<sub>2</sub>. Purification of the crude product was achieved by flash column chromatography using petrol ether as eluent to yield the desired compound as greenish solid (13.8 mg, 60%).

**<sup>1</sup>H NMR** (CDCl<sub>3</sub>, 300 MHz, ppm):  $\delta$  7.92 (m, 1H), 7.89 (d,  $J$  = 8.4 Hz, 1H), 7.71 (d,  $J$  = 8.4 Hz, 2H), 7.67 (d,  $J$  = 8.0 Hz, 1H), 7.51-7.4 (m, 4H), 7.32 (t,  $J$  = 7.6 Hz, 1H), 6.99 (s, 1H), 6.80 (t,  $J$  = 3.2 Hz, 1H), 6.61 (d,  $J$  = 4 Hz, 1H).

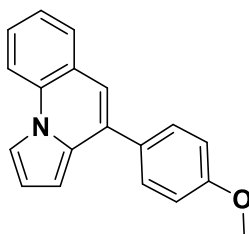
**<sup>13</sup>C NMR** (CDCl<sub>3</sub>, 75 MHz, ppm):  $\delta$  139.3, 133.0, 132.9, 131.1, 129.0, 128.7, 128.6, 128.3, 127.8, 124.5, 123.9, 118.3, 114.3, 113.0, 112.8, 103.6.

**4-(*p*-Tolyl)pyrrolo[1,2-*a*]quinoline (3b)<sup>[47]</sup>**

The compound was prepared according to the general procedure using 22.2 mg of 1-(2-bromophenyl)-1*H*-pyrrole, 9.5 mg of Rh-6G, 253.6  $\mu$ L of 1-ethynyl-4-methylbenzene, 38.3  $\mu$ L of DIPEA and 1.5 mL dry DMSO. The reaction mixture was irradiated for 3 hours under N<sub>2</sub>. Purification of the crude product was achieved by flash column chromatography using petrol ether as eluent to yield the desired compound as greenish solid (12.4 mg, 51%).

**<sup>1</sup>H NMR** (CDCl<sub>3</sub>, 300 MHz, ppm):  $\delta$  7.91–7.87 (m, 2H), 7.66–7.64 (m, 1H), 7.60 (d, *J* = 8.1 Hz, 2H), 7.50–7.45 (m, 1H), 7.32–7.30 (m, 1H), 7.29–7.27 (m, 2H), 6.96 (s, 1H), 6.79–6.78 (m, 1H), 6.61–6.60 (m, 1H), 2.43 (s, 3H).

**<sup>13</sup>C NMR** (CDCl<sub>3</sub>, 75 MHz, ppm):  $\delta$  137.8, 136.1, 132.64, 132.59, 130.9, 129.2, 128.6, 128.2, 127.4, 124.3, 123.6, 117.7, 114.0, 112.7, 112.5, 103.3, 21.3.

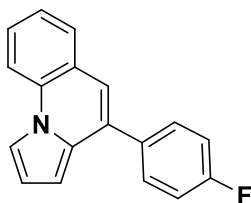
**4-(4-Methoxyphenyl)pyrrolo[1,2-*a*]quinoline (3c)<sup>[48]</sup>**

The compound was prepared according to the general procedure using 22.2 mg of 1-(2-bromophenyl)-1*H*-pyrrole, 9.5 mg of Rh-6G, 259.3  $\mu$ L of 1-ethynyl-4-methoxybenzene, 38.3  $\mu$ L of DIPEA and 1.5 mL dry DMSO. The reaction mixture was irradiated for 2.5 hours under N<sub>2</sub>. Purification of the crude product was achieved by flash column chromatography using petrol ether as eluent to yield the desired compound as greenish solid (13 mg, 50%).

**<sup>1</sup>H NMR** (CDCl<sub>3</sub>, 300 MHz, ppm):  $\delta$  7.85–7.80 (m, 2H), 7.59–7.57 (m, 3H), 7.42–7.38 (m, 1H), 7.26–7.22 (m, 1H), 6.94 (dd, *J* = 2.2, 6.6 Hz, 2H), 6.87 (s, 1H), 6.72 (t, *J* = 3.3 Hz, 1H), 6.54 (dd, *J* = 1.5, 3.7 Hz, 1H), 3.80 (s, 3H).

**<sup>13</sup>C NMR** (CDCl<sub>3</sub>, 75 MHz, ppm):  $\delta$  159.5, 132.5, 132.3, 131.4, 131.0, 129.4, 128.5, 127.3, 124.3, 123.6, 117.5, 114.0, 113.9, 112.7, 112.5, 103.2, 55.3.

**4-(4-Fluorophenyl)pyrrolo[1,2-a]quinoline (3d)<sup>[46]</sup>**

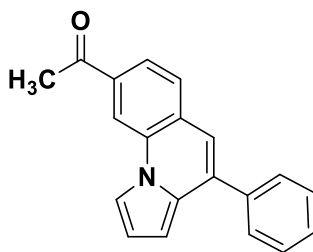


The compound was prepared according to the general procedure using 22.2 mg of 1-(2-bromophenyl)-1*H*-pyrrole, 9.5 mg of Rh-6G, 229.2  $\mu$ L of 1-ethynyl-4-fluorobenzene, 38.3  $\mu$ L of DIPEA and 1.5 mL dry DMSO. The reaction mixture was irradiated for 2.5 hours under N<sub>2</sub>. Purification of the crude product was achieved by flash column chromatography using petrol ether as eluent to yield the desired compound as light green solid (11.9 mg, 48%).

**<sup>1</sup>H NMR** (CDCl<sub>3</sub>, 300 MHz, ppm):  $\delta$  7.93 (dd,  $J$  = 3.2, 1.6 Hz, 1H), 7.89 (d,  $J$  = 8.4 Hz, 1H), 7.68 (m, 3H), 7.51 (t,  $J$  = 7.2 Hz, 1H), 7.35 (t,  $J$  = 6.8 Hz, 1H), 7.17 (t,  $J$  = 8.8 Hz, 2H), 6.95 (s, 1H), 6.80 (dd,  $J$  = 3.6, 2.8 Hz, 1H), 6.56 (dd,  $J$  = 4.0, 1.6 Hz, 1H).

**<sup>13</sup>C NMR** (CDCl<sub>3</sub>, 75 MHz, ppm):  $\delta$  164.0, 161.6, 135.2, 135.1, 132.8, 131.8, 131.0, 130.3, 130.2, 130.1, 128.9, 127.9, 124.3, 124.0, 118.3, 118.3, 115.8, 115.6, 114.3, 113.0, 112.9, 104.9, 103.4.

**1-(4-Phenylpyrrolo[1,2-a]quinolin-8-yl)ethan-1-one (3e)**



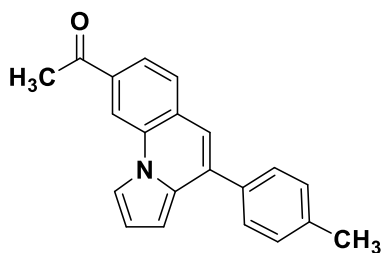
The compound was prepared according to the general procedure using 26.4 mg of 1-(4-bromo-3-(1*H*-pyrrol-1-yl)phenyl)ethan-1-one, 9.5 mg of Rh-6G, 219.6  $\mu$ L of phenylacetylene, 38.3  $\mu$ L of DIPEA and 1.5 mL dry DMSO. The reaction mixture was irradiated for 3 hours under N<sub>2</sub>. Purification of the crude product was achieved by flash column chromatography using petrol ether/ethyl acetate (5:5) as eluent to yield the desired compound as yellow solid (16.5 mg, 58%).

**<sup>1</sup>H NMR** (CDCl<sub>3</sub>, 300 MHz, ppm): δ 8.52 (s, 1H), 8.08 (dd, *J* = 3, 1.4 Hz, 1H), 7.88 (dd, *J* = 8.1, 1.4 Hz, 1H), 7.72 (d, *J* = 8.1 Hz, 3H), 7.60 – 7.46 (m, 3H), 6.99 (s, 1H), 6.84 (dd, *J* = 3.6, 3.3 Hz, 1H), 6.68 (dd, *J* = 4.7, 0.9 Hz, 1H), 2.73 (s, 3H).

**<sup>13</sup>C NMR** (CDCl<sub>3</sub>, 75 MHz, ppm): δ 197.4, 138.6, 135.5, 128.8, 128.7, 128.5, 128.4, 123.8, 117.3, 114.2, 114.0, 113.5, 105.0, 27.0.

**HRMS** [*M*+*H*]<sup>+</sup> C<sub>20</sub>H<sub>15</sub>NO calculated 286.1226 found 286.1229.

**1-(4-(*p*-Tolyl)pyrrolo[1,2-*a*]quinolin-8-yl)ethan-1-one (3f)**



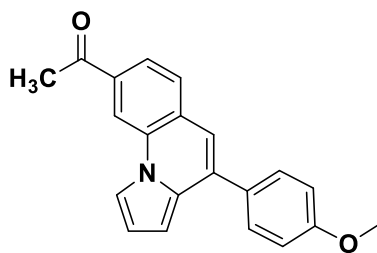
The compound was prepared according to the general procedure using 26.4 mg of 1-(4-bromo-3-(1*H*-pyrrol-1-yl)phenyl)ethan-1-one, 9.5 mg of Rh-6G, 253.6 μL of 1-ethynyl-4-methylbenzene, 38.3 μL of DIPEA and 1.5 mL dry DMSO. The reaction mixture was irradiated for 3 hours under N<sub>2</sub>. Purification of the crude product was achieved by flash column chromatography using petrol ether/ethyl acetate (5:5) as eluent to yield the desired compound as yellow solid (16.2 mg, 54%).

**<sup>1</sup>H NMR** (CDCl<sub>3</sub>, 300 MHz, ppm): δ 8.52 (s, 1H), 8.07 (dd, *J* = 3.0, 1.4 Hz, 1H), 7.87 (dd, *J* = 8.2, 1.6 Hz, 1H), 7.71 (d, *J* = 8.2 Hz, 1H), 7.67 – 7.57 (m, 2H), 7.42 – 7.28 (m, 2H), 6.97 (s, 1H), 6.84 (dd, *J* = 3.9, 2.9 Hz, 1H), 6.68 (dd, *J* = 3.9, 1.2 Hz, 1H), 2.73 (s, 3H), 2.45 (s, 3H).

**<sup>13</sup>C NMR** (CDCl<sub>3</sub>, 75 MHz, ppm): δ 197.4, 138.6, 135.7, 135.6, 135.4, 132.5, 129.5, 128.7, 128.5, 128.4, 123.7, 117.0, 114.2, 113.9, 113.5, 105.0, 27.0, 21.5.

**HRMS** [*M*<sup>+</sup>] C<sub>21</sub>H<sub>17</sub>NO calculated 299.1304 found 299.1305.

**1-(4-(4-Methoxyphenyl)pyrrolo[1,2-a]quinolin-8-yl)ethan-1-one (3g)**



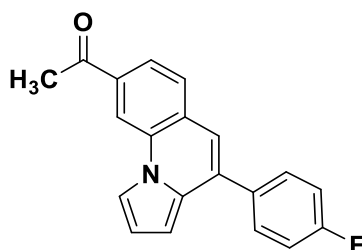
The compound was prepared according to the general procedure using 26.4 mg of 1-(4-bromo-3-(1*H*-pyrrol-1-yl)phenyl)ethan-1-one, 9.5 mg of Rh-6G, 259.3  $\mu$ L of 1-ethynyl-4-methoxybenzene, 38.3  $\mu$ L of DIPEA and 1.5 mL dry DMSO. The reaction mixture was irradiated for 2.5 hours under N<sub>2</sub>. Purification of the crude product was achieved by flash column chromatography using petrol ether/ethyl acetate (5:5) as eluent to yield the desired compound as yellow solid (23.6 mg, 75%).

**<sup>1</sup>H NMR** (CDCl<sub>3</sub>, 300 MHz, ppm):  $\delta$  8.52 (s, 1H), 8.07 (dd, *J* = 2.9, 1.4 Hz, 1H), 7.88 (dd, *J* = 8.1, 1.6 Hz, 1H), 7.72 (d, *J* = 8.1 Hz, 1H), 7.69 – 7.65 (m, 2H), 7.06 – 7.01 (m, 2H), 6.96 (s, 1H), 6.84 (dd, *J* = 3.8, 2.9 Hz, 1H), 6.68 (dd, *J* = 3.9, 1.3 Hz, 1H), 3.90 (s, 3H), 2.73 (s, 3H).

**<sup>13</sup>C NMR** (CDCl<sub>3</sub>, 151 MHz, ppm):  $\delta$  197.4, 160.1, 135.4, 135.3, 132.5, 131.2, 131.1, 129.7, 128.7, 128.6, 123.8, 116.8, 114.3, 114.2, 113.9, 113.5, 105.0, 55.6, 27.0.

**HRMS** [*M*<sup>+</sup>] C<sub>21</sub>H<sub>17</sub>NO<sub>2</sub> calculated 315.1253 found 315.1255.

**1-(4-(4-Fluorophenyl)pyrrolo[1,2-a]quinolin-8-yl)ethan-1-one (3h)**



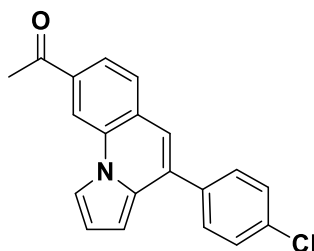
The compound was prepared according to the general procedure using 26.4 mg of 1-(4-bromo-3-(1*H*-pyrrol-1-yl)phenyl)ethan-1-one, 9.5 mg of Rh-6G, 229.2  $\mu$ L of 1-ethynyl-4-fluorobenzene, 38.3  $\mu$ L of DIPEA and 1.5 mL dry DMSO. The reaction mixture was irradiated for 2.5 hours under N<sub>2</sub>. Purification of the crude product was achieved by flash column chromatography using petrol ether/ethyl acetate (5:5) as eluent to yield the desired compound as yellow solid (15.1 mg, 50%).

**$^1\text{H}$  NMR** ( $\text{CDCl}_3$ , 300 MHz, ppm):  $\delta$  8.52 (s, 1H), 8.08 (dd,  $J = 3.0, 1.4$  Hz, 1H), 7.88 (dd,  $J = 8.2, 1.6$  Hz, 1H), 7.79 – 7.60 (m, 3H), 7.19 (t,  $J = 8.7$  Hz, 2H), 6.96 (s, 1H), 6.84 (dd,  $J = 3.9, 2.9$  Hz, 1H), 6.62 (dd,  $J = 3.9, 1.4$  Hz, 1H), 2.73 (s, 3H).

**$^{13}\text{C}$  NMR** ( $\text{CDCl}_3$ , 75 MHz, ppm):  $\delta$  197.4, 164.7, 161.4, 135.7, 134.68, 134.63, 132.6, 130.9, 130.2, 130.1, 128.8, 128.3, 123.8, 117.3, 116.0, 115.7, 114.2, 114.1, 113.6, 104.9, 27.0.

**HRMS** [ $\text{M}^+$ ]  $\text{C}_{20}\text{H}_{14}\text{FNO}$  calculated 303.1053 found 303.1051.

#### 1-(4-(4-Chlorophenyl)pyrrolo[1,2-*a*]quinolin-8-yl)ethan-1-one (3i)



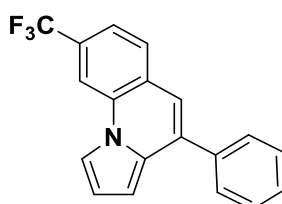
The compound was prepared according to the general procedure using 26.4 mg of 1-(4-bromo-3-(1*H*-pyrrol-1-yl)phenyl)ethan-1-one, 9.5 mg of Rh-6G, 273 mg of 1-chloro-4-ethynylbenzene, 38.3  $\mu\text{L}$  of DIPEA and 1.5 mL dry DMSO. The reaction mixture was irradiated for 2.5 hours under  $\text{N}_2$ . Purification of the crude product was achieved by flash column chromatography using petrol ether/ethyl acetate (5:5) as eluent to yield the desired compound as yellow solid (15.9 mg, 50%).

**$^1\text{H}$  NMR** ( $\text{CDCl}_3$ , 600 MHz, ppm):  $\delta$  8.53 (s, 1H), 8.08 (dd,  $J = 2.9, 1.4$  Hz, 1H), 7.89 (dd,  $J = 8.1, 1.6$  Hz, 1H), 7.73 (d,  $J = 8.1$  Hz, 1H), 7.70 – 7.56 (m, 2H), 7.55 – 7.40 (m, 2H), 6.97 (s, 1H), 6.85 (dd,  $J = 3.9, 2.9$  Hz, 1H), 6.62 (dd,  $J = 3.9, 1.4$  Hz, 1H), 2.73 (s, 3H).

**$^{13}\text{C}$  NMR** ( $\text{CDCl}_3$ , 151 MHz, ppm):  $\delta$  197.4, 137.1, 135.8, 134.6, 134.5, 132.7, 130.7, 129.8, 129.8, 129.1, 128.9, 128.2, 123.9, 117.4, 114.3, 114.2, 113.6, 104.9, 27.0.

**HRMS** [ $\text{M}^+$ ]  $\text{C}_{20}\text{H}_{14}\text{ClNO}$  calculated 319.0758 found 319.0759.

#### 4-Phenyl-8-(trifluoromethyl)pyrrolo[1,2-*a*]quinoline (3j)



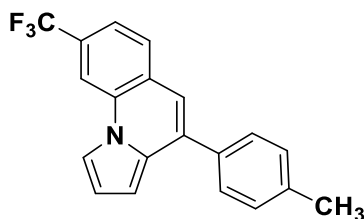
The compound was prepared according to the general procedure using 29 mg of 1-(2-bromo-5-(trifluoromethyl)phenyl)-1*H*-pyrrole, 9.5 mg of Rh-6G, 219.6  $\mu$ L of phenylacetylene, 38.3  $\mu$ L of DIPEA and 1.5 mL dry DMSO. The reaction mixture was irradiated for 4 hours under N<sub>2</sub>. Purification of the crude product was achieved by flash column chromatography using petrol ether as eluent to yield the desired compound as light green solid (15 mg, 52%).

**<sup>1</sup>H NMR** (CDCl<sub>3</sub>, 600 MHz, ppm):  $\delta$  8.14 (s, 1H), 7.99 (dd, *J* = 2.8, 1.2 Hz, 1H), 7.78 (d, *J* = 8.2 Hz, 1H), 7.75 – 7.62 (m, 2H), 7.59 – 7.48 (m, 4H), 7.00 (s, 1H), 6.86 (dd, *J* = 3.9, 2.9 Hz, 1H), 6.67 (dd, *J* = 3.9, 1.3 Hz, 1H).

**<sup>13</sup>C NMR** (CDCl<sub>3</sub>, 151 MHz, ppm):  $\delta$  138.6, 135.3, 132.4, 131.1, 129.4, 129.3, 128.8, 128.7, 127.1, 125.2, 123.4, 121.6, 120.26, 120.24, 117.1, 113.8, 113.5, 111.7, 111.67, 111.64, 111.62, 104.8.

**HRMS [M<sup>+</sup>]** C<sub>19</sub>H<sub>12</sub>F<sub>3</sub>N calculated 311.0916 found 311.0907.

#### 4-(*p*-Tolyl)-8-(trifluoromethyl)pyrrolo[1,2-*a*]quinoline (3k)

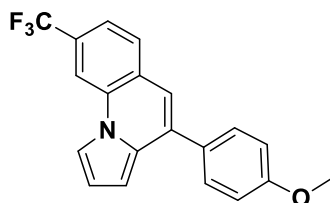


The compound was prepared according to the general procedure using 29 mg of 1-(2-bromo-5-(trifluoromethyl)phenyl)-1*H*-pyrrole, 9.5 mg of Rh-6G, 253.6  $\mu$ L of 1-ethynyl-4-methylbenzene, 38.3  $\mu$ L of DIPEA and 1.5 mL dry DMSO. The reaction mixture was irradiated for 4 hours under N<sub>2</sub>. Purification of the crude product was achieved by flash column chromatography using petrol ether as eluent to yield the desired compound as light green solid (18.2 mg, 56%).

**<sup>1</sup>H NMR** (CDCl<sub>3</sub>, 300 MHz, ppm):  $\delta$  8.13 (s, 1H), 7.97 (dd, *J* = 2.9, 1.4 Hz, 1H), 7.76 (d, *J* = 8.1 Hz, 1H), 7.70 – 7.59 (m, 2H), 7.59 – 7.49 (m, 1H), 7.40 – 7.27 (m, 2H), 6.98 (s, 1H), 6.85 (dd, *J* = 3.9, 2.9 Hz, 1H), 6.68 (dd, *J* = 3.9, 1.3 Hz, 1H), 2.46 (s, 3H).

**<sup>13</sup>C NMR** (CDCl<sub>3</sub>, 75 MHz, ppm):  $\delta$  138.6, 135.7, 135.2, 132.3, 131.1, 129.5, 129.3, 128.4, 127.1, 120.24, 116.8, 113.7, 113.5, 111.6, 104.8, 21.5.

**HRMS [M<sup>+</sup>]** C<sub>20</sub>H<sub>14</sub>F<sub>3</sub>N calculated 325.1072 found 325.1064.

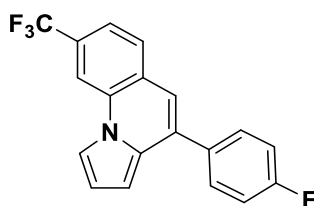
**4-(4-Methoxyphenyl)-8-(trifluoromethyl)pyrrolo[1,2-*a*]quinoline (3l)**

The compound was prepared according to the general procedure using 29 mg of 1-(2-bromo-5-(trifluoromethyl)phenyl)-1*H*-pyrrole, 9.5 mg of Rh-6G, 259.3  $\mu$ L of 1-ethynyl-4-methoxybenzene, 38.3  $\mu$ L of DIPEA and 1.5 mL dry DMSO. The reaction mixture was irradiated for 4 hours under N<sub>2</sub>. Purification of the crude product was achieved by flash column chromatography using petrol ether as eluent to yield the desired compound as green solid (14 mg, 41%).

**<sup>1</sup>H NMR** (CDCl<sub>3</sub>, 300 MHz, ppm):  $\delta$  8.14 (s, 1H), 7.97 (dd, *J* = 3.0, 1.3 Hz, 1H), 7.76 (d, *J* = 8.1 Hz, 1H), 7.72 – 7.62 (m, 2H), 7.54 (dd, *J* = 8.1, 1.0 Hz, 1H), 7.12 – 7.00 (m, 2H), 6.96 (s, 1H), 6.85 (dd, *J* = 3.7, 2.9 Hz, 1H), 6.68 (dd, *J* = 3.8, 1.3 Hz, 1H), 3.90 (s, 3H).

**<sup>13</sup>C NMR** (CDCl<sub>3</sub>, 151 MHz, ppm):  $\delta$  160.1, 134.9, 132.3, 131.2, 131.0, 129.7, 129.2, 129.1, 128.8, 127.2, 127.0, 125.2, 123.4, 121.6, 120.25, 120.23, 120.21, 120.18, 116.6, 114.3, 113.5, 111.66, 111.63, 111.60, 111.57, 104.8, 55.6.

**HRMS** [*M*<sup>+</sup>] C<sub>20</sub>H<sub>14</sub>F<sub>3</sub>NO calculated 341.1020 found 341.1019.

**4-(4-Fluorophenyl)-8-(trifluoromethyl)pyrrolo[1,2-*a*]quinoline (3m)**

The compound was prepared according to the general procedure using 29 mg of 1-(2-bromo-5-(trifluoromethyl)phenyl)-1*H*-pyrrole, 9.5 mg of Rh-6G, 229.2  $\mu$ L of 1-ethynyl-4-fluorobenzene, 38.3  $\mu$ L of DIPEA and 1.5 mL dry DMSO. The reaction mixture was irradiated for 4 hours under N<sub>2</sub>. Purification of the crude product was achieved by flash column chromatography using petrol ether as eluent to yield the desired compound as green solid (13.5 mg, 41%).

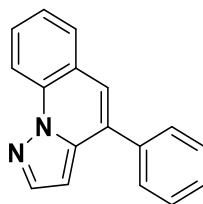


**<sup>1</sup>H NMR** (600 MHz, CDCl<sub>3</sub>, ppm): δ 8.1 (s, 1H), 7.98 (dd, *J* = 2.8, 1.3 Hz, 1H), 7.77 (d, *J* = 8.1 Hz, 1H), 7.72 – 7.65 (m, 2H), 7.55 (dd, *J* = 8 Hz, 1H), 7.23 – 7.16 (m, 2H), 6.96 (s, 1H), 6.86 (dd, *J* = 3.7, 2.9 Hz, 1H), 6.62 (dd, *J* = 3.8, 1.2 Hz, 1H).

**<sup>13</sup>C NMR** (151 MHz, CDCl<sub>3</sub>, ppm): δ 163.9, 162.2, 134.6, 134.5, 134.2, 132.4, 131.0, 130.2, 129.5, 129.2, 126.9, 123.3, 120.34, 120.32, 117.1, 115.9, 115.8, 113.8, 113.7, 111.7, 111.6, 104.7.

**HRMS** [**M**+**H**]<sup>+</sup> C<sub>19</sub>H<sub>11</sub>F<sub>4</sub>N calculated 330.09 found 330.09.

#### 4-Phenylpyrazolo[1,5-a]quinoline (3n)



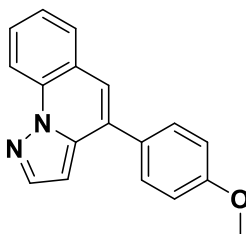
The compound was prepared according to the general procedure using 22.3 mg of 1-(2-bromophenyl)-1*H*-pyrazole, 9.5 mg of Rh-6G, 219.6 μL of phenylacetylene, 38.3 μL of DIPEA and 1.5 mL dry DMSO. The reaction mixture was irradiated for 24 hours under N<sub>2</sub>. Purification of the crude product was achieved by flash column chromatography using petrol ether/ ethyl acetate (1:4) as eluent to yield the desired compound as light green solid (9.5 mg, 39%).

**<sup>1</sup>H NMR** (300 MHz, CDCl<sub>3</sub>, ppm): δ 8.60 (d, *J* = 8.4 Hz, 1H), 8.06 (d, *J* = 2.1 Hz, 1H), 7.82-7.65 (m, 4H), 7.55-7.46 (m, 4H), 7.43 (s, 1H), 6.75 (d, *J* = 2.1 Hz, 1H).

**<sup>13</sup>C NMR** (75 MHz, CDCl<sub>3</sub>, ppm): δ 141.4, 138.4, 138.3, 134.3, 131.1, 129.4, 129.0, 128.7, 128.6, 128.3, 125.1, 123.8, 123.3, 115.7, 100.4.

**HRMS** [**M**<sup>+</sup>] C<sub>17</sub>H<sub>12</sub>N<sub>2</sub> calculated 244.0995 found 244.0991.

#### 4-(4-Methoxyphenyl)pyrazolo[1,5-a]quinoline (3o)



The compound was prepared according to the general procedure using 22.3 mg of 1-(2-bromophenyl)-1*H*-pyrazole, 9.5 mg of Rh-6G, 259.3 μL of 1-ethynyl-4-methoxybenzene, 38.3 μL of DIPEA and 1.5 mL dry DMSO. The reaction mixture was irradiated for 24 hours

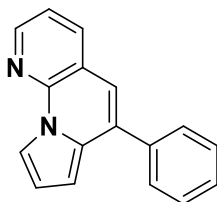
under N<sub>2</sub>. Purification of the crude product was achieved by flash column chromatography using petrol ether/ ethyl acetate (1:4) as eluent to yield the desired compound as light green solid (10 mg, 35%).

**<sup>1</sup>H NMR** (300 MHz, CDCl<sub>3</sub>, ppm): δ 8.59 (d, *J* = 8.4 Hz, 1H), 8.05 (d, *J* = 2.1 Hz, 1H), 7.79 (dd, *J* = 7.9, 1.1 Hz, 1H), 7.68-7.63 (m, 3H), 7.48- 7.42 (m, 1H), 7.38 (s, 1H), 7.07-7.02 (m, 2H), 6.73 (d, *J* = 2.1 Hz, 1H), 3.89 (s, 3H).

**<sup>13</sup>C NMR** (75 MHz, CDCl<sub>3</sub>, ppm): δ 160.0, 141.4, 138.6, 134.1, 130.7, 130.7, 129.5, 129.1, 128.5, 125.1, 122.7, 115.7, 114.4, 100.3, 55.6.

**HRMS** [*M*<sup>+</sup>] C<sub>18</sub>H<sub>14</sub>N<sub>2</sub>O calculated 274.1100 found 274.1103.

### 6-Phenylpyrrolo[1,2-*a*][1,8]naphthyridine (3p)



The compound was prepared according to the general procedure using 22.3 mg of 3-bromo-2-(1*H*-pyrrol-1-yl)pyridine, 9.5 mg of Rh-6G, 219.6 μL of phenylacetylene, 38.3 μL of DIPEA and 1.5 mL dry DMSO. The reaction mixture was irradiated for 16 hours under N<sub>2</sub>. Purification of the crude product was achieved by flash column chromatography using

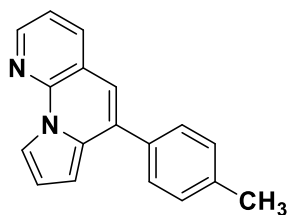
petrol ether/ethyl acetate (1:4) as eluent to yield the desired compound as yellow solid (12 mg, 49%).

**<sup>1</sup>H NMR** (300 MHz, CDCl<sub>3</sub>, ppm): δ 8.55 (dd, *J* = 4.8, 1.8 Hz, 1H), 8.44 (dd, *J* = 2.9, 1.4 Hz, 1H), 7.98 (dd, *J* = 7.7, 1.7 Hz, 1H), 7.73-7.69 (m, 2H), 7.53-7.74 (m, 3H), 7.31 (dd, *J* = 7.7, 4.7 Hz, 1H), 6.91 (s, 1H), 6.83 (dd, *J* = 3.7, 3 Hz, 1H), 6.67 (dd, *J* = 3.8, 1.5 Hz, 1H).

**<sup>13</sup>C NMR** (75 MHz, CDCl<sub>3</sub>, ppm): δ 146.8, 144.1, 138.6, 136.3, 134.3, 128.8, 128.6, 128.5, 120.2, 119.3, 116.3, 114.5, 113.4, 105.3.

**HRMS** [*M*<sup>+</sup>] C<sub>17</sub>H<sub>12</sub>N<sub>2</sub> calculated 244.0995 found 244.0999.

**6-(*p*-Tolyl)pyrrolo[1,2-*a*][1,8]naphthyridine (3q)**



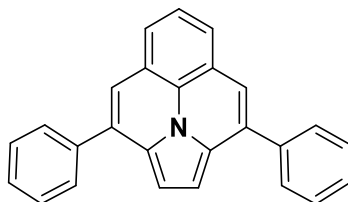
The compound was prepared according to the general procedure using 22.3 mg of 3-bromo-2-(1*H*-pyrrol-1-yl)pyridine, 9.5 mg of Rh-6G, 253.6  $\mu$ L of 1-ethynyl-4-methylbenzene, 38.3  $\mu$ L of DIPEA and 1.5 mL dry DMSO. The reaction mixture was irradiated for 16 hours under N<sub>2</sub>. Purification of the crude product was achieved by flash column chromatography using petrol ether: ethyl acetate (1:4) as eluent to yield the desired compound as yellow solid (13mg, 50%).

**<sup>1</sup>H NMR** (300 MHz, CDCl<sub>3</sub>, ppm):  $\delta$  8.53 (dd, *J* = 4.7, 1.7 Hz, 1H), 8.43 (dd, *J* = 2.8, 1.4 Hz, 1H), 7.96 (dd, *J* = 7.8, 1.7 Hz, 1H), 7.63-7.59 (m, 2H), 7.32- 7.26 (m, 3H), 6.89 (s, 1H), 6.83 (dd, *J* = 3.7, 3.0 Hz, 1H), 6.68 (dd, *J* = 3.7, 1.5 Hz, 1H), 2.45 (s, 3H).

**<sup>13</sup>C NMR** (75 MHz, CDCl<sub>3</sub>, ppm):  $\delta$  146.7, 144.0, 138.5, 136.2, 135.7, 134.2, 131.7, 129.5, 128.4, 120.1, 119.3, 116.0, 114.4, 113.3, 105.2, 21.5.

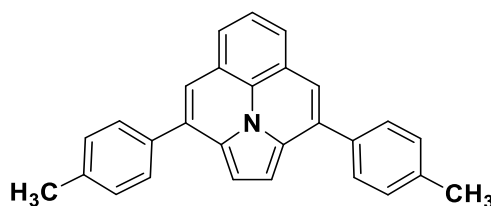
**HRMS** [*M*<sup>+</sup>] C<sub>18</sub>H<sub>14</sub>N<sub>2</sub> calculated 258.11515 found 258.11516.

**3,9-Diphenylindolizino[6,5,4,3-*ija*]quinoline (3r)<sup>[49]</sup>**



**<sup>1</sup>H NMR** (600 MHz, CDCl<sub>3</sub>, ppm):  $\delta$  7.83 – 7.78 (m, 4H), 7.53 (s, 7H), 7.24 (s, 2H), 7.07 (s, 2H).

**<sup>13</sup>C NMR** (151 MHz, CDCl<sub>3</sub>, ppm):  $\delta$  138.9, 133.7, 132.8, 128.9, 128.5, 128.4, 127.0, 126.0, 124.0, 119.7, 119.5, 106.2.

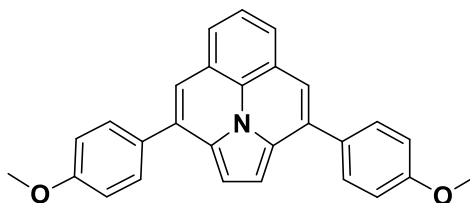
**3,9-di-*p*-Toly lindolizino[6,5,4,3-*ija*]quinoline (3s)**

The compound was prepared according to the general procedure using 30 mg of 1-(2,6-dibromophenyl)-1*H*-pyrrole, 9.5 mg of Rh-6G, 253.6  $\mu$ L of 1-ethynyl-4-methylbenzene, and 38.3  $\mu$ L of DIPEA. The reaction mixture was irradiated for 24 hours under  $N_2$ . Purification of the crude product was achieved by flash column chromatography using petrol ether as eluent to yield the desired compound as yellow solid (11.1 mg, 30%).

**$^1H$  NMR** (600 MHz,  $CDCl_3$ ):  $\delta$  7.72 – 7.69 (m, 4H), 7.49 – 7.45 (m, 2H), 7.42 (m, 1H), 7.35 – 7.32 (m, 4H), 7.21 (s, 2H), 7.06 (s, 2H), 2.46 (s, 6H).

**$^{13}C$  NMR** ( $CDCl_3$ , 151 MHz, ppm):  $\delta$  138.3, 136.0, 133.6, 132.7, 129.65, 129.6, 128.2, 127.0, 126.1, 124.0, 119.4, 119.2, 106.1, 21.5.

**EI-MS [ $M^+$ ]**  $C_{28}H_{21}N$  calculated 371.16685 found 371.16695.

**3,9-Bis(4-methoxyphenyl)indolizino[6,5,4,3-*ija*]quinoline (3t)**

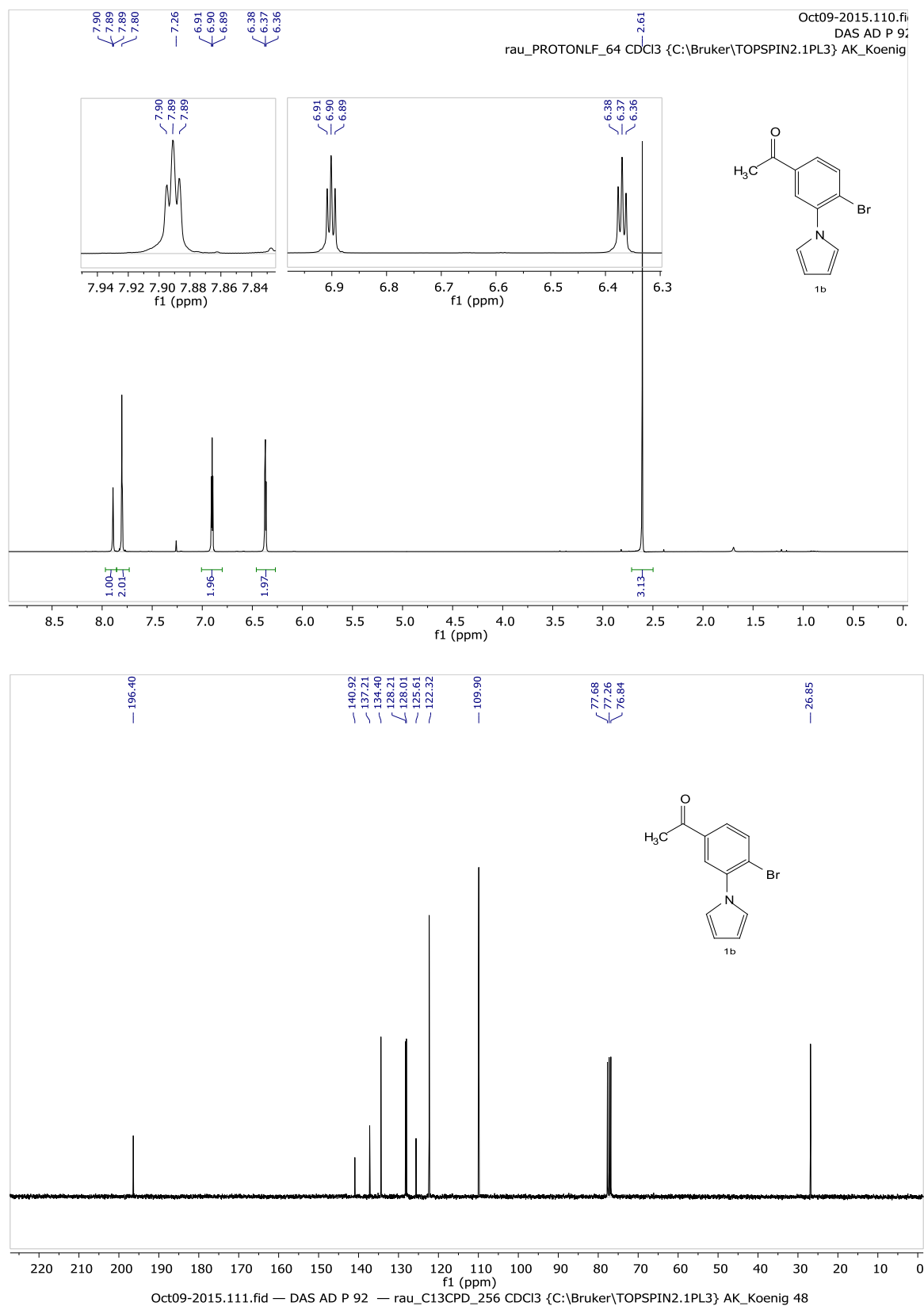
The compound was prepared according to the general procedure using 30 mg of 1-(2,6-dibromophenyl)-1*H*-pyrrole, 9.5 mg of Rh-6G, 259.3  $\mu$ L of 1-ethynyl-4-methoxybenzene, and 38.3  $\mu$ L of DIPEA. The reaction mixture was irradiated for 24 hours under  $N_2$ . Purification of the crude product was achieved by flash column chromatography using petrol ether as eluent to yield the desired compound as yellow solid (12.1 mg, 30%).

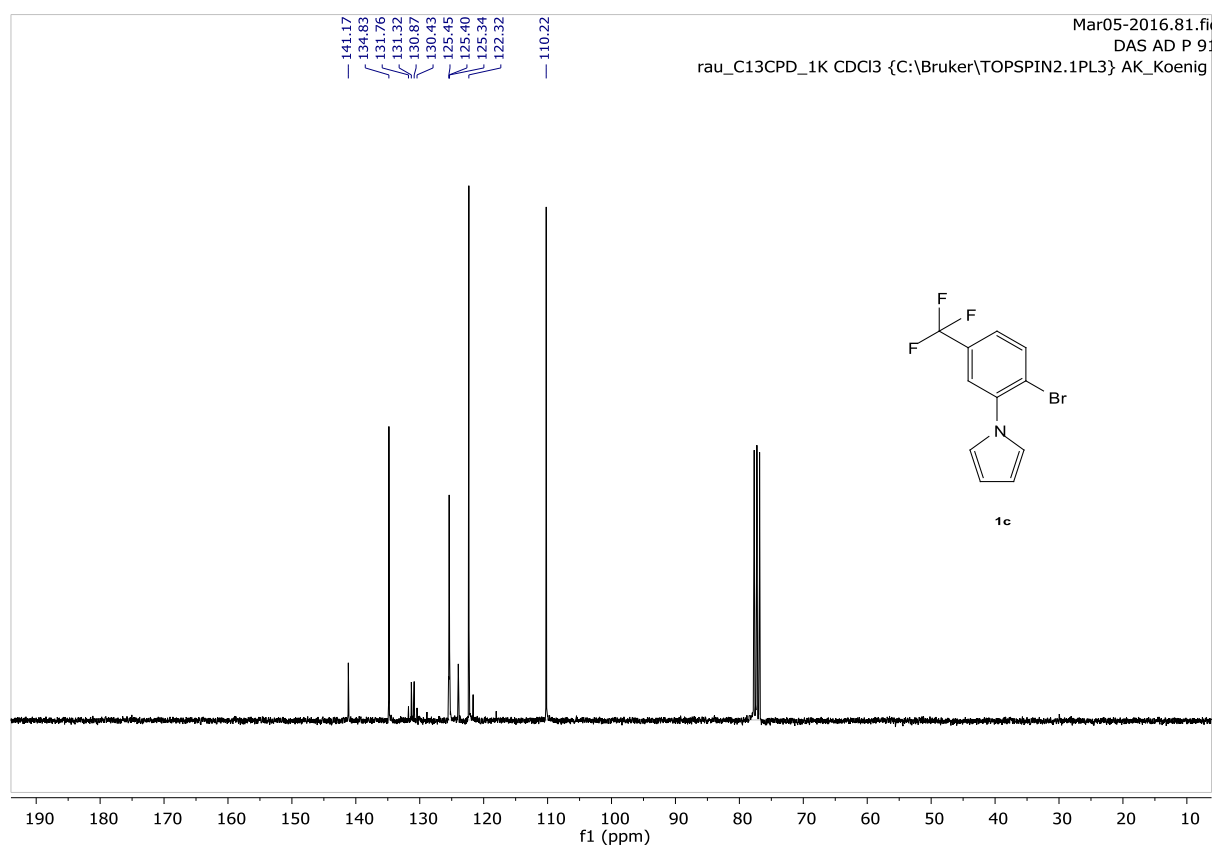
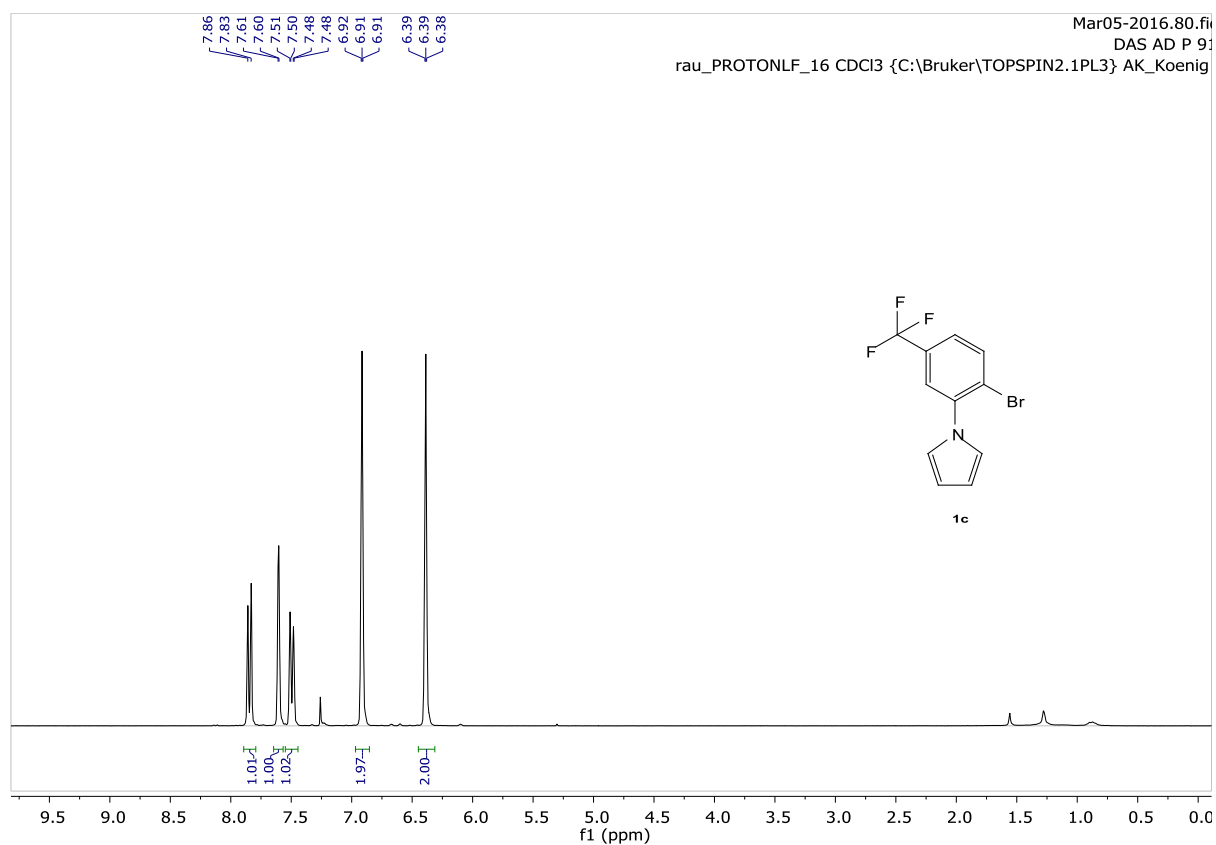
**$^1H$  NMR** (600 MHz,  $CDCl_3$ ):  $\delta$  7.75 – 7.72 (m, 4H), 7.46 – 7.70 (m, 3H), 7.39 (s, 2H), 7.07 – 7.04 (m, 6H), 3.90 (s, 6H).

**$^{13}C$  NMR** ( $CDCl_3$ , 151 MHz, ppm):  $\delta$  159.9, 134.2, 133.2, 132.5, 131.4, 129.5, 127.1, 126.1, 124.0, 119.3, 118.9, 114.3, 106.1, 55.6.

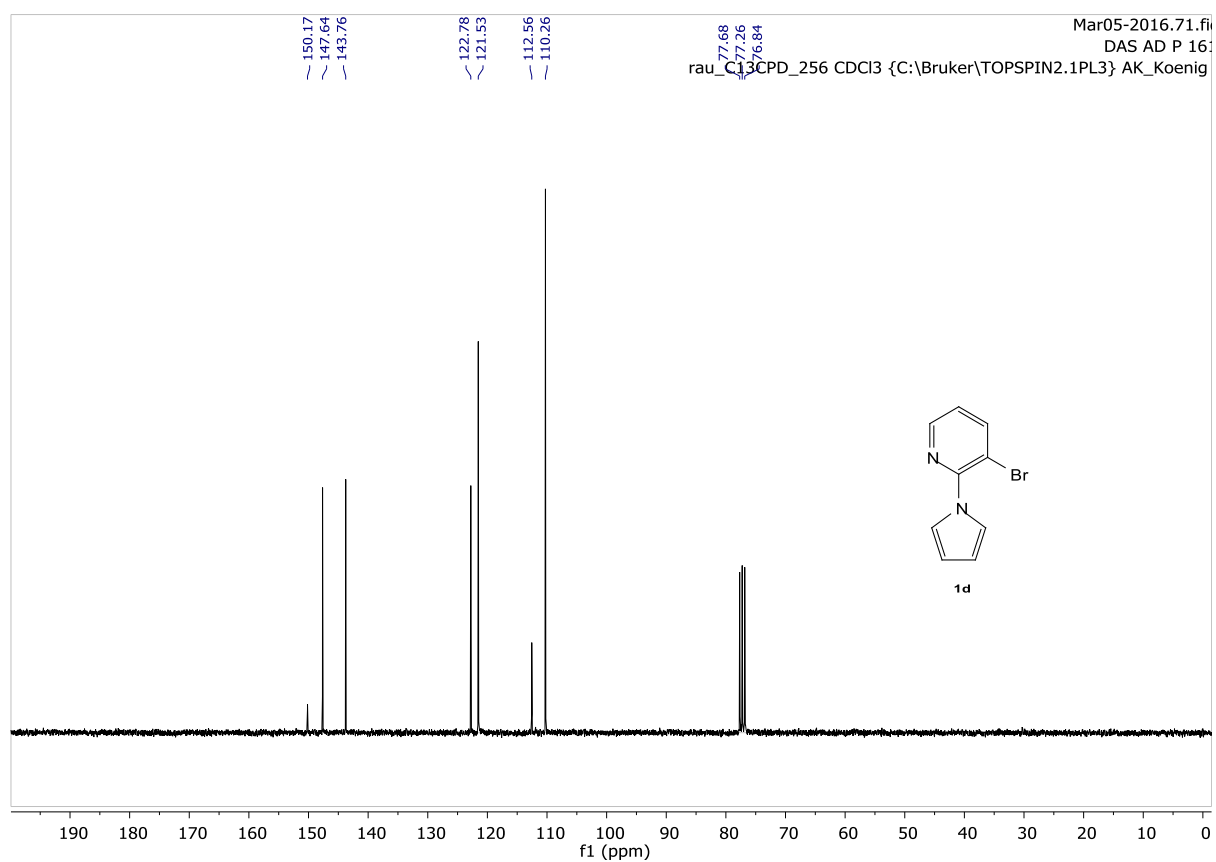
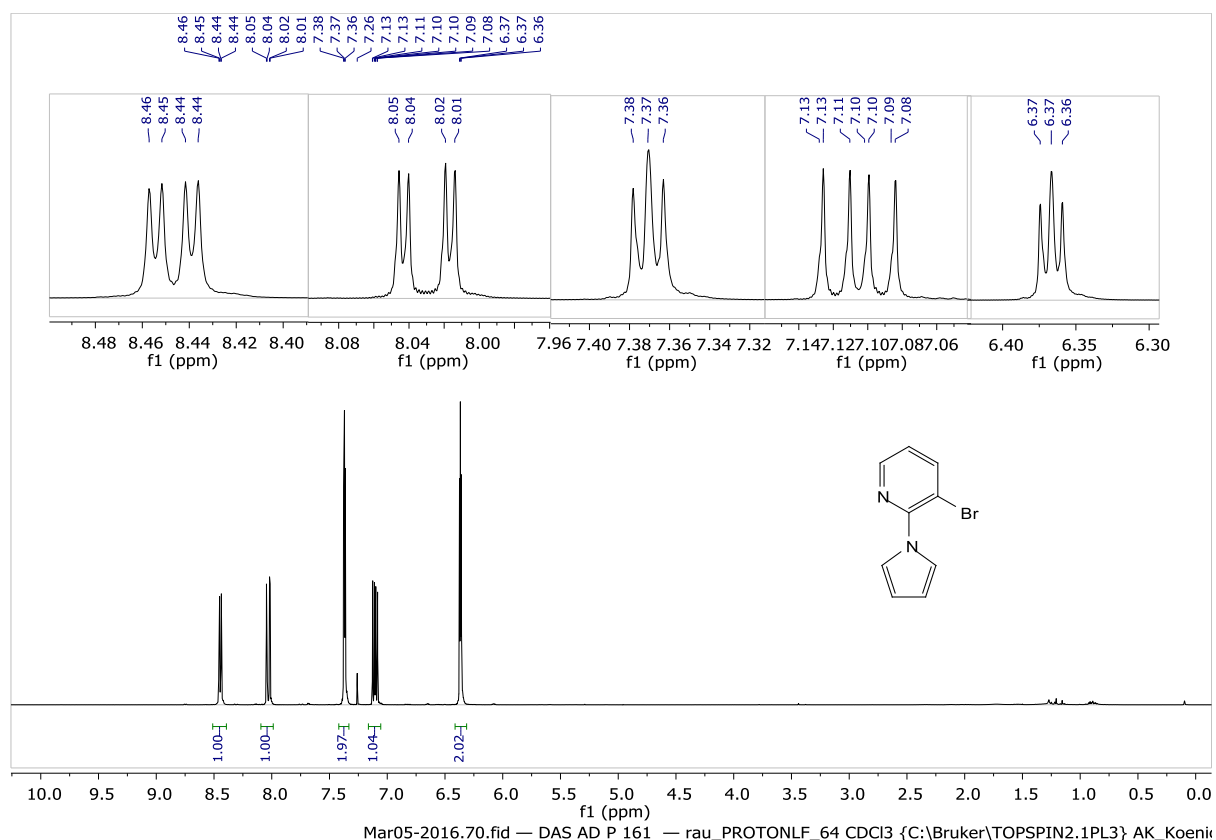
**EI-MS [ $M^+$ ]**  $C_{28}H_{21}NO_2$  calculated 403.15668 found 403.15664.

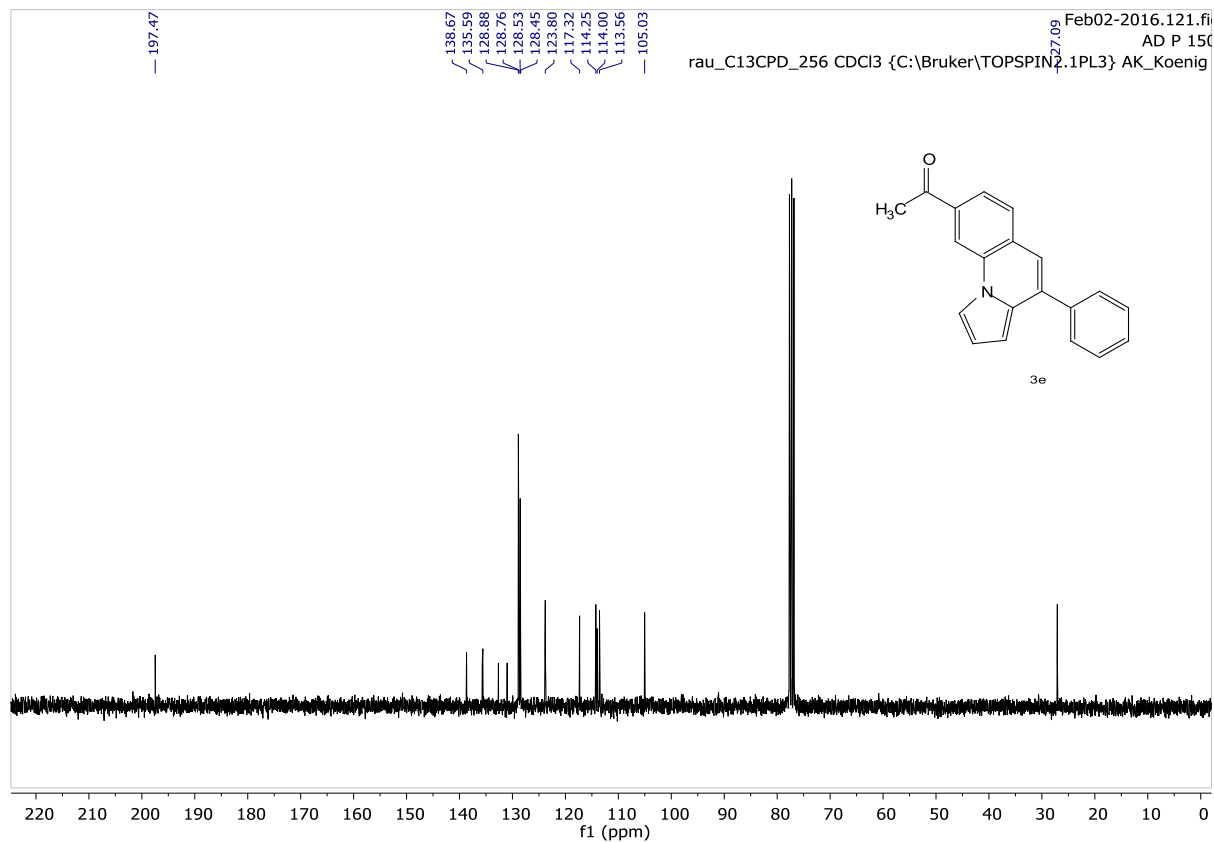
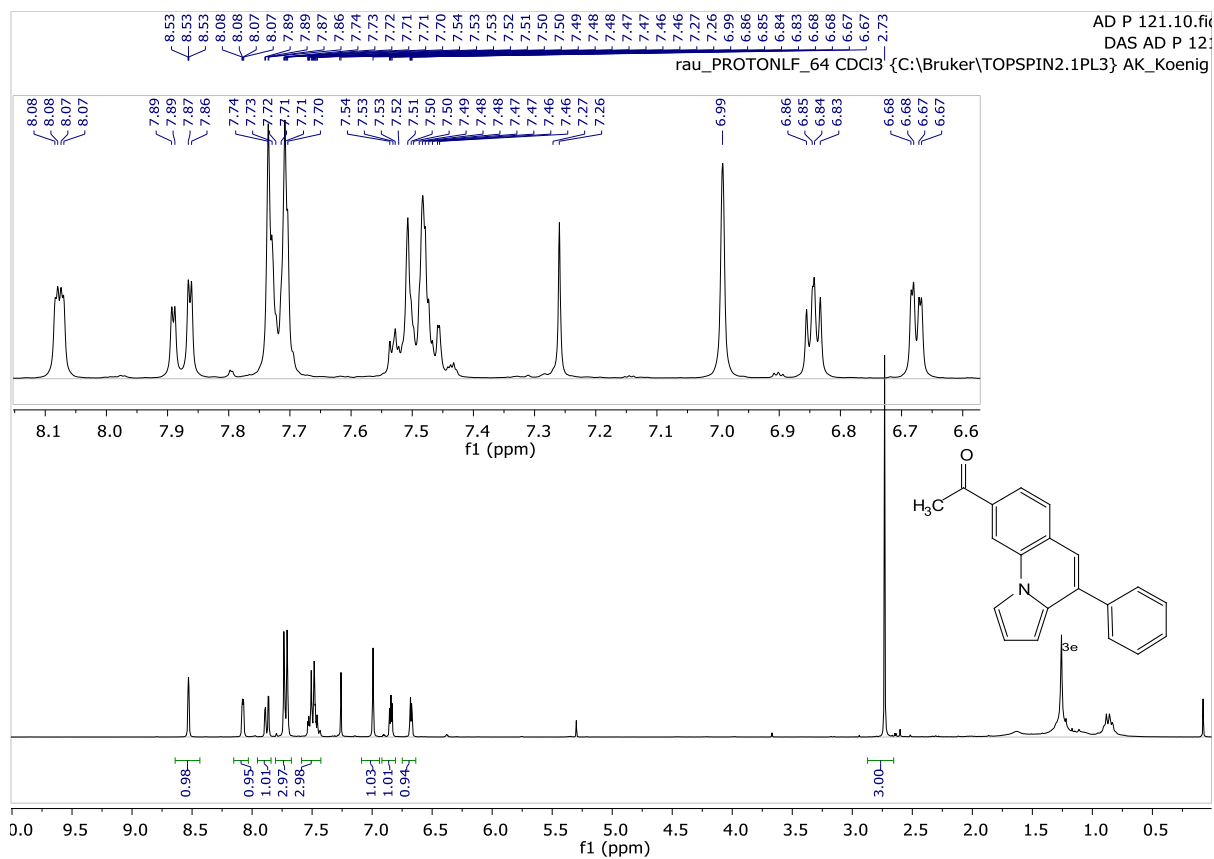
## 2.4.6 $^1\text{H}$ - and $^{13}\text{C}$ NMR spectra of synthesized compounds





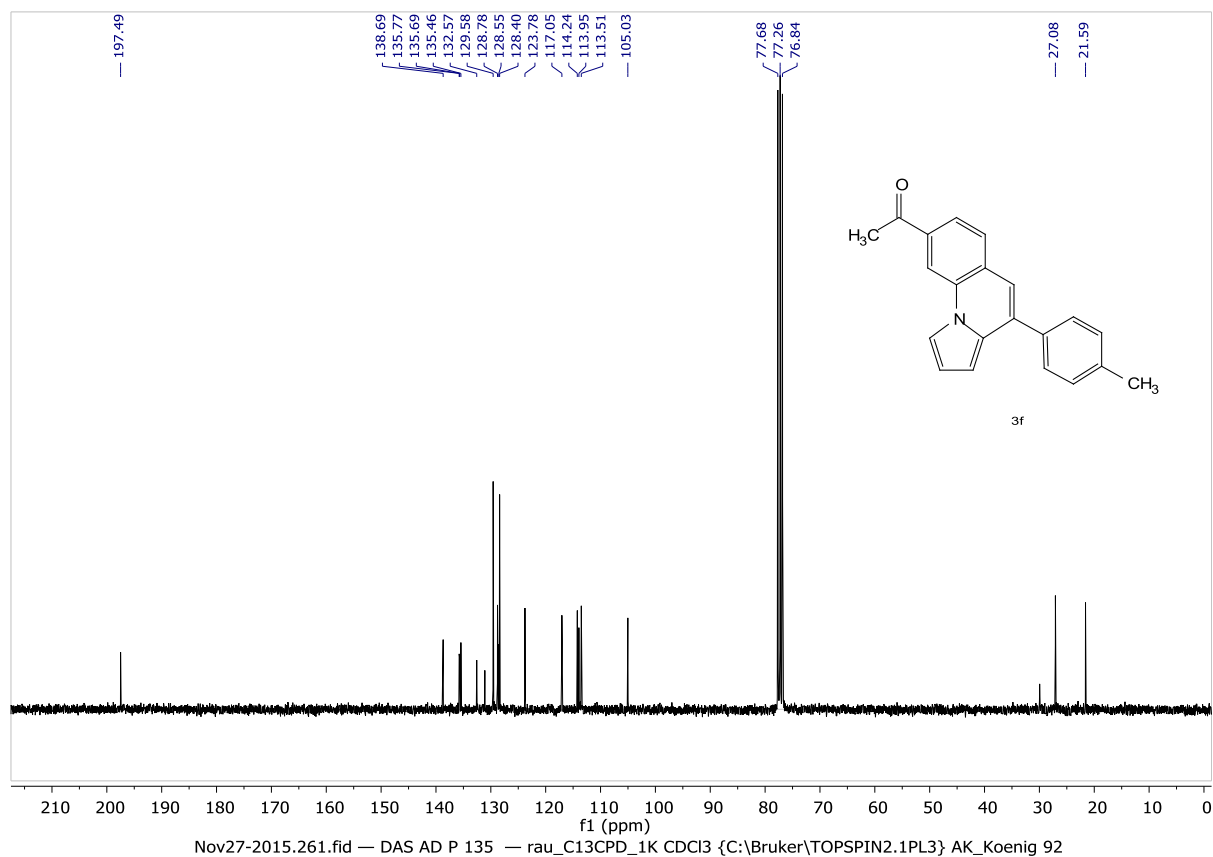
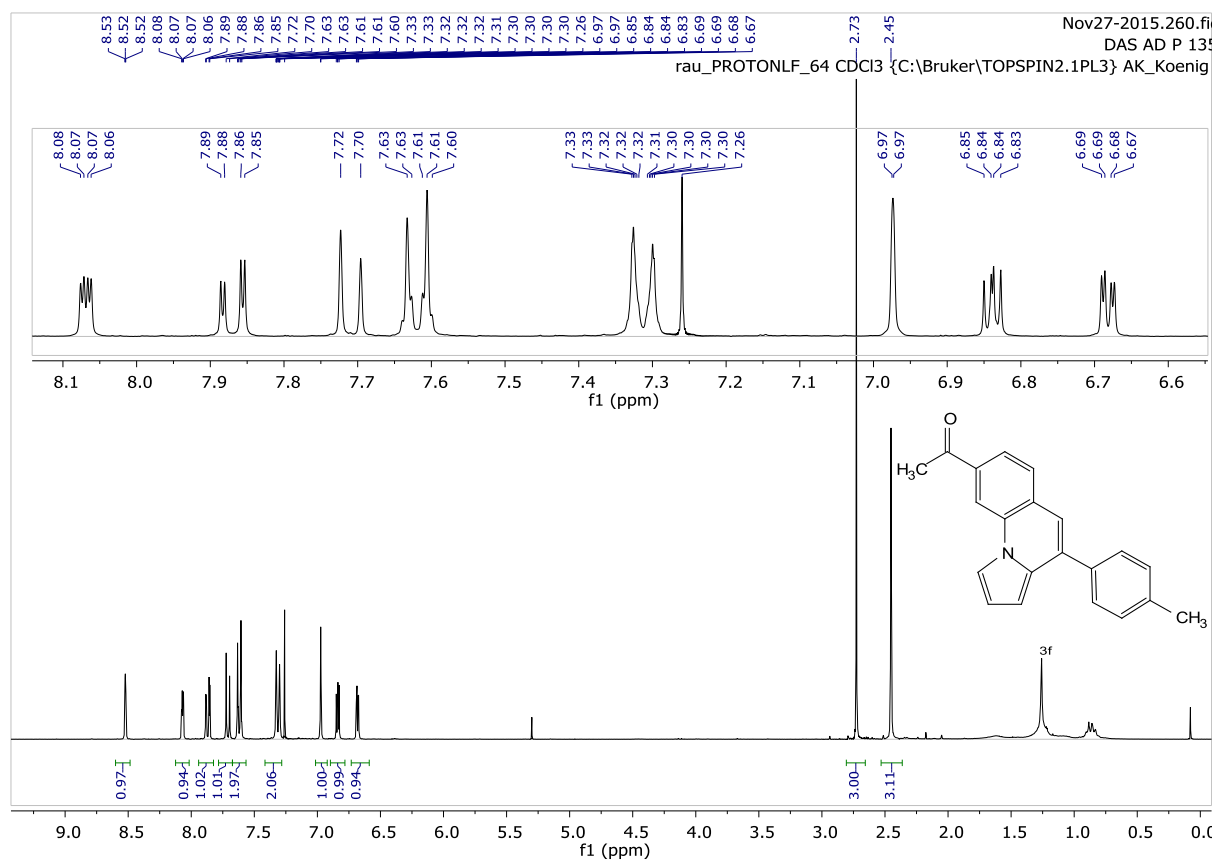
**Synthesis of Pyrrolo[1,2-a]quinolines and Ullazines by Visible Light Mediated One- and Two Fold Annulation of N-arylpyrroles with Arylalkynes**





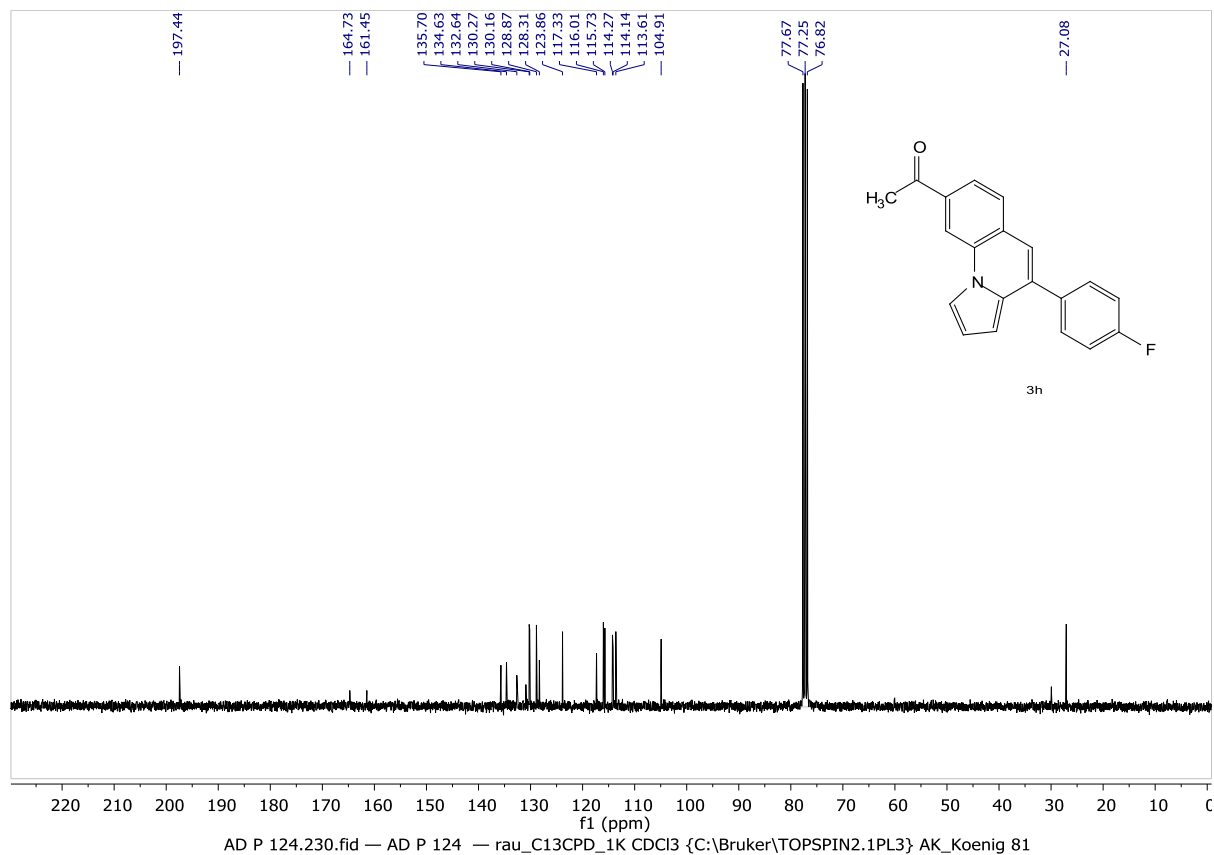
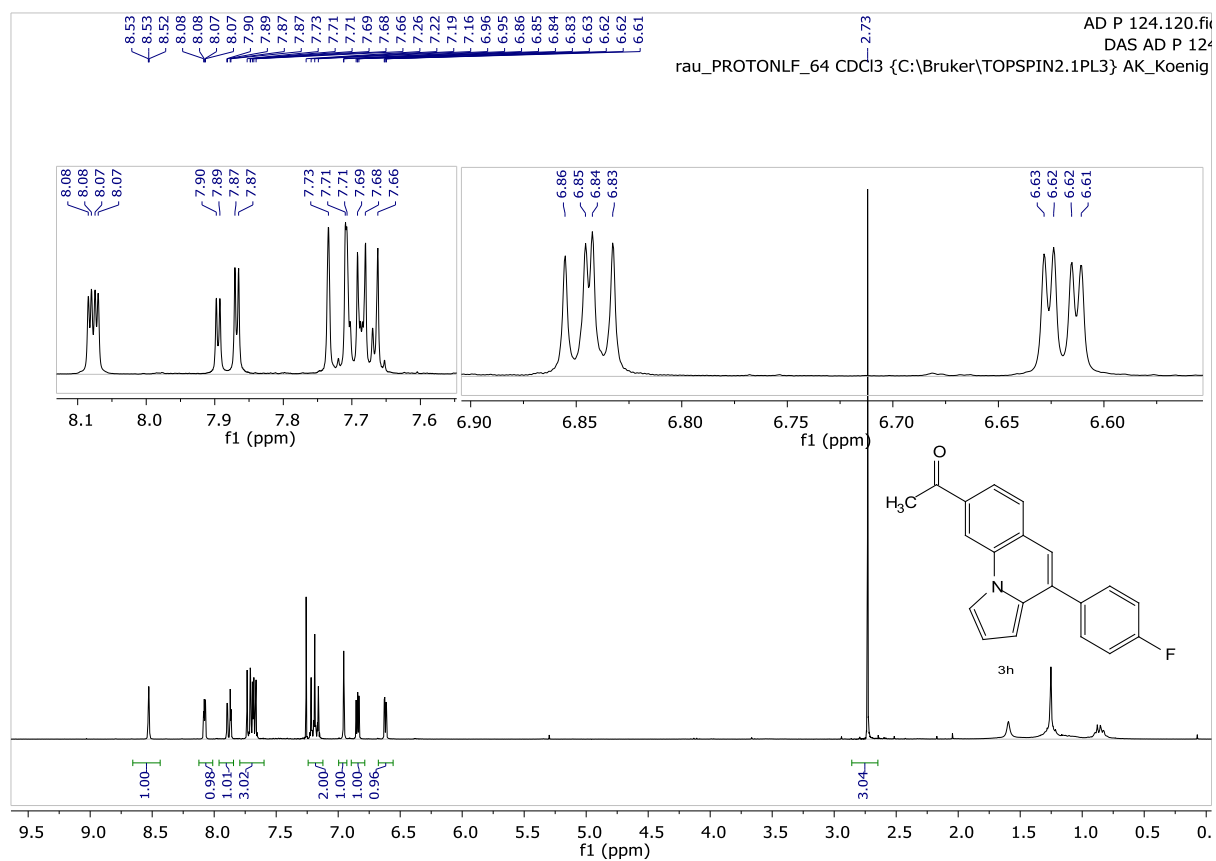


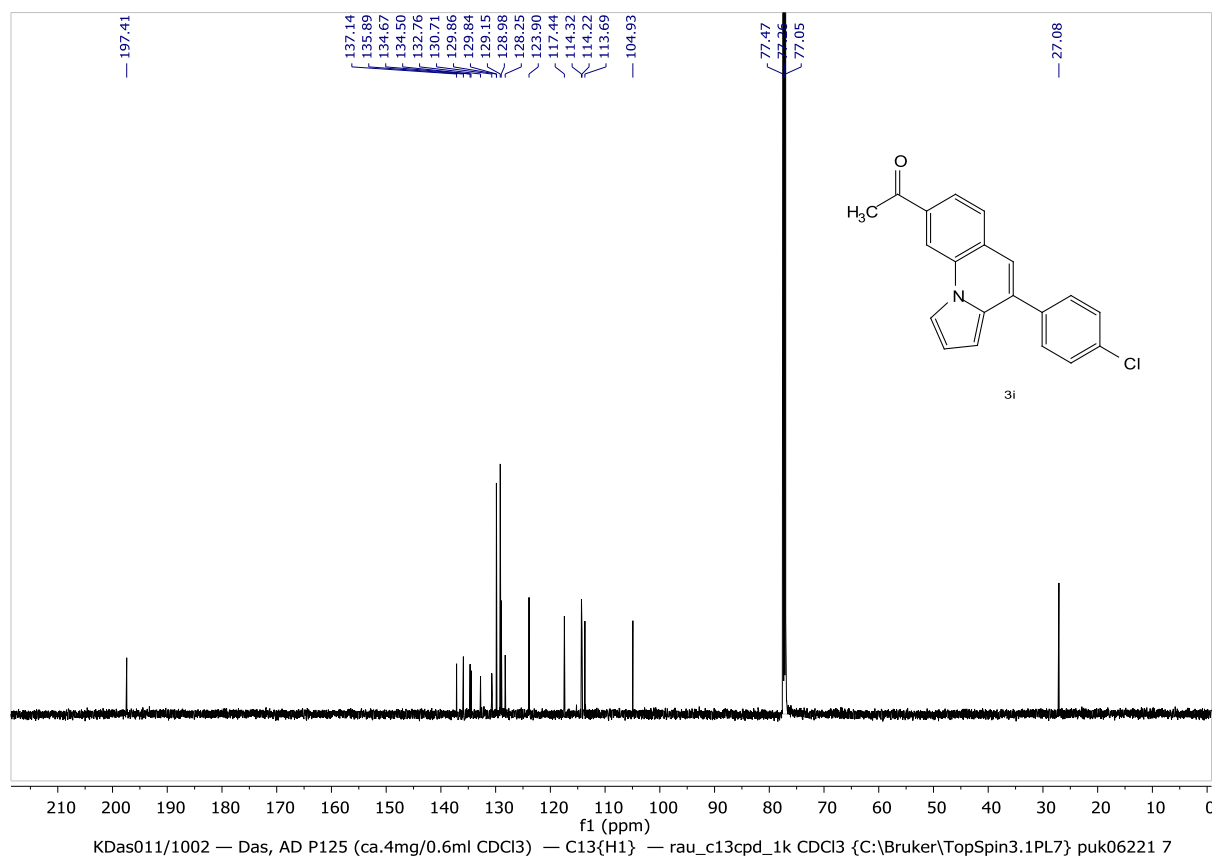
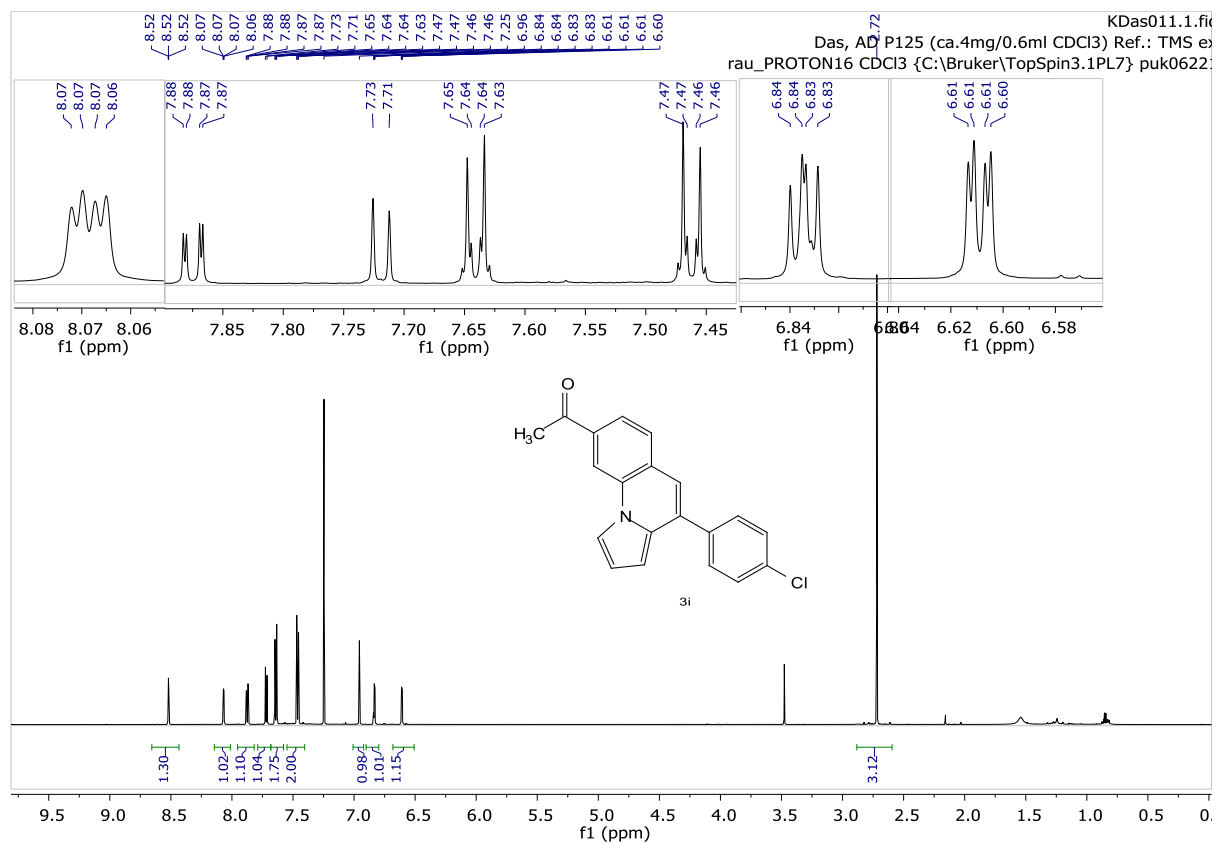
**Synthesis of Pyrrolo[1,2-a]quinolines and Ullazines by Visible Light Mediated One- and Two Fold Annulation of N-arylpyrroles with Arylalkynes**



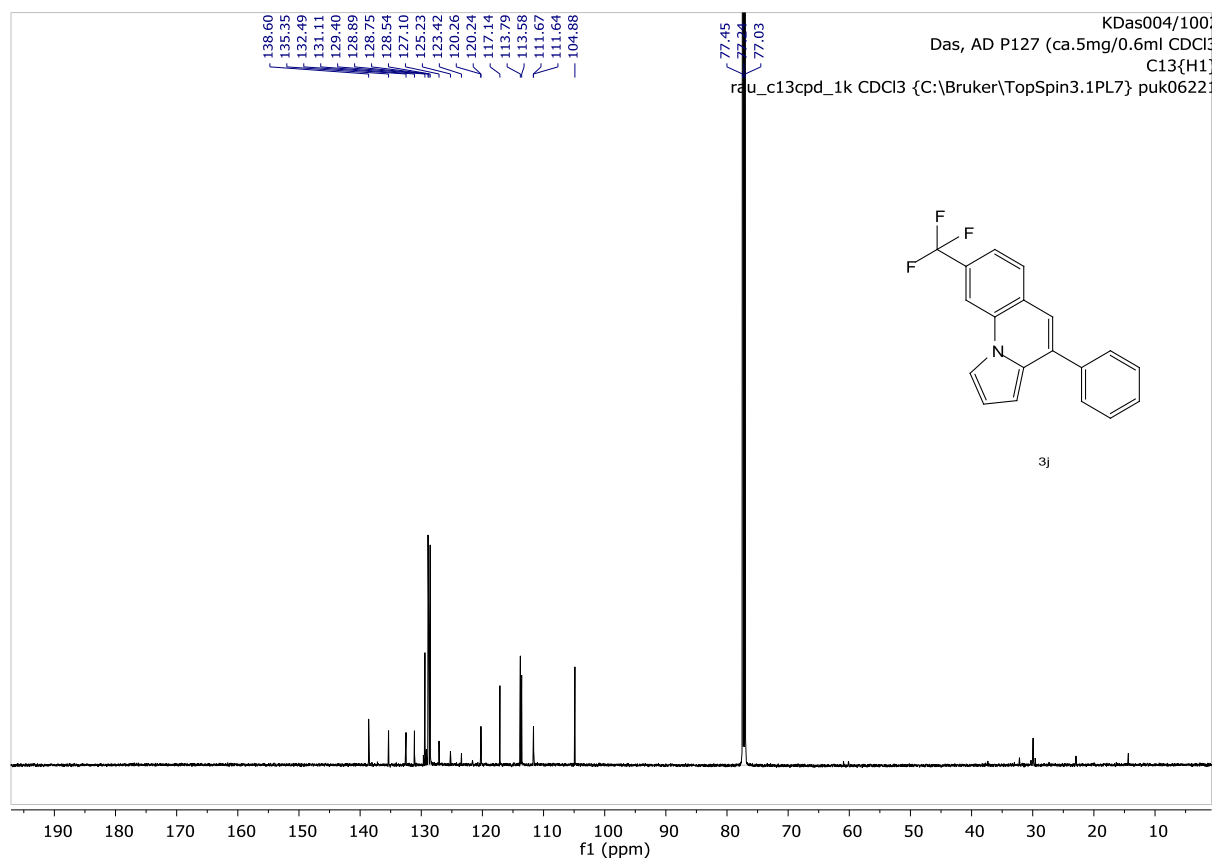
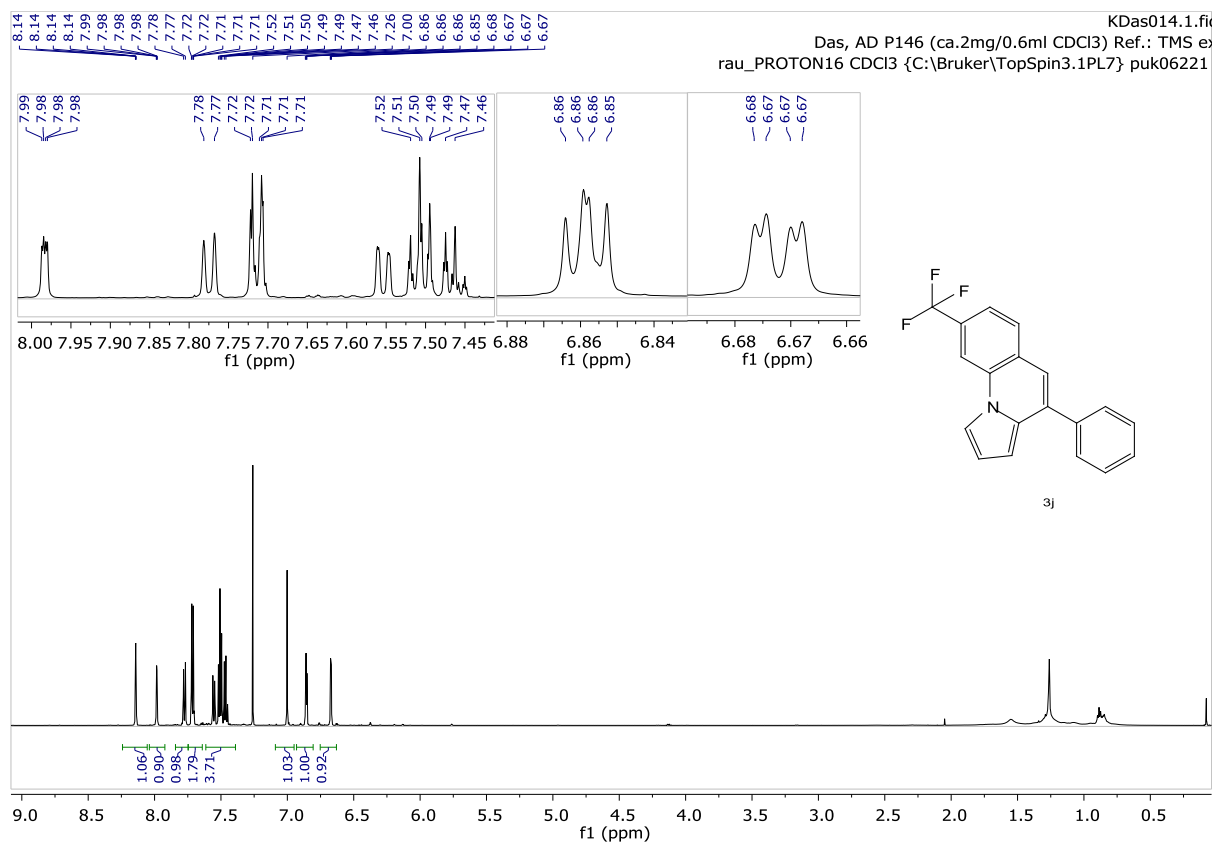


**Synthesis of Pyrrolo[1,2-a]quinolines and Ullazines by Visible Light Mediated One- and Two Fold Annulation of N-arylpyrroles with Arylalkynes**

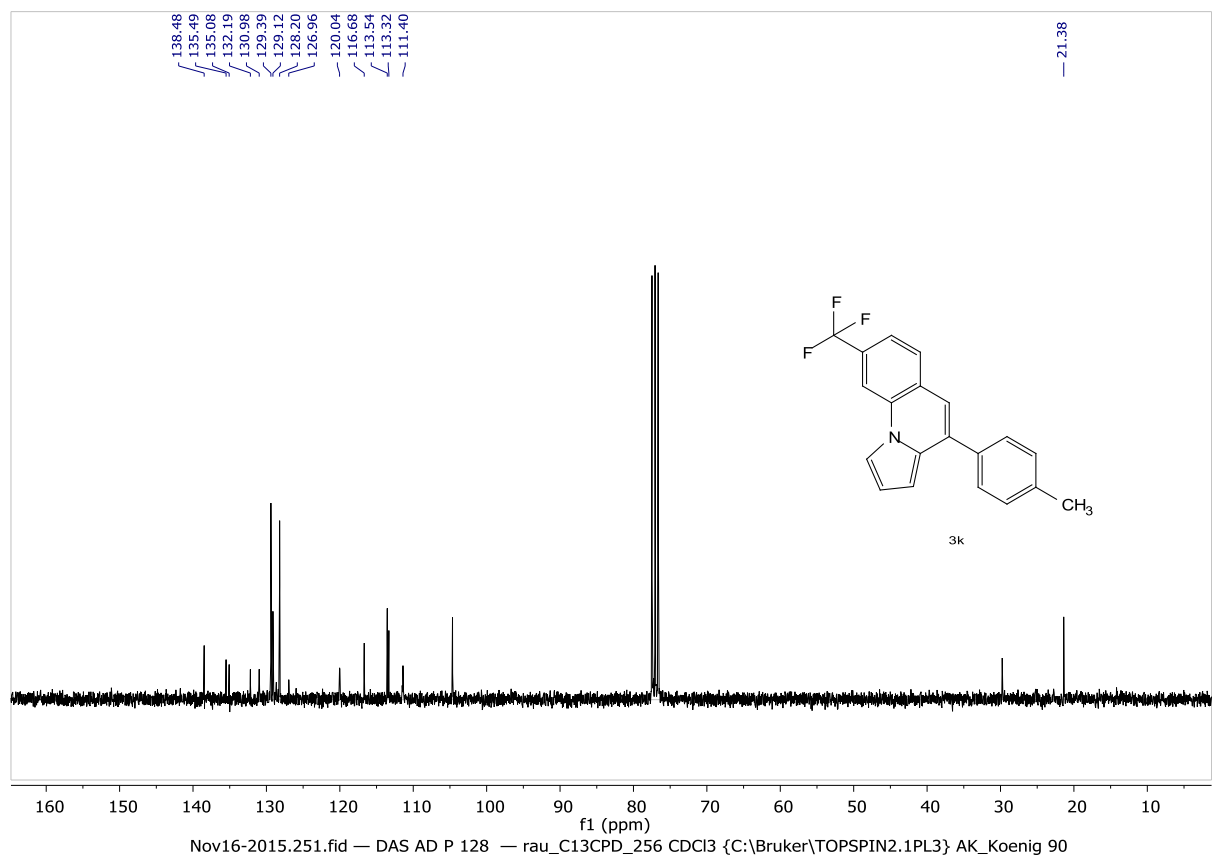
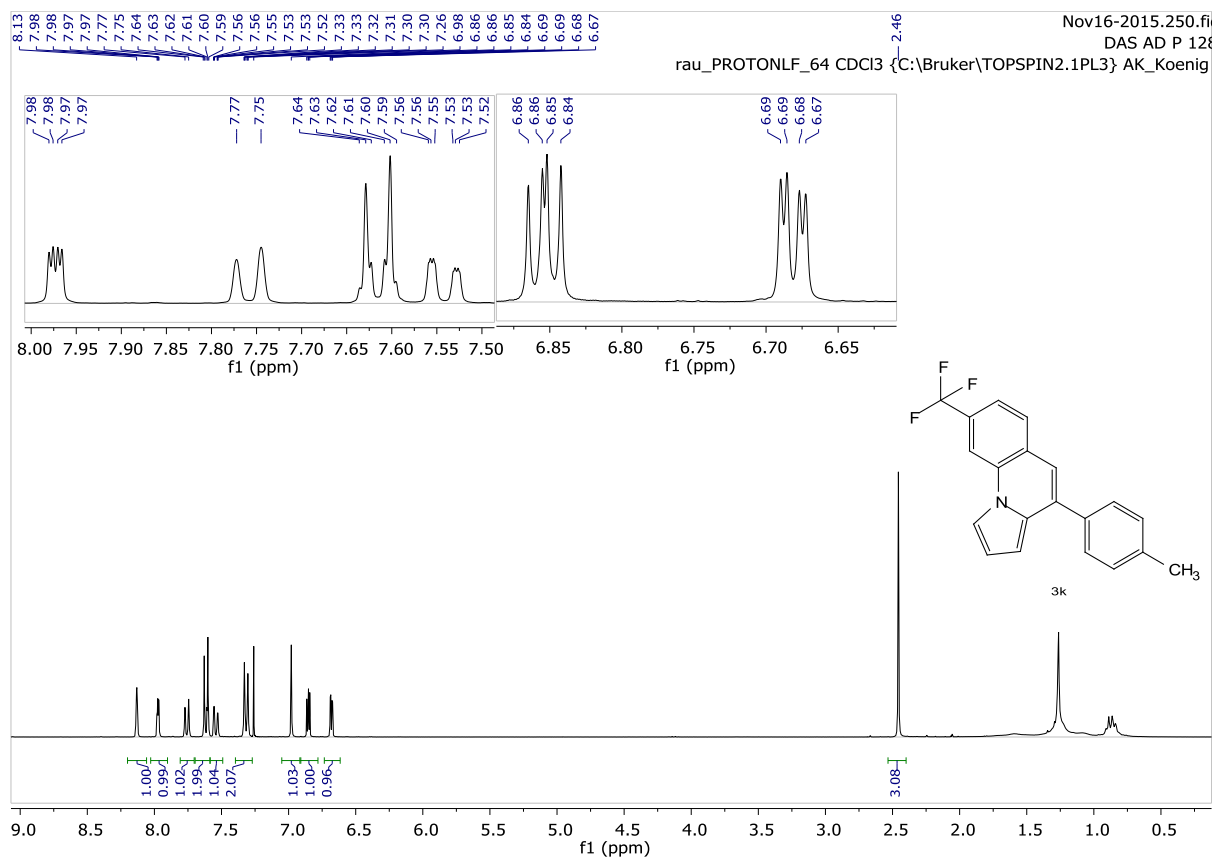




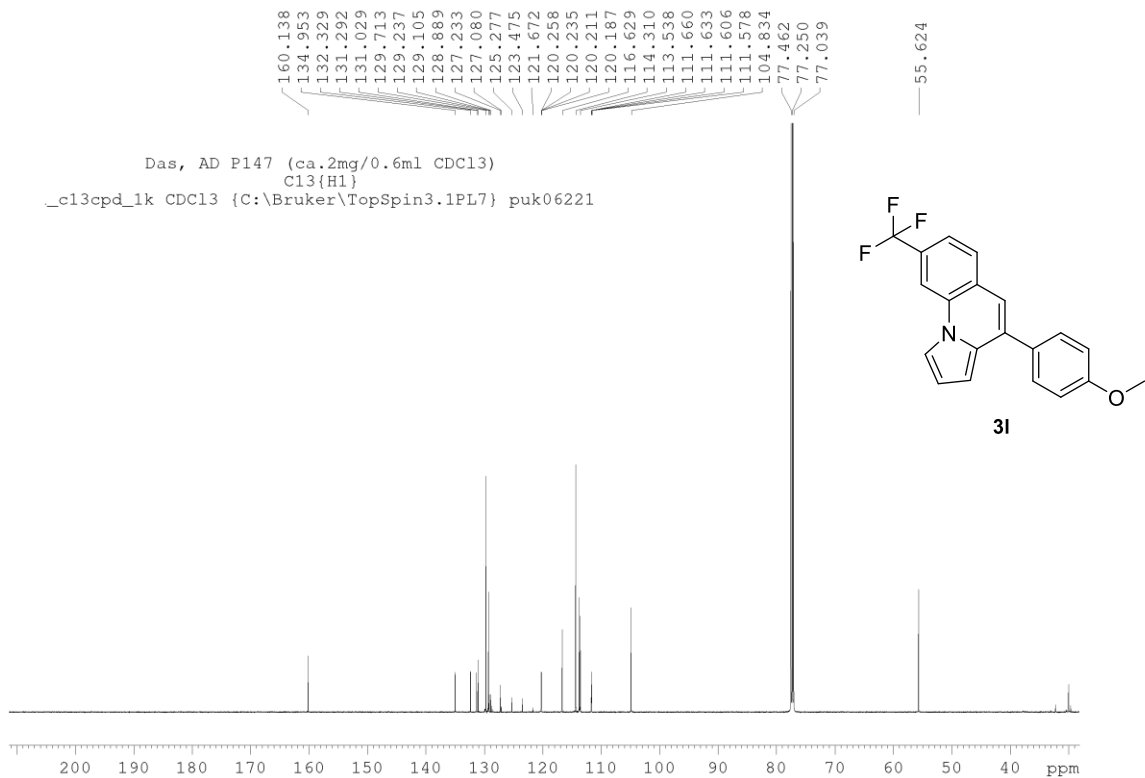
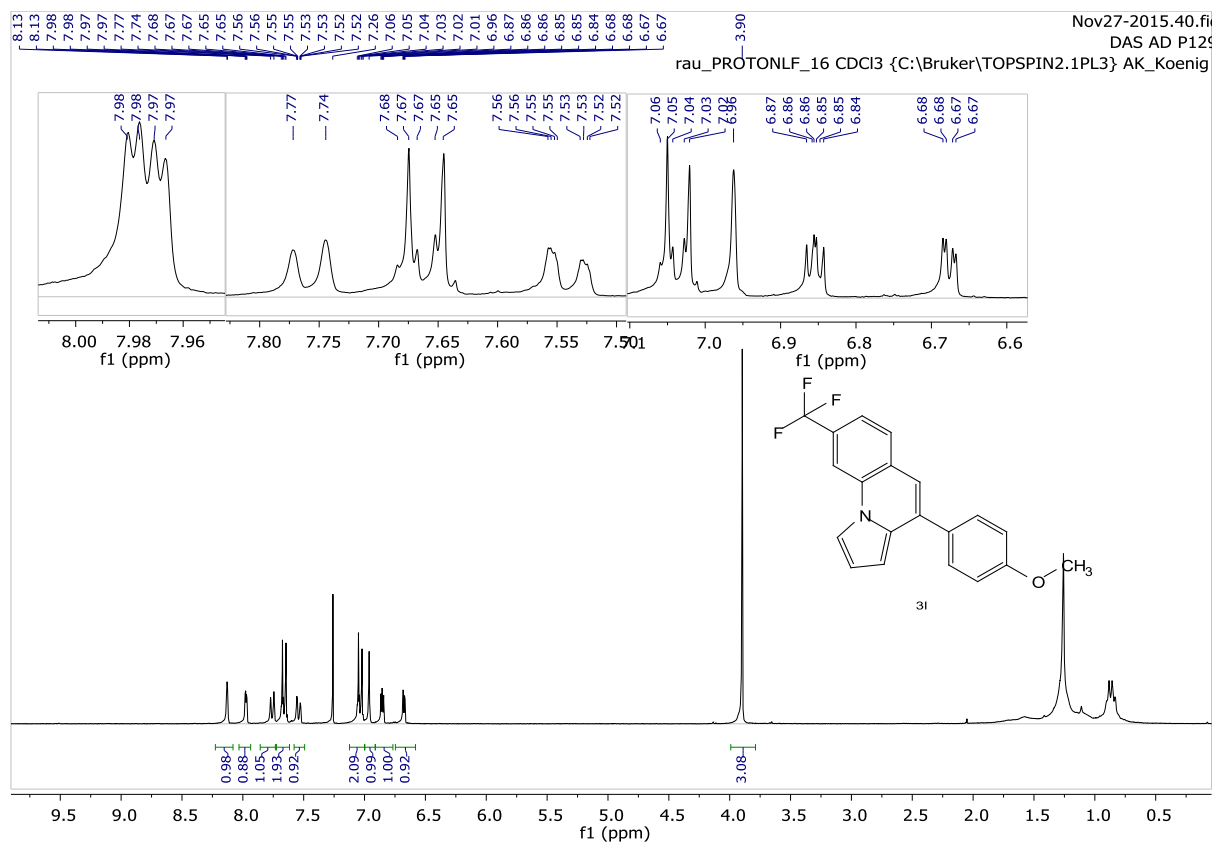
# Synthesis of Pyrrolo[1,2-a]quinolines and Ullazines by Visible Light Mediated One- and Two Fold Annulation of N-arylpyrroles with Arylalkynes



## Chapter 2

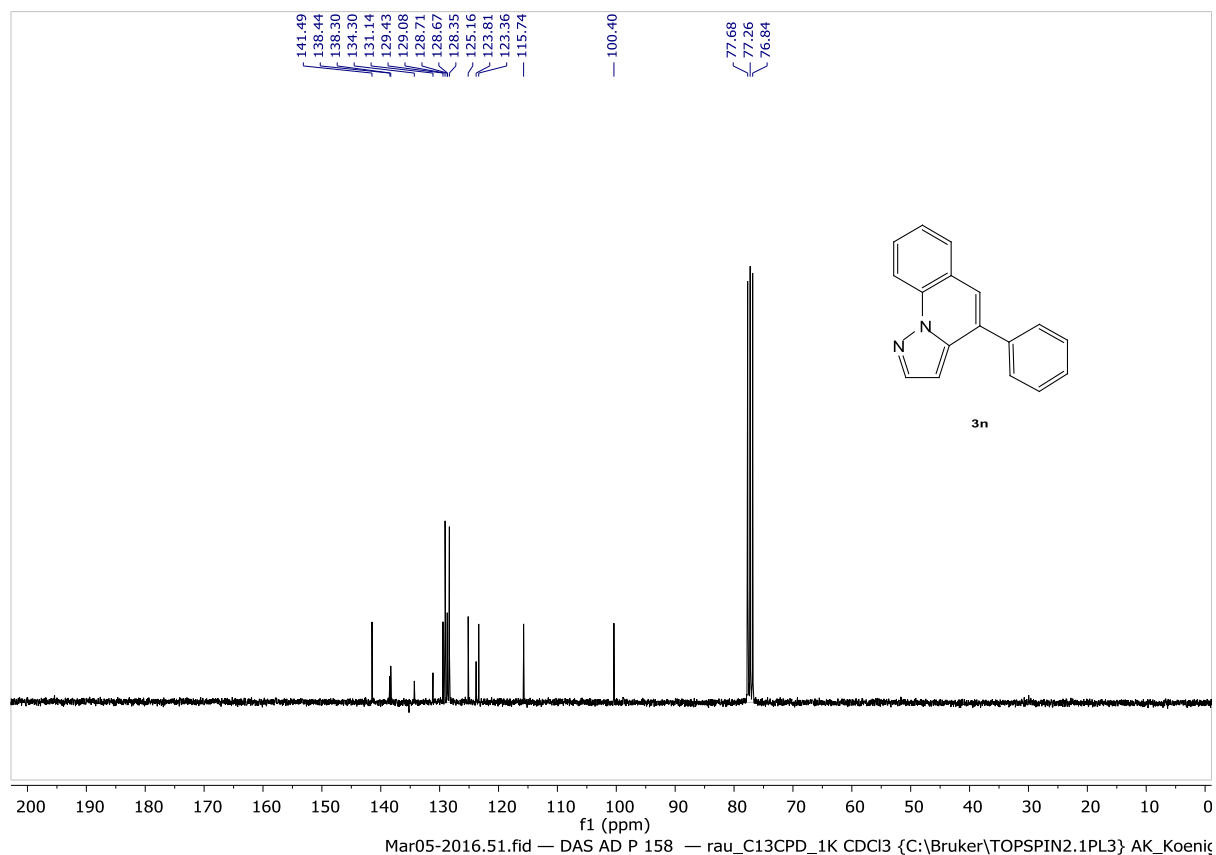


**Synthesis of Pyrrolo[1,2-a]quinolines and Ullazines by Visible Light Mediated One- and Two Fold Annulation of N-arylpyrroles with Arylalkynes**

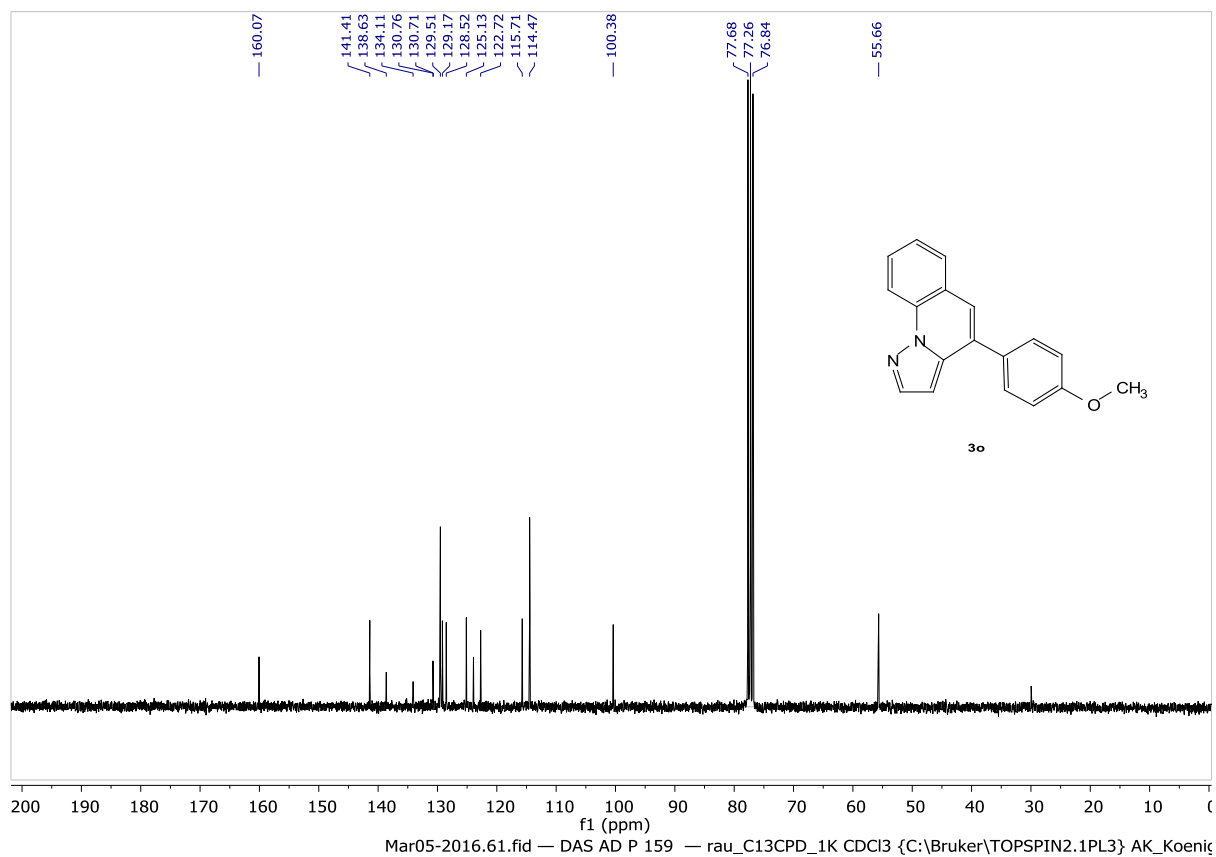
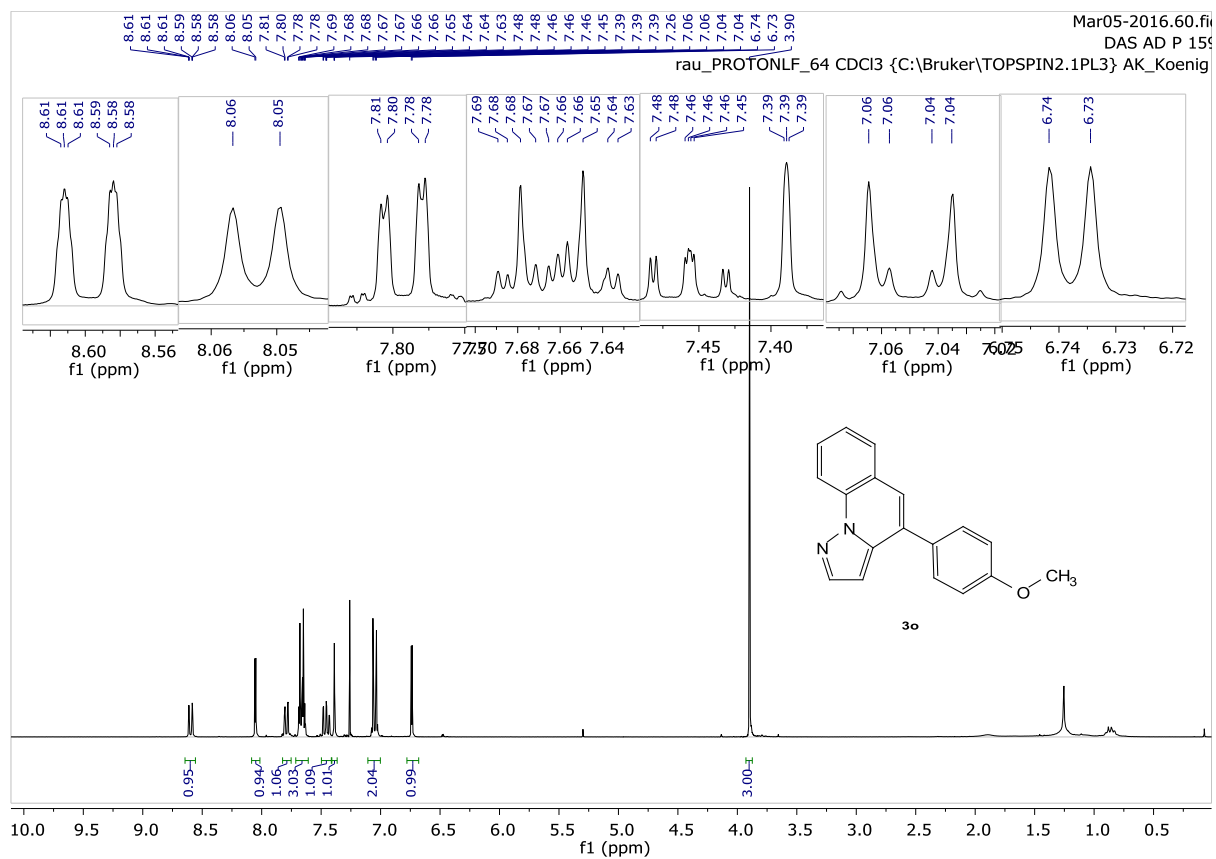




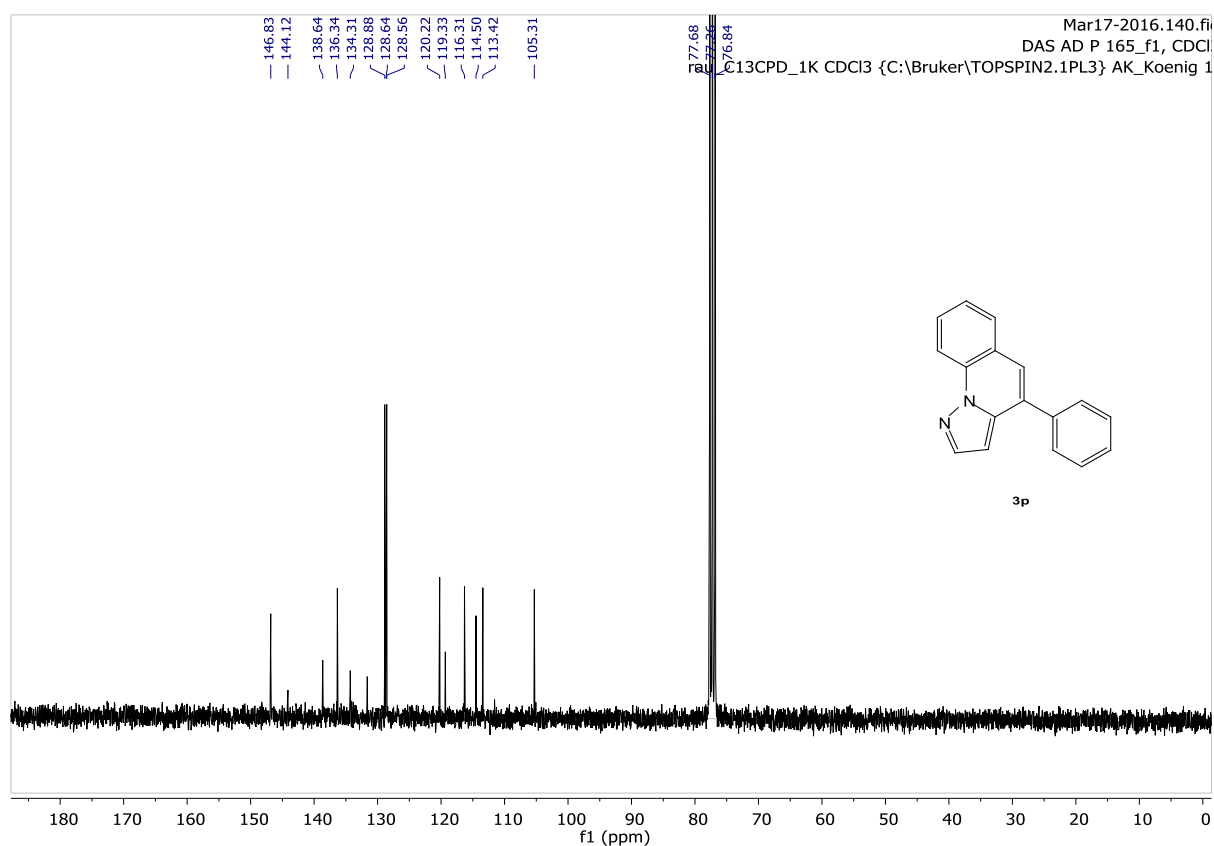
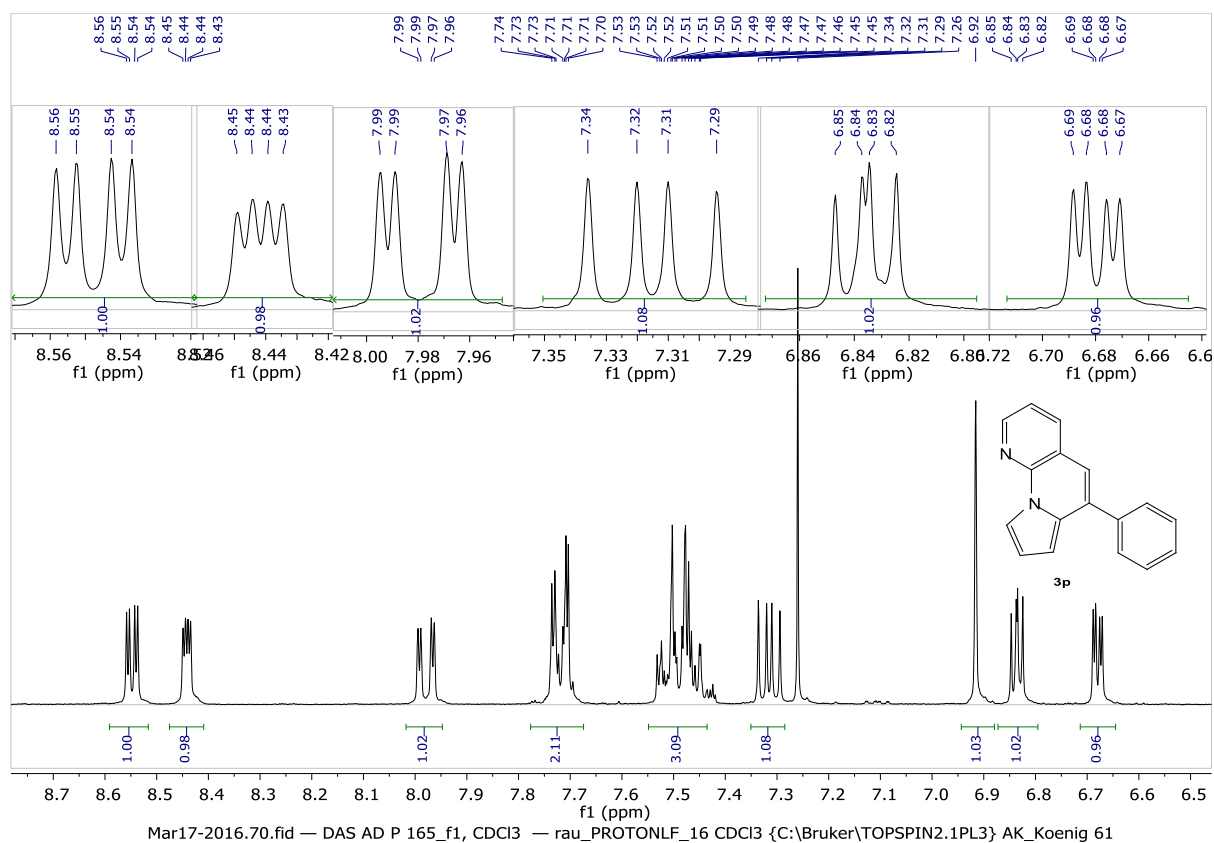


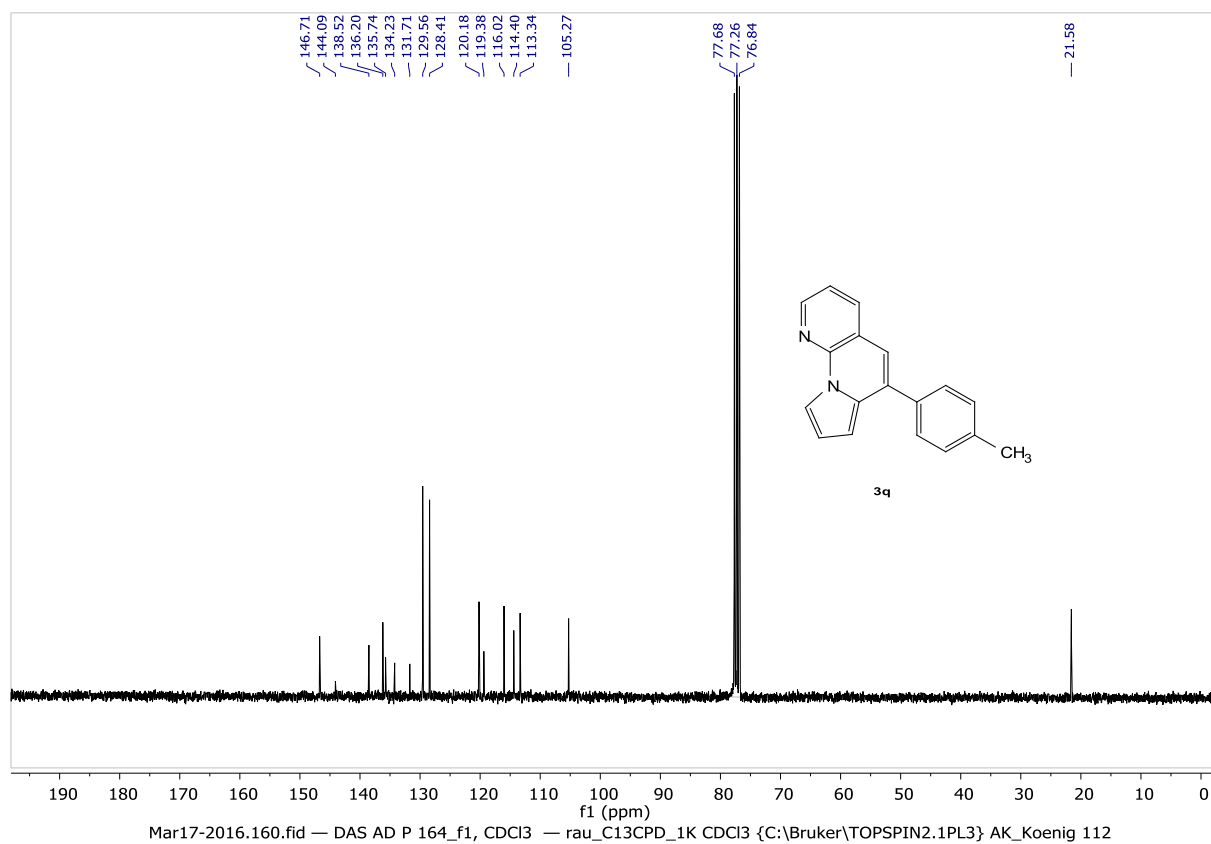
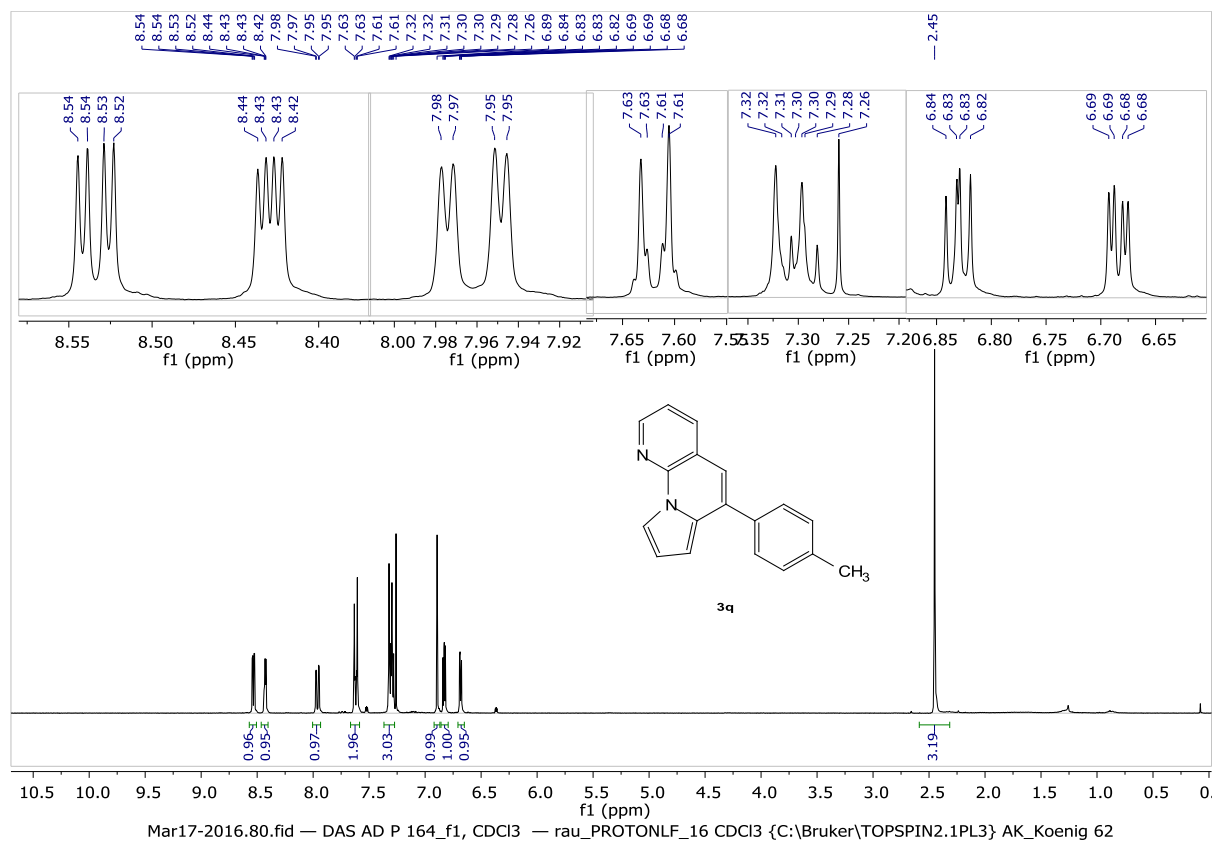


## Chapter 2



**Synthesis of Pyrrolo[1,2-a]quinolines and Ullazines by Visible Light Mediated One- and Two Fold Annulation of N-arylpyrroles with Arylalkynes**



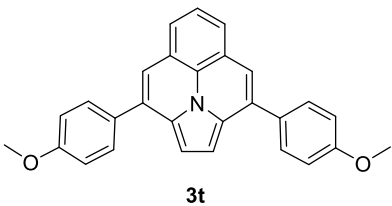
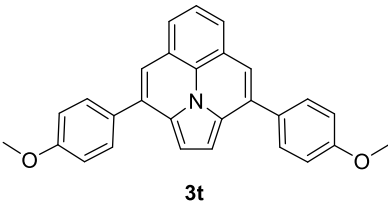


Das, AD P134 (ca.2mg/0.6ml CDCl<sub>3</sub>) Ref.: TMS ex  
rau\_PROTON16 CDCl<sub>3</sub> {C:\Bruker\TopSpin3.1PL7} puk0622

Chemical structure of **3s** is shown above the spectrum.

Integration values (from left to right): 4.18, 2.17, 1.35, 4.07, 2.07, 2.15, 6.00.





## 2.5 References

1. G. W. Gribble, *Comprehensive Heterocyclic Chemistry II*, Pergamon, 2nd edn, **1996**, p. 207.
2. A. Facchetti, *Chem. Mater.* **2011**, *23*, 733-758.
3. A. Carbone, M. Pennati, B. Parrino, A. Lopergolo, P. Barraja, A. Montalbano, V. Spano, S. Sbarra, V. Doldi, M. De Cesare, G. Cirrincione, P. Diana, N. Zaffaroni, *J. Med. Chem.* **2013**, *56*, 7060-7072.
4. K. Tsuji, H. Tsubouchi, H. Ishikawa, *Chem. Pharm. Bull.* **1995**, *43*, 1678-1682.
5. S. M. Gomha, K. M. Dawood, *J. Chem. Res.* **2014**, *38*, 515-576.
6. S. Cai, J. Drewe, S. Jiang, S. Kasibhatla, J. Kuemmerle, N. Sirisoma, H. Z. Zhang, *Substituted 1-benzoyl-3-cyano-pyrrolo [1,2-a] quino- lines and analogs as activators of caspases and inducers of apoptosis*, US20050014759 A1, **2005**.
7. L. Zhu, E.-G. Kim, Y. Yi, E. Ahmed, S. A. Jenekhe, V. Coropceanu, J.-L. Bredas, *J. Phys. Chem. C.* **2010**, *114*, 20401-20409.
8. E. B. Schwartz, C. B. Knobler, D. J. Cram, *J. Am. Chem. Soc.* **1992**, *114*, 10775-10784.
9. P. J. Dijkstra, M. Skowronska-Ptasinska, D. N. Reinhoudt, H. J. Den Hertog, J. Van Eerden, S. Harkema, D. De Zeeuw, *J. Org. Chem.* **1987**, *52*, 4913-4921.
10. S. Chandrasekhar, G. S. Ranganath, *Rep. Prog. Phys.* **1990**, *53*, 57-84.
11. K. Praefcke, B. Kohne, D. Singer, *Angew. Chem. Int. Ed.* **1990**, *29*, 177.
12. G. Winters, G. Odasso, G. Galliani, L. J. Lerner, *2-Phenylpyrazolo-[1,5-a]quinoline compounds*, US4024149 A, **1977**.
13. A. Dualeh, R. Humphry-Baker, J. H. Delcamp, M. K. Nazeeruddin, M. Grätzel, *Adv. Energy Mater.* **2013**, *3*, 496-504.
14. S. P. Shukla, R. K. Tiwari, A. K. Verma, *J. Org. Chem.* **2012**, *77*, 10382.
15. D. G. Hulcoop, M. Lautens, *Org. Lett.* **2007**, *9*, 1761-1764.
16. C. Baik, D. Kim, M.-S. Kang, K. Song, S. O. Kang, J. Ko, *Tetrahedron.* **2009**, *65*, 5302-5307.
17. D. M. Schultz, J. P. Wolfe, *Org. Lett.* **2010**, *12*, 1028-1031.
18. J. Takaya, S. Udagawa, H. Kusama, N. Iwasawa, *Angew. Chem. Int. Ed.* **2008**, *47*, 4906-4909.
19. E. Ahmed, A. L. Briseno, Y. Xia, S. A. Jenekhe, *J. Am. Chem. Soc.* **2008**, *130*, 1118-1119.

20. A. Ohsawa, T. Kawaguchi, H. Igeta, *Synthesis*. **1983**, 12, 1037-1040.
21. K. M. Wald, A. A. Nada, G. Sziagyi, H. Wamhoff, *Chem. Ber.* **1980**, 113, 2884-2890.
22. M. Nayak, I. Kim, *Org. Biomol. Chem.* **2015**, 13, 9697-9708.
23. D. I. Chai, M. Lautens, *J. Org. Chem.* **2009**, 74, 3054-3061.
24. A. K. Verma, T. Kesharwani, J. Singh, V. Tandon, R. C. Larock, *Angew. Chem., Int. Ed.* **2009**, 48, 1138-1143.
25. M. Baumann, I. R. Baxendale, *J. Org. Chem.* **2015**, 80, 10806-10816.
26. N. Umeda, K. Hirano, T. Satoh, N. Shibata, H. Sato, M. Miura, *J. Org. Chem.* **2011**, 76, 13-24.
27. R. Morioka, K. Nobushige, T. Satoh, K. Hirano, M. Miura, *Org. Lett.* **2015**, 17, 3130-3133.
28. F. Dumitrascu, E. Georgescu, F. Georgescu, M. Popa, D. Dumitrescu, *Molecules*. **2013**, 18, 2635-2645.
29. S. Linde, A. Loschberger, T. Klein, M. Heidbreder, S. Wolter, M. Heilemann, M. Sauer, *Nat. Protoc.* **2011**, 6, 991-1009.
30. I. Ghosh, B. König, *Angew. Chem. Int. Ed.* **2016**, 55, 7676-7679.
31. J. M. R. Narayanam, C. R. J. Stephenson, *Chem. Soc. Rev.* **2011**, 40, 102-113.
32. C. K. Prier, D. A. Rankic, D. W. C. MacMillan, *Chem. Rev.* **2013**, 113, 5322-5363.
33. . I. Ghosh, T. Ghosh, J. I. Bardagi, B. König, *Science*. **2014**, 346, 725-728.
34. H. Kim, C. Lee, *Angew. Chem. Int. Ed.* **2012**, 51, 12303-12306.
35. J. D. Nguyen, E. M. D'Amato, J. M. Narayanam, C. R. Stephenson, *Nat. Chem.* **2012**, 4, 854-859.
36. C. Costentin, M. Robert, J.-M. Saveant, *J. Am. Chem. Soc.* **2004**, 126, 16051-16057.
37. A. H. Jackson, P. Smith, *Chem. Commun.* **1967**, DOI: 10.1039/C19670000264.
38. H. Balli, M. Zeller, *Helv. Chim. Acta.* **1983**, 66, 2135-2139.
39. K.-I. Kanno, Y. Liu, A. Iesato, K. Nakajima, T. Takahashi, *Org. Lett.* **2005**, 7, 5453-5456.
40. J. H. Delcamp, A. Yella, T. W. Holcombe, M. K. Nazeeruddin, M. Graetzel, *Angew. Chem. Int. Ed.* **2013**, 52, 376-380.
41. S. van de Linde, I. Krstic, T. Prisner, S. Doose, M. Heilemann, M. Sauer, *Photochem. Photobiol. Sci.* **2011**, 10, 499-506.
42. C. K. Lee, J. H. Jun, J. S. Yu, *J. Heterocycl. Chem.* **2000**, 37, 15-24.
43. A. Fürstner, V. Mamane, *J. Org. Chem.* **2002**, 67, 6264-6267.



44. J. H. Delcamp, A. Yella, T. W. Holcombe, M. K. Nazeeruddin, M. Graetzel, *Angew. Chem. Int. Ed.* **2013**, 52, 376-380.
45. F. Diness, D. P. Fairlie, *Angew. Chem. Int. Ed.* **2012**, 51, 8012-8016.
46. D. I. Chai, M. J. Lautens, *J. Org. Chem.* **2009**, 74, 3054-3061.
47. A. K. Verma, S. P. Shukla, J. Singh, V. Rustagi, *J. Org. Chem.* **2011**, 76, 5670-5673.
48. S. P. Shukla, R. K. Tiwari, A. K. Verma, *J. Org. Chem.* **2012**, 77, 10382-10392.
49. H. Balli, M. Zeller, *Helv. Chim. Acta.* **1983**, 66, 2135-2139.



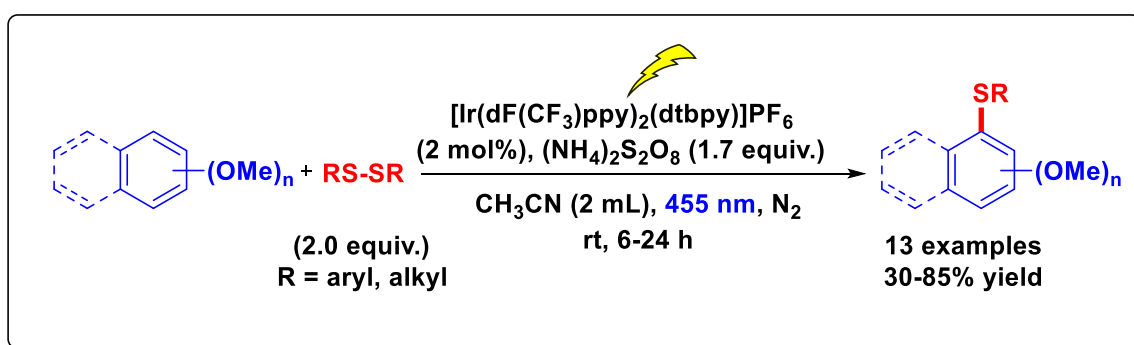
# *Chapter 3*

## *3. Synthesis of Aryl Sulfides via Radical-Radical Cross Coupling of Electron Rich Arenes using Visible Light Photoredox Catalysis*



## Abstract

Electron rich arenes react with aryl and alkyl disulfides in the presence of catalytic amounts of  $[\text{Ir}(\text{dF}(\text{CF}_3)\text{ppy})_2(\text{dtbpy})]\text{PF}_6$  and  $(\text{NH}_4)_2\text{S}_2\text{O}_8$  under blue light irradiation to form aryl thiols. The reaction proceeds at room temperature and avoids the use of pre-functionalized arenes. Experimental evidence suggests a radical-radical cross coupling mechanism.



---

**This chapter is a manuscript, prepared for submission to a journal:**

A. Das, M. Maity, B. König; manuscript in progress.

A.D. performed all the experimental work and wrote the manuscript. M. M. performed the spectroscopic experiments and some photocatalytic reactions. B.K. supervised the project and is the corresponding author.

### 3.1 Introduction

The generation of carbon-sulfur bonds has become an important task in organic synthesis because of their abundance in natural products and drugs.<sup>[1-3]</sup> They are used as organic semiconductors, antidepressant or as antileukotriene agents (**Figure 1**). Three of five most selling drugs in the market in 2015 were organosulfur compounds. The vast majority of methods for C-S bond synthesis use transition metal catalyzed cross coupling of thiols and their derivatives with organohalides,<sup>[4a-c]</sup> arylboronic acids,<sup>[5]</sup> aryl triflates<sup>[6]</sup> and diazonium salts.<sup>[7]</sup> The metals used are palladium,<sup>[8a-c]</sup> copper,<sup>[9a-h]</sup> nickel,<sup>[10a-c]</sup> iron,<sup>[11a-e]</sup> cobalt<sup>[12a-c]</sup> and rhodium.<sup>[13a-b]</sup> Aryl sulfides are also synthesized by cross coupling of thiols and aryl Grignard/aryl zinc reagents.<sup>[14a-b]</sup> However, most of these methods require harsh reaction conditions, external additives and high temperatures. These transformations need pre-functionalized arenes, while direct C-S sulfonylation by C-H functionalization would be more desirable and cost effective. So far, only a few reports on direct C-H functionalization using transition metals and metal free<sup>[15]</sup> condition and different sources of sulfur, for example arylsulfonyl chlorides, sodium arylsulfonates, sulfinic acids and arylsulfonyl hydrazides have been reported (**Scheme 1**). The protocols require pre-functionalized sulfonylating reagents, which must be synthesized. Recently Lei and co-workers reported a DDQ mediated selective radical-radical cross-coupling between electron rich arenes and thiols.<sup>[16]</sup> Miyake *et. al.*, reported the visible light promoted cross coupling reaction between aryl halides and aryl thiols *via* an intermolecular charge transfer using Cs<sub>2</sub>CO<sub>3</sub> as base.<sup>[17]</sup> Two recent reports showed the synthesis of C-3 sulfonylated indoles and 3-sulfonylimidazopyridine *via* C-H functionalization using Rose Bengal as photocatalyst.<sup>[18-19]</sup> In general, the arylation reactions use the reductive cycle of the photocatalyst and for this, electron poor arenes are required. In this article, we report the development of a mild and efficient oxidative photocatalytic method of thiolation of electron rich di- and trimethoxybenzene arenes with aryl disulfides and (NH<sub>4</sub>)<sub>2</sub>S<sub>2</sub>O<sub>8</sub> as an external oxidant (**Scheme 2**).

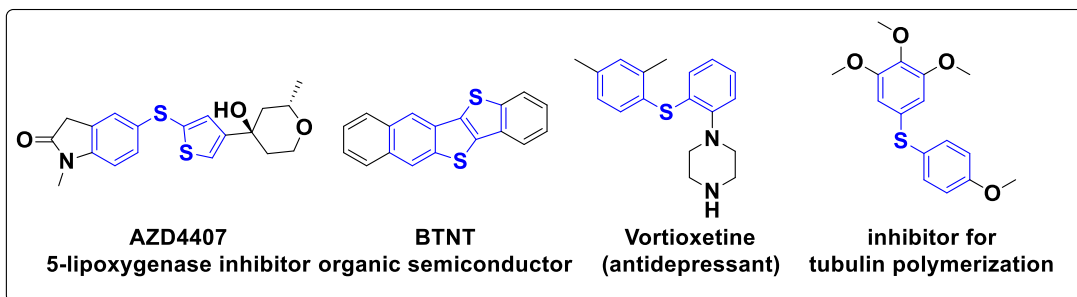
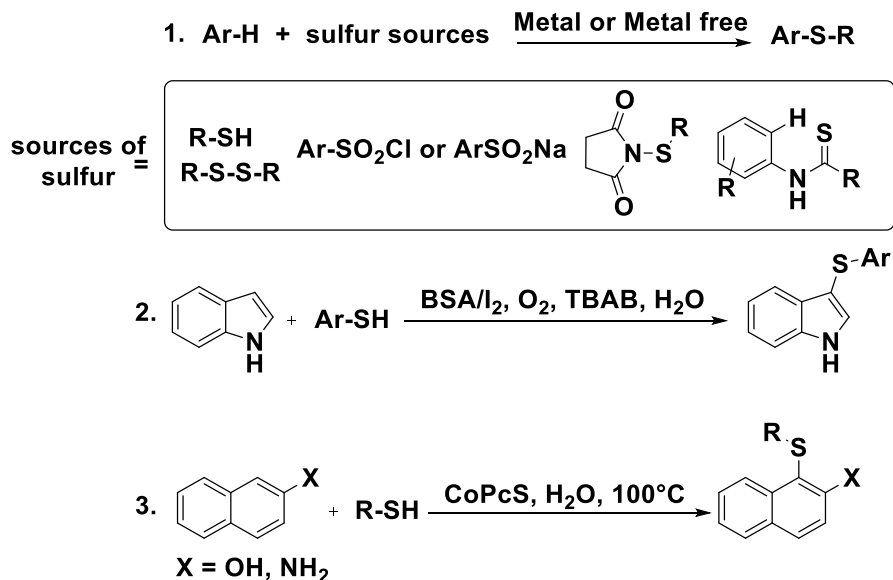
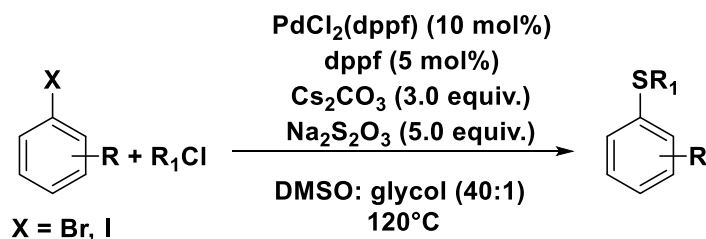


**Figure 1:** Selected examples of sulfenylated heterocycles used in pharmaceutical and material chemistry.

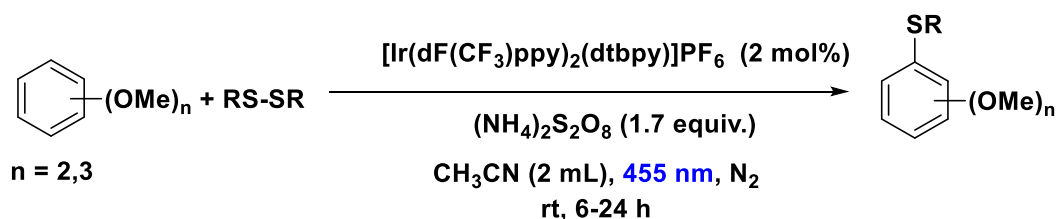


**Scheme 1:** Synthetic routes to organosulfur compounds.

## Palladium catalyzed aryl thiol synthesis



## Our photocatalyzed method



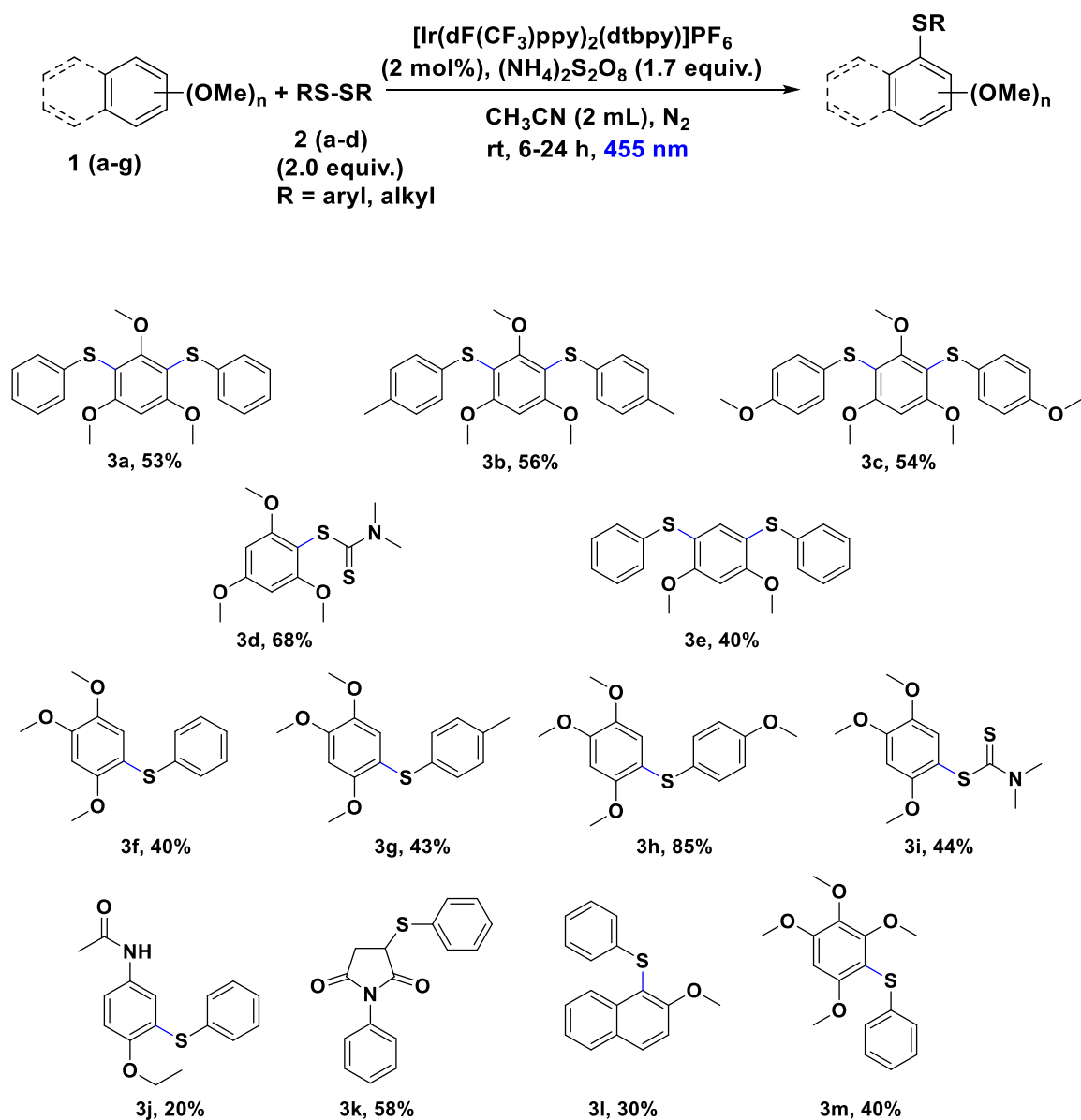
Scheme 2: Aryl sulfide synthesis.

## 3.2 Results and discussions

1,2,4 Trimethoxybenzene and diphenyl disulfide were employed as the model substrates to test our proposal and to optimize the reaction conditions. Our developed photocatalytic method allows the activation of electron rich alkoxyarenes for the direct C-H sulfenylation reaction using visible light and  $[\text{Ir}(\text{dF}(\text{CF}_3)\text{ppy})_2(\text{dtbbpy})]\text{PF}_6$  as the photocatalyst. The reaction was carried out under nitrogen under visible light irradiation at 455 nm. The oxidation potential of this test arene is 1.02 V *vs* SCE, which could be easily oxidized by  $[\text{Ir}(\text{dF}(\text{CF}_3)\text{ppy})_2(\text{dtbbpy})]\text{PF}_6$  having an excited state oxidation potential of 1.21 V *vs* SCE. Other photocatalysts like  $\text{Ru}(\text{bpy})_3\text{Cl}_2$ ,  $\text{Ru}(\text{bpz})_3\text{PF}_6$ , DDQ, acridinium dyes, Eosin Y, Eosin Y disodium salt and 4-CzIPN were tried for this transformation, but under our reaction conditions either the conversion was poor or the degradation of the photocatalyst was observed. (see Supporting Information **Table 1**). The organic dye 9-mesityl-10-phenylacridinium tetrafluoroborate completely decomposed in the presence of excess disulfide within 30 minutes of irradiation.  $[\text{Ir}(\text{dF}(\text{CF}_3)\text{ppy})_2(\text{dtbbpy})]\text{PF}_6$  was found to be the best photocatalyst and in this case,  $\text{CH}_3\text{CN}$  was the best solvent compared to DMF, DMSO and DCE. When thiophenol was used as the sulfur source, diphenyl disulfide was obtained

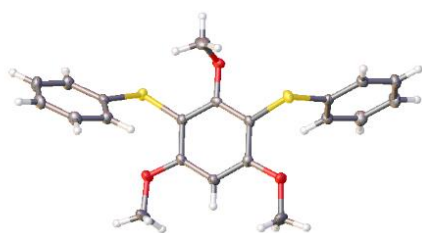


as a major side product, which in turn hindered the arylation process and resulted in lots of other oxidized products of thiophenol. So, the easily available diphenyl disulfide was added as the thiolating agent. Addition of excess disulfide (*e.g.*, 5 equivalents) resulted in the formation of thiophenol as a major side product along with other oxidized sulfur species. So, after screening the amounts of disulfide from 0.5 equivalents to 5 equivalents, we observed, the addition of two equivalents of disulfide was optimal. The photocatalytic reaction was very slow when air was used as an oxidant, also it led to various oxidation products of the sulfur and the degradation of the photocatalyst was observed upon irradiation. So,  $(\text{NH}_4)_2\text{S}_2\text{O}_8$  was used as an external oxidant. Addition of *tert*-butyl hydroperoxide (TBHP) as an oxidant completely led to degradation of the reaction mixture, also when nitrobenzene ( $\text{PhNO}_2$ ) was used as oxidant, trace amounts of product were observed along with the formation of aniline, likely arising from the regeneration of the catalyst. Control experiments concluded that both the light and photocatalyst were necessary to carry out the arylation reaction (see Supporting Information **Table 2**). With these conditions in hand, we carried out the reaction on electron rich di- and trimethoxyarenes. The reactions were complete within 6 to 24 hours and the products were obtained in moderate yields. The best yield of 85% was observed when the electron rich bis(4-methoxyphenyl) disulfide was employed as the thiolating agent (**3h**). With symmetrical arenes, diarylation was observed as the mono arylated product formed initially in the reaction was more reactive than the starting material and reacted again to form the diaryl thiol product. When 1-phenyl-1 *H*-pyrrole-2,5-dione was employed as the arene, the sulfenylation occurred exclusively at the double bond instead at the arene to give the product **3k** in 58% yield and trace amount of diarylation product at the aromatic ring was observed. With 1-phenyl-1 *H*-pyrrole-2,5-dione was employed as the arene, the sulfenylation occurred exclusively at the double bond instead at the arene to give the product **3k** in 58% yield and trace amount of diarylation product at the aromatic ring was observed. When 2-methoxynaphthalene was used as the substrate, the product was obtained in 30% yield (**3l**) which shows the limitation of our photocatalytic method. The oxidation potential for this arene is 1.5 V *vs* SCE and therefore is higher than the excited state oxidation potential of the photocatalyst.

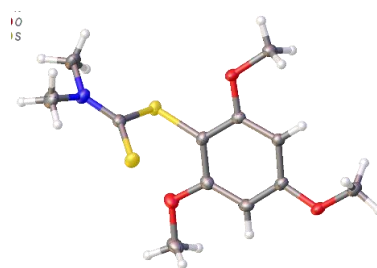


The reactions were performed with 1(a-g) (0.1 mmol) and 2(a-d) (2.0 equiv.),  $(\text{NH}_4)_2\text{S}_2\text{O}_8$  (1.7 equiv.) and  $[\text{Ir}(\text{dF}(\text{CF}_3)\text{ppy})_2(\text{dtbpy})]\text{PF}_6$  (2 mol%) in 2 mL of  $\text{CH}_3\text{CN}$ . For reaction times see experimental section.

**Scheme 3:** Substrate scope for aryl thiol syntheses.



**3a**



**3d**

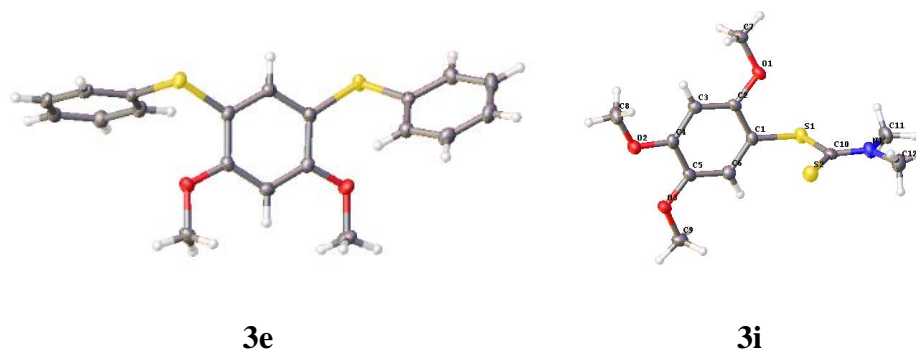
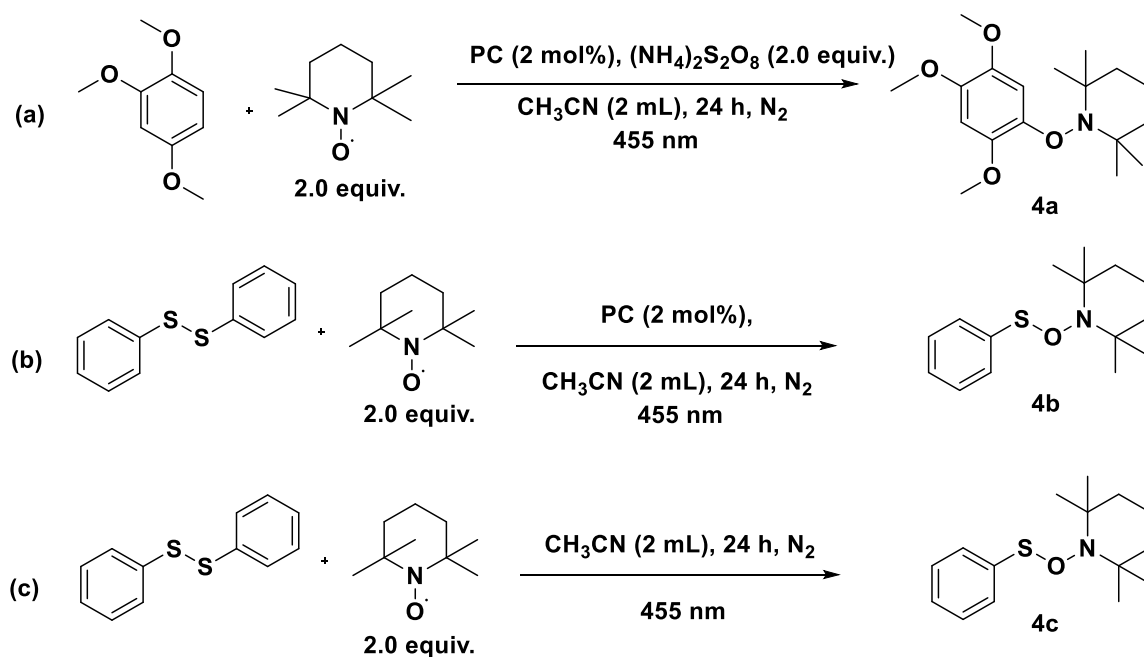


**Figure 2:** Crystal structures of compounds **3a**, **3e**, **3d** and **3i**.

Various control experiments were performed to support the proposed reaction mechanism, which is shown in **Scheme 4**. Two equivalents of 2,2,6,6-tetramethylpiperidin-1-oxyl (TEMPO), a radical scavenger were added to 1,2,4-trimethoxybenzene (**Scheme 4a**), in the presence of  $[\text{Ir}(\text{dF}(\text{CF}_3)\text{ppy})_2(\text{dtbpy})]\text{PF}_6$ , ammonium thiosulfate and 455 nm LED irradiation. The reaction mixture was analyzed by mass spectrometry, which showed the molecular ion indicating the formation of the proposed TEMPO adduct with the arene radical intermediate. Also, when diphenyl disulfide was irradiated with TEMPO in the presence and absence of the photocatalyst, (**Scheme 4b and 4c**) the adduct 2,2,6,6-tetramethyl-1-((phenylthio)oxy)piperidine was obtained in both cases (see experimental section) for the HRMS analysis of TEMPO adduct. These radical trapping experiments show that, initially the radical cation of the arene is formed by the excited photocatalyst, which then is trapped by the radical scavenger TEMPO. S-S bond cleavage has been reported for alkyl- and aryl- disulfides in an oxidative<sup>[20-22]</sup> and triplet sensitized mechanism.<sup>[23]</sup> Also, it is well known in literature that the aromatic disulfides are cleaved homolytically under UV irradiation yielding the corresponding radicals.<sup>[24]</sup> A recent study from Nicewicz showed that an aryl disulfide could be cleaved by irradiation with visible light.<sup>[25]</sup>



**Scheme 4:** Radical trapping experiments.

Some spectroscopic investigations (**Figure 3**) gave valuable information about the mechanism of the photoredox catalytic cycle. The luminescence intensity of  $[\text{Ir}(\text{dF}(\text{CF}_3)\text{ppy})_2(\text{dtbpy})]\text{PF}_6$  was quenched upon successive addition of 1,2,4-trimethoxybenzene (oxidation potential +1.02 V *vs* SCE) (**Figure 3a**). The values are similar to the estimated excited state oxidation potential of  $[\text{Ir}(\text{dF}(\text{CF}_3)\text{ppy})_2(\text{dtbpy})]\text{PF}_6$  (+1.21 V *vs* SCE in acetonitrile). On the other hand, the luminescence was quenched negligible on addition of diphenyl disulfide (**Figure 3b**). Stern Volmer quenching studies showed that the arene is quenched at a much higher rate than the disulfide (**Figure 3c**). This indicated that the oxidation of the arene was the key step in initiating the C-H sulfenylation reaction. Anisole does not quench the luminescence of  $[\text{Ir}(\text{dF}(\text{CF}_3)\text{ppy})_2(\text{dtbpy})]\text{PF}_6$  and also did not give a sulfenylated product under our photocatalytic conditions. This is rationalized by the oxidation potential of anisole of +1.76 V *vs* SCE, which is higher than the estimated excited state oxidation potential of the photocatalyst.

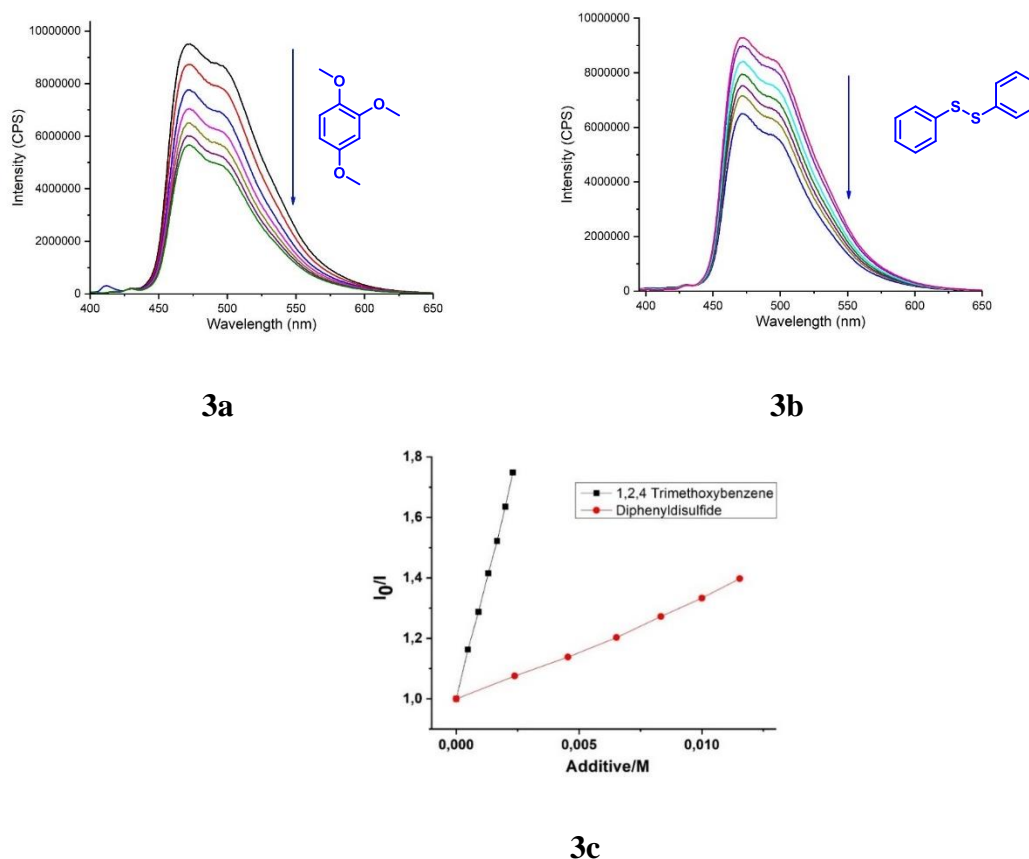
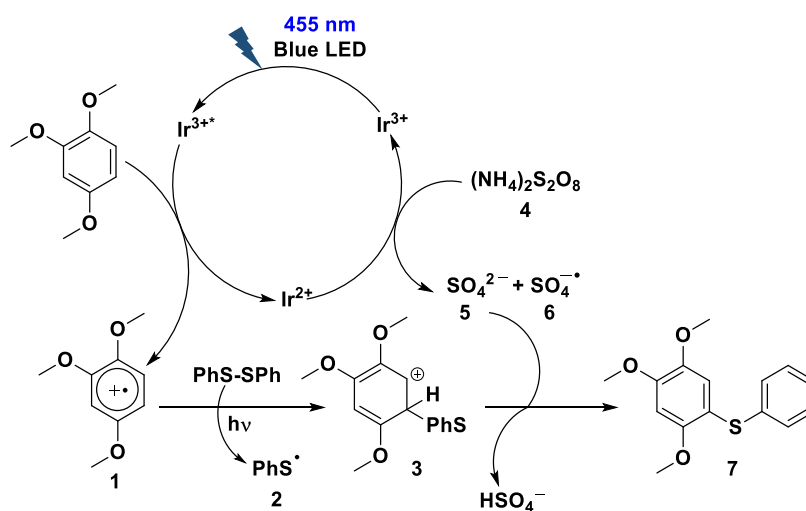


**Figure 3:** (a) Changes in the fluorescence spectra (in this case intensity,  $\lambda_{\text{Ex}} = 455 \text{ nm}$ ) of  $[\text{Ir}(\text{dF}(\text{CF}_3)\text{ppy})_2(\text{dtbbpy})]\text{PF}_6$  upon the addition of 1,2,4-trimethoxybenzene in  $\text{CH}_3\text{CN}$ . (b) Changes in the fluorescence spectra upon the addition of diphenyl disulfide in  $\text{CH}_3\text{CN}$ . (c) Stern Volmer quenching plot of Iridium catalyst in the presence of 1,2,4-trimethoxybenzene and diphenyl disulfide.  $K_q(\text{arene}) = 318 \pm 2.6 \text{ M}^{-1}\text{L}$  and  $K_q(\text{disulfide}) = 36 \pm 0.7 \text{ M}^{-1}\text{L}$ .

Based on the above experimental results, spectroscopic investigations and literature reports, we propose a photocatalytic mechanism (**Scheme 5**). Upon photoexcitation,  $[\text{Ir}(\text{dF}(\text{CF}_3)\text{ppy})_2(\text{dtbbpy})]\text{PF}_6$  forms an excited state  $^*[\text{Ir}(\text{dF}(\text{CF}_3)\text{ppy})_2(\text{dtbbpy})]\text{PF}_6$  which accepts an electron from the arene and converts it to its corresponding radical cation **1**. Ammonium persulfate present in the reaction mixture could oxidize the reduced photocatalyst and complete the catalytic cycle forming the sulfate dianion **5** and sulfate radical anion **6**. The phenyl sulfide radical **2** formed upon homolytic cleavage of diphenyl disulfide then adds to the radical cation of the arene to form the unstable cationic intermediate **3**, hydrogen atom abstraction by  $\text{SO}_4^{\cdot-}$  followed by aromatization leads to the desired product **7**.



**Scheme 5:** Proposed mechanism for visible light mediated direct C-H sulfenylation.

### 3.3. Conclusion

In conclusion, we have developed a photocatalytic method for synthesis of aryl sulfides via a radical-radical cross coupling of electron rich arenes with aryl and alkyl disulfides. The reaction conditions are mild, proceeds at room temperature and avoids the use of pre-functionalized arenes.

### 3.4. X-ray crystallographic data

X-ray crystallographic data for **3a** (CCDC 1847083), **3d** (CCDC 1847084), **3e** (CCDC 1847085 and **3i** (CCDC 1847086). These data can be obtained free of charge from The Cambridge Crystallographic Data Centre.

## 3.5 Experimental section

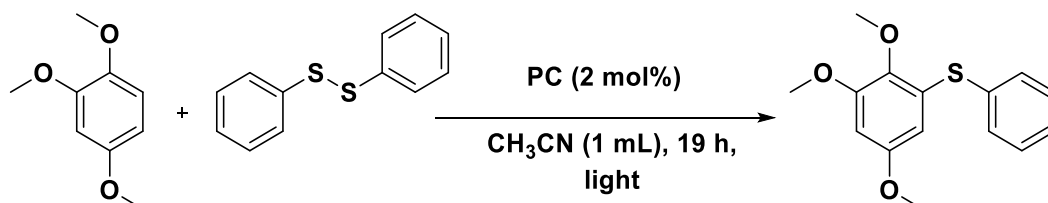
### 3.5.1 Materials and methods

Solvents and reagents were obtained from commercial sources and used without further purification. Spectroscopic grade DMF and DMSO were dried with 3 Å molecular sieves according to a reported procedure.<sup>[26]</sup>  $[\text{Ir}(\text{dF}(\text{CF}_3)\text{ppy})_2(\text{dtbbpy})]\text{PF}_6$  was synthesized according to the general procedure.<sup>[27]</sup> Proton NMR spectra were recorded on a Bruker Avance 300 MHz spectrometer and 600 MHz spectrometer in  $\text{CDCl}_3$  solution with internal solvent signal peak at 7.26 ppm. Carbon NMR were recorded at 75 MHz spectrometer and 151 MHz spectrometer in  $\text{CDCl}_3$  solution and referenced to the internal solvent signal at 77.26 ppm. Proton NMR data are reported as follows: chemical shift (ppm), multiplicity (s = singlet, d = doublet, t = triplet, q = quartet, quint = quintet, dd = doublet of doublets, ddd = doublet of doublet of doublets, td = triplet of doublets, qd = quartet of doublets, m = multiplet, br. s. = broad singlet), and coupling constants (Hz). High resolution mass spectra (HRMS) were obtained from the central analytic mass spectrometry facilities of the Faculty of Chemistry and Pharmacy, Regensburg University and are reported according to the IUPAC recommendations 2013. All reactions were monitored by thin-layer chromatography using Merck silica gel plates 60 F254; visualization was accomplished with short wave length UV light (254 nm). UV–Vis and fluorescence measurements were performed with Varian Cary 50 UV/Vis spectrophotometer and FluoroMax-4 spectrofluorometer, respectively. Electrochemical studies were carried out under argon atmosphere. The measurements were performed in acetonitrile ( $\text{CH}_3\text{CN}$ ) containing 0.1 M tetra-n-butylammonium tetrafluoroborate using ferrocene/ferrocenium ( $\text{Fc}/\text{Fc}^+$ ) as an internal reference. A glassy carbon electrode (working electrode), platinum wire (counter electrode), and silver wire (quasi-reference electrode) were employed. Spectroelectrochemical studies were carried out in an optically transparent thin layer electrochemical cell (OTTLE). Suitable crystals were selected and mounted on a MITIGEN holder oil on a GV1000/SuperNova, TitanS2 diffractometer or Atlas diffractometer. Using **Olex2** (Dolomanov et al., 2009), the structure was solved with the **ShelXT** (Sheldrick, 2015) structure solution program, using the Intrinsic Phasing solution method. The model was refined with ShelXL (Sheldrick, 2015) using Least Squares minimisation.

Standard flash chromatography was performed using silica gel of particle size 40–63  $\mu\text{m}$ . Photooxidation reactions were performed with 455 nm LEDs (OSRAM Oslon SSL 80 royal-blue LEDs ( $\lambda = 455 \text{ nm} (\pm 15 \text{ nm})$ , 3.5 V, 700 mA).

### 3.5.2 Optimization of the reactions and control experiments

**Table 1:**



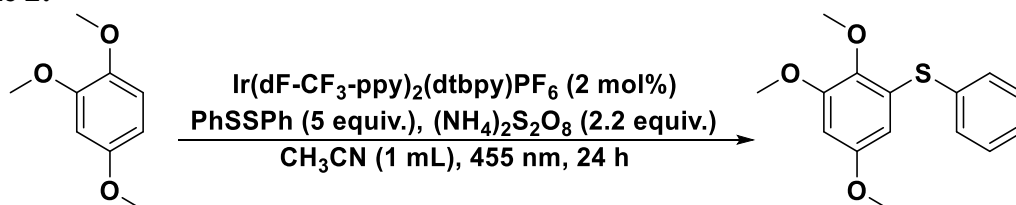
| Entry | Photocatalyst   | Oxidant                               | Light source | Air / $\text{N}_2$ | Comments   |
|-------|---|---------------------------------------|--------------|--------------------|--|
| 1     | $\text{Ir}(\text{dF-CF}_3\text{-ppy})_2(\text{dtbpy})^{3+}$ | $(\text{NH}_4)_2\text{S}_2\text{O}_8$ | 455 nm       | $\text{N}_2$       | Full conversion to product was observed in 6 hours   |
| 2     | $\text{Ir}(\text{dF-CF}_3\text{-ppy})_2(\text{dtbpy})^{3+}$ | air                                   | 455 nm       | air                | Degradation of catalyst is observed upon irradiation |
| 3     | 4-CzIPN   | air                                   | 455 nm       | air                | Degradation of catalyst is observed upon irradiation |
| 4     | 4-CzIPN   | $(\text{NH}_4)_2\text{S}_2\text{O}_8$ | 455 nm       | $\text{N}_2$       | 30% conversion of the starting material was observed |
| 5     | Eosin Y   | air                                   | 530 nm       | air                | PC bleached in 2 hours                               |
| 6     | Eosin Y   | $(\text{NH}_4)_2\text{S}_2\text{O}_8$ | 530 nm       | $\text{N}_2$       | Degradation of catalyst is observed upon irradiation |
| 7     | Eosin Y- $\text{Na}_2$                                      | air                                   | 530 nm       | air                | Degradation of catalyst is observed upon irradiation |



**Synthesis of Aryl Sulfides via Radical-Radical Cross Coupling of Electron Rich Arenes using Visible Light Photoredox Catalysis**

|   |                         |   |        |                |  |
|---|-------------------------|---|--------|----------------|--|
| 8 | Eosin Y-Na <sub>2</sub> | (NH <sub>4</sub> ) <sub>2</sub> S <sub>2</sub> O <sub>8</sub> | 530 nm | N <sub>2</sub> | 10% conversion of the starting material was observed |
|---|-------------------------|---|--------|----------------|--|

**Table 2:**

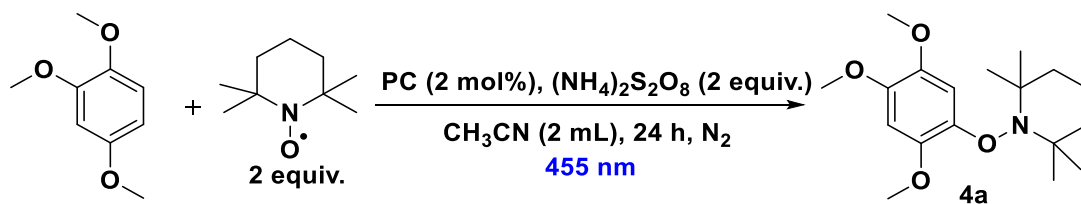


| Entry | Photocatalyst | Oxidant | N <sub>2</sub> /<br>air | Light/<br>dark | Comments  |
|-------|---------------|---------|-------------------------|----------------|---|
| 1     | ✓             | ✓       | N <sub>2</sub>          | dark           | Only Starting material, no conversion   |
| 2     | ✓             | ✓       | N <sub>2</sub>          | 455 nm         | Full conversion to product  |
| 3     | ✓             | ✓       | air                     | dark           | Only Starting material, some oxidative side reactions of the disulphide, no product formation |
| 4     | ✓             | ✓       | air                     | 455 nm         | Catalyst bleached immediately   |
| 5     | ✓             | ✗       | N <sub>2</sub>          | dark           | Only Starting material, no conversion   |
| 6     | ✓             |         | N <sub>2</sub>          | 455 nm         | 10% conversion by GC  |
| 7     | ✓             | ✗       | air                     | dark           | Only Starting material, no conversion   |
| 8     | ✓             |         | air                     | 455 nm         | Catalyst bleached immediately   |

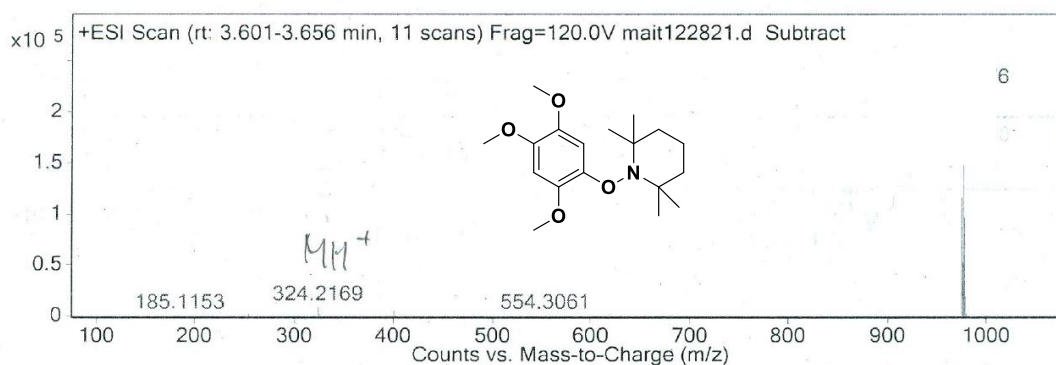
**HRMS analysis of the TEMPO adduct**

A solution of 1,2,4 trimethoxybenzene in CH<sub>3</sub>CN with 2 mol% [Ir(dF(CF<sub>3</sub>)ppy)<sub>2</sub>(dtbbpy)]PF<sub>6</sub>, 2.2 equivalents (NH<sub>4</sub>)<sub>2</sub>S<sub>2</sub>O<sub>8</sub> and 2 equivalents TEMPO was irradiated with a 455 nm LED under N<sub>2</sub> at 25 °C. The reaction mixture was analyzed by

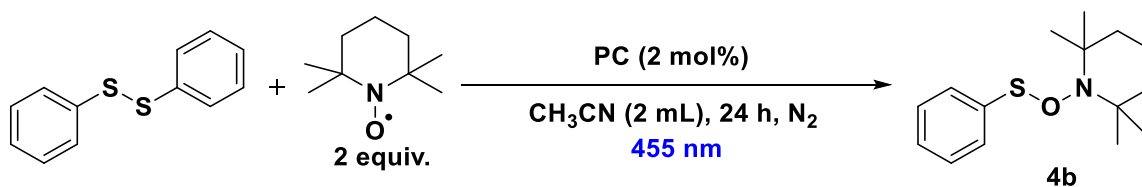
HRMS, which showed the exact molecular ion indicating the formation of the proposed TEMPO adduct to the aryl radical cation intermediate.



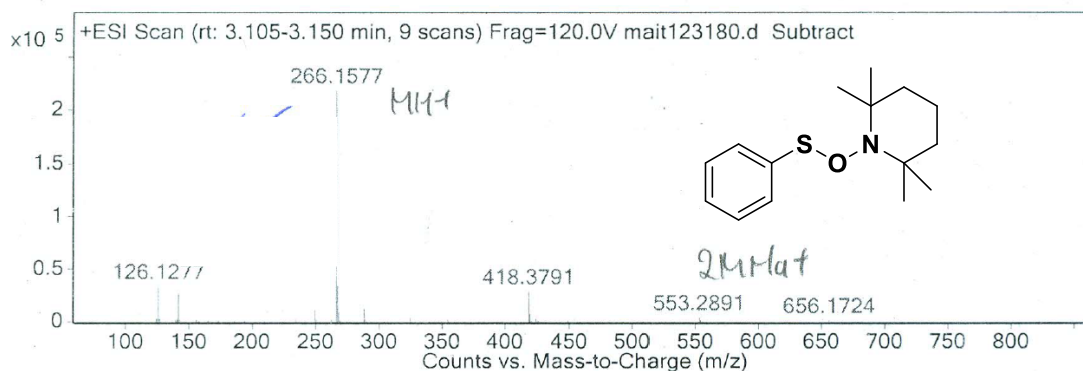
**HRMS [M+H]<sup>+</sup> C<sub>18</sub>H<sub>29</sub>NO<sub>4</sub> calculated 324.2175 found 324.2169**



A solution of diphenyl disulfide in CH<sub>3</sub>CN with 2 mol% [Ir(dF(CF<sub>3</sub>)ppy)<sub>2</sub>(dtbpy)]PF<sub>6</sub> and 2 equivalents TEMPO was irradiated with a 455 nm LED under N<sub>2</sub> at 25 °C. The reaction mixture was analyzed by HRMS, which showed the exact molecular ion indicating the formation of the proposed TEMPO adduct to the aryl radical cation intermediate.



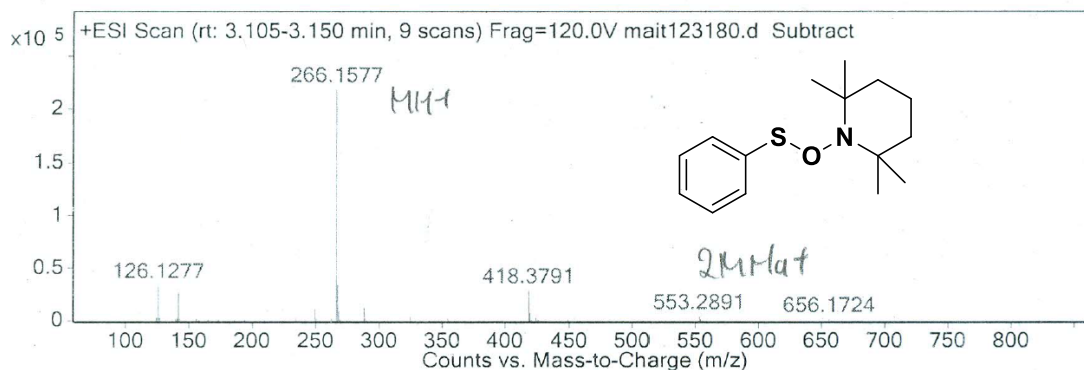
**HRMS [M+H]<sup>+</sup> C<sub>15</sub>H<sub>23</sub>NOS calculated 266.1579 found 266.1577**



### *Synthesis of Aryl Sulfides via Radical-Radical Cross Coupling of Electron Rich Arenes using Visible Light Photoredox Catalysis*

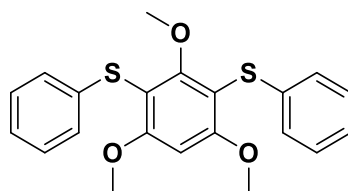
A solution of diphenyl disulfide in CH<sub>3</sub>CN and 2 equivalents TEMPO was irradiated with a 455 nm LED under N<sub>2</sub> at 25 °C. The reaction mixture was analyzed by HRMS, which showed the exact molecular ion indicating the formation of the proposed TEMPO adduct to the aryl radical cation intermediate.

**HRMS [M+H]<sup>+</sup> C<sub>15</sub>H<sub>23</sub>NOS** calculated 266.1579 found 266.1577



### 3.5.3 General procedure for C–H sulfenylation

In a 5 mL snap vial with magnetic stirring bar, the arene (0.1 mmol, 1.0 equiv.), the aryl disulfide (2.0 equiv.), (NH<sub>4</sub>)<sub>2</sub>S<sub>2</sub>O<sub>8</sub> (1.7 equiv.) and [Ir(dF(CF<sub>3</sub>)ppy)<sub>2</sub>(dtbpy)]PF<sub>6</sub> (0.002 mmol, 0.02 equiv.) were added. Dry CH<sub>3</sub>CN (2.0 mL) were added under N<sub>2</sub> and the mixture was degassed by “pump-freeze-thaw” cycles (×3) via a syringe needle. This reaction mixture was irradiated through the plane bottom side of the snap vial using a 455 nm LED under nitrogen at 25°C. The reaction progress was monitored by GC analysis. After 6 h to 24 h of irradiation, the reaction mixture was transferred to separating funnel, diluted with ethyl acetate and washed with 15 mL of water. The aqueous layer was washed three times (3 × 15 mL) with ethyl acetate. The combined organic phases were dried over MgSO<sub>4</sub>, filtered and concentrated in vacuum. Purification of the crude product was achieved by flash column chromatography using petrol ether/ethyl acetate as eluent.

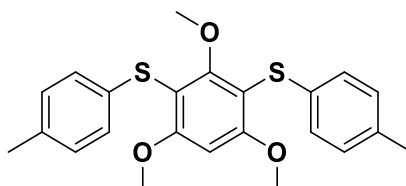
**Synthesis of (2,4,6-trimethoxy-1,3-phenylene)bis(phenylsulfane) (3a)<sup>[28]</sup>**

The compound was prepared according to the general procedure using 16.8 mg of 1,3,5-trimethoxybenzene, 2.2 mg of  $[\text{Ir}(\text{dF}(\text{CF}_3)\text{ppy})_2(\text{dtbpy})]\text{PF}_6$ , 43.6 mg of diphenyl disulfide, 40 mg of  $(\text{NH}_4)_2\text{S}_2\text{O}_8$  and 2.0 mL dry  $\text{CH}_3\text{CN}$ . The reaction mixture was irradiated for 6 hours under  $\text{N}_2$ . Purification of the crude product was achieved by flash column chromatography using petrol ether/ ethylacetate (85:15) as eluent to yield the desired compound as white solid (20.4 mg, 53%).

**$^1\text{H}$  NMR** ( $\text{CDCl}_3$ , 300 MHz, ppm):  $\delta$  7.25-7.15 (m, 4H), 7.08-7.05 (m, 4H), 6.43 (s, 1H), 3.87 (s, 6H), 3.76 (s, 3H).

**$^{13}\text{C}$  NMR** ( $\text{CDCl}_3$ , 75 MHz, ppm):  $\delta$  166.3, 163.7, 138.4, 128.8, 126.2, 125.0, 106.8, 92.5, 62.5, 56.5.

**HRMS** [ $\text{M}^+$ ]  $\text{C}_{21}\text{H}_{20}\text{O}_3\text{S}_2$  calculated 384.0848 found 384.0852.

**Synthesis of (2,4,6-trimethoxy-1,3-phenylene)bis(p-tolylsulfane) (3b)**

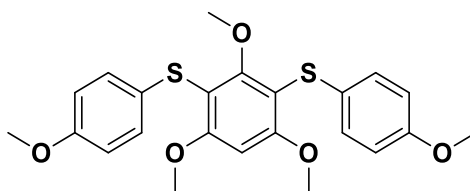
The compound was prepared according to the general procedure using 16.8 mg of 1,3,5-trimethoxybenzene, 2.2 mg of  $[\text{Ir}(\text{dF}(\text{CF}_3)\text{ppy})_2(\text{dtbpy})]\text{PF}_6$ , 49.2 mg of 1,2-di-*p*-tolylsulfane, 40 mg of  $(\text{NH}_4)_2\text{S}_2\text{O}_8$  and 2.0 mL dry  $\text{CH}_3\text{CN}$ . The reaction mixture was irradiated for 6 h under  $\text{N}_2$ . Purification of the crude product was achieved by flash column chromatography using petrol ether/ ethylacetate (85:15) as eluent to yield the desired compound as white solid (23.1 mg, 56%).

**$^1\text{H}$  NMR** ( $\text{CDCl}_3$ , 300 MHz, ppm):  $\delta$  6.99 (s, 8H), 6.41 (s, 1H), 3.86 (s, 6H), 3.76 (s, 3H), 2.26 (s, 6H).

**$^{13}\text{C}$  NMR** ( $\text{CDCl}_3$ , 75 MHz, ppm):  $\delta$  166.1, 163.5, 134.8, 129.6, 126.6, 107.4, 92.5, 62.5, 56.5, 21.1.

**HRMS** [ $\text{M}^+$ ]  $\text{C}_{23}\text{H}_{24}\text{O}_3\text{S}_2$  calculated 412.1161 found 412.1170.

**Synthesis of (2,4,6-trimethoxy-1,3-phenylene)bis((4-methoxyphenyl)sulfane) (3c)**



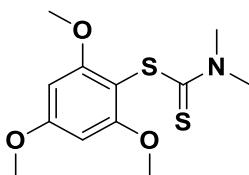
The compound was prepared according to the general procedure using 16.8 mg of 1,3,5-trimethoxybenzene, 2.2 mg of  $[\text{Ir}(\text{dF}(\text{CF}_3)\text{ppy})_2(\text{dtbpy})]\text{PF}_6$ , 55.6 mg of 1,2-bis(4-methoxyphenyl)disulfane, 40 mg of  $(\text{NH}_4)_2\text{S}_2\text{O}_8$  and 2.0 mL dry  $\text{CH}_3\text{CN}$ . The reaction mixture was irradiated for 6 hours under  $\text{N}_2$ . Purification of the crude product was achieved by flash column chromatography using petrol ether/ ethylacetate (85:15) as eluent to yield the desired compound as white solid (24.0 mg, 54%).

**$^1\text{H}$  NMR** ( $\text{CDCl}_3$ , 300 MHz, ppm):  $\delta$  7.11-7.08 (m, 4H), 6.75-6.72 (m, 4H), 6.36 (s, 1H), 3.84 (s, 6H), 3.79 (s, 3H), 3.73 (s, 6H).

**$^{13}\text{C}$  NMR** ( $\text{CDCl}_3$ , 75 MHz, ppm):  $\delta$  165.6, 163.1, 158.0, 129.3, 128.9, 114.5, 108.6, 92.6, 62.5, 56.5, 55.5.

**HRMS**  $[\text{M}+\text{H}]^+$   $\text{C}_{23}\text{H}_{24}\text{O}_5\text{S}_2$  calculated 445.1138 found 445.1140.

**Synthesis of 2,4,6-trimethoxyphenyl dimethylcarbamodithioate (3d)**

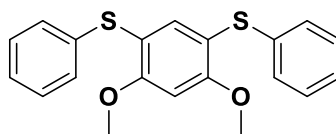


The compound was prepared according to the general procedure using 16.8 mg of 1,3,5-trimethoxybenzene, 2.2 mg of  $[\text{Ir}(\text{dF}(\text{CF}_3)\text{ppy})_2(\text{dtbpy})]\text{PF}_6$ , 47.8 mg of tetramethylthiuramdisulfid, 40 mg of  $(\text{NH}_4)_2\text{S}_2\text{O}_8$  and 2.0 mL dry  $\text{CH}_3\text{CN}$ . The reaction mixture was irradiated for 24 hours under  $\text{N}_2$ . Purification of the crude product was achieved by flash column chromatography using petrol ether/ ethylacetate (80:20) as eluent to yield the desired compound as white solid (19.6 mg, 68%).

**$^1\text{H}$  NMR** ( $\text{CDCl}_3$ , 300 MHz, ppm):  $\delta$  6.21 (s, 2H), 3.85 (s, 3H), 3.83 (s, 6H), 3.54 (s, 6H).

**$^{13}\text{C}$  NMR** ( $\text{CDCl}_3$ , 75 MHz, ppm):  $\delta$  197.6, 164.0, 162.7, 100.1, 91.4, 56.6, 55.5.

**HRMS**  $[\text{M}+\text{H}]^+$   $\text{C}_{12}\text{H}_{17}\text{NO}_3\text{S}_2$  calculated 288.0723 found 288.0727.

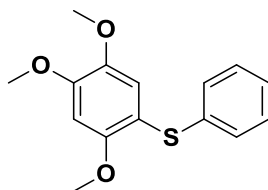
**Synthesis of (4,6-dimethoxy-1,3-phenylene)bis(phenylsulfane) (3e)**

The compound was prepared according to the general procedure using 12.7  $\mu\text{L}$  of 1,2-dimethoxybenzene, 2.2 mg of  $[\text{Ir}(\text{dF}(\text{CF}_3)\text{ppy})_2(\text{dtbpy})]\text{PF}_6$ , 43.6 mg of diphenyl disulfide, 40 mg of  $(\text{NH}_4)_2\text{S}_2\text{O}_8$  and 2.0 mL dry  $\text{CH}_3\text{CN}$ . The reaction mixture was irradiated for 6 hours under  $\text{N}_2$ . Purification of the crude product was achieved by flash column chromatography using petrol ether/ ethylacetate (85:15) as eluent to yield the desired compound as yellowish white solid (14.2 mg, 40%).

**$^1\text{H}$  NMR** ( $\text{CDCl}_3$ , 300 MHz, ppm):  $\delta$  7.39 (s, 1H), 7.25-7.10 (m, 10H), 6.55 (s, 1H), 3.88 (s, 6H).

**$^{13}\text{C}$  NMR** ( $\text{CDCl}_3$ , 75 MHz, ppm):  $\delta$  160.82, 141.35, 136.74, 129.01, 128.59, 126.04, 113.44, 96.22, 56.39.

**HRMS**[ $\text{M}^+$ ]  $\text{C}_{20}\text{H}_{18}\text{O}_2\text{S}_2$  calculated 354.0742 found 354.0743.

**Synthesis of phenyl(2,4,5-trimethoxyphenyl)sulfane (3f)<sup>[29]</sup>**

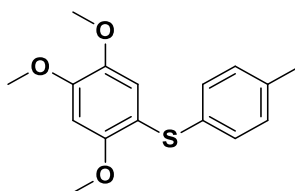
The compound was prepared according to the general procedure using 15.0  $\mu\text{L}$  of 1,2,4-trimethoxybenzene, 2.2 mg of  $[\text{Ir}(\text{dF}(\text{CF}_3)\text{ppy})_2(\text{dtbpy})]\text{PF}_6$ , 43.6 mg of diphenyl disulfide, 40 mg of  $(\text{NH}_4)_2\text{S}_2\text{O}_8$  and 2.0 mL dry  $\text{CH}_3\text{CN}$ . The reaction mixture was irradiated for 6 hours under  $\text{N}_2$ . Purification of the crude product was achieved by flash column chromatography using petrol ether/ ethylacetate (85:15) as eluent to yield the desired compound as pale yellow liquid (11.2 mg, 40%).

**$^1\text{H}$  NMR** ( $\text{CDCl}_3$ , 300 MHz, ppm):  $\delta$  7.26-7.22 (m, 3H), 7.20-7.11 (m, 2H), 6.95 (s, 1H), 6.59 (s, 1H), 3.93 (s, 3H), 3.82 (s, 3H), 3.78 (s, 3H)

**$^{13}\text{C}$  NMR** ( $\text{CDCl}_3$ , 75 MHz, ppm):  $\delta$  154.6, 150.9, 143.6, 137.9, 129.0, 127.7, 119.0, 110.0, 98.1, 57.2, 56.7, 56.3.

**HRMS**[ $\text{M}^+$ ]  $\text{C}_{15}\text{H}_{16}\text{O}_3\text{S}$  calculated 276.0814 found 276.0817.

**Synthesis of p-tolyl(2,4,5-trimethoxyphenyl)sulfane (3g)<sup>[29]</sup>**



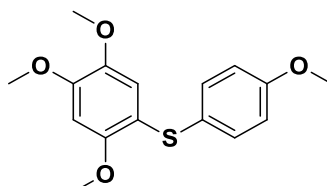
The compound was prepared according to the general procedure using 15.0  $\mu\text{L}$  of 1,2,4-trimethoxybenzene, 2.2 mg of  $[\text{Ir}(\text{dF}(\text{CF}_3)\text{ppy})_2(\text{dtbpy})]\text{PF}_6$ , 49.2 mg of 1,2-di-*p*-tolylidisulfane, 40 mg of  $(\text{NH}_4)_2\text{S}_2\text{O}_8$  and 2.0 mL dry  $\text{CH}_3\text{CN}$ . The reaction mixture was irradiated for 24 hours under  $\text{N}_2$ . Purification of the crude product was achieved by flash column chromatography using petrol ether/ ethylacetate (85:15) as eluent to yield the desired compound as white solid (12.5 mg, 43%).

**$^1\text{H}$  NMR** ( $\text{CDCl}_3$ , 300 MHz, ppm):  $\delta$  7.10-7.02 (m, 4H), 6.87 (s, 1H), 6.57 (s, 1H), 3.91 (s, 3H), 3.81 (s, 3H), 3.75 (s, 3H), 2.28 (s, 3H).

**$^{13}\text{C}$  NMR** ( $\text{CDCl}_3$ , 75 MHz, ppm):  $\delta$  154.0, 150.0, 143.5, 135.9, 133.6, 129.8, 128.8, 118.2, 98.1, 57.1, 56.7, 56.3, 21.1.

**HRMS**[ $\text{M}^+$ ]  $\text{C}_{16}\text{H}_{18}\text{O}_3\text{S}$  calculated 290.0971 found 290.0977.

**Synthesis of (4-methoxyphenyl)(2,4,5-trimethoxyphenyl)sulfane (3h)<sup>[30]</sup>**



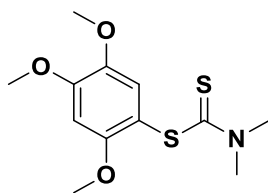
The compound was prepared according to the general procedure using 15.0  $\mu\text{L}$  of 1,2,4-trimethoxybenzene, 2.2 mg of  $[\text{Ir}(\text{dF}(\text{CF}_3)\text{ppy})_2(\text{dtbpy})]\text{PF}_6$ , 55.6 mg of 1,2-bis(4-methoxyphenyl)disulfane, 40 mg of  $(\text{NH}_4)_2\text{S}_2\text{O}_8$  and 2.0 mL dry  $\text{CH}_3\text{CN}$ . The reaction mixture was irradiated for 6 hours under  $\text{N}_2$ . Purification of the crude product was achieved by flash column chromatography using petrol ether/ ethylacetate (86:14) as eluent to yield the desired compound as pale yellow liquid (26.0 mg, 85%).

**$^1\text{H}$  NMR** ( $\text{CDCl}_3$ , 300 MHz, ppm):  $\delta$  7.25-7.22 (m, 2H), 6.83-6.80 (m, 2H), 6.71 (s, 1H), 6.53 (s, 1H), 3.87 (s, 3H), 3.82 (s, 3H), 3.76 (s, 3H), 3.69 (s, 3H).

**$^{13}\text{C}$  NMR** ( $\text{CDCl}_3$ , 75 MHz, ppm):  $\delta$  159.0, 152.8, 149.7, 143.6, 132.5, 126.4, 116.5, 114.8, 114.4, 98.1, 57.0, 56.7, 56.3, 55.5.

**HRMS**[ $\text{M}^+$ ]  $\text{C}_{16}\text{H}_{18}\text{O}_4\text{S}$  calculated 306.0920 found 306.0926.

### Synthesis of 2,4,5-trimethoxyphenyl dimethylcarbamodithioate (3i)



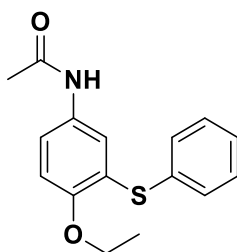
The compound was prepared according to the general procedure using 15.0  $\mu\text{L}$  of 1,2,4-trimethoxybenzene, 2.2 mg of  $[\text{Ir}(\text{dF}(\text{CF}_3)\text{ppy})_2(\text{dtbpy})]\text{PF}_6$ , 47.8 mg of tetramethylthiuramdisulfid, 40 mg of  $(\text{NH}_4)_2\text{S}_2\text{O}_8$  and 2.0 mL dry  $\text{CH}_3\text{CN}$ . The reaction mixture was irradiated for 24 hours under  $\text{N}_2$ . Purification of the crude product was achieved by flash column chromatography using petrol ether/ ethylacetate (80:20) as eluent to yield the desired compound as yellow solid (12.7 mg, 44%).

**$^1\text{H}$  NMR** ( $\text{CDCl}_3$ , 300 MHz, ppm):  $\delta$  6.89 (s, 1H), 6.61 (s, 1H), 3.94 (s, 3H), 3.86 (s, 3H), 3.84 (s, 3H), 3.54 (d,  $J = 11.1$  Hz, 6H).

**$^{13}\text{C}$  NMR** ( $\text{CDCl}_3$ , 75 MHz, ppm):  $\delta$  197.8, 156.0, 152.4, 143.3, 121.1, 109.5, 97.7, 57.3, 56.6, 56.1, 45.9, 42.1.

**HRMS**  $[\text{M}+\text{H}]^+$   $\text{C}_{12}\text{H}_{17}\text{NO}_3\text{S}_2$  calculated 288.0723 found 288.0724.

### Synthesis of *N*-(4-ethoxy-3-(phenylthio)phenyl)acetamide (3j)



The compound was prepared according to the general procedure using 17.9 mg of *N*-(4-ethoxyphenyl)acetamide, 2.2 mg of  $[\text{Ir}(\text{dF}(\text{CF}_3)\text{ppy})_2(\text{dtbpy})]\text{PF}_6$ , 43.6 mg of diphenyl disulfide, 40 mg of  $(\text{NH}_4)_2\text{S}_2\text{O}_8$  and 2.0 mL dry  $\text{CH}_3\text{CN}$ . The reaction mixture was irradiated for 24 hours under  $\text{N}_2$ . Purification of the crude product was achieved by flash column chromatography using petrol ether/ ethylacetate (85:15) as eluent to yield the desired compound as white solid (5.8 mg, 20%)

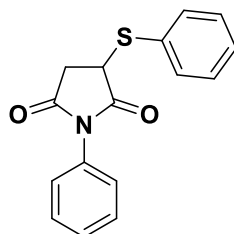
**$^1\text{H}$  NMR** ( $\text{CDCl}_3$ , 600 MHz, ppm):  $\delta$  8.23 (d,  $J = 9$  Hz, 1H), 7.86 (bs, 1H), 7.33-7.29 (m, 1H), 7.25-7.24 (m, 1H), 7.17 (t,  $J = 7.2$  Hz, 1H), 7.11 (d,  $J = 7.5$  Hz, 2H), 7.07 (d,  $J = 2.8$  Hz, 1H), 6.96 (dd,  $J = 9$  Hz, 2.8 Hz, 1H), 3.98 (q,  $J = 6.9$  Hz, 2H), 2.00 (s, 3H), 1.38 (t,  $J = 7$  Hz, 3H).



**<sup>13</sup>C NMR** (CDCl<sub>3</sub>, 150 MHz, ppm): δ 168.2, 155.5, 135.6, 133.0, 129.5, 127.7, 126.6, 122.8, 122.1, 121.4, 116.8, 64.0., 24.6, 14.9.

**HRMS** [M+H]<sup>+</sup> C<sub>16</sub>H<sub>17</sub>NO<sub>2</sub>S calculated 288.1053 found 288.1046.

**Synthesis of 1-(2-(phenylthio)phenyl)-1H-pyrrole-2,5-dione (3k)**



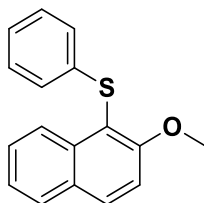
The compound was prepared according to the general procedure using 17.3 mg of 1-(2-(phenylthio)phenyl)-1H-pyrrole-2,5-dione, 2.2 mg of [Ir(dF(CF<sub>3</sub>)ppy)<sub>2</sub>(dtbpy)]PF<sub>6</sub>, 43.6 mg of diphenyl disulfide, 40 mg of (NH<sub>4</sub>)<sub>2</sub>S<sub>2</sub>O<sub>8</sub> and 2.0 mL dry CH<sub>3</sub>CN. The reaction mixture was irradiated for 24 hours under N<sub>2</sub>. Purification of the crude product was achieved by flash column chromatography using petrol ether/ ethylacetate (85:15) as eluent to yield the desired compound as white solid (16.5 mg, 58%).

**<sup>1</sup>H NMR** (CDCl<sub>3</sub>, 600 MHz, ppm): δ 7.59-7.56 (m, 2H), 7.45-7.36 (m, 7H), 7.06-7.03 (m, 2H).

**<sup>13</sup>C NMR** (CDCl<sub>3</sub>, 151 MHz, ppm): δ 174.7, 173.7, 135.3, 133.8, 131.7, 129.9, 129.7, 129.3, 129.0, 126.5, 44.3, 36.6.

**HRMS** [M+H]<sup>+</sup> C<sub>16</sub>H<sub>13</sub>NO<sub>2</sub>S calculated 284.0740 found 284.0734.

**Synthesis of (2-methoxynaphthalen-1-yl)(phenyl)sulfane (3l)**



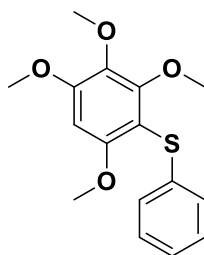
The compound was prepared according to the general procedure using 15.8 mg of (2-methoxynaphthalen-1-yl)(phenyl)sulfane, 2.2 mg of [Ir(dF(CF<sub>3</sub>)ppy)<sub>2</sub>(dtbpy)]PF<sub>6</sub>, 43.6 mg of diphenyl disulfide, 40 mg of (NH<sub>4</sub>)<sub>2</sub>S<sub>2</sub>O<sub>8</sub> and 2.0 mL dry CH<sub>3</sub>CN. The reaction mixture was irradiated for 24 hours under N<sub>2</sub>. Purification of the crude product was achieved by flash column chromatography using petrol ether/ ethylacetate (85:15) as eluent to yield the desired compound as white solid (8 mg, 30%).

**<sup>1</sup>H NMR** (CDCl<sub>3</sub>, 300 MHz, ppm): δ 8.48 (d, *J* = 8.4 Hz, 1H), 7.98 (d, *J* = 9.0 Hz, 1H), 7.84 (d, *J* = 8.1 Hz, 1H), 7.54-7.48 (m, 1H), 7.42-7.37 (m, 2H), 7.17-7.14 (m, 5H), 3.97 (s, 3H).

**<sup>13</sup>C NMR** (CDCl<sub>3</sub>, 75 MHz, ppm): δ 159.4, 138.3, 136.5, 132.3, 129.7, 128.9, 128.5, 127.9, 126.4, 125.6, 124.9, 124.3, 113.6, 113.1, 57.1.

**HRMS**[M<sup>+</sup>.] C<sub>17</sub>H<sub>14</sub>OS calculated 266.07599 found 266.0752.

#### Synthesis of phenyl(2,3,4,6-tetramethoxyphenyl)sulfane (3m):



The compound was prepared according to the general procedure using 19.8 mg of phenyl(2,3,4,6-tetramethoxyphenyl)sulfane, 2.2 mg of [Ir(dF(CF<sub>3</sub>)ppy)<sub>2</sub>(dtbpy)]PF<sub>6</sub>, 43.6 mg of diphenyl disulfide, 40 mg of (NH<sub>4</sub>)<sub>2</sub>S<sub>2</sub>O<sub>8</sub> and 2.0 mL dry CH<sub>3</sub>CN. The reaction mixture was irradiated for 24 hours under N<sub>2</sub>. Purification of the crude product was achieved by flash column chromatography using petrol ether/ ethylacetate (85:15) as eluent to yield the desired compound as white solid (12.2 mg, 40%).

**<sup>1</sup>H NMR** (CDCl<sub>3</sub>, 300 MHz, ppm): δ 7.199-7.149 (m, 2H), 7.072-7.021 (m, 3H), 6.375 (s, 1H), 3.936 (s, 3H), 3.831 (s, 3H), 3.801 (s, 3H), 3.796 (s, 3H).

**<sup>13</sup>C NMR** (CDCl<sub>3</sub>, 75 MHz, ppm): δ 157.7, 156.5, 155.6, 138.9, 137.2, 128.8, 126.2, 124.9, 92.9, 61.8, 61.4, 56.8, 56.2.

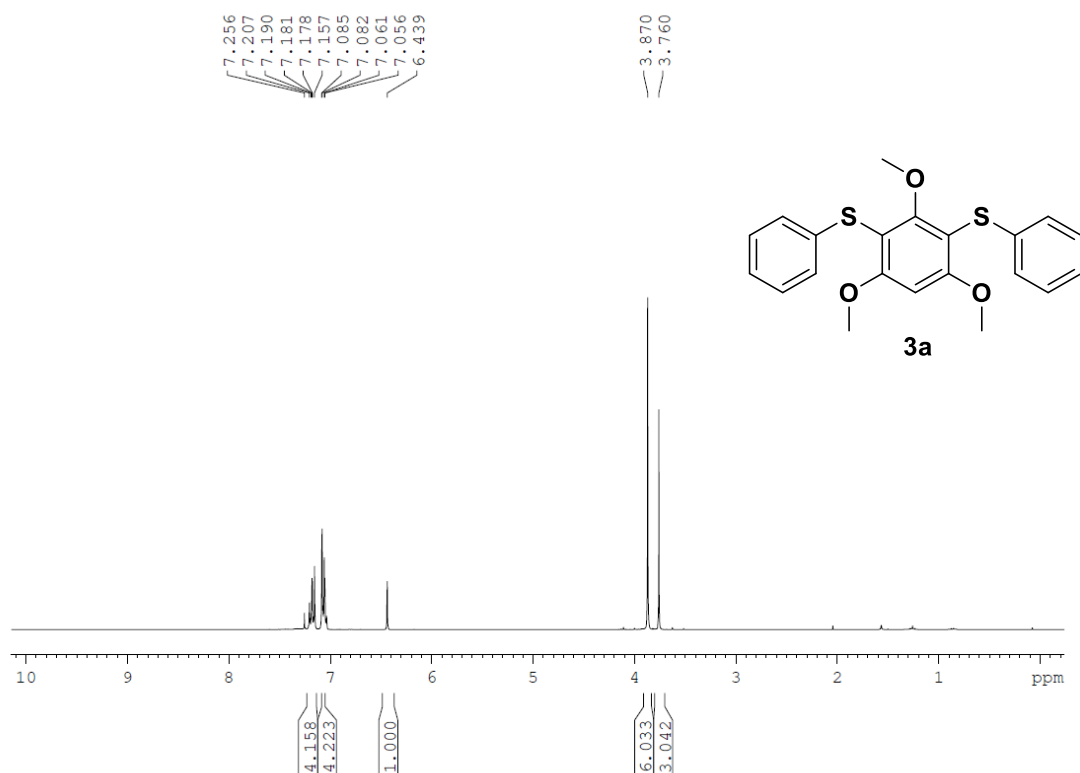
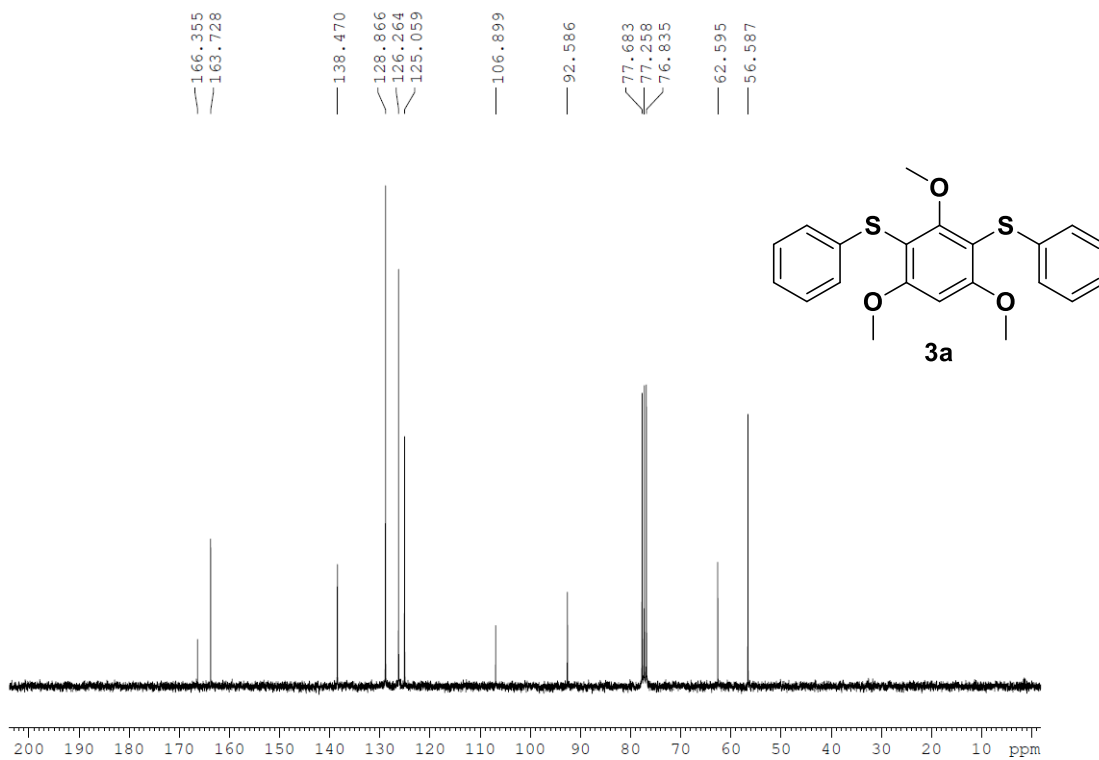
**HRMS**[M<sup>+</sup>.] C<sub>16</sub>H<sub>18</sub>O<sub>4</sub>S calculated 306.0920 found 306.0922.

### 3.5.4 Crystallographic Data

Single crystals of **3d**, **3e** and **3i** were obtained by recrystallization from DCM/PE and Single crystals of **3a** was obtained by recrystallization from EA/PE.

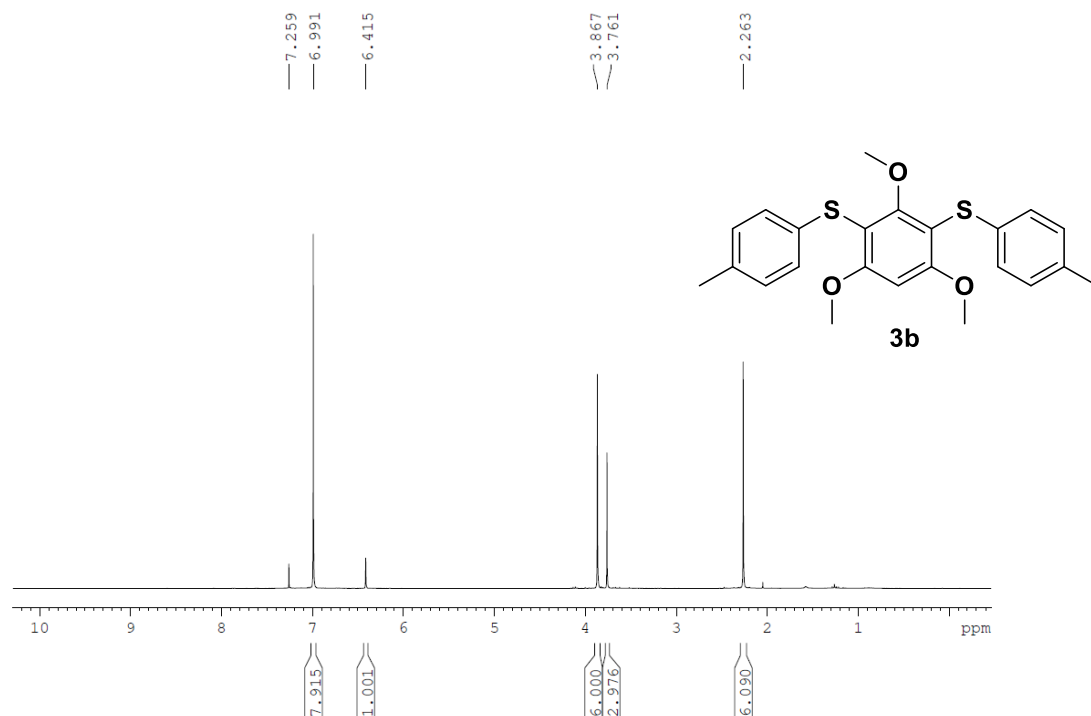
**Synthesis of Aryl Sulfides via Radical-Radical Cross Coupling of Electron Rich Arenes  
using Visible Light Photoredox Catalysis**

| Compound                     | 3a  | 3d   | 3e  | 3i   |
|------------------------------|---|--|---|--|
| CCDC No                      |   |  |   |  |
| Formula                      | C <sub>21</sub> H <sub>20</sub> O <sub>3</sub> S <sub>2</sub> | C <sub>12</sub> H <sub>17</sub> NO <sub>3</sub> S <sub>2</sub> | C <sub>20</sub> H <sub>18</sub> O <sub>2</sub> S <sub>2</sub> | C <sub>12</sub> H <sub>17</sub> NO <sub>3</sub> S <sub>2</sub> |
| $D_{calc.}/\text{g cm}^{-3}$ | 1.324   | 1.420  | 1.363   | 1.343  |
| $\mu/\text{mm}^{-1}$         | 2.645   | 3.604  | 2.863   | 3.410  |
| Formula Weight               | 384.49  | 287.38   | 354.46  | 287.38   |
| Colour                       | clear colourless  | clear colourless   | clear colourless  | Clear colourless   |
| Shape                        | plate   | block  | plate   | plate  |
| Max Size/mm                  | 0.28  | 0.12   | 0.19  | 0.13   |
| Mid Size/mm                  | 0.17  | 0.10   | 0.14  | 0.08   |
| Min Size/mm                  | 0.07  | 0.08   | 0.06  | 0.02   |
| $T/\text{K}$                 | 122.99(10)  | 123.01(11)   | 122.9(2)  | 122.9(2)   |
| Crystal System               | monoclinic  | monoclinic   | monoclinic  | triclinic  |
| Space Group                  | $P2_1/c$  | $P2_1/n$   | $P2_1/c$  | P-1  |
| $a/\text{\AA}$               | 14.5868(3)  | 7.51380(10)  | 10.3054(4)  | 7.3374(3)  |
| $b/\text{\AA}$               | 17.6123(3)  | 7.37880(10)  | 11.0809(4)  | 10.3449(5)   |
| $c/\text{\AA}$               | 7.5316(2)   | 24.3461(4)   | 15.6403(5)  | 10.3830(8)   |
| $\alpha/^\circ$              | 90  | 90   | 90  | 74.208(6)  |
| $\beta/^\circ$               | 94.518(2)   | 95.064(2)  | 104.792(4)  | 75.907(5)  |
| $\gamma/^\circ$              | 90  | 90   | 90  | 72.065(4)  |
| $V/\text{\AA}^3$             | 1928.91(7)  | 1344.55(3)   | 1726.82(11)   | 710.46(8)  |
| $Z$                          | 4   | 4  | 4   | 2  |
| $Z'$                         | 1   | 1  | 1   | 1  |
| Wavelength/ $\text{\AA}$     | 1.54184   | 1.54184  | 1.54184   | 1.54184  |
| Radiation type               | CuK $\alpha$  | CuK $\alpha$   | CuK $\alpha$  | CuK $\alpha$   |
| $\theta_{min}/^\circ$        | 3.942   | 3.645  | 4.437   | 4.494  |
| $\theta_{max}/^\circ$        | 73.926  | 73.882   | 74.823  | 75.226   |
| Measured Refl.               | 40564   | 17615  | 24757   | 2858   |
| Independent Refl.            | 3891  | 2702   | 3513  | 2858   |
| Reflections Used             | 3496  | 2472   | 3070  | 2321   |
| $R_{int}$                    | 0.0555  | 0.0299   | 0.0465  | 0.0469   |
| Parameters                   | 238   | 168  | 219   | 169  |
| Restraints                   | 0   | 0  | 0   | 0  |
| Largest Peak                 | 0.259   | 0.321  | 0.242   | 0.564  |
| Deepest Hole                 | -0.232  | -0.303   | -0.325  | -0.392   |
| GooF                         | 1.032   | 1.042  | 1.050   | 1.090  |
| $wR_2$ (all data)            | 0.0759  | 0.0703   | 0.0798  | 0.1515   |
| $wR_2$                       | 0.0718  | 0.0676   | 0.0763  | 0.1391   |
| $R_I$ (all data)             | 0.0344  | 0.0297   | 0.0372  | 0.0749   |
| $R_I$                        | 0.0296  | 0.0263   | 0.0306  | 0.0614   |

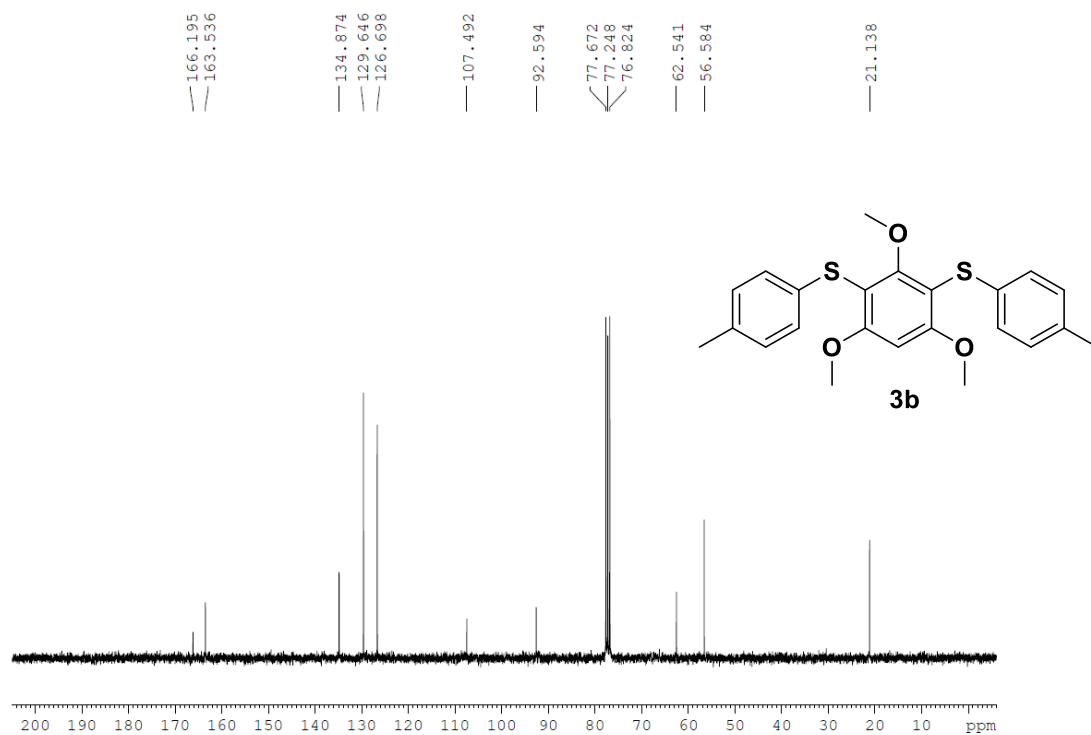
3.5.5  $^1\text{H}$ - and  $^{13}\text{C}$  NMR spectra of synthesized compounds $^1\text{H}$  spectra of compound 3a ( $\text{CDCl}_3$ , 300 MHz) $^{13}\text{C}$  spectra of compound 3a ( $\text{CDCl}_3$ , 75 MHz)

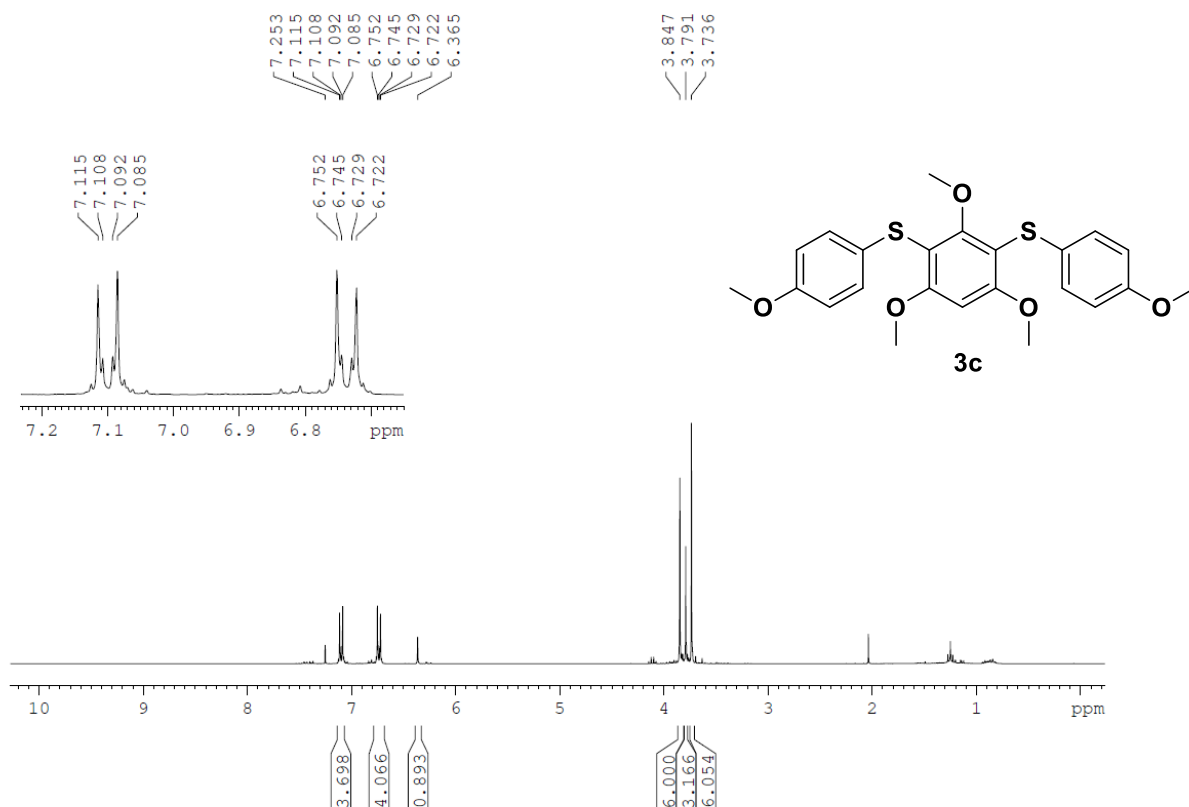
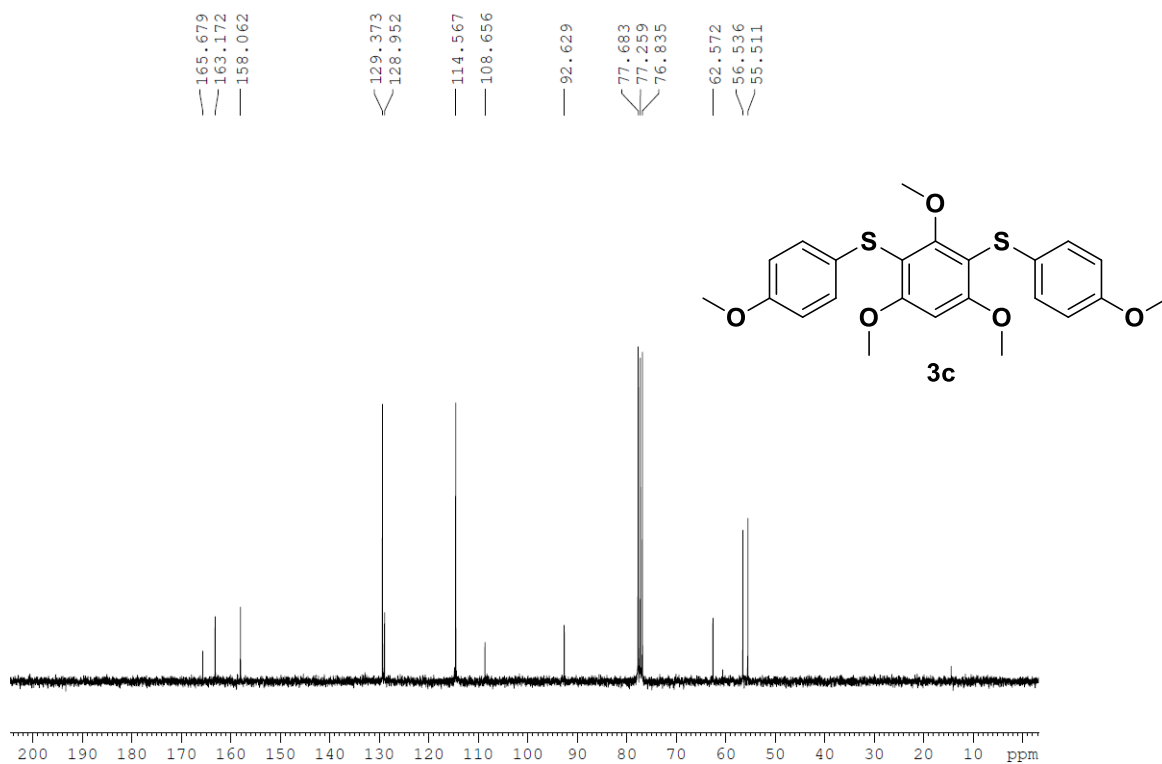
*Synthesis of Aryl Sulfides via Radical-Radical Cross Coupling of Electron Rich Arenes  
using Visible Light Photoredox Catalysis*

**<sup>1</sup>H spectra of compound 3b (CDCl<sub>3</sub>, 300 MHz)**



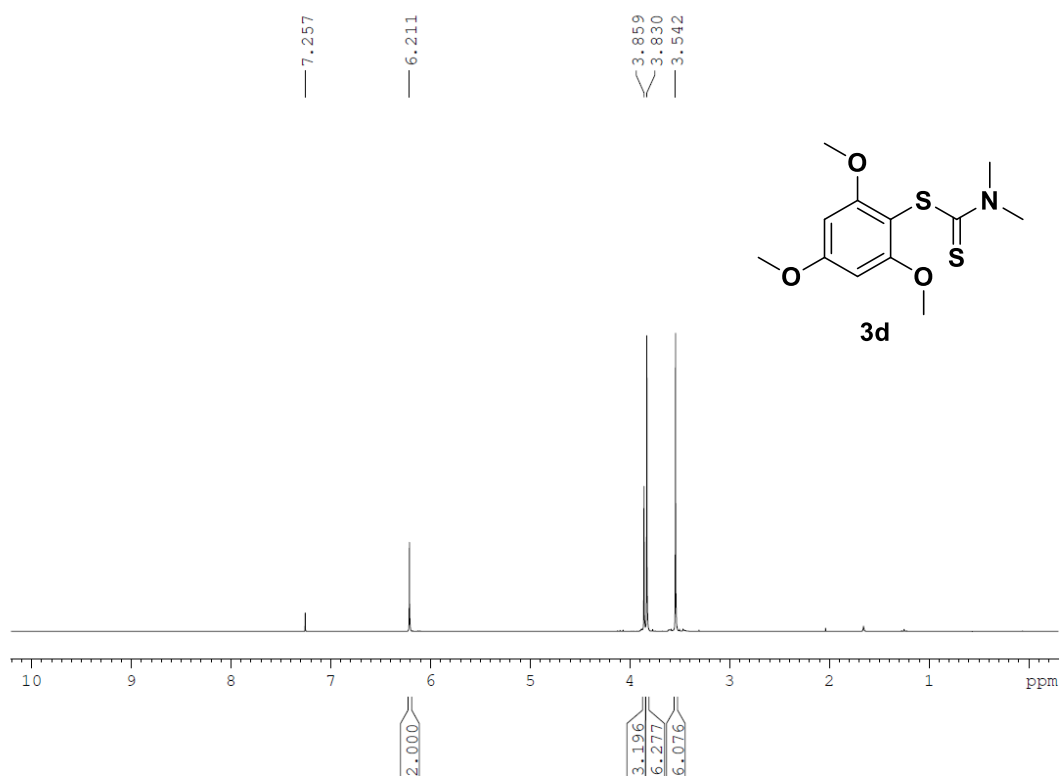
**<sup>13</sup>C spectra of compound 3b (CDCl<sub>3</sub>, 75 MHz)**



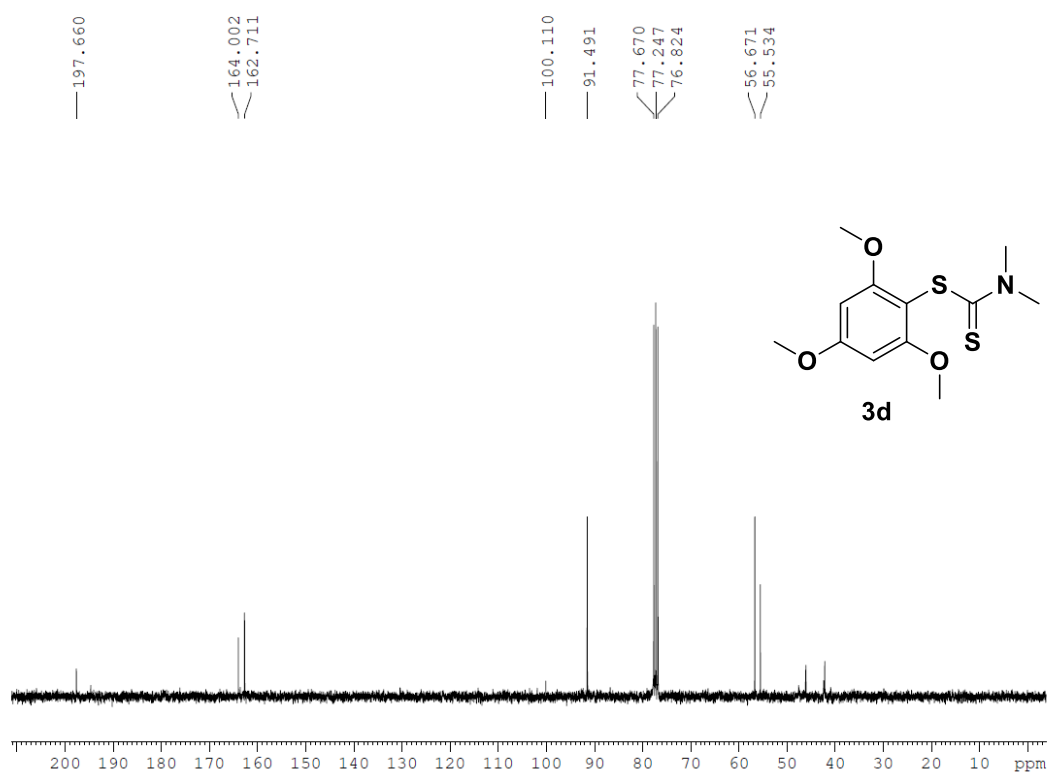
**$^1\text{H}$  spectra of compound 3c ( $\text{CDCl}_3$ , 300 MHz)** **$^{13}\text{C}$  spectra of compound 3c ( $\text{CDCl}_3$ , 75 MHz)**

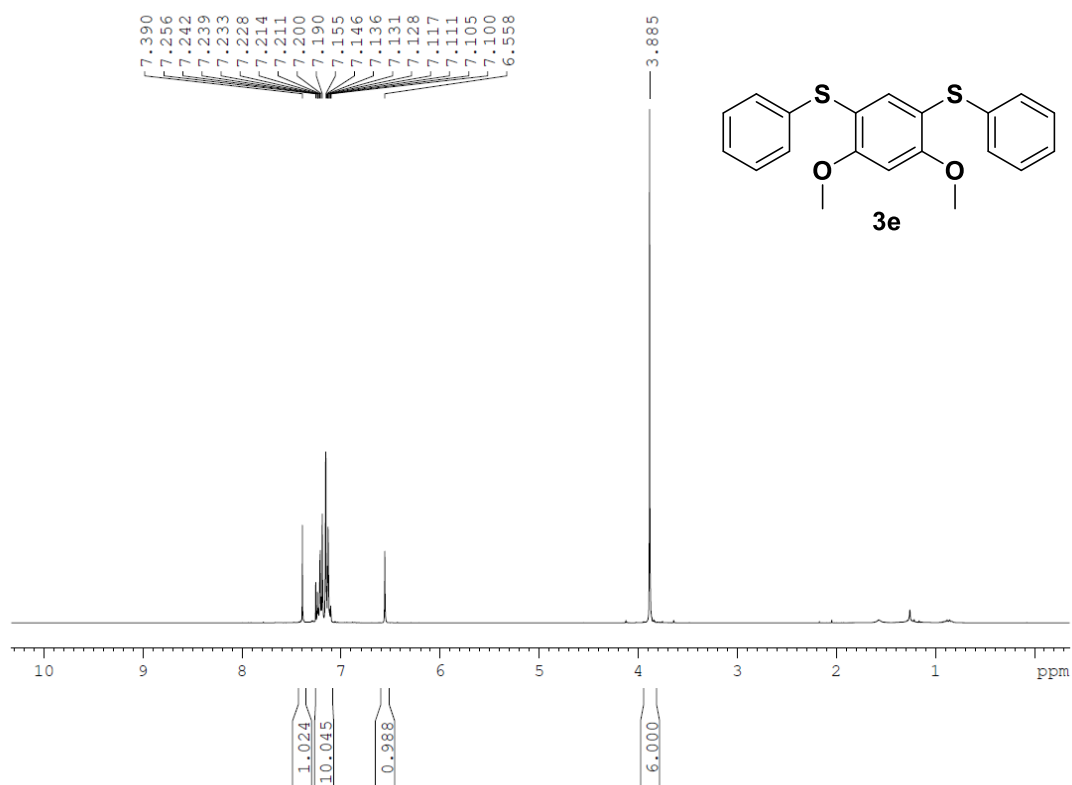
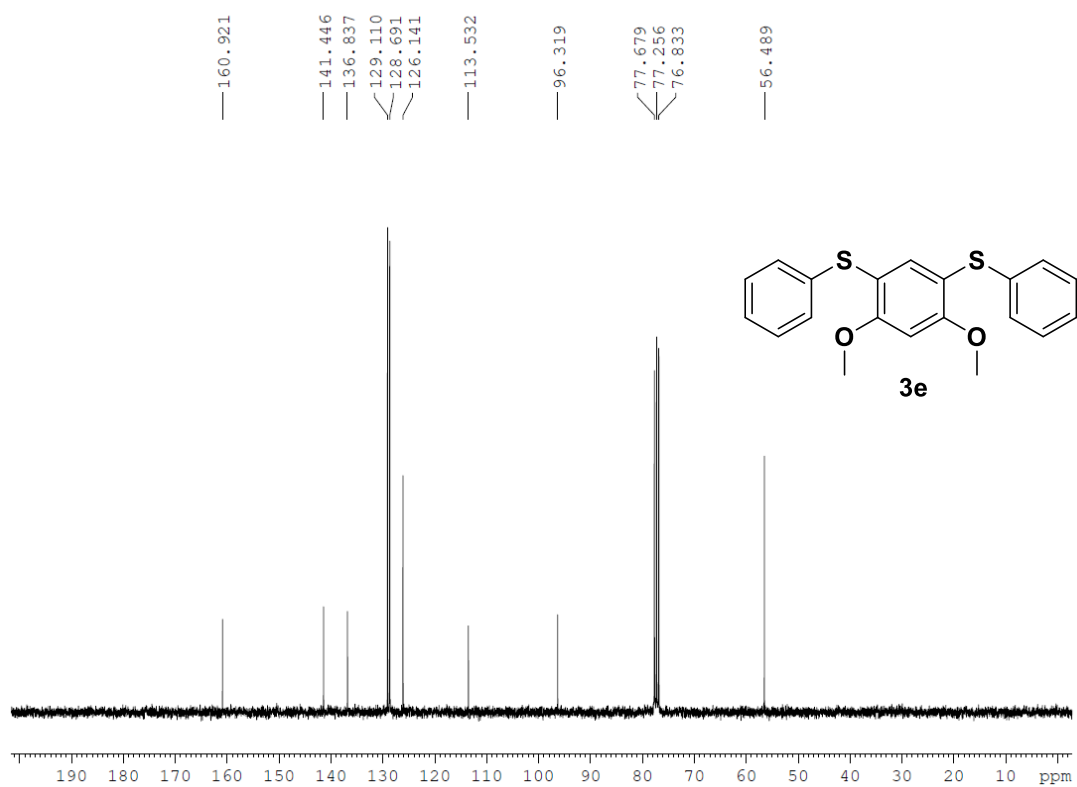
*Synthesis of Aryl Sulfides via Radical-Radical Cross Coupling of Electron Rich Arenes  
using Visible Light Photoredox Catalysis*

**<sup>1</sup>H spectra of compound 3d (CDCl<sub>3</sub>, 300 MHz)**



**<sup>13</sup>C spectra of compound 3d (CDCl<sub>3</sub>, 75 MHz)**

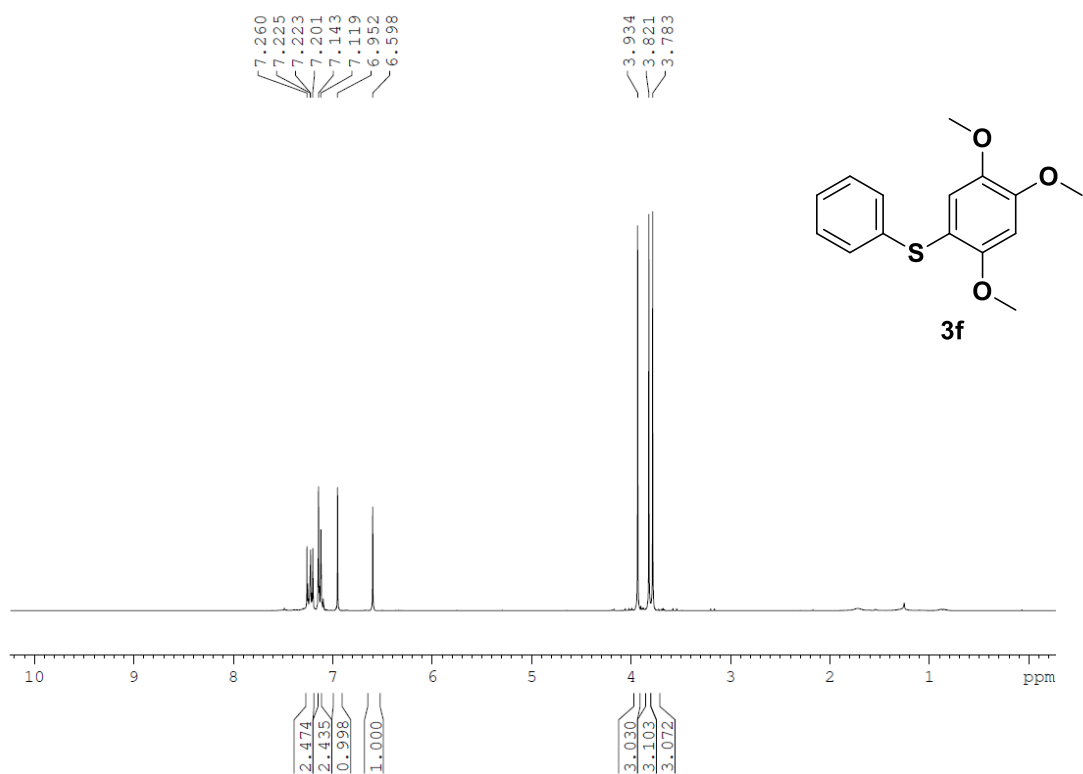


**$^1\text{H}$  spectra of compound 3e ( $\text{CDCl}_3$ , 300 MHz)** **$^{13}\text{C}$  spectra of compound 3e ( $\text{CDCl}_3$ , 75 MHz)**

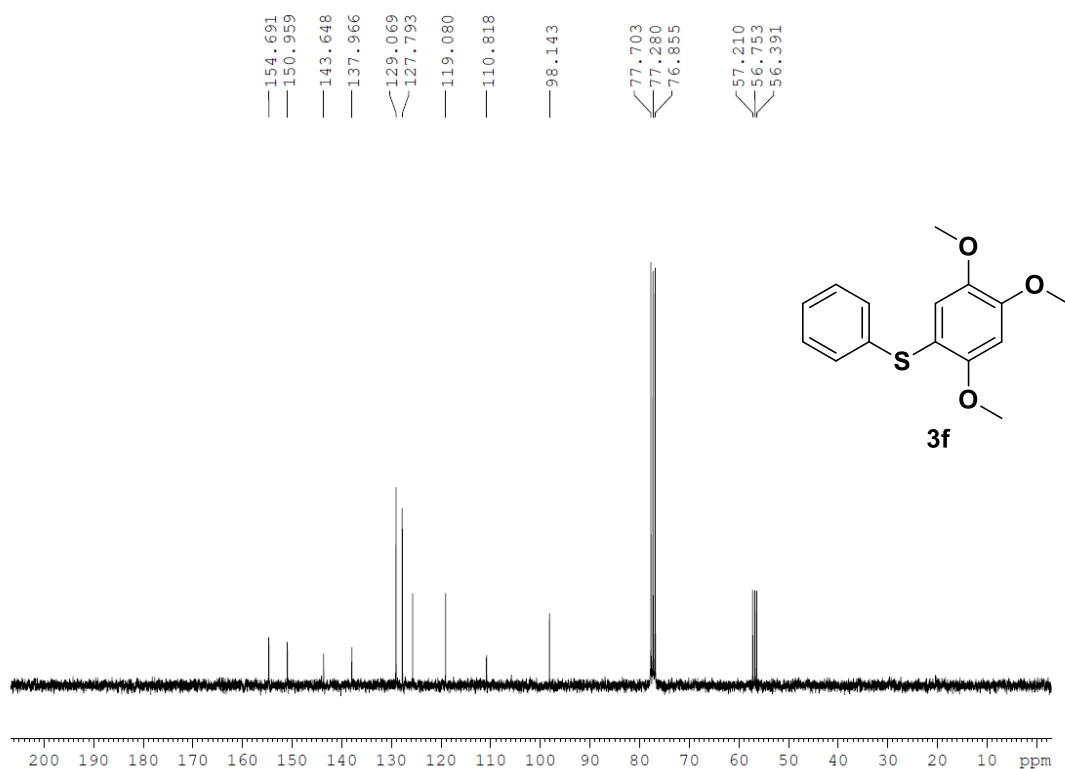


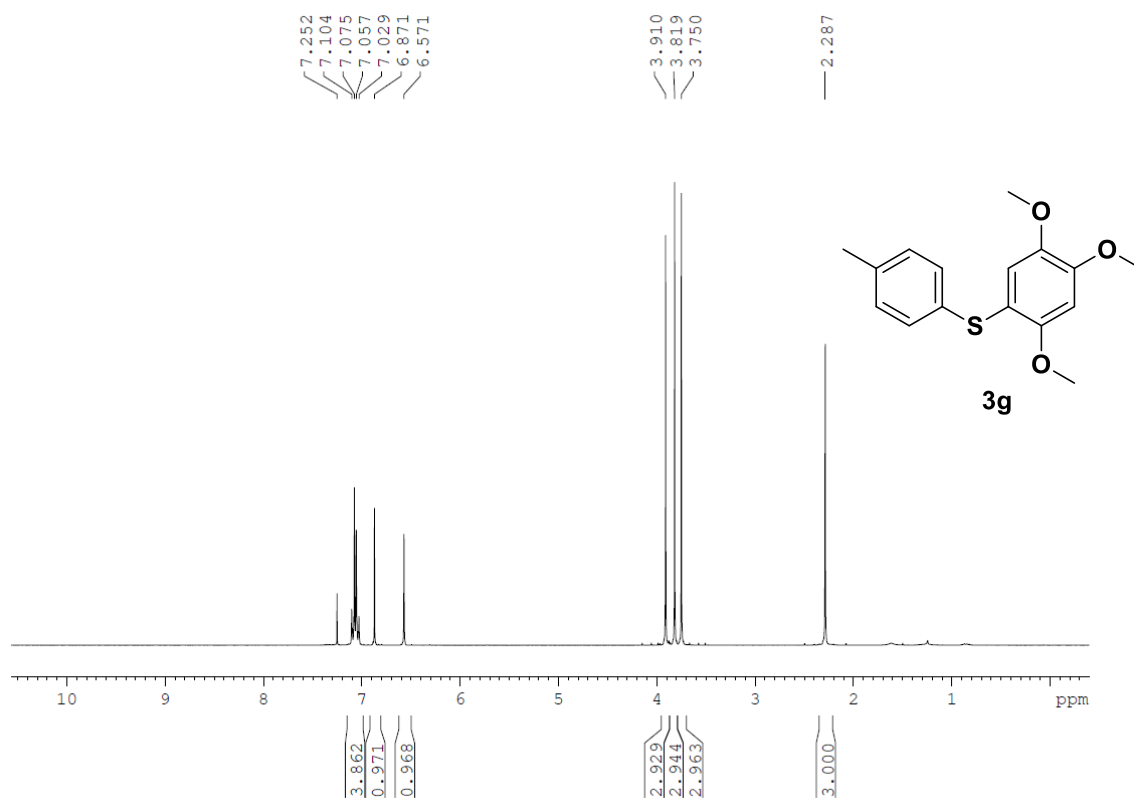
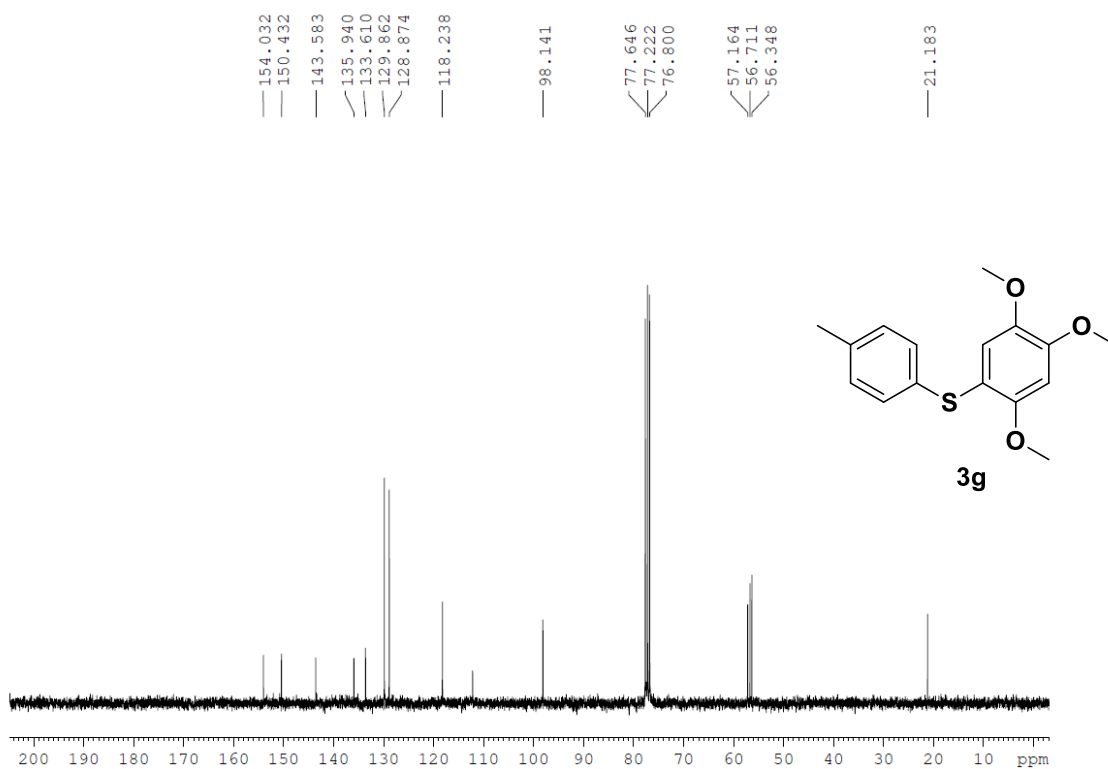
*Synthesis of Aryl Sulfides via Radical-Radical Cross Coupling of Electron Rich Arenes  
using Visible Light Photoredox Catalysis*

**<sup>1</sup>H spectra of compound 3f (CDCl<sub>3</sub>, 300 MHz)**



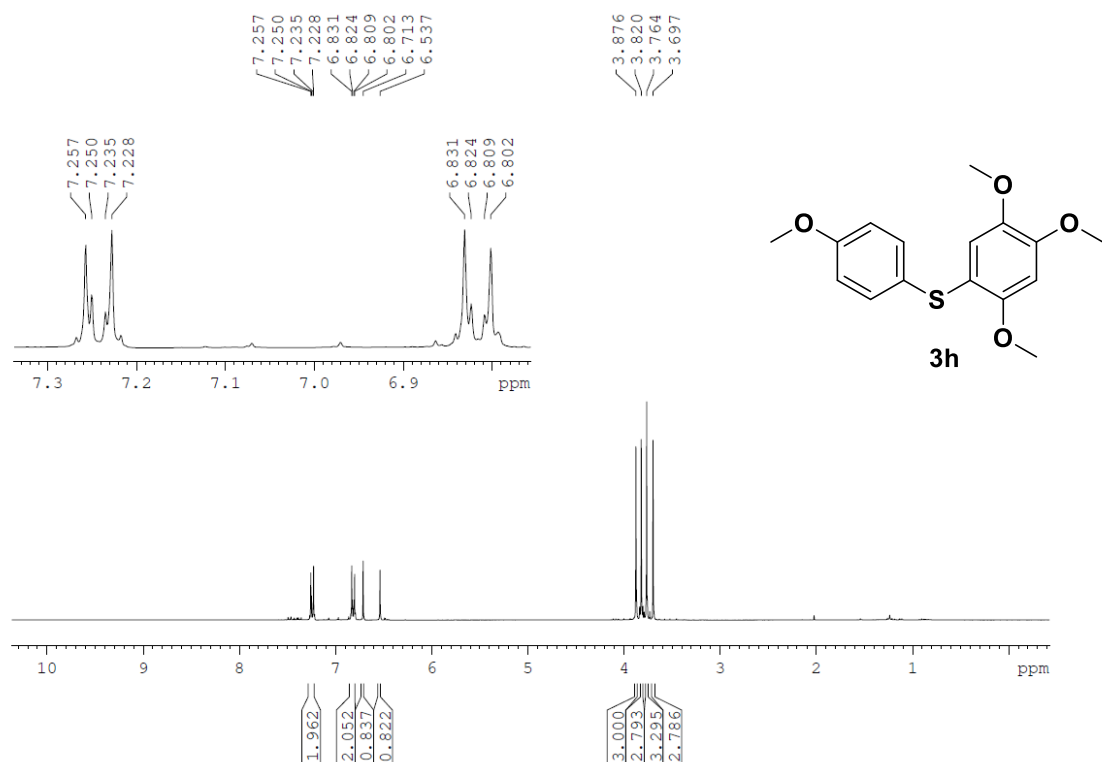
**<sup>13</sup>C spectra of compound 3f (CDCl<sub>3</sub>, 75 MHz)**



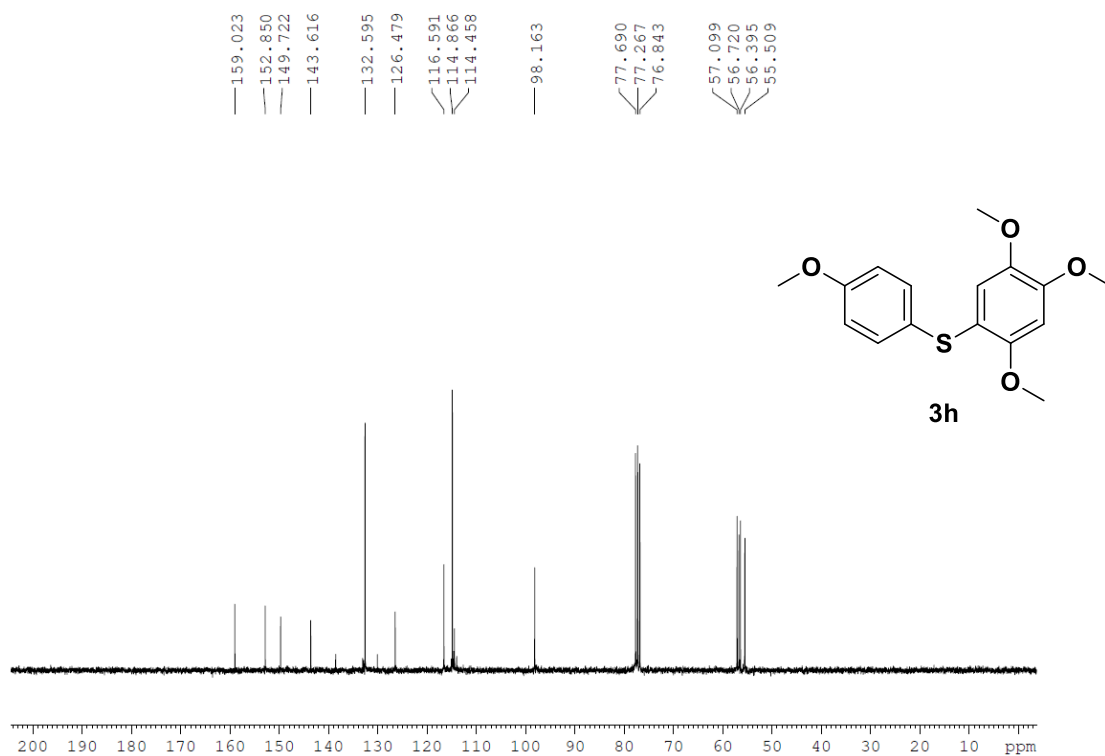
**$^1\text{H}$  spectra of compound 3g ( $\text{CDCl}_3$ , 300 MHz)** **$^{13}\text{C}$  spectra of compound 3g ( $\text{CDCl}_3$ , 75 MHz)**

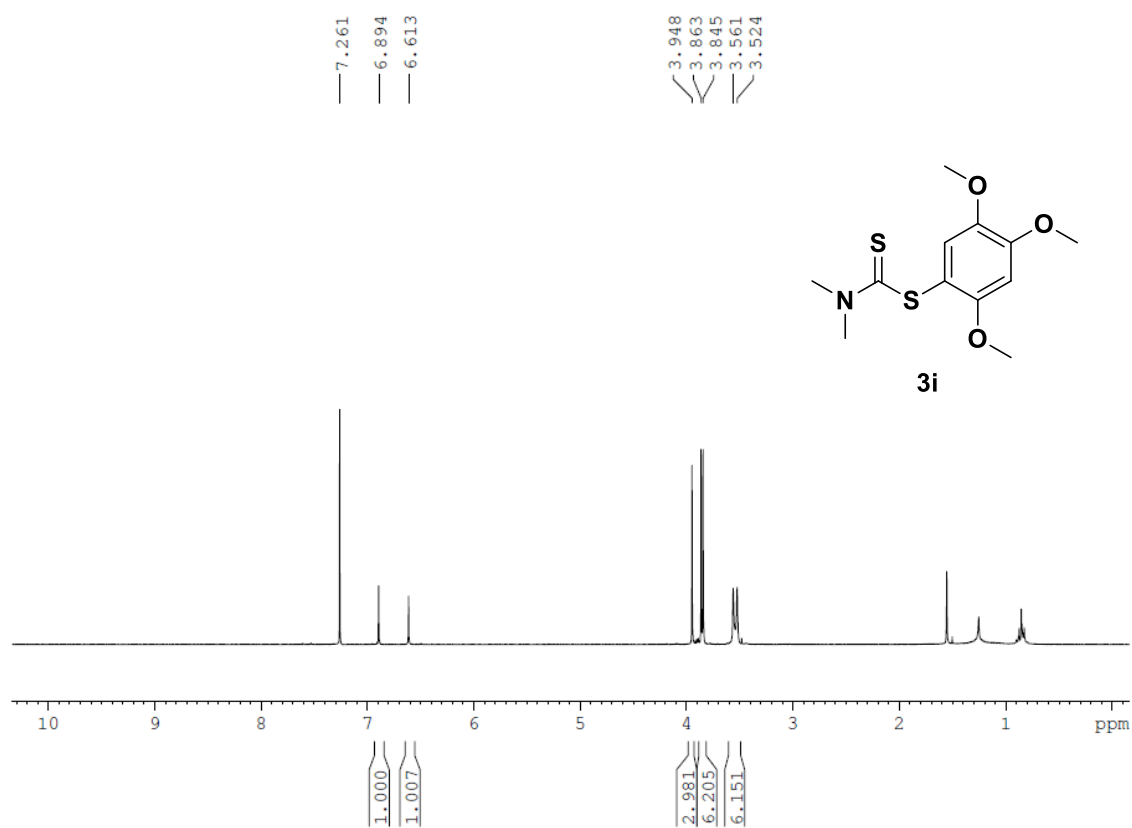
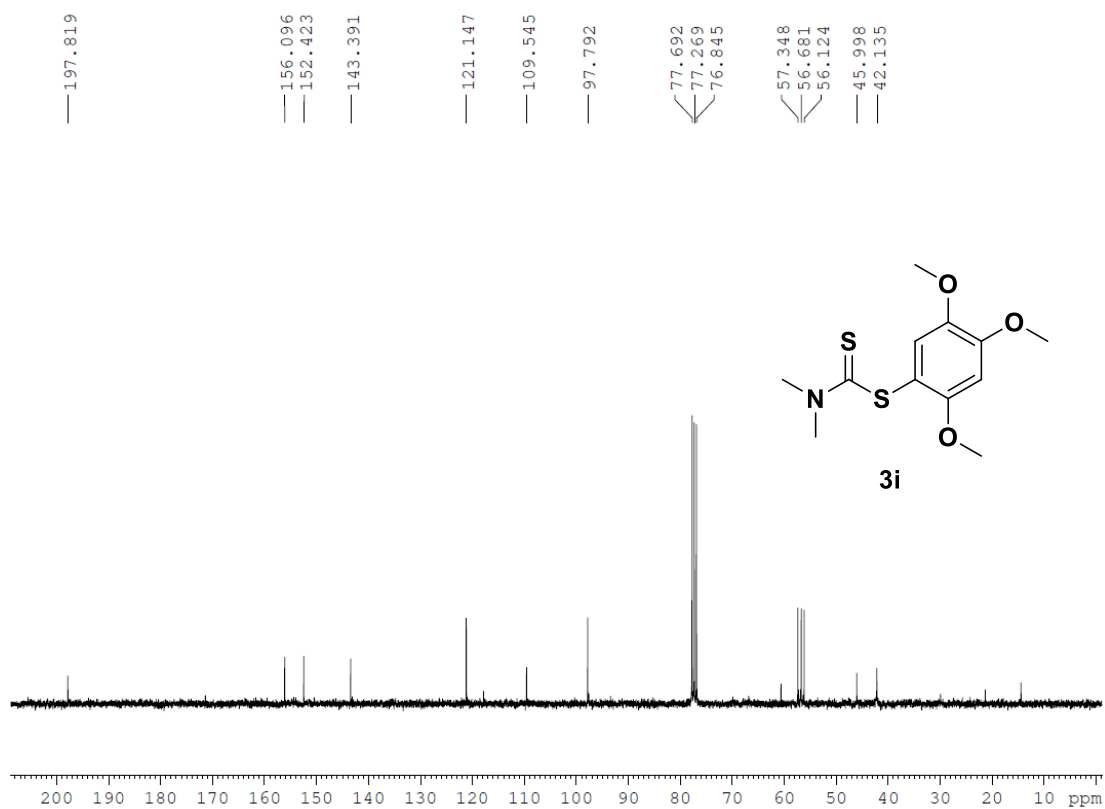
***Synthesis of Aryl Sulfides via Radical-Radical Cross Coupling of Electron Rich Arenes  
using Visible Light Photoredox Catalysis***

**<sup>1</sup>H spectra of compound 3h (CDCl<sub>3</sub>, 300 MHz)**



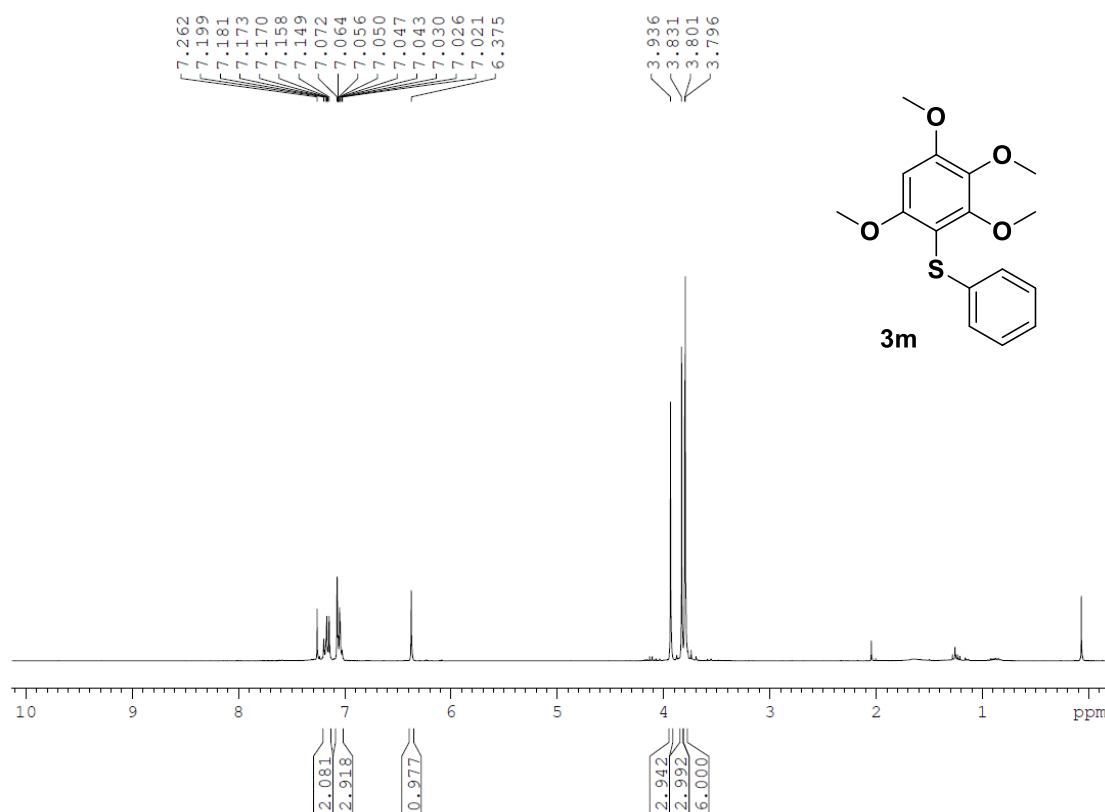
**<sup>13</sup>C spectra of compound 3h (CDCl<sub>3</sub>, 75 MHz)**



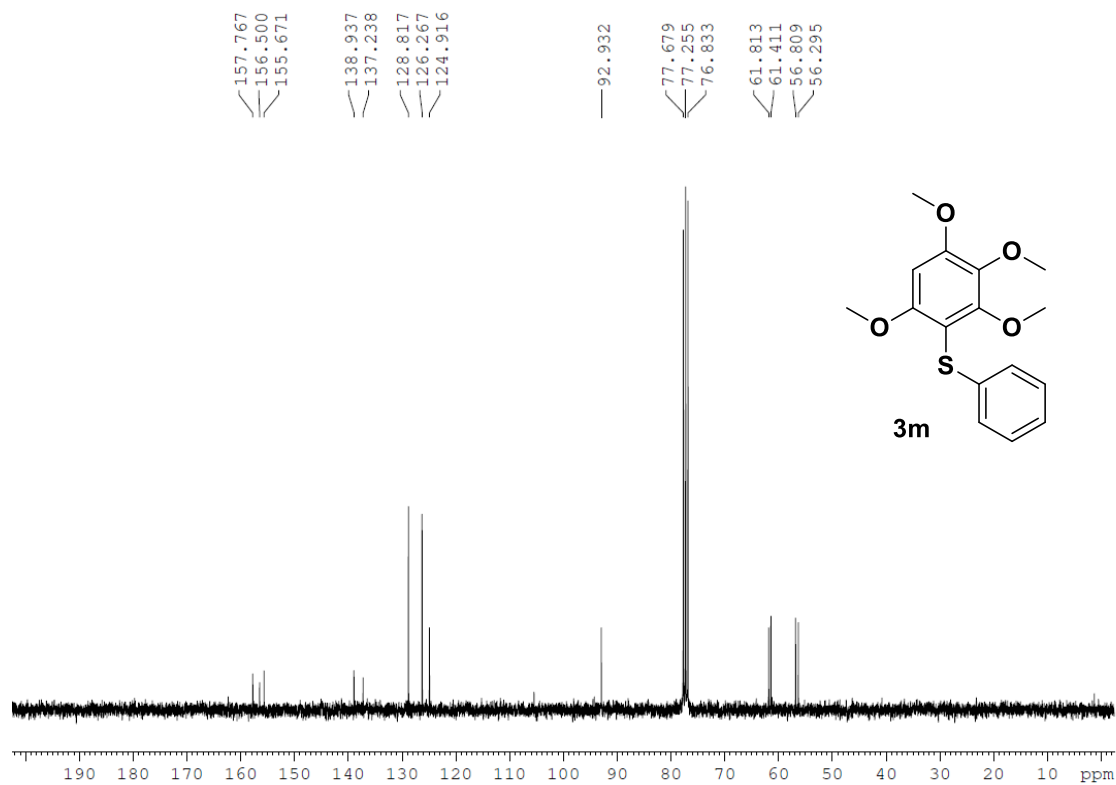
**<sup>1</sup>H spectra of compound 3i (CDCl<sub>3</sub>, 300 MHz)****<sup>13</sup>C spectra of compound 3i (CDCl<sub>3</sub>, 75 MHz)**

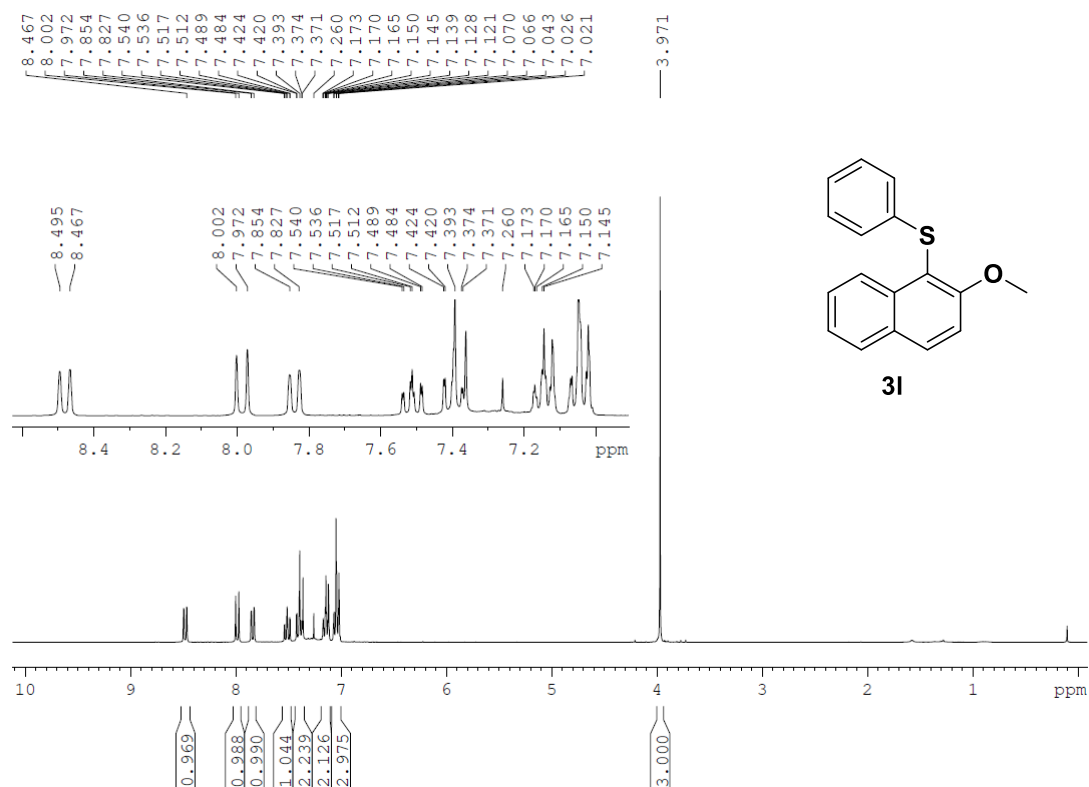
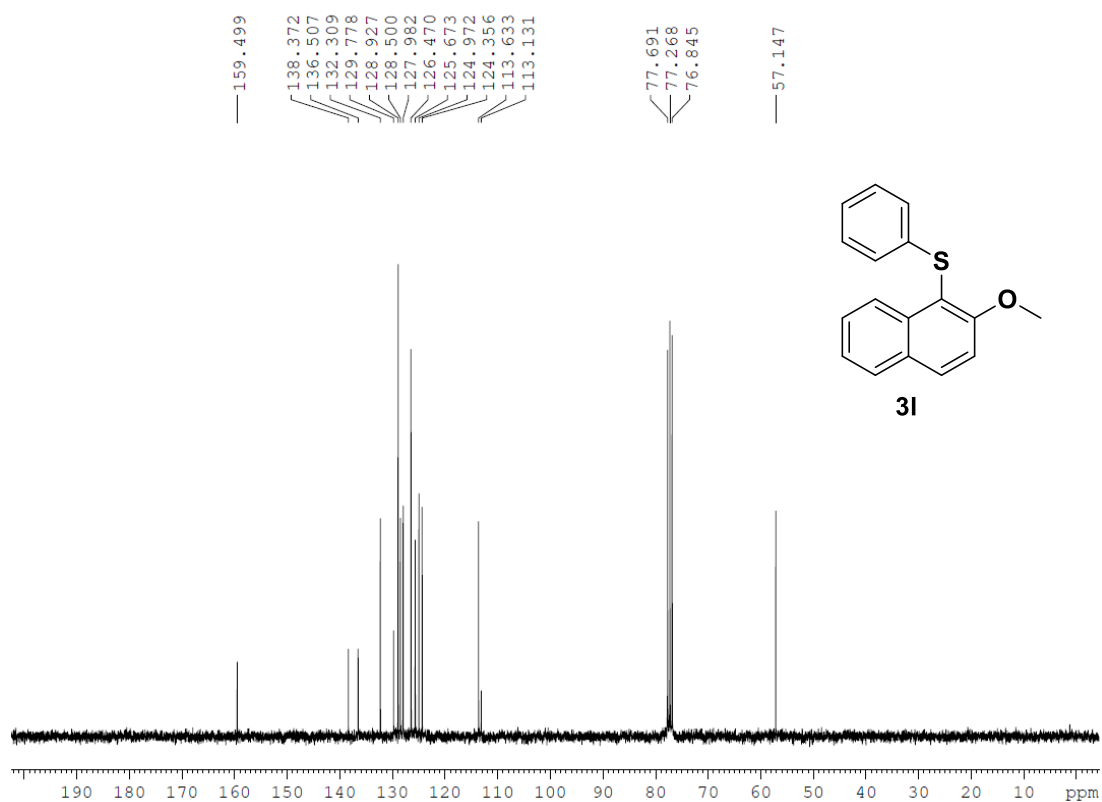
*Synthesis of Aryl Sulfides via Radical-Radical Cross Coupling of Electron Rich Arenes  
using Visible Light Photoredox Catalysis*

**<sup>1</sup>H spectra of compound 3m (CDCl<sub>3</sub>, 300 MHz)**



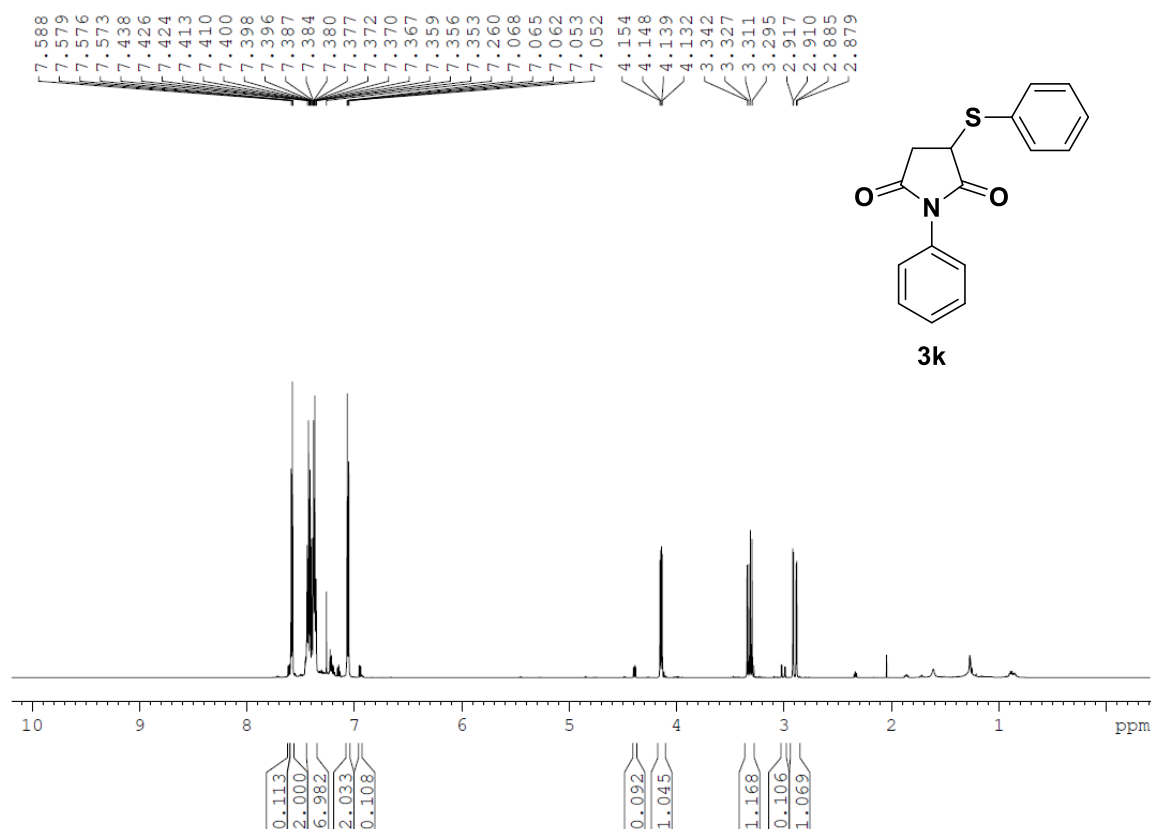
**<sup>13</sup>C spectra of compound 3m (CDCl<sub>3</sub>, 75 MHz)**



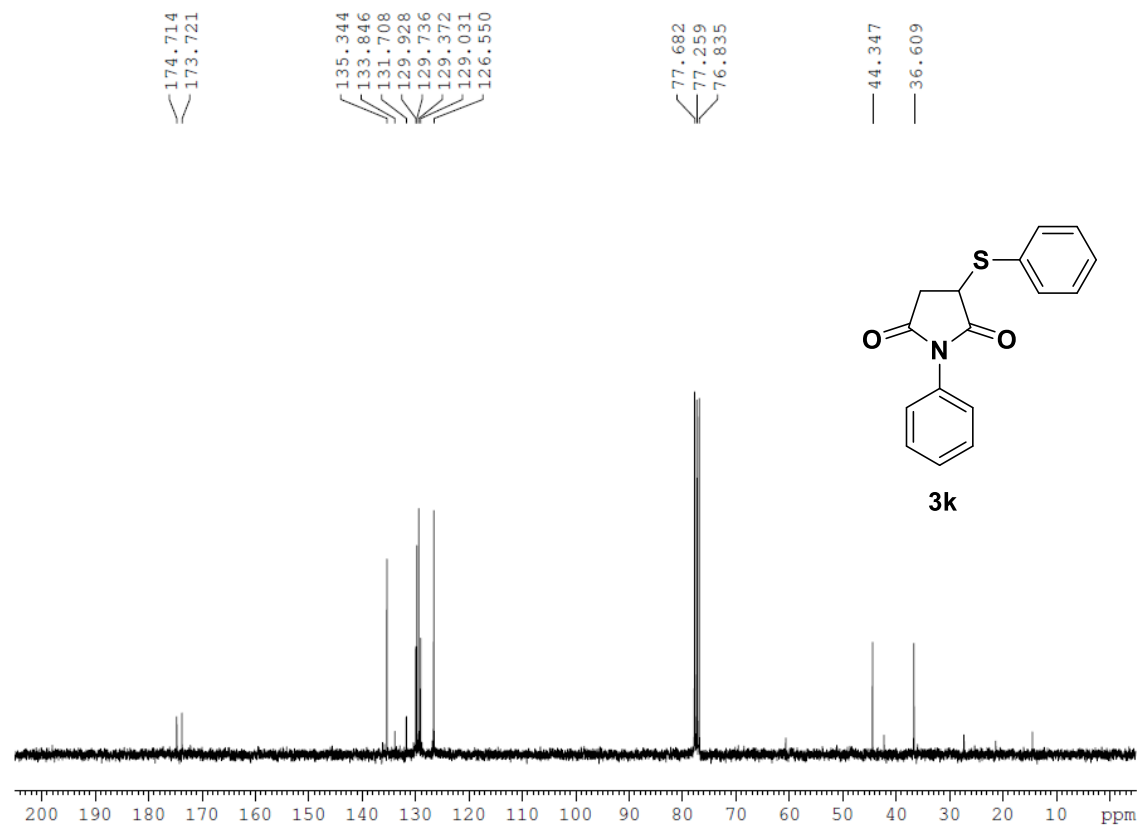
**$^1\text{H}$  spectra of compound 3l ( $\text{CDCl}_3$ , 300 MHz)** **$^{13}\text{C}$  spectra of compound 3l ( $\text{CDCl}_3$ , 75 MHz)**

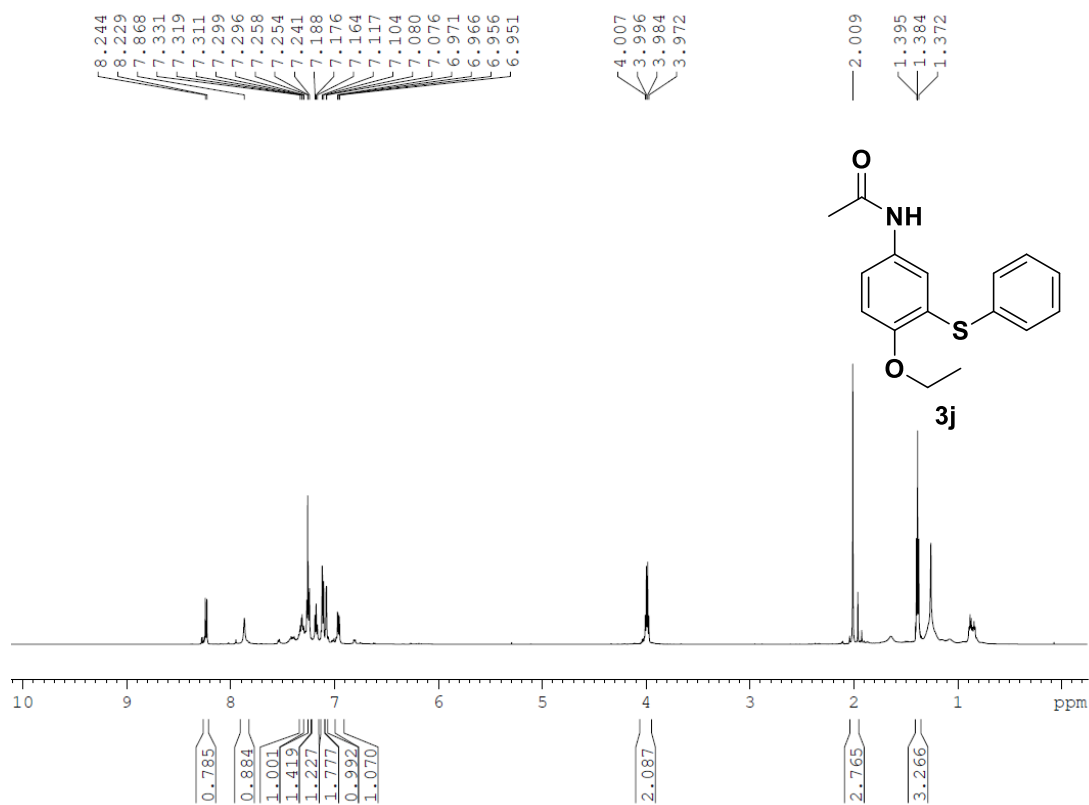
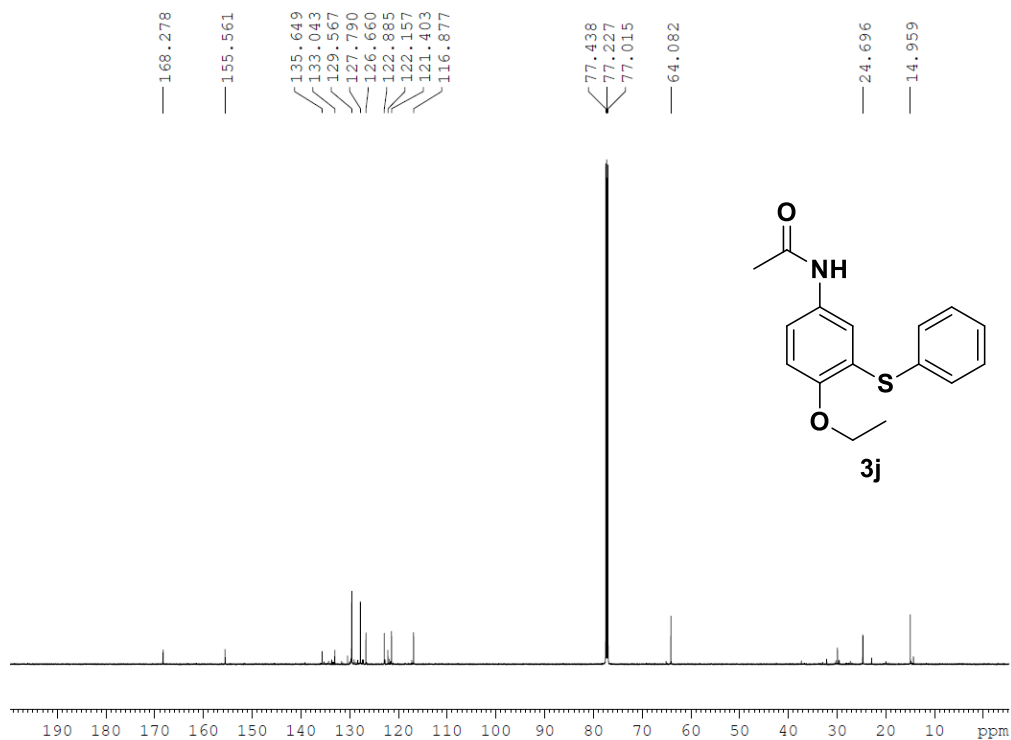
*Synthesis of Aryl Sulfides via Radical-Radical Cross Coupling of Electron Rich Arenes  
using Visible Light Photoredox Catalysis*

**<sup>1</sup>H spectra of compound 3k (CDCl<sub>3</sub>, 600 MHz)**



**<sup>13</sup>C spectra of compound 3k (CDCl<sub>3</sub>, 151 MHz)**



**$^1\text{H}$  spectra of compound 3j ( $\text{CDCl}_3$ , 600 MHz)** **$^{13}\text{C}$  spectra of compound 3j ( $\text{CDCl}_3$ , 151 MHz)**



### 3.4 References

1. K. L. Dunbar, D. H. Scharf, A. Litomska, C. Hertweck, *Chem. Rev.* **2017**, *117*, 5521-5577.
2. M. A. Vazquez-Prieto, R. M. Miatello, *Mol. Aspects. Med.* **2010**, *31*, 540-545.
3. F. Minghao, T. Bingging, S. H, Liang, X, Jiang, *Curr. Top. Med. Chem.* **2016**, *16*, 1200-1216.
4. a) T. Kondo, T. Mitsudo, *Chem. Rev.* **2000**, *100*, 3205-3220. b) C. C. Eichman, J. P. Stambuli, *Molecules.* **2011**, *16*, 590-608. c) Y. C. Wong, T. T. Jayanth, C. H. Cheng, *Org. Lett.* **2006**, *8*, 5613-5616.
5. a) R. Singh, B. K. Allam, N. Singh, K. Kumari, S. K. Singh, K. N Singh, *Adv. Synth. Catal.* **2015**, *357*, 1181-1186.
6. V. G. Pandya, S. B. Mhaske, *Org. Lett.* **2014**, *16*, 3836-3839.
7. Y. Li, W. Xie, X. Jiang, *Chem. Eur. J.* **2015**, *21*, 16059-16065.
8. a) G. Y. Li, *Angew. Chem. Int. Ed.* **2001**, *40*, 1513-1516. b) M. A. Fernández-Rodríguez, J. F. Hartwig, *Chem. Eur. J.* **2010**, *16*, 2355-2359. c) G. Teverovskiy, D. S. Surry, S. L. Buchwald, *Angew. Chem. Int. Ed.* **2011**, *50*, 7312-7314.
9. a) J. Gan, D. Ma, *Org. Lett.* **2009**, *11*, 2788-2790. b) A. Saha, D. Saha, B. C. Ranu, *Org. Biomol. Chem.* **2009**, *7*, 1652-1657. c) D. Ma, S. Xie, P. Xue, X. Zhang, J. Dong, Y. Jiang, *Angew. Chem. Int. Ed.* **2009**, *48*, 4222-4225. d) D. Ma, Q. Geng, H. Zhang, Y. Jiang, *Angew. Chem. Int. Ed.* **2010**, *49*, 1291-1294. e) C. K. Chen, Y. W. Chen, C. H. Lin, H. P. Lin, C. F. Lee, *Chem. Commun.* **2010**, *46*, 282-284. f) D. Ma, X. Lu, L. Shi, H. Zhang, Y. Jiang, X. Liu, *Angew. Chem. Int. Ed.* **2011**, *50*, 1118-1121. g) H. Deng, Z. Li, F. Ke, X. Zhou. *Chem. Eur. J.* **2012**, *18*, 4840-4843. h) C. Uyeda, Y. Tan, G. C. Fu, J. C Peters, *J. Am. Chem. Soc.* **2013**, *135*, 9548-9552.
10. a) Y. Zhang, K. C. Ngeow, J. Y. Ying, *Org. Lett.* **2007**, *9*, 3495-3498. b) S. Jammi, P. Barua, L. Rout, P. Saha, T. Punniyamurthy, *Tetrahedron Lett.* **2008**, *49*, 1484-1487. c) C. P. Zhang, D. A. Vicic, *J. Am. Chem. Soc.* **2012**, *134*, 183-185.
11. a) A. Correa, O. G. Mancheño, C. Bolm, *Chem. Soc. Rev.* **2008**, *37*, 1108-1117. b) A. Correa, M. Carril, C. Bolm, *Angew. Chem. Int. Ed.* **2008**, *47*, 2880-2883. c) W. Y. Wu, J. C. Wang, F. Y. Tsai, *Green. Chem.* **2009**, *11*, 326-329. d) C. F. Lee, J. R. Wu, C. H. Lin, *Chem. Commun.* **2009**, 4450-4452. e) Y. Y. Lin, Y. J. Wang, C. H. Lin, J. H. Cheng, C. F. Lee, *J. Org. Chem.* **2012**, *77*, 6100-6106.

12. a) Y. C. Wong, T. T. Jayanth, C. H. Cheng, *Org. Lett.* **2006**, 8, 5613-5616. b) M. T. Lan, W. Y. Wu, S. H. Huang, K. L. Luo, F. Y. Tsai, *RSC. Adv.* **2011**, 1, 1751-1755. c) X. Huang, Y. Chen, S. Zhen, L. Song, M. Gao, P. Zhang, H. Li, B. Yuan, G. Yang, *J. Org. Chem.* DOI: 10.1021/acs.joc.7b02718.
13. a) K. Ajiki, M. Hirano, K. Tanaka, *Org. Lett.* **2005**, 7, 4193-4195. b) M. Arisawa, T. Suzuki, T. Ishikawa, M. Yamaguchi, *J. Am. Chem. Soc.* **2008**, 130, 12214-12215.
14. a) J. H. Cheng, C. Ramesh, H. L. Kao, Y. J. Wang, C. C. Chan, C. F. Lee, *J. Org. Chem.* **2012**, 77, 10369-10374. b) I. M. Yonova, C. A. Osborne, N. S. Morrisette, E. R. Jarvo, *J. Org. Chem.* **2014**, 79, 1947-1953.
15. a) C. Shen, P. Zhang, Q. Sun, S. Bai, T. S. A. Hor, X. Liu, *Chem. Soc. Rev.* **2015**, 44, 291-314. b) S. K. R. Parumala, R. K. Peddinti, *Green. Chem.* **2015**, 17, 4068-4072. c) W. Zhao, P. Xie, Z. Bian, A. Zhou, H. Ge, B. Niu, Y. Ding, *RSC. Adv.* **2015**, 5, 59861-59864.
16. Z. Huang, D. Zhang, X. Qi, Z. Yan, M. Wang, H. Yan, A. Lei, *Org. Lett.* **2016**, 18, 2351-2354.
17. G. M. Miyake, C. Lim, B. Liu, *J. Am. Chem. Soc.* **2017**, 139, 13616-13619.
18. W. Guo, W. Tan, L. Zheng, Y. Wu, D. Chen, X. Fan, *RSC. Adv.* **2017**, 7, 37739-37742.
19. R. Rahaman, S. Das, P. Barman, *Green Chem.* **2018**, 20, 141-147.
20. J. Giordan, H. Bock, *Chem. Ber.* **1982**, 115, 2548-2559.
21. S. Töteberg-Kaulen, E. Steckhan, *Tetrahedron.* **1988**, 44, 4389-4397.
22. P. Lakkaraju, H. Roth, *J. Chem. Soc., Perkin Trans.* **1998**, 2, 1119-1122.
23. W. L. Wallace, R. P. Van Duyne, F. D. Lewis, *J. Am. Chem. Soc.* **1976**, 98, 5319-5326.
24. F. Denes, M. Pichowicz, G. Povie, P. Renaud, *Chem. Rev.* **2014**, 114, 2587-2693.
25. N. A. Romero, D. A. Nicewicz, *J. Am. Chem. Soc.* **2014**, 136, 17024-17035.
26. D. B. G. Williams, M. J. Lawton, *J. Org. Chem.* **2010**, 75, 8351-8354.
27. M. S. Lowry, J. I. Goldsmith, J. D. Slinker, R. Rohl, R. A. Pascal, G. G. Malliaras, *Chem. Mater.* **2005**, 17, 5712-5719.
28. L. Chen, P. Liu, J. Wu, B. Dai, *Tetrahedron.* **2018**, 74, 1513-1519.
29. K. Yan, D. Yang, P. Sun, W. Wei, Y. Liu, G. Li, S. Lu, H. Wang, *Tetrahedron. Lett.* **2015**, 56, 4792-4795.

30. M. R. Reddy, G. S Kumar, H. M. Meshram, *Tetrahedron. Lett.* **2016**, 57, 3622-3624.



# *Chapter 4*

## ***4. Photochemical versus Photocatalytic Oxidation of Benzyl alcohols – A Comparison***



## 4.1 Introduction

Photochemical reactions are initiated by the direct absorption of light by a molecule. Most organic molecules have strong absorption only below 300 nm and therefore typically UV B or UV C irradiation is required for their excitation. In contrast, in a photocatalyzed reaction, activation of organic molecules with a visible light absorbing photocatalyst is possible either by electron transfer or energy transfer. Due to the smaller energies involved and specific energy pathways, reactions can be more specific. Advances in light emitting diode (LED) technology during the last decades have increased the interest in photochemistry and photocatalysis, as they offer a high power, flexible and cheap light source with small bandwidth needed for the controlled irradiation of the reactant molecules in a solution. Recently, high power UV-LEDs have become available, which offers the opportunity to compare photoreactions initiated by direct UV irradiation and photocatalyzed reactions with excitation in the visible spectrum. The irradiation power of the LEDs can now be comparable to both cases and the irradiation time could be decreased to a minimum to prevent further thermal reactions in the batch allowing for a better comparison of the two activation mechanisms concerning their efficiency and selectivity. Under such controlled reaction conditions, a data-based evaluation becomes feasible, if a photocatalyzed or a photochemical reaction pathway is preferable.

An interesting model system of photoredox catalysis for mechanistic investigations is the photooxidation of 4-methoxybenzyl alcohol (**MBA**) catalyzed by riboflavin tetraacetate (**RFTA**).<sup>[1]</sup> The reaction is initiated by visible light excitation of **RFTA**. The 4-methoxybenzylalcohol undergoes an one electron oxidation<sup>[2,3]</sup> while the excited flavin is reduced to the radical anion (**RFTA**<sup>•-</sup>) by taking up an electron from the alcohol to form a spin-correlated radical-ion pair. Subsequently, a proton transfer occurs, followed by a second electron and proton transfer to complete the reaction.

---

**This chapter is a manuscript, prepared for submission to a journal:**

Amrita Das (A.D) performed all the photochemical experiments. Matthias Block (M.B) (LMU Munich) performed the transient measurements. A.D and M.B wrote the manuscript. Tim den Hartog synthesized the compounds. Burkhard König (B.K) and Eberhard Riedle (E.R). supervised the project and are corresponding authors.

Therefore, the crucial reaction step is the electron transfer (eT) from the substrate **MBA** to the light induced formed triplet state of the **RFTA** resulting in a spin-correlated radical-ion pair. Since, the overall efficiency of the reaction strongly depends on the electron transfer characteristics, properties can be modified by substituents on the arene with different electronic properties.

We have first investigated the efficiency of the **MBA** photo-oxidation by direct UV excitation and compared with flavin catalyzed visible light photo-oxidation. The second reaction is based on early studies.<sup>[4]</sup>

## 4.2 Quantum Yield of **MBA** Photo-oxidation in MeOH

The direct photo-oxidation of **MBA** to the corresponding aldehyde (**MBAld**) by UV irradiation is studied and its quantum yield ( $\Phi_{UV}$ ) is compared to the quantum yield ( $\Phi_{PC}$ ) for the photocatalyzed reaction with **RFTA**.

For the direct UV irradiation, a solution of **MBA** in MeOH with a concentration of  $c_{MBA} = 21.5$  mM was prepared in a  $d = 1$  cm *Hellma* quartz glass cuvette with a sample volume of  $V = 2$  mL. The solution was irradiated in a quantum yield determination setup (QYDS).<sup>[4]</sup> In order to avoid a strong excitation of the aldehyde a *LG Innotek 278 nm* high power UV-LED was chosen in combination with an *Asahi XUS0300* shortpass optical filter with a center wavelength of about  $\lambda_{LED} = 278$  nm. The absorbed optical power was  $P_{abs} = 44.9$  mW and the solution was irradiated for  $T_{max} = 120$  min. In order to determine the concentrations of alcohol and aldehyde after a certain irradiation time, aliquots were taken prior to the irradiation and every 30 min. The aliquots were then analyzed in a commercial gas chromatograph *Agilent 6890 GC* with FID detector. For the quantification of the concentrations the GC response was determined by carefully preparing known concentrations of the alcohol and the aldehyde, which gives a linear correlation of the integrated FID signal of the peaks and the concentration (see experimentail section, **Figure 6-8** for the GC response function. For the flavin-catalyzed visible light photo-oxidation, a solution of **RFTA** and **MBA** was prepared in MeOH. The concentration of flavin was  $c_{RFTA} = 1.0$  mM and of **MBA**  $c_{MBA} = 20.0$  mM. The volume and cuvette thickness were the same as for the UV irradiation. The light source was a high power *OSRAM LDCQ7P-1U3U* LED with a center wavelength of about  $\lambda_{LED} = 435$  nm. The absorbed optical power was  $P_{abs} = 50.1$  mW and aliquots were taken every 30 minutes with a maximum irradiation time



of 120 minutes.

The results are shown in **Figure. 1** and it can be seen in (a) and (c) that the benzyl alcohol signal at a retention time of about 21.2 minutes decreases with increasing illumination time and the aldehyde signal around 19.0 min appears. In the case of the UV irradiation, the aldehyde signal did not increase to the same extent as the alcohol signal decreases. Additional peaks appear, which indicates already the formation of side or decomposition products. The product aldehyde absorbs UV light, which may initiate further conversion or decomposition. With flavin as photocatalyst, the alcohol is cleanly and selectively converted into the aldehyde as the only product.

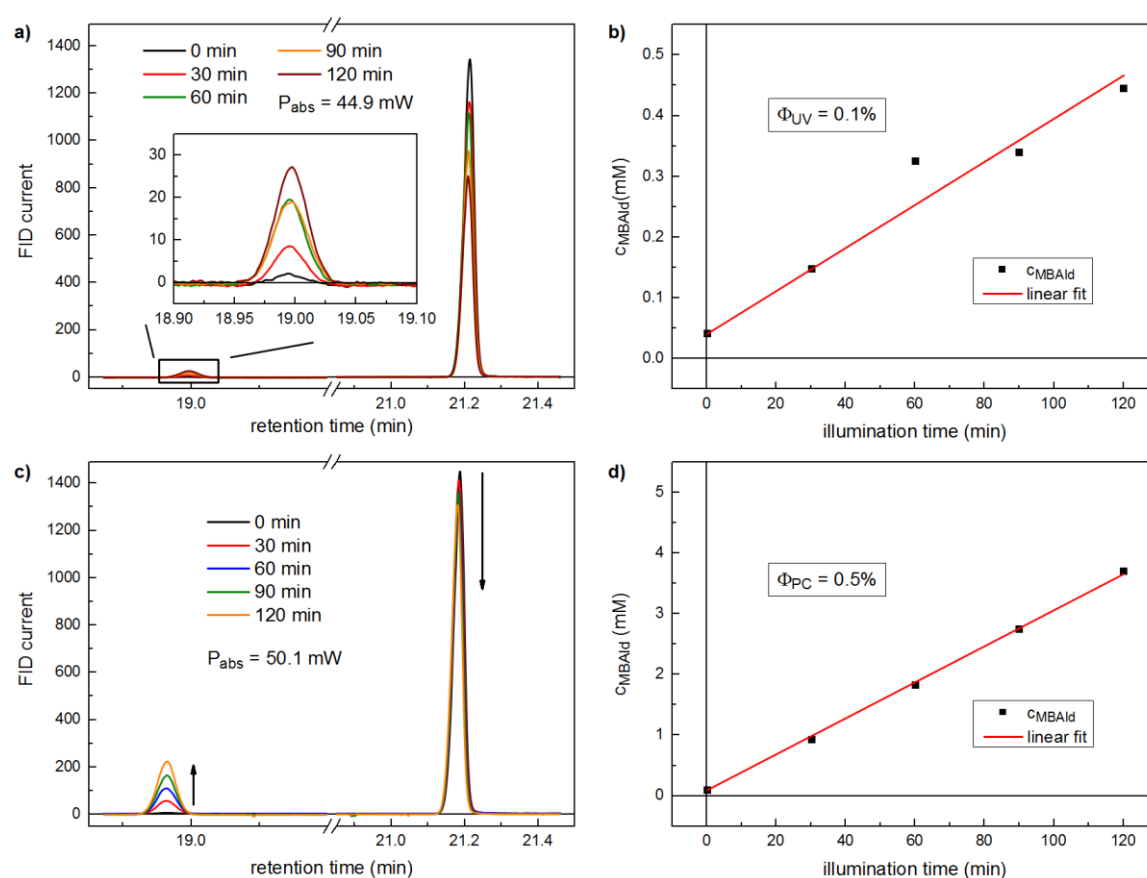


**Figure 1:** Results of the illumination in the QYDS. (a) GC traces of the UV irradiated solution. (b) Corresponding concentrations of the aldehyde of the UV irradiated solution. (c) GC traces of the visible light irradiated solution. (d) Corresponding concentrations of the aldehyde of the visible light irradiated solution.

It can also be seen by comparing (a) and (c) that the photocatalyzed reaction is more

efficient for the aldehyde formation than the UV irradiation. The graphs in **(b)** and **(d)** depicts the aldehyde concentration versus the illumination time and a linear correlation is observed. With the slope of the linear function, the quantum yield for the photooxidation can be estimated *via*:

$$\Phi = \frac{c_{\text{MBAld}}}{T} \cdot \frac{V \cdot N_A \cdot h \cdot c}{P_{\text{abs}} \cdot \lambda_{\text{LED}}} \quad (1)$$

A quantum yield of UV irradiation of  $\Phi_{\text{UV}} = 0.1\%$  and for visible light irradiation of  $\Phi_{\text{PC}} = 0.5\%$  is derived from the experimental data. The photocatalyzed oxidation is about five times more efficient and shows a better selectivity for the product.

The product yield was also confirmed by transient absorption (TA) spectroscopy. Transient absorption on the ns- $\mu$ s time scale was performed with an *ESKPLA NT242-PGD035* ns-laser system as the pump source with electronically adjustable delay. A detailed description of the TA setup can be found in the following references.<sup>[5,6]</sup> At first, a sample containing only flavin was measured in order to determine its singlet and triplet lifetime in MeOH. The flavin concentration was  $c_{\text{RFTA}} = 1.0$  mM and the solution was circulated in a flow cell with film thickness of  $d = 250$   $\mu$ m at ambient conditions. The pump wavelength was  $\lambda_{\text{pump}} = 455$  nm. Applying a global fit routine provided the lifetimes, species spectra of the singlet and triplet state and the triplet yield of **RFTA** in MeOH. The values are:  $\tau_{0\text{S1}} = 6.8$  ns,  $\tau_{0\text{T1}} = 484$  ns and  $\Phi_{\text{ISC}} = 0.6$ .

To study the photooxidation of **MBA** in MeOH, a solution of **RFTA** and **MBA** in MeOH was prepared with concentrations of flavin  $c_{\text{RFTA}} = 1.0$  mM and of **MBA**  $c_{\text{MBA}} = 20.0$  mM. The pump wavelength was  $\lambda_{\text{pump}} = 455$  nm providing a selective excitation of the flavin. The transient absorption profile and the resulting species spectra and yields are shown in **Figure 2**.

The product yield is then:

$$\Phi_{\text{tot}} \leq \Phi_{\text{ISC}} \cdot \Phi_{\text{ET}} \cdot \Phi_{\text{PT}} = 0.3 \cdot 0.03 \cdot 0.61 = 0.055 = 0.55\% \quad (2)$$

The value is in good agreement with the one obtained from the QYDS measurement.

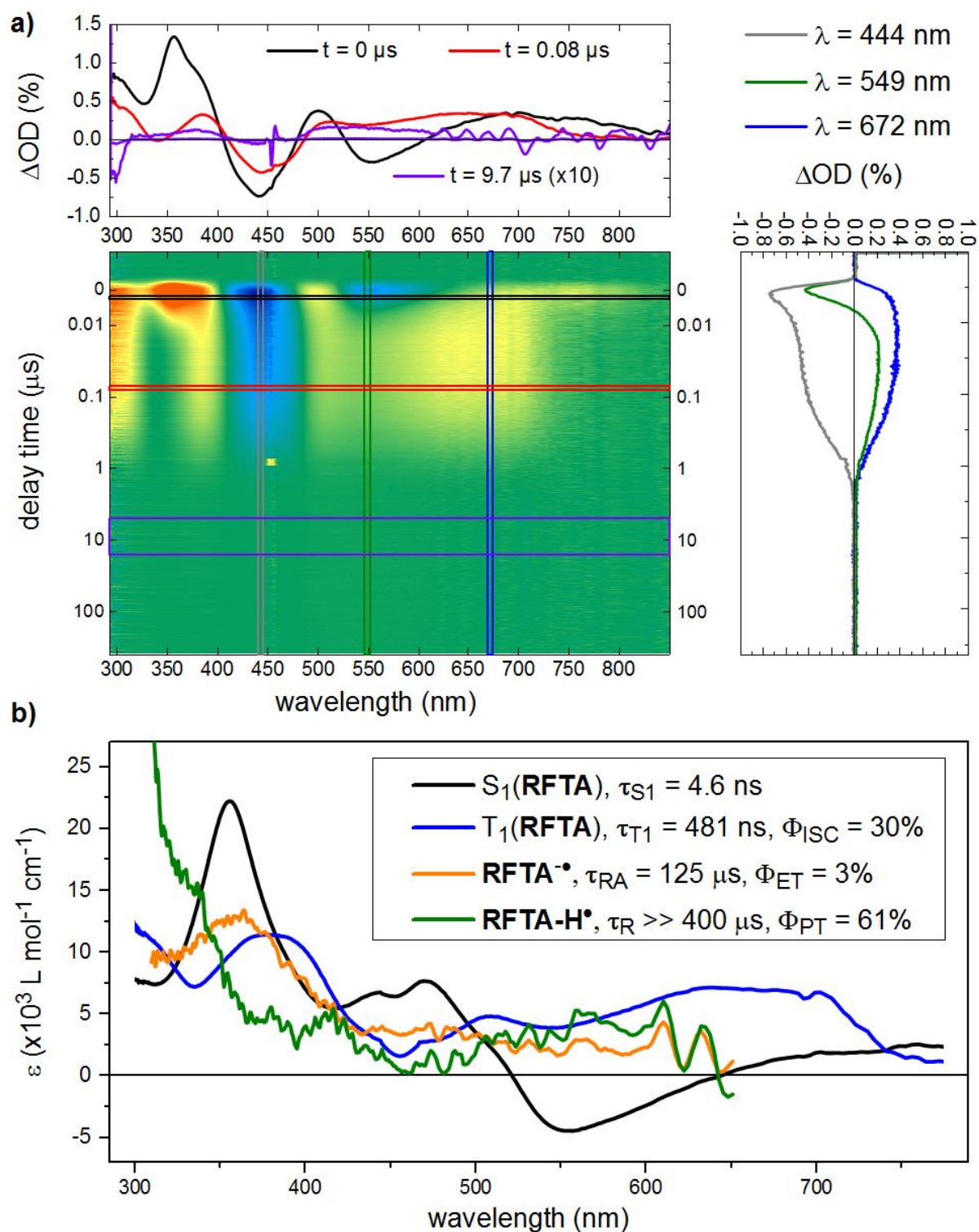


**Figure 2:** Transient absorption of  $[\text{RFTA}] = 1$  mM and  $[\text{MBA}] = 20$  mM in MeOH: (a) Profile. (b) SAS and yields.

As discussed in the previous section, the rate of electron transfer plays an important role in the efficient oxidation of benzyl alcohol to the aldehyde. Therefore, we have investigated

a series of differently methoxy-substituted 1,3 diols with increasing electron density and compare their electron transfer efficiencies using time-resolved spectroscopic studies.

### **4.3 Photocatalyzed oxidation of lignin substructure - benzylic alcohols**

Lignin represents 30% of non-fossil organic carbon on earth and is considered as the largest renewable feedstock on earth. The primary structure of lignin is a randomly crosslinked polymer of phenyl propane units joined by many different linkages. The most common precursors are the three monolignol monomers all of which are methoxylated to various degrees: coumaryl alcohol, coniferyl alcohol and sinapyl alcohol. These are incorporated in the lignin in the form of phenyl propanoids. (**Figure. 3**). A controlled depolymerization of these fragments could be an ideal source of aromatic organic compounds as starting material in synthesis. Oxidative flavin photocatalysis offers a potential pathway for the selective degradation of lignin.

Among the different linkages in lignin, the  $\beta$ -O-4 linkage consists of >50% of all linkages found in lignocellulose. The degree of oxidation of these linkages depends on the methoxy substitution on the aromatic moiety. In our study, we have investigated the substitution effect and oxidation of a substructure of lignin that contains 1,3 diol unit. We have performed transient absorption (TA) studies to investigate the effect of the substitution pattern on the arene ring on the efficiency of the photocatalyzed reaction and subsequent processes. Our analysis is based on the detailed spectroscopic study of the mechanism and the quantum yields of the flavin catalyzed photo-oxidation of **MBA**.<sup>[7]</sup>

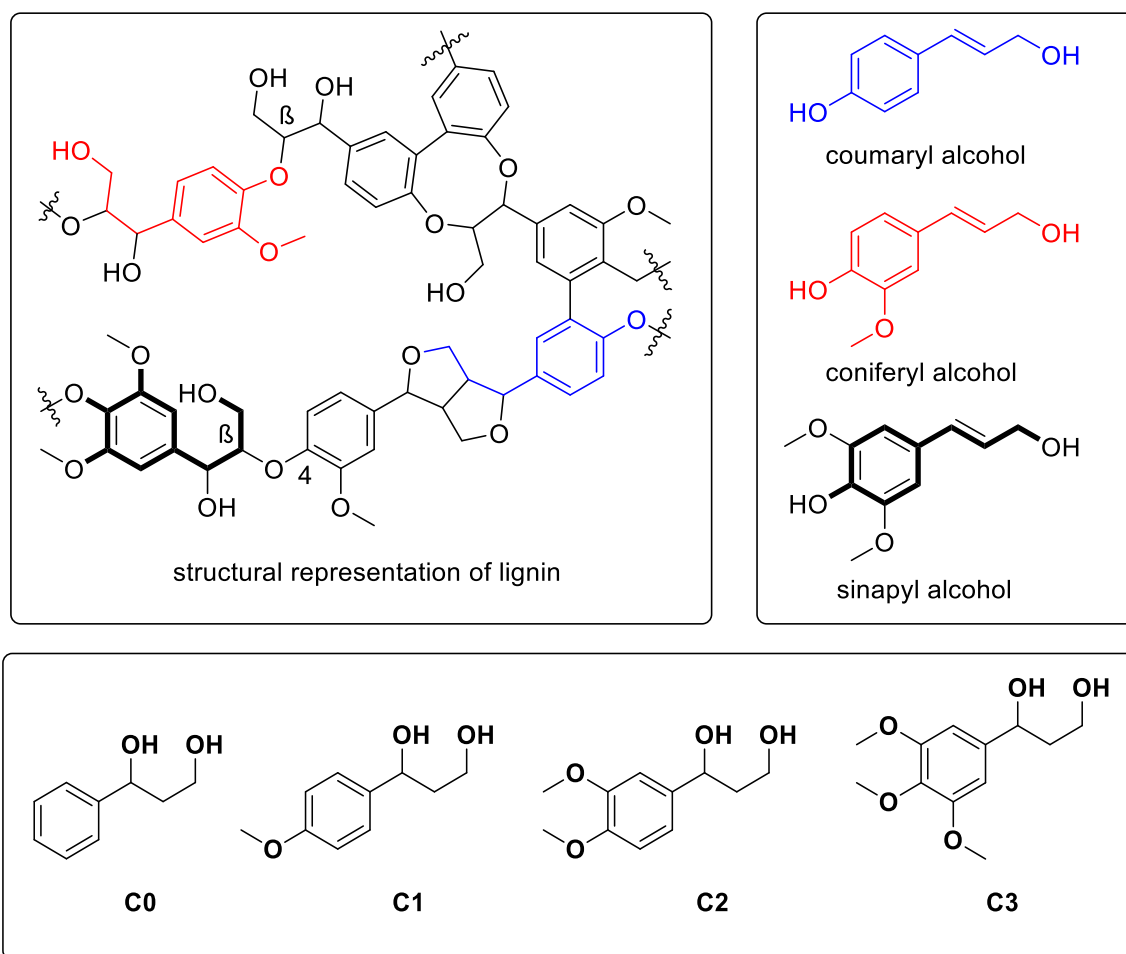
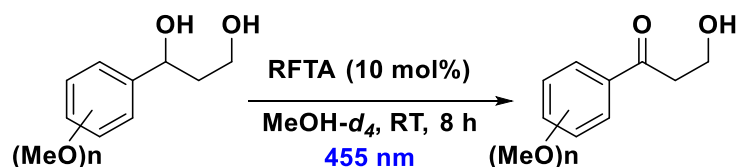


**Figure 3:** (a) Schematic representation of a lignin polymer (b) Three important monolignol subunits. (c) Substrates for transient absorption studies.

In the previously discussed experiments, we have observed that the overall efficiency of the photo-oxidation of **MBA** is increased under visible light induced photocatalyzed condition using **RFTA** as the photocatalyst. Furthermore, the lifetimes and yields of the intermediate states can be obtained by transient absorption spectroscopy. In principle, the efficiency for eT should increase with an increasing ability of the substrate to stabilize the intermediate radical cation after electron transfer. Consequently, this should also improve the entire product quantum yield (PQY). Thus, under identical photocatalytic reaction conditions the total chemical yield of the four substrates (**C-0** to **C-3**, **Figure 3c**) was determined by NMR. It turned out that with increasing electron donating character, the chemical yield first increased from **C-0** to **C-1**, but then decreased to zero from **C-1** to **C-3** (**Scheme 1**, **Table 1**).



Scheme 1: Oxidation of 1,3 diol with RFTA.

Table 1: Benzylic oxidation of 1,3 diols

| Entry | Substrate | Product <sup>a</sup>   |
|-------|-----------|--|
| 1     | <br>C0    | <br>20%  |
| 2     | <br>C1    | <br>46%  |
| 3     | <br>C2    | <br>12%  |
| 4     | <br>C3    | <p style="text-align: center;">0%<br/>Partial degradation of the starting material</p> |

<sup>a</sup>the yields were calculated by NMR experiment using 1,3,5-trimethoxybenzene as an internal standard.

According to our hypothesis, there could be two possible explanations for this anomalous observation. Firstly, Marcus theory might provide an explanation. As the electron donating character in the substrate increases, the total amount of Gibbs' free energy ( $\Delta G^0$ ), that will be released by the reaction will also increase. Thus, in our case, it might be possible that the total Gibbs' free energy of electron transfer is lowered so much, that according to

Marcus theory, the electron transfer occurs in the inverted region increasing the activation energy of the reaction, thus decreasing the total product yield (**Figure 4**). This hypothesis can be checked by the determination of electron transfer rate and correspondingly the total electron transfer yield *via* time resolved absorption spectroscopy. If the electron transfer rate is decreased from C1 to C3 with otherwise identical reaction conditions, *i.e.*, solvent, temperature *etc.*, Marcus theory can provide a good explanation.

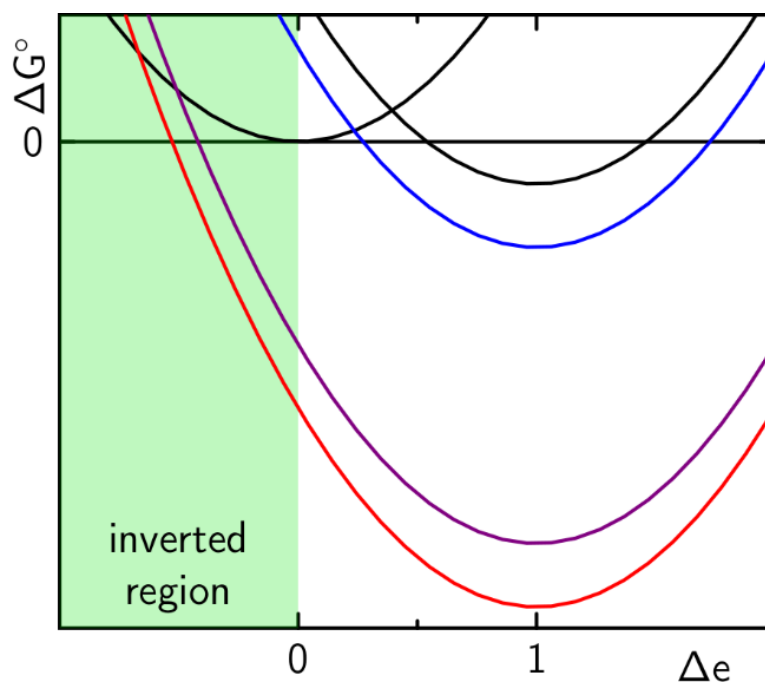


**Figure 4:** Hypothesis 1 explained by Marcus theory.

Secondly, on the other hand, the origin of the drop in the product yield could arise from potentially increased unproductive recombination reactions of the spin-correlated ionic radical pair. Since intersystem crossing (ISC) must occur first within the triplet-born ionic radical pair before radical pair recombination can occur, it is possible that the increased stabilization of the cation radical might simultaneously decrease its reactivity, increasing its lifetime and, thus, decreasing the chance for further productive processes. Therefore, the spin-correlated radical pair will have an enhanced probability undergoing ISC and finally recombine following the unproductive pathway of the photocatalytic cycle (**Figure 5**). The bold arrows here represents the probability of the molecule to remain in that particular state.

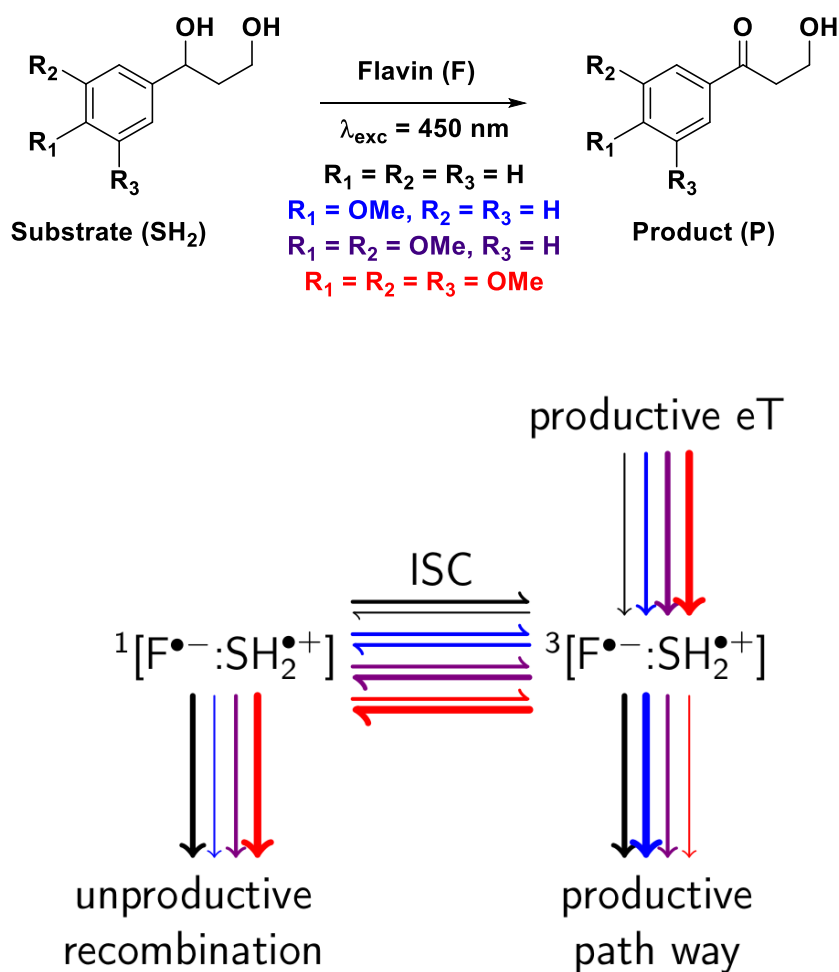


**Figure 5:** Hypothesis 2 explained by the productive and unproductive pathways arising from spin recombination after intersystem crossing.

In order to understand the varying yields and exclude one of the possible explanations, transient absorption on the ns- $\mu\text{s}$  time scale was carried out with substrates **C1**, **C2** and **C3**. The summary of electron transfer (eT) rates and yields for the RFTA/MBA system is presented in **Table 2**.

**Table 2:**

| Entry | CX [mM] | $^1\Phi_{\text{eT}}^{\text{a}}$<br>(MeCN/H <sub>2</sub> O<br>50:50 v/v) | $^3\Phi_{\text{eT}}^{\text{b}}$<br>(MeCN/H <sub>2</sub> O<br>50:50 v/v) | $^1\Phi_{\text{eT}}^{\text{a}}$<br>(MeOH) | $^3\Phi_{\text{eT}}^{\text{b}}$<br>(MeOH) |
|-------|---------|---|---|---|---|
| C1    | 20      | 0.27  | 0.26  | 0.31                                      | 0.06 <sup>c</sup>                         |



|    |     |      |      |      |      |
|----|-----|------|------|------|------|
| C1 | 100 | 0.60 | 0.52 | 0.60 | 0.03 |
| C2 | 20  | 0.33 | 0.97 | 0.39 | 0.95 |
| C2 | 100 | 0.68 | 0.99 | 0.65 | 0.99 |
| C3 | 20  | 0.16 | 0.97 | 0.24 | 0.91 |
| C3 | 100 | --   | --   | --   | --   |

<sup>a</sup> calculated by  $^1\Phi_{eT} = 1 - (k_{S1}^0 - k_{S1}^0)$ , <sup>b</sup> calculated by  $^3\Phi_{eT} = 1 - (k_{T1}^0 - k_{T1}^0)$ , <sup>c</sup> the data set with 20 mM C1 in MeOH showed a stronger triplet quenching compared to 100 mM C1.

Considering only the case with 20 mM substrate in ACN/H<sub>2</sub>O (50:50 v/v), shows that the electron transfer (eT) efficiencies for the S<sub>1</sub> and T<sub>1</sub> reaction are 27% and 26%, respectively, in case of C1. In contrast, the efficiencies are 33% and 97%, respectively, in case of C2 and 16% and 97%, respectively, in case of C3. In MeOH, the eT efficiencies with C2 and C3 are also maximal and thus, much more efficient than with C1. Interestingly, in MeOH the eT efficiency between the triplet flavin and the C1 is close to zero, which is in contrast to the situation in ACN/H<sub>2</sub>O (50:50 v/v) where it reaches 26%. Thus, every encounter between a triplet flavin and either C2 or C3 results in an efficient electron transfer. In case of C1, the efficiency is only about 6 to 26% depending on the solvent conditions. This observation suggests that, the total Gibb's free energy for electron transfer is lowered with more electron donating character in the substrate, enhancing the electron transfer rates. If the activation energy is increased according to Marcus theory, the electron transfer rate should decrease from C1 to C3, which is not the case here. However, since the overall product yield is reduced with more electron donating character, we conclude that the overall recombination rates and correspondingly, the yields for the unproductive processes increase simultaneously following the second hypothesis (**Figure 5**). Therefore, the enhancement of the unproductive pathway is a likely explanation of our experimental results.

## 4.4 Conclusion

In conclusion, we could show that with the high power UV-LEDs we can compare the photoreactions initiated by direct UV irradiation with photocatalyzed reactions. We concluded that the photocatalyzed oxidation of 4-methylbenzyl alcohol is five times faster than the direct photochemical oxidation with UV light. We have also studied the rate of

oxidation of four differently substituted benzylic 1,3 diols. Transient absorption spectroscopic studies showed that, with increase in methoxy substitution, the rate of electron transfer increases. However, as the overall product yield is decreased, we hypothesized that, with the increase in stability of the radical cation, *i.e.*, with the increase in the life time of the spin-correlated radical ion pair, the unproductive recombination pathway of this radical ion pair back to the starting material increases, hence the rate of oxidation decreases.

## 4.5 Experimental section

### 4.5.1 Materials and methods

Solvents and reagents were obtained from commercial sources and used without further purification. Spectroscopic grade DMF and DMSO were dried with 3 Å molecular sieves. Riboflavin tetraacetate was synthesized according to the general procedure.<sup>[8]</sup> Proton NMR spectra were recorded on a Bruker Avance 300 MHz spectrometer in CDCl<sub>3</sub> solution with internal solvent signal peak at 7.26 ppm. Carbon NMR were recorded at 75 MHz spectrometer in CDCl<sub>3</sub> solution and referenced to the internal solvent signal at 77.26 ppm. Proton NMR data are reported as follows: chemical shift (ppm), multiplicity (s = singlet, d = doublet, t = triplet, q = quartet, quint = quintet, dd = doublet of doublets, ddd = doublet of doublet of doublets, td = triplet of doublets, qd = quartet of doublets, m = multiplet, br. s. = broad singlet), and coupling constants (Hz). High resolution mass spectra (HRMS) were obtained from the central analytic mass spectrometry facilities of the Faculty of Chemistry and Pharmacy, Regensburg University and are reported according to the IUPAC recommendations 2013. All reactions were monitored by thin-layer chromatography using Merck silica gel plates 60 F254; visualization was accomplished with short wave length UV light (254 nm). UV-Vis and fluorescence measurements were performed with Varian Cary 50 UV/Vis spectrophotometer and FluoroMax-4 spectrofluorometer, respectively. Electrochemical studies were carried out under argon atmosphere. The measurements were performed in acetonitrile (CH<sub>3</sub>CN) containing 0.1 M tetra-n-butylammonium tetrafluoroborate using ferrocene/ferrocenium (Fc/Fc<sup>+</sup>) as an internal reference. A glassy carbon electrode (working electrode), platinum wire counter electrode, and Ag quasi-

reference electrode were employed. Spectroelectrochemical studies were carried out in an optically transparent thin layer electrochemical cell (OTTLE). Standard flash chromatography was performed using silica gel of particle size 40–63  $\mu\text{m}$ . Photooxidation reactions were performed with 455 nm LEDs (OSRAM Oslon SSL 80 royal-blue LEDs ( $\lambda = 455 \text{ nm} (\pm 15 \text{ nm})$ ), 3.5 V, 700 mA).

#### 4.5.2 Gas Chromatographic traces for different concentrations of MBA and MBAld in MeOH

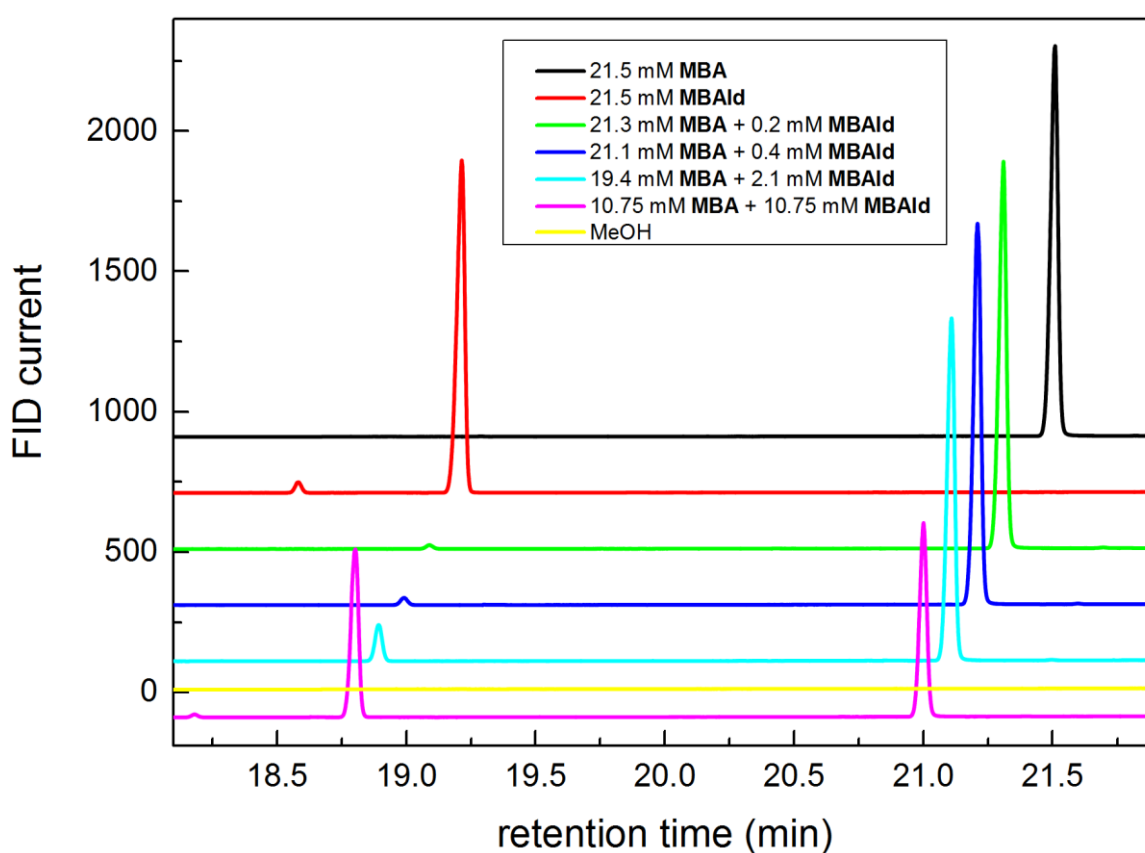


**Figure 6:** GC traces of various prepared concentrations of MBA and MBAld in MeOH.

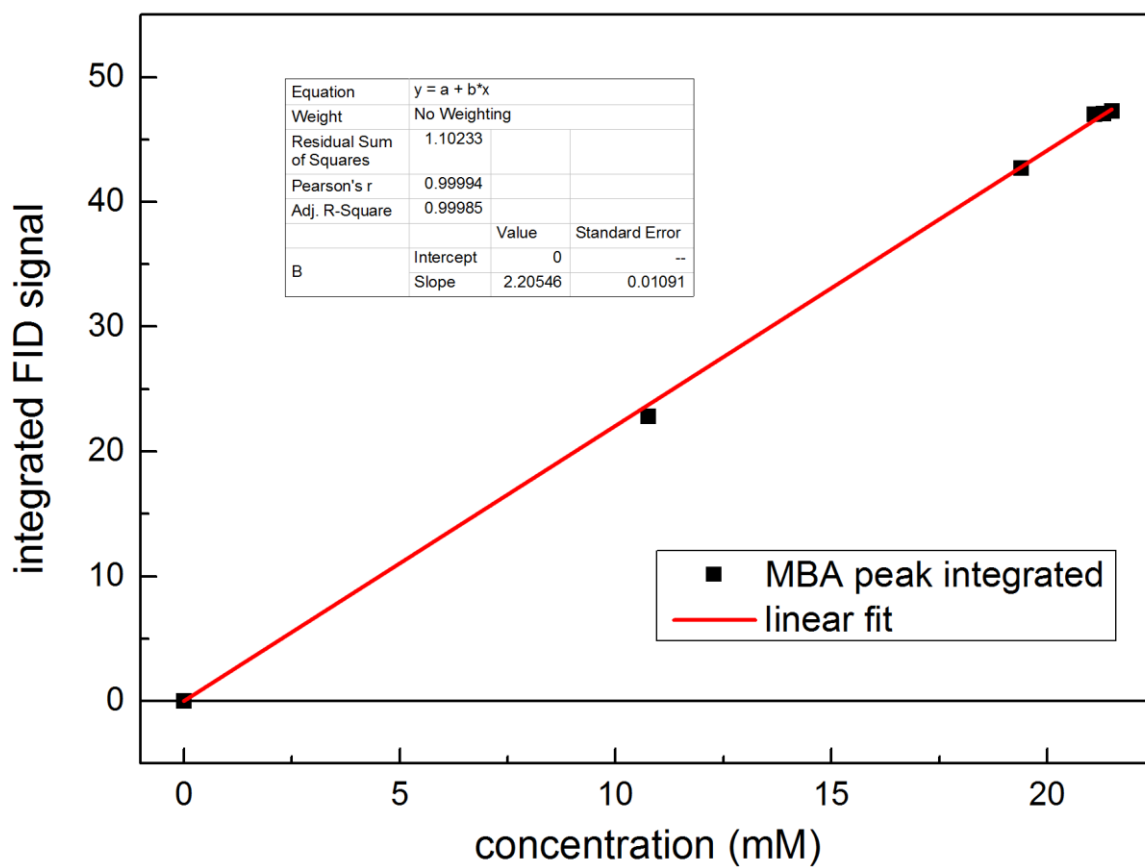


**Figure 7:** Integrated MBA peak *versus* the concentration in MeOH.

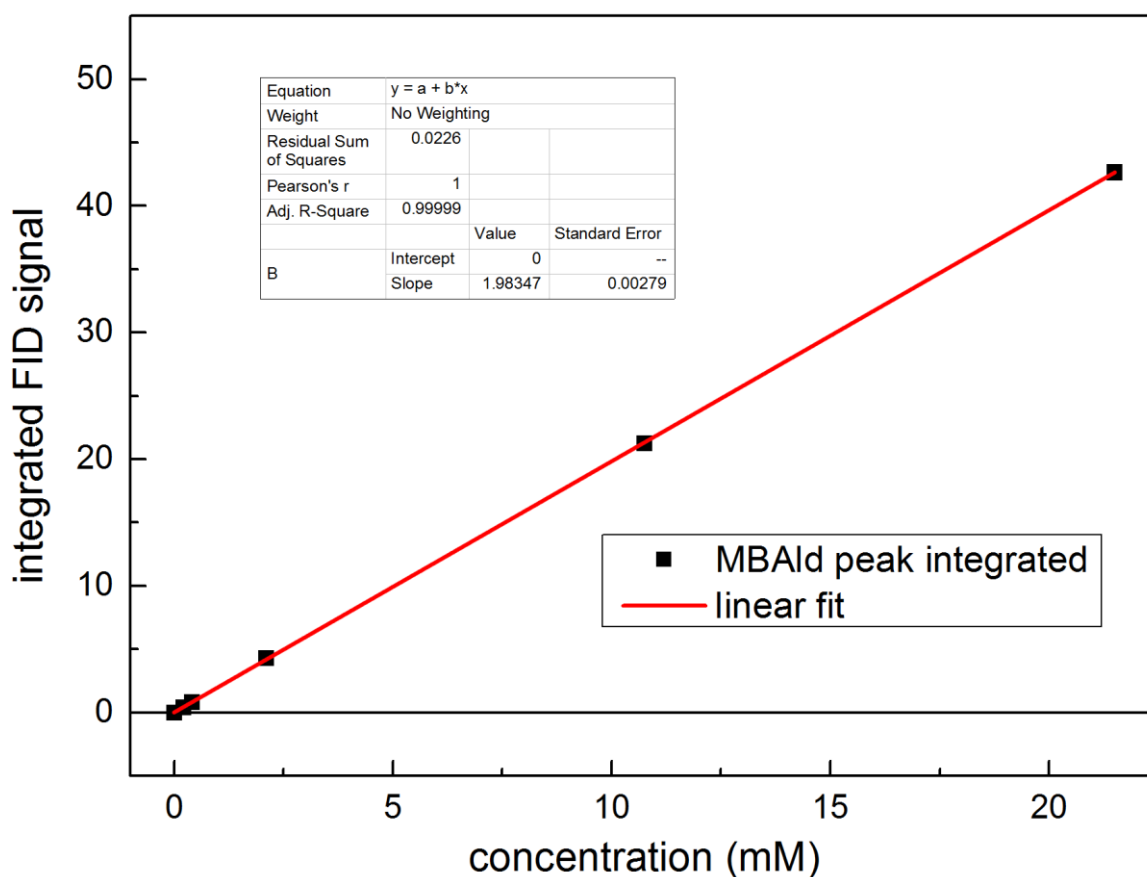
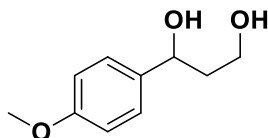


**Figure 8:** Integrated MBAld peak versus the concentration in MeOH.

### 4.5.3 Synthesis of the 1,3 diols

The 1,3 diols are synthesized according to the literature procedures.<sup>[9]</sup> All the compounds are obtained as white solids.

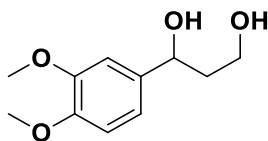
#### Synthesis of 1-(4-methoxyphenyl)propane-1,3-diol (2)



<sup>1</sup>H NMR (CDCl<sub>3</sub>, 300 MHz, ppm):  $\delta$  7.25 (d,  $J$  = 9 Hz, 2H), 6.85 (d,  $J$  = 8.7 Hz, 2H), 4.83 (dd,  $J$  = 8.7 Hz, 3.87 Hz, 1H), 3.77-3.74 (m, 5H), 3.25 (bs, 2H), 2.00-1.87 (m, 2H).

<sup>13</sup>C NMR (CDCl<sub>3</sub>, 75 MHz, ppm):  $\delta$  158.9, 136.6, 126.9, 113.8, 73.5, 61.1, 55.3, 40.4

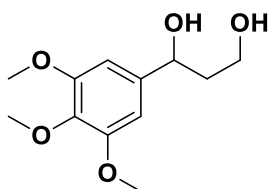
These data are in accordance with the literature procedure.

**Synthesis of 1-(3,4-dimethoxyphenyl)propane-1,3-diol (3)**

**<sup>1</sup>H NMR** (CDCl<sub>3</sub>, 300 MHz, ppm): δ 6.88-6.77 (m, 3H), 4.83 (dd, *J* = 8.5 Hz, 3.9 Hz, 1H), 3.84-3.77 (m, 8H), 2.02 (bs, 2H), 1.99-1.81 (m, 2H).

**<sup>13</sup>C NMR** (CDCl<sub>3</sub>, 75 MHz, ppm): δ 149.1, 148.4, 137.2, 117.9, 111.0, 108.9, 74.0, 61.4, 56.0, 55.9, 40.6.

These data are in accordance with the literature procedure.

**Synthesis of 1-(3,4,5-trimethoxyphenyl)propane-1,3-diol (4)**

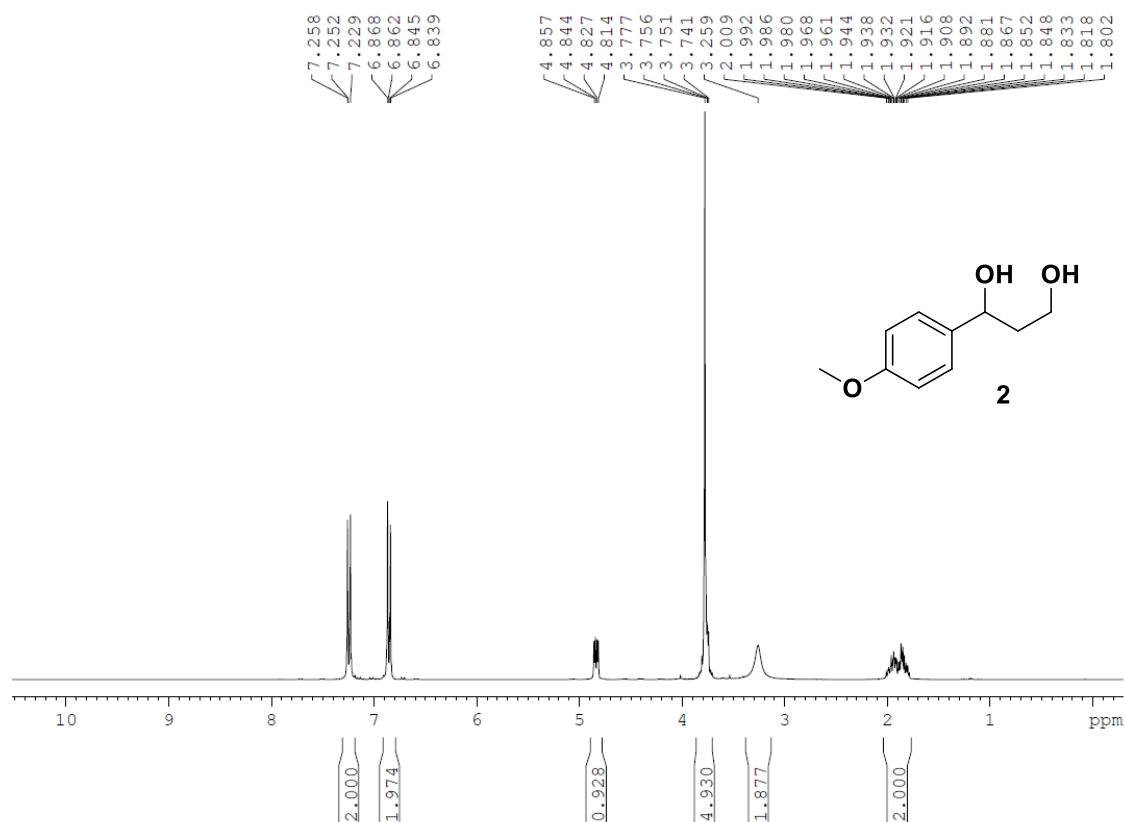
**<sup>1</sup>H NMR** (CDCl<sub>3</sub>, 300 MHz, ppm): δ 6.51 (s, 2H), 4.79 (dd, *J* = 8.5 Hz, 3.9 Hz, 1H), 3.78-3.76 (m, 1H), 3.42 (bs, 2H), 1.98-1.79 (m, 2H).

**<sup>13</sup>C NMR** (CDCl<sub>3</sub>, 75 MHz, ppm): δ 153.2, 140.0, 136.8, 102.5, 74.2, 61.3, 60.9, 56.1, 40.6.

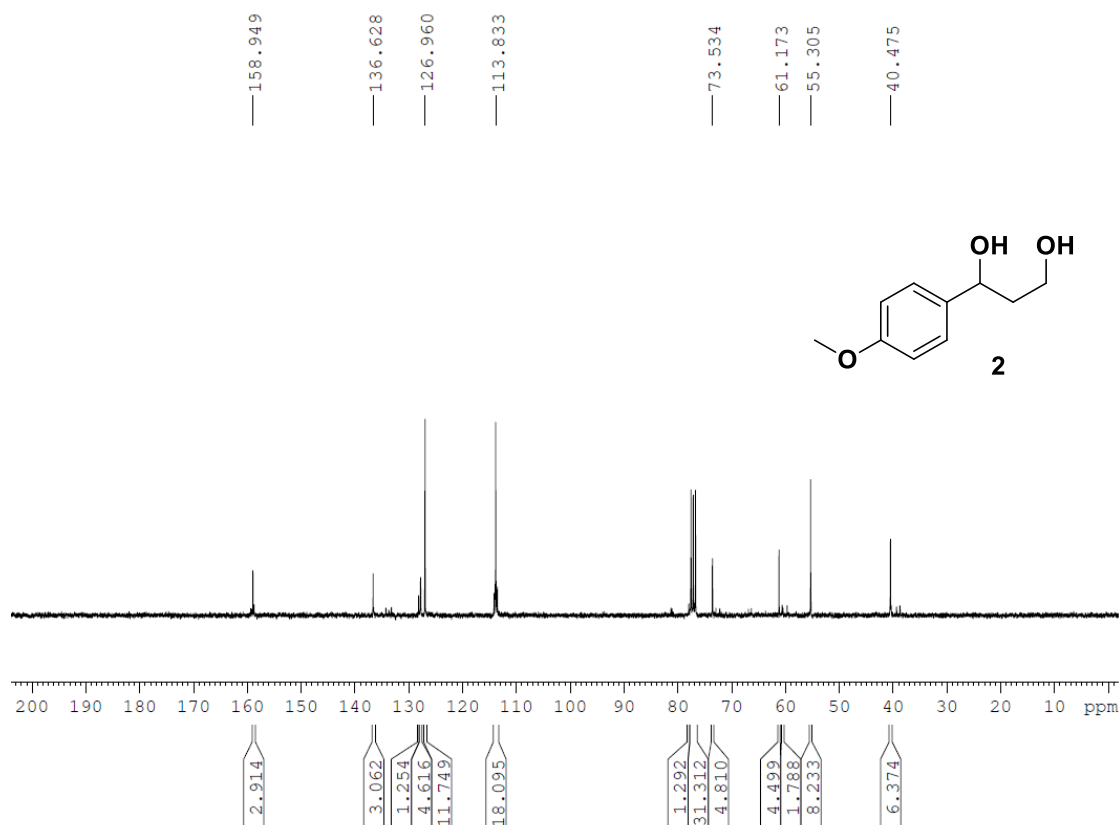
These data are in accordance with the literature procedure.

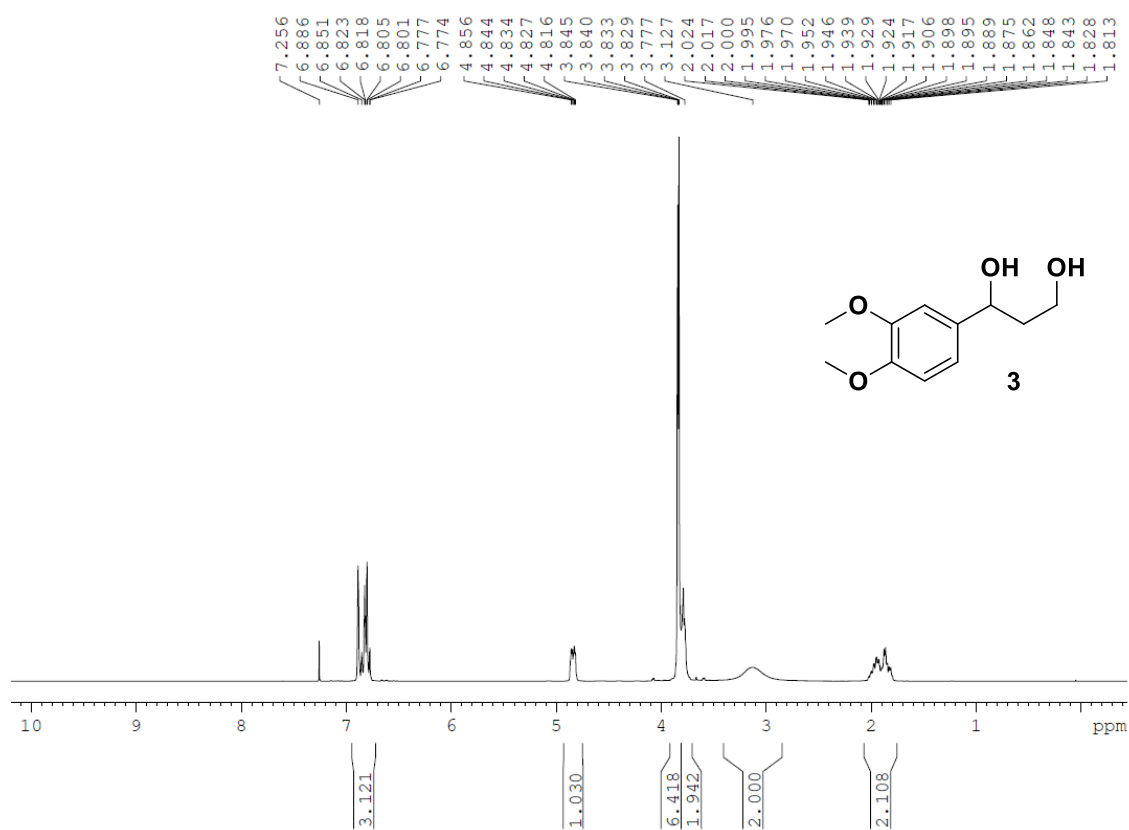
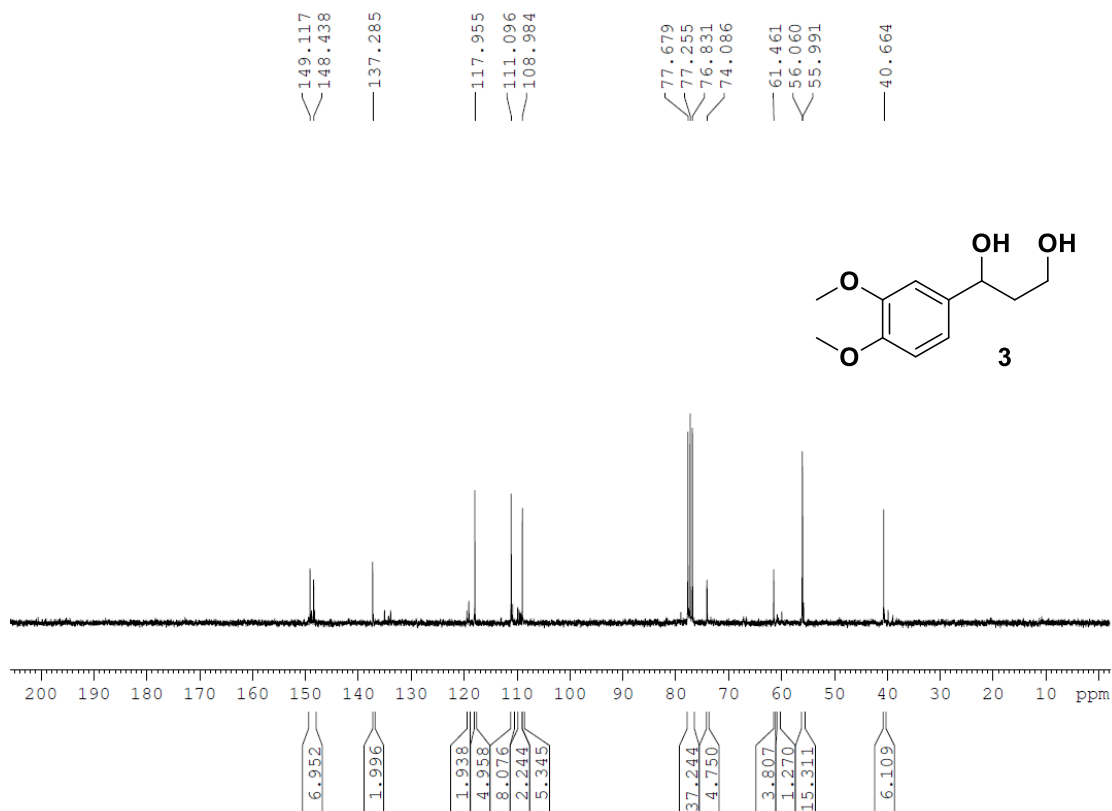
#### 4.5.4 $^1\text{H}$ - and $^{13}\text{C}$ NMR spectra of synthesized compounds

##### $^1\text{H}$ NMR of compound 2 ( $\text{CDCl}_3$ , 300 MHz)



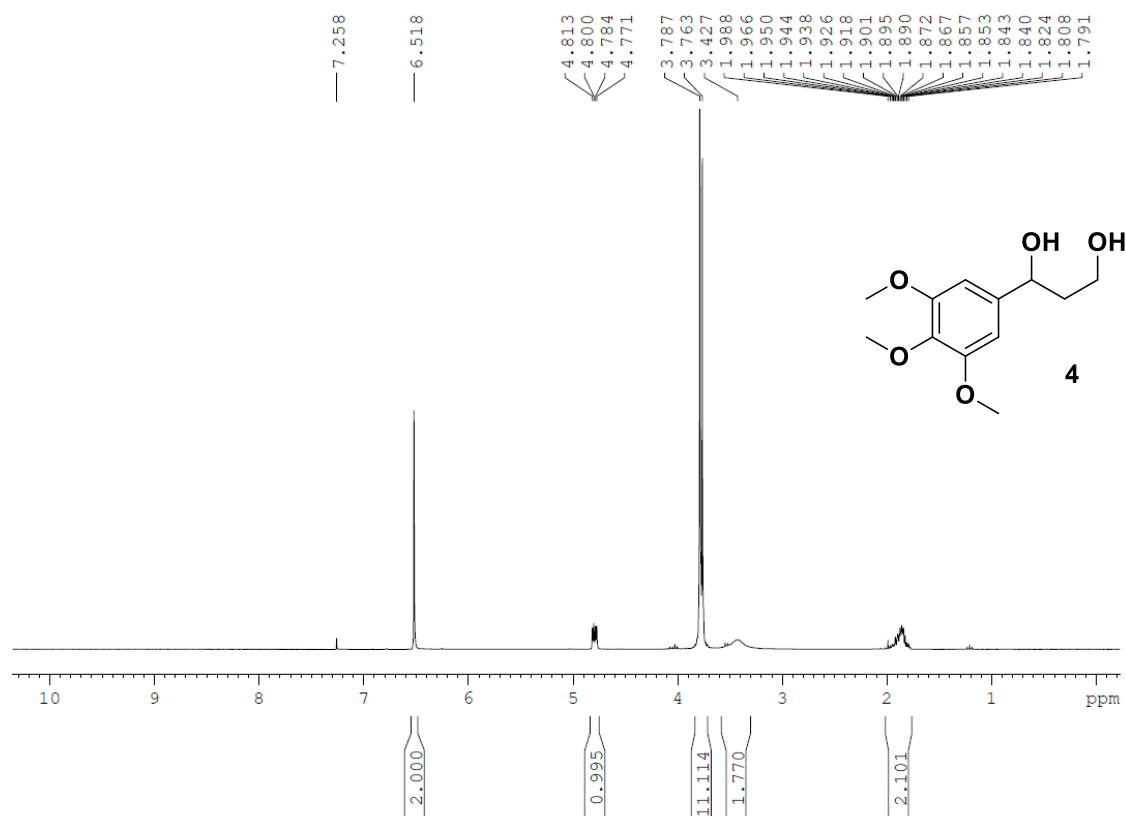
##### $^{13}\text{C}$ NMR of compound 2 ( $\text{CDCl}_3$ , 75 MHz)



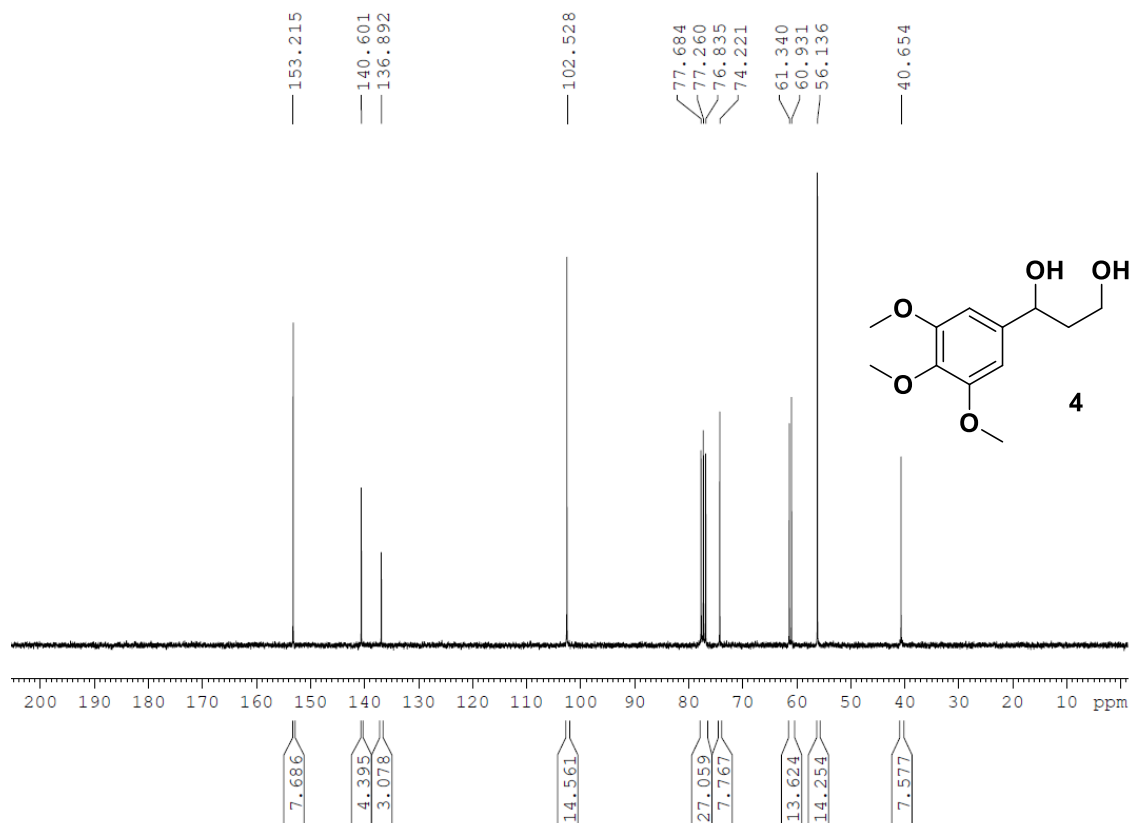
**$^1\text{H}$  NMR of compound 3 ( $\text{CDCl}_3$ , 300 MHz)** **$^{13}\text{C}$  NMR of compound 3 ( $\text{CDCl}_3$ , 75 MHz)**



**<sup>1</sup>H NMR of compound 4 (CDCl<sub>3</sub>, 300 MHz)**



**<sup>13</sup>C NMR of compound 4 (CDCl<sub>3</sub>, 75 MHz)**



## 4.6 References

1. P. F. Heelis, *Chem. Soc. Rev.* **1982**, *11*, 15-39.
2. a) P. Hemmerich, V. Massey, G. Weber, *Nature*. **1967**, *213*, 728-730. b) W. H. Walker, P. Hemmerich, V. Massey, *Helv. Chem. Acta*. **1967**, *50*, 2269-2279.
3. W. H. Walker, P. Hemmerich, V. Massey, *Eur. J. Biochem.* **1970**, *13*, 258-266.
4. U. Megerle, R. Lechner, B. König, E. Riedle, *Photochem. Photobiol. Sci.* **2010**, *9*, 1400-1406.
5. U. Megerle, I. Pugliesi, C. Schrieffer, C. F. Sailer, E. Riedle, *Appl. Phys. B.* **2009**, *96*, 215-231.
6. E. Riedle, and M. Wenninger in *Chemical Photocatalysis* (Ed.: B. König), D. Gruyter, Berlin, **2013**.
7. U. Megerle, M. Wenninger, R.-J. Kutta, R. Lechner, B. König, B. Dick, E. Riedle, *Phys. Chem. Chem. Phys.* **2011**, *13*, 8869-8880.
8. A. Barthel, L. Trieschmann, D. Ströhl, R. Kluge, G. Böhm, R. Csuk, *Arch. Pharm.* **2009**, *342*, 445-452.
9. K. A. De. Castro, J. Ko, D. Park, S. Park, H. Rhee, *Org. Process. Res. Dev.* **2011**, *11*, 919-921.

# *Chapter 5*

## *5. Attempts Towards the Photochemical Generation of Amidinyl Radicals and Syntheses of Oxadiazole and Quinazolinone Derivatives*



## 5.1 Introduction

Nitrogen containing compounds are found in many natural products, biologically active molecules and have widespread applications in chemical and pharmaceutical industries and also in material science. Over the decades, different strategies for C-N bond construction have gained interests. Despite of tremendous advances in this field, there are significant challenges to solve due to harsh reaction conditions required to generate radicals on nitrogen, their high affinity to abstract hydrogen atoms and to involve in other degradation pathways. Traditional methods to construct C-N bonds are based on copper mediated Ullman and Goldberg couplings<sup>[1]</sup> or the palladium catalyzed Buchwald-Hartwig amination/amidation strategy.<sup>[2]</sup> However, these methods require very high temperatures and pre-functionalized substrates. Free radicals have attracted considerable attention due to their high efficiency and unique reactivity. Although carbon centered radicals are widely known in literature, nitrogen centered radicals are relatively unexplored due to the lack of a convenient method to generate the radicals. Typically, nitrogen radicals are generated by thermolysis, photolysis or stoichiometric radical initiators.<sup>[3]</sup> The earliest example of nitrogen centered radical generation is the Hofmann-Löffler-Freytag reaction for the synthesis of five membered ring compounds via a thermal or photochemical decomposition of N-halo amines.<sup>[4]</sup> The generation of the free aminyl radical was first observed by H. Wieland in 1911, who found that tetraphenylhydrazine could generate a diphenylaminyl radical when irradiated with UV light.<sup>[5]</sup> Traditionally, radical initiators such as di-*tert*-butylperoxide (DTBP), *tert*butylhydroperoxide (TBHP)/I<sub>2</sub>, AIBN, (nBu<sub>3</sub>Sn)<sub>2</sub>/hν, Et<sub>3</sub>B/O<sub>2</sub> or UV irradiation are used for the generation of nitrogen radicals. Recently, visible light photoredox catalysis has emerged as a powerful technique to generate N-centered radical or radical cation species under mild conditions via a single-electron transfer (SET) process between N-H bonds or N-centered radical precursors with N-X (X = O, Cl, Br, N etc.) bonds.<sup>[6]</sup>

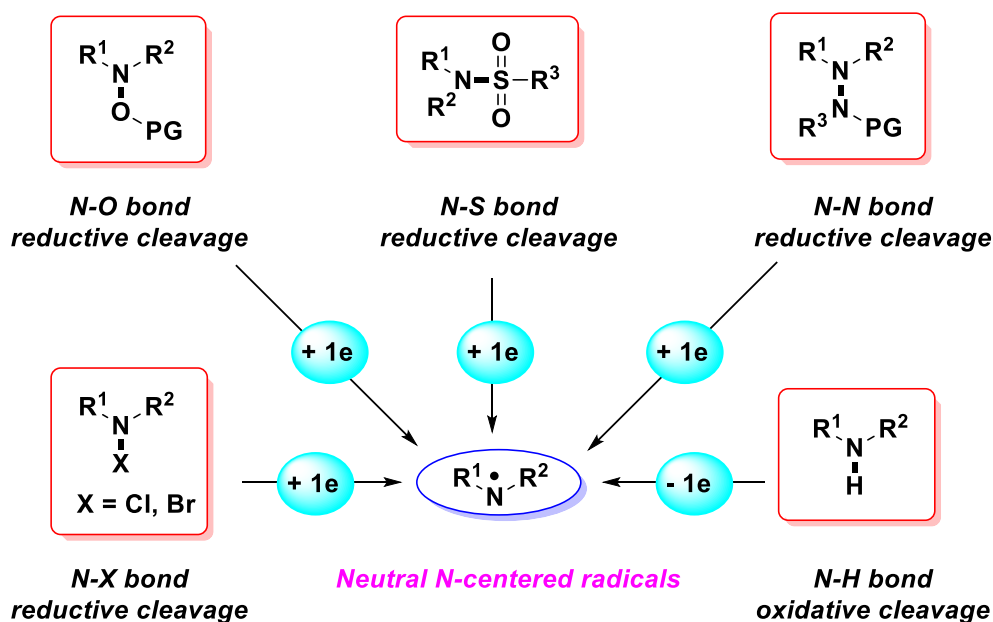
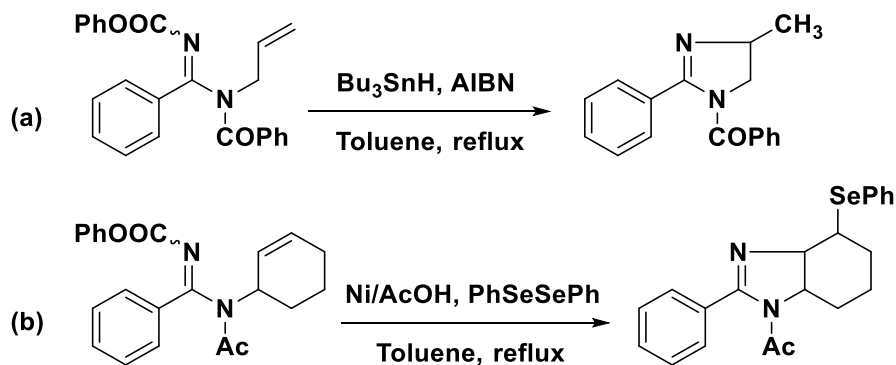


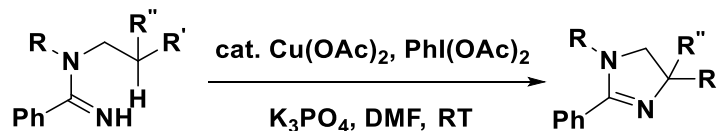
**Figure 1:** General scheme for generation of neutral N-centered radicals.

Amidines are a class of oxoacid derivatives where the  $\text{-OH}$  group and  $\text{=O}$  group are replaced by an  $\text{-NH}_2$  and  $\text{=NH}$  group. These amidines are very interesting due to their basicity, biological activity and their application as intermediates in the synthesis of some metallocyclic complexes and heterocyclic complexes. In the last decades, there have been few reports on the generation of amidinyl radicals and their transformations into heterocycles. In 2003, Zhang *et. al.* reported the generation of an amidinyl radical from amidoxime benzoates by treatment with  $\text{Bu}_3\text{SnH}$ / AIBN, resulting in the formation of imidazolines and imidazoles (**Scheme 1a**).<sup>[7]</sup> They also showed that amidinyl radicals could be generated by electron transfer from metallic nickel (Ni) to the amidoxime esters (**Scheme 1b**).<sup>[8]</sup>

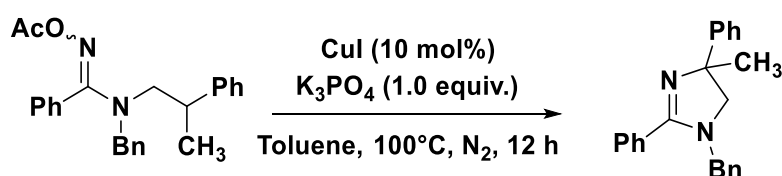


**Scheme 1:** Generation of amidinyl radical from amidoxime benzoates.

Chiba *et. al.* disclosed a Cu-catalyzed  $\text{PhI}(\text{OAc})_2$ -mediated C–H amination of N-alkyl amidines for the synthesis of dihydroimidazoles (**Scheme 2**)<sup>[9]</sup>, and the copper-catalyzed redox-neutral C–H amination with amidoximes (**Scheme 3**).<sup>[10]</sup>



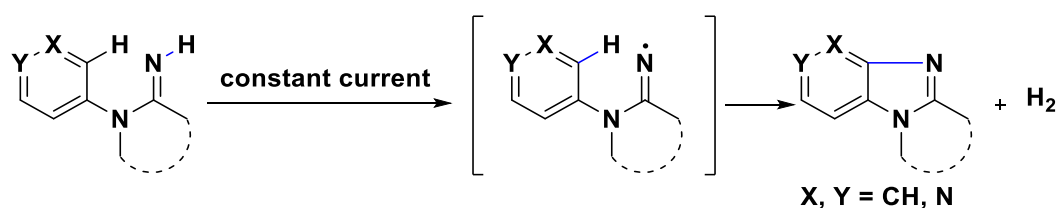
**Scheme 2:** Cu-catalyzed C-H amination of *N*-alkylamidines.



**Scheme 3:** Redox neutral C-H amination with amidoxime.

However, all these methods suffer from several disadvantages like long reaction times, high temperatures and the use of stoichiometric oxidants.

A recent report showed a metal and reagent free method to access amidinyl radicals through the anodic cleavage of a N–H bond (**Scheme 4**).<sup>[11]</sup>



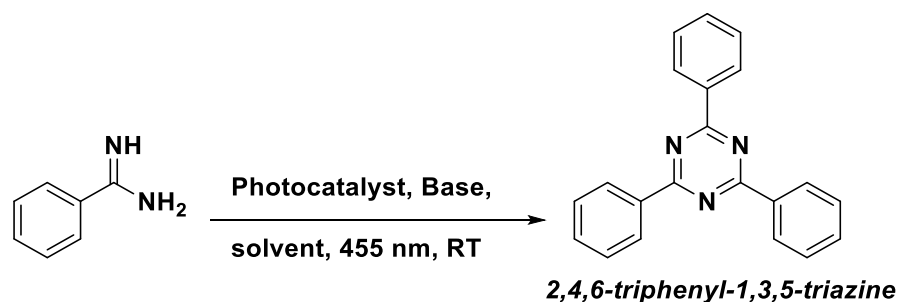
**Scheme 4:** Amidinyl radical formation through anodic N–H bond cleavage.

So far, to our knowledge, no photochemical method for the generation of an amidinyl radical is reported. Therefore, we envisaged to develop a method to generate an amidinyl radical in a photocatalytic way.

## 5.2 Results and discussions

### 5.2.1 Generation of amidinyl radical from benzamidine

We started with the simplest amidine, benzamidine and subjected it to different photochemical conditions. Our idea was to generate an amidinyl radical via N-H bond scission. Using Ru(bpy)<sub>3</sub>Cl<sub>2</sub>, Ir(ppy)<sub>3</sub> or Eosin Y as the photocatalyst under blue light irradiation, the amidine was converted to its trimerized product 2,4,6-triphenyl-1,3,5-triazine in some cases (**Scheme 5**). In other cases, either the bleaching of the catalyst or degradation of the starting material was observed. When phenyl acetylene was used as the reagent to trap the amidinyl radical, it remained unreacted in the reaction mixture.



**Scheme 5:** Trimerization of benzamidine under our photocatalytic conditions.

Later, we found that leaving the benzamidine in solution under air for a longer time also resulted in this trimerized product. Benzamidine hydrochloride is more stable than benzamidine and it is not susceptible to aerial oxidation. Using this as a choice of substrate also did not generate the amidinyl radical. The N-H bond dissociation energy of benzamidine is nearly 102.0 kcal/mol<sup>[12]</sup> making this bond rather difficult to break under our photocatalytic conditions. Therefore, we moved on to different kind of substrates for the generation of N-radicals.



### 5.2.2 Generation of amidinyl radicals from sulfonyl amidoximes

We synthesized a series of sulfonyl amidoximes as model compounds (**Figure 2**) for the generation of nitrogen centered radicals following a reported procedure.<sup>[13]</sup> The N-O bond dissociation energies of these amidoximes are in the range of 52.0 kcal/mol, hence they are easier to cleave than the benzamidines.

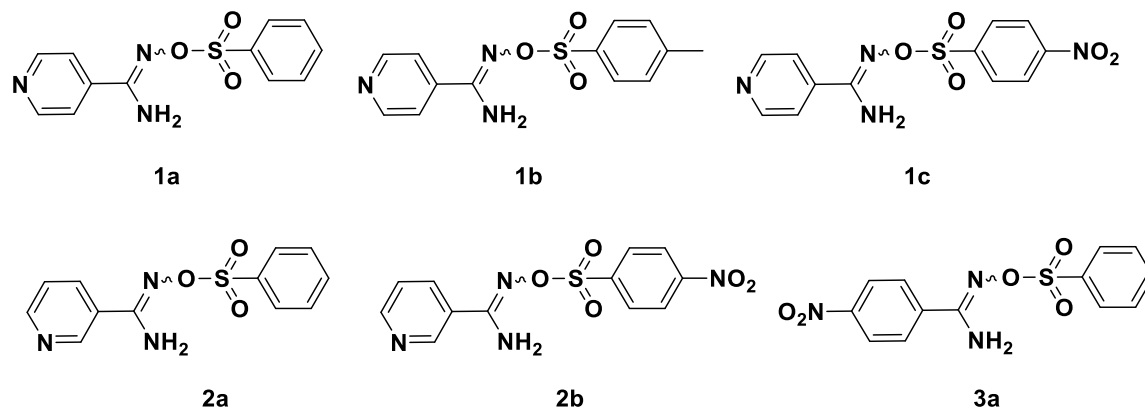
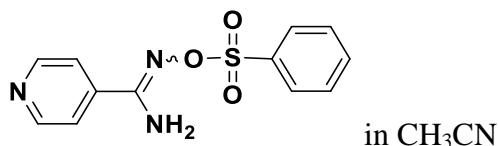
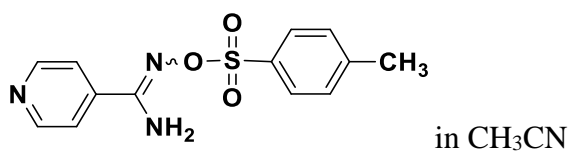
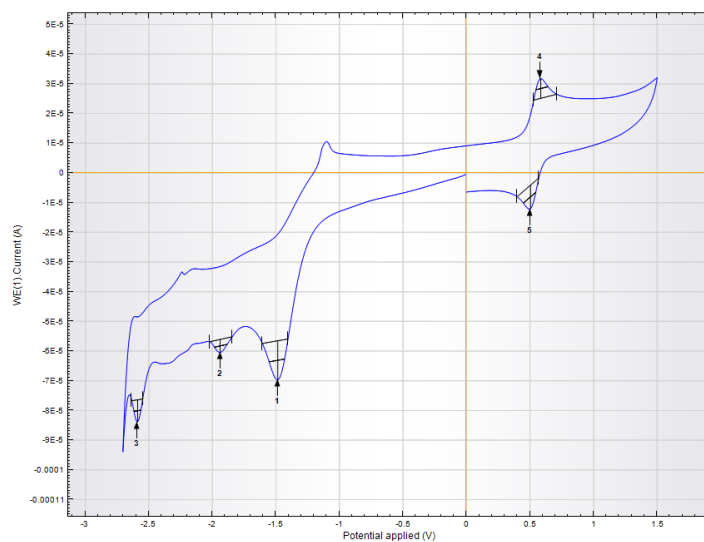


**Figure 2:** Structures of sulfonyl amidoximes synthesized.

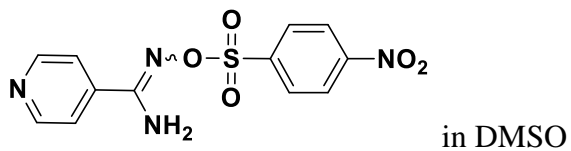
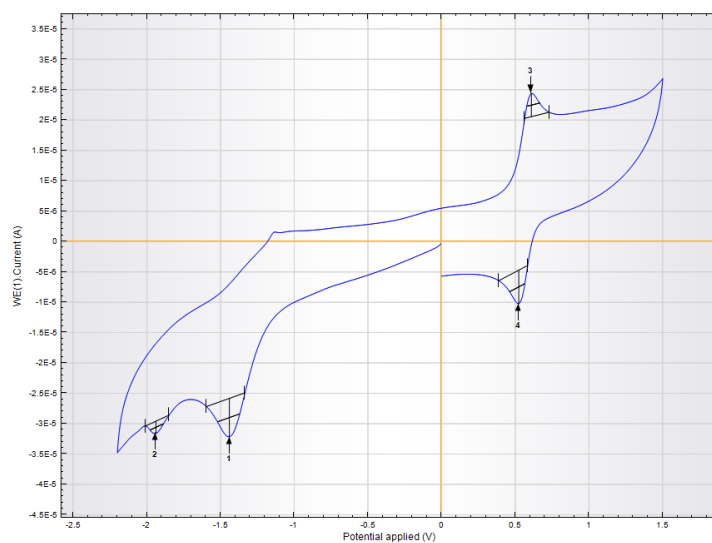
These sulfonyl amidoximes also have reduction potentials in the range of the generally used photocatalysts. Here, we will consider the first reduction potential.



$E^0 = -1.64 \text{ V}, -2.09 \text{ V}, -2.74 \text{ V vs SCE}$

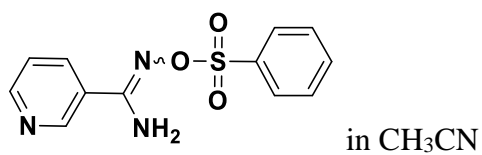
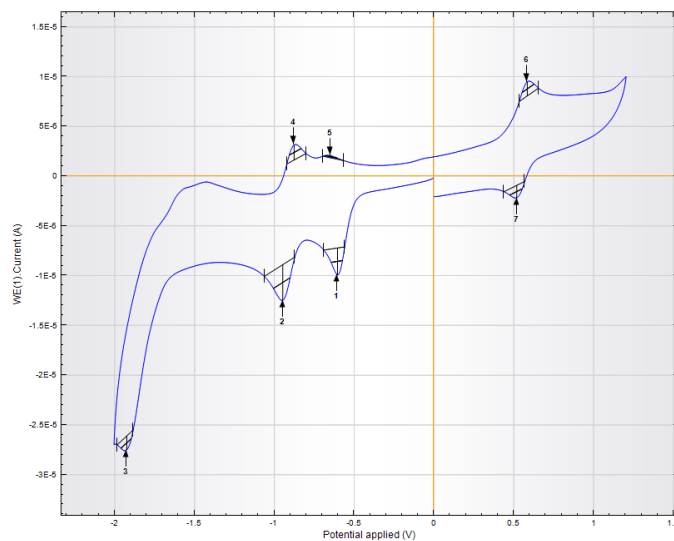


$E^0 = -1.62 \text{ V}, -2.11 \text{ V vs SCE}$

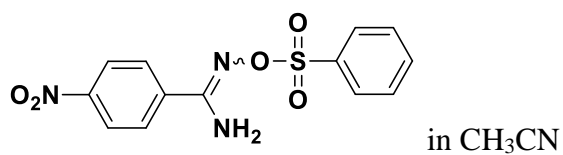
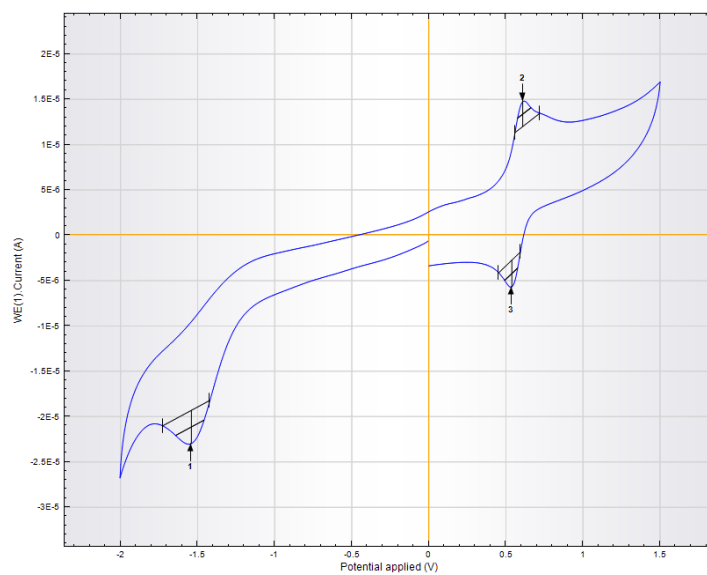


$E^0 = -0.775 \text{ V}, -1.117 \text{ V}, -2.09 \text{ V vs SCE}$

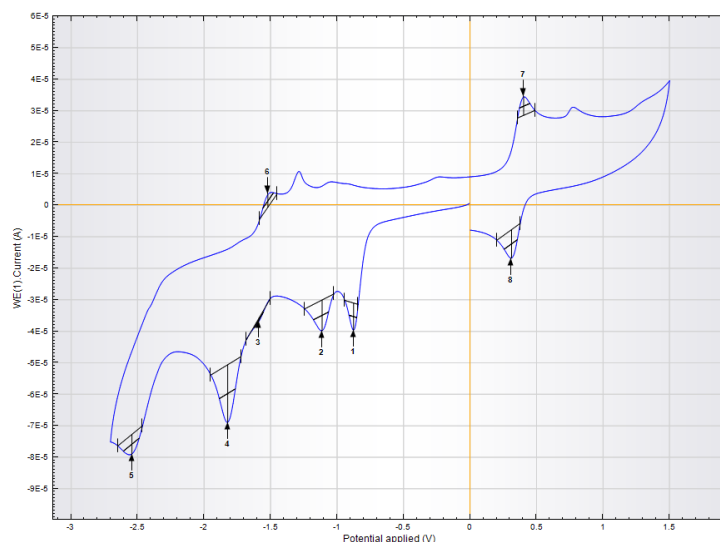
*Attempts Towards the Photochemical Generation of Amidinyl Radicals and Syntheses of Oxadiazole and Quinazolinone Derivatives*



$E^0 = -1.73 \text{ V vs SCE}$

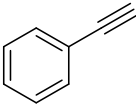


$E^0 = -0.85 \text{ V}, -1.08 \text{ V}, -1.79 \text{ V}, -2.51 \text{ V vs SCE}$

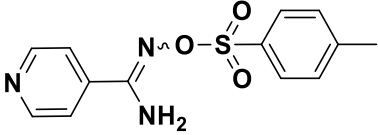
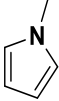


We aimed to generate a nitrogen radical by cleaving the N-O bond under photocatalytic conditions and to trap this radical with an alkene or alkyne. However, we did not obtain the desired products. In all the cases, the cleavage of the N-O bond occurred, generating a N-radical, however, the hydrogen abstraction step was much faster than coupling with the trapping reagents and we obtained the corresponding amidines in almost quantitative amounts. We hypothesized that changing the solvent from polar to nonpolar could affect the rate of hydrogen abstraction, although, there was no improvement. Few of the trial reactions are shown in **Table 1**.

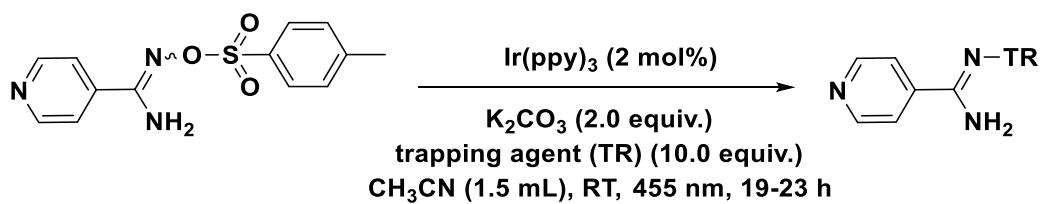
**Table 1:**

| Entry | Starting material | Trapping reagent  | Catalyst             | Reaction condition   | Observations  |
|-------|-------------------|---|----------------------|--|---|
| 1     |                   |  | Ir(ppy) <sub>3</sub> | Hantzsch ester (2 equiv.), K <sub>2</sub> CO <sub>3</sub> (2 equiv.), DMSO, 455 nm, RT, 24 h | Complete oxidation of the Hantzsch ester.<br>Starting material was converted to the amidine |

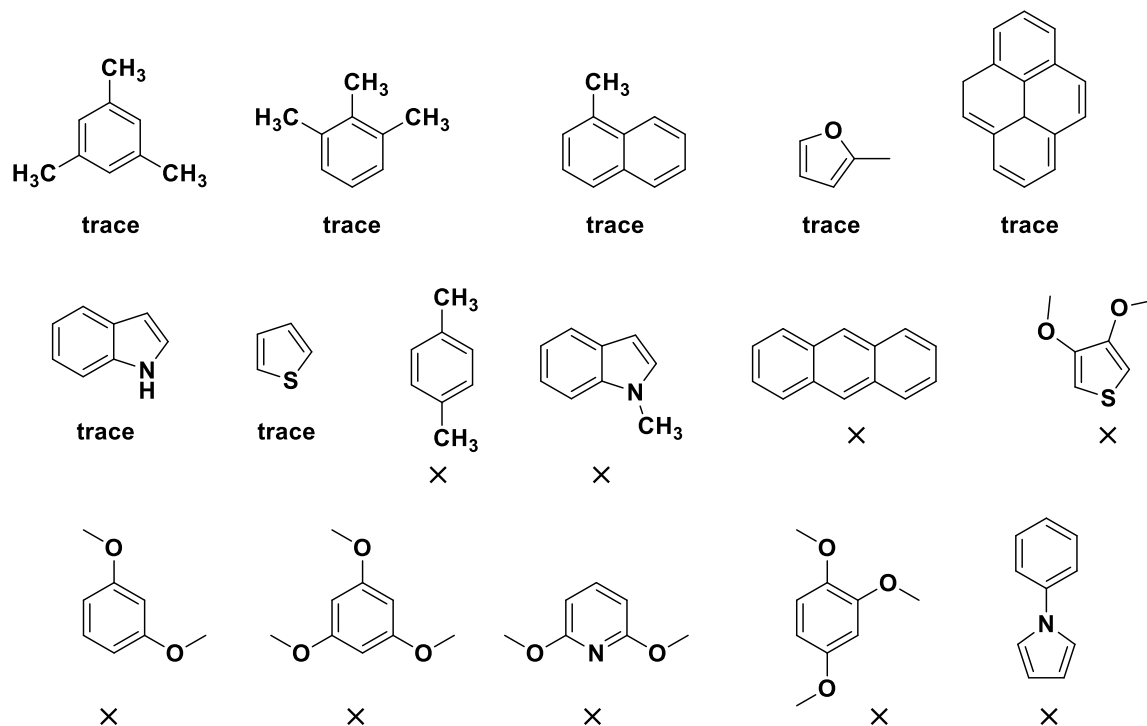
*Attempts Towards the Photochemical Generation of Amidinyl Radicals and Syntheses of Oxadiazole and Quinazolinone Derivatives*

|   |   |   |                      |  |                                |
|---|---|---|----------------------|--|--------------------------------|
| 2 |  |   | Rh-6G                | DIPEA, DMSO,<br>455 nm, RT, 24 h   | degradation                    |
| 3 |   | ----  | Rh-6G                | DIPEA, DMSO,<br>455 nm, RT, 24 h   | Degradation                    |
| 4 |   | ----  | ----                 | Et <sub>3</sub> N, CH <sub>3</sub> CN,<br>455 nm, RT   | No EDA<br>complex<br>formation |
| 5 |   |  | Ir(ppy) <sub>3</sub> | K <sub>2</sub> CO <sub>3</sub> (2 equiv.),<br>CH <sub>3</sub> CN, 455 nm,<br>RT  | No reaction                    |
| 6 |   | ----  | Ir(ppy) <sub>3</sub> | 9,10<br>dihydroanthracen<br>e (2 equiv.),<br>K <sub>2</sub> CO <sub>3</sub> (2 equiv.),<br>CH <sub>3</sub> CN, 455 nm,<br>RT | No reaction                    |
| 7 |   | ----  | Ir(ppy) <sub>3</sub> | 1,4 CHD (2<br>equiv.), K <sub>2</sub> CO <sub>3</sub> (2<br>equiv.), CH <sub>3</sub> CN,<br>455 nm, RT                       | No reaction                    |

We then tried to trap the radical with other reagents used in large excess to the starting material to avoid the hydrogen abstraction process. We were able to observe the desired products with a few heterocycles shown below (**Scheme 6**). The formation of the products were detected by mass spectroscopy. We tried to optimize the reaction conditions to obtain better yields. In this regard, we chose 2-methylfuran as the trapping reagent for the optimization (**Table 2**).

Synthesis of *N*-(het)aryl isonicotinimides

Trapping reagents:



Scheme 6: Attempts to trap aminidyl radical with heterocycles.

## Optimization of reaction: (Solvent and base)

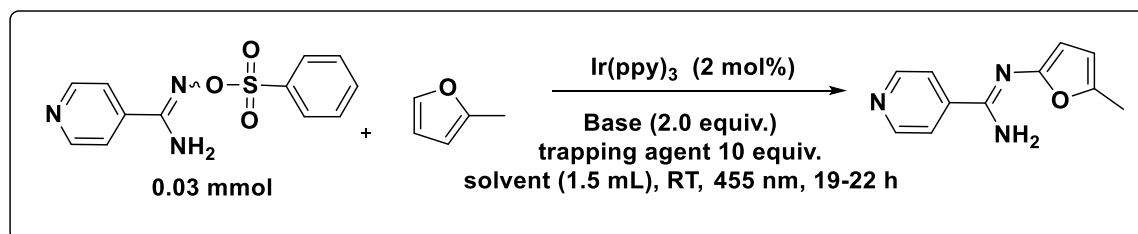


**Table 2:**

| Entry | Base                             | Solvent            | Time (h) | Observations ( <i>product detected by mass spectroscopy</i> ) |
|-------|----------------------------------|--------------------|----------|---|
| 1     | K <sub>2</sub> CO <sub>3</sub>   | CH <sub>3</sub> CN | 22       | Product formation   |
| 2     | K <sub>2</sub> CO <sub>3</sub>   | DMSO               | 22       | Product formation   |
| 3     | K <sub>2</sub> CO <sub>3</sub>   | DMF                | 22       | Product formation   |
| 4     | K <sub>2</sub> CO <sub>3</sub>   | DCE                | 22       | Starting material   |
| 5     | Na <sub>2</sub> CO <sub>3</sub>  | CH <sub>3</sub> CN | 22       | Starting material   |
| 6     | Na <sub>2</sub> CO <sub>3</sub>  | DMSO               | 22       | Starting material   |
| 7     | Na <sub>2</sub> CO <sub>3</sub>  | DMF                | 22       | Product formation (better)                                    |
| 8     | Na <sub>2</sub> CO <sub>3</sub>  | DCE                | 22       | Only starting material  |
| 9     | NaHCO <sub>3</sub>               | CH <sub>3</sub> CN | 22       | Only starting material  |
| 10    | Na <sub>2</sub> HPO <sub>4</sub> | CH <sub>3</sub> CN | 19       | Starting materials, catalyst bleached, no product.            |
| 11    | Na <sub>2</sub> HPO <sub>4</sub> | DMSO               | 19       | Starting materials, catalyst bleached, no product.            |
| 12    | Na <sub>2</sub> HPO <sub>4</sub> | DMF                | 19       | Starting materials, catalyst bleached, no product.            |
| 13    | Na <sub>2</sub> HPO <sub>4</sub> | DCE                | 19       | Starting materials, catalyst bleached, no product.            |
| 14    | K <sub>2</sub> HPO <sub>4</sub>  | CH <sub>3</sub> CN | 19       | Starting materials, catalyst bleached, no product.            |
| 15    | ---                              | CH <sub>3</sub> CN | 19       | Starting materials, catalyst bleached, no product.            |

The products could be detected by mass spectroscopy, but, the yields could not be improved and we could not isolate any product. This may be due to the high polarity of the products. We imagined that the free NH<sub>2</sub> group in the amidoxime could be one reason for very high polarity of the products, impeding their isolation. Therefore, we tried to alkylate the primary amine (**Table 3**). Upon alkylation/arylation, it could be possible to perform an intramolecular reaction, which could be thermodynamically more favorable than the intermolecular reaction.

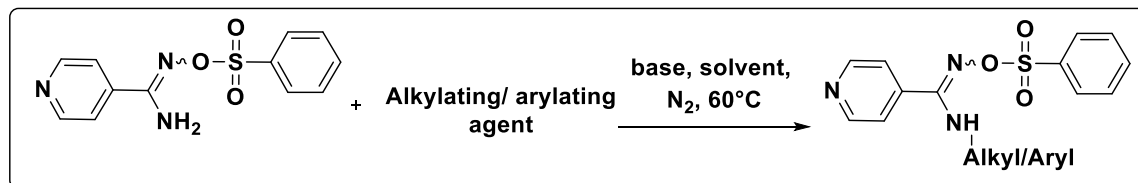
5.2.3 Synthesis of *N*-aryl sulfoxynylamidines

Table 3:

| Entry | Alkylating agent                 | Base  | Solvent (2 mL)        | Reaction yield (%) |
|-------|----------------------------------|---|-----------------------|--------------------|
| 1     | Allyl bromide                    | K <sub>2</sub> CO <sub>3</sub> , RT                                   | DMF                   | 0                  |
| 2     | Allyl bromide                    | K <sub>2</sub> CO <sub>3</sub>  | DMF                   | 0                  |
| 3     | Allyl bromide                    | Pd(PPh) <sub>4</sub> Cl <sub>2</sub> , RT                             | THF                   | 0                  |
| 4     | Allyl bromide                    | Pd(PPh) <sub>4</sub> Cl <sub>2</sub> , K <sub>2</sub> CO <sub>3</sub> | THF                   | 0                  |
| 5     | Allyl bromide                    | KO <sup>t</sup> Bu  | THF: H <sub>2</sub> O | 0                  |
| 6     | Allyl bromide                    | KO <sup>t</sup> Bu  | DMF                   | 0                  |
| 7     | PhCH <sub>2</sub> Br             | K <sub>2</sub> CO <sub>3</sub>  | Acetone               | 0                  |
| 8     | PhCH <sub>2</sub> Br             | NaOH  | DMSO                  | 0                  |
| 9     | PhCH <sub>2</sub> Br             | KO <sup>t</sup> Bu  | DMF                   | 0                  |
| 10    | <i>p</i> -CNPhCH <sub>2</sub> Br | K <sub>2</sub> CO <sub>3</sub>  | Acetone               | 0                  |
| 11    | <i>p</i> -CNPhCH <sub>2</sub> Br | NaOH  | DMSO                  | 0                  |
| 12    | <i>p</i> -CNPhCH <sub>2</sub> Br | KO <sup>t</sup> Bu  | DMF                   | 0                  |
| 13    | PhCOCl                           | KO <sup>t</sup> Bu  | DMF                   | 0                  |

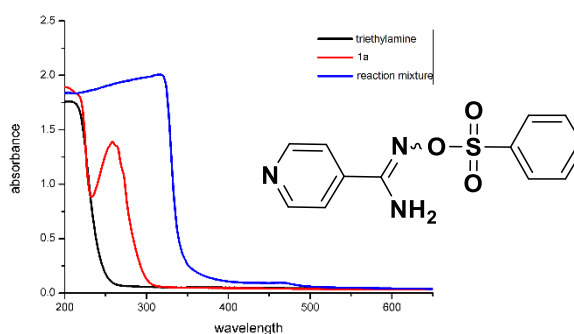
Different alkyl/aryl halides and different bases were used. Unfortunately, we were not able to obtain any alkylated/arylated product.



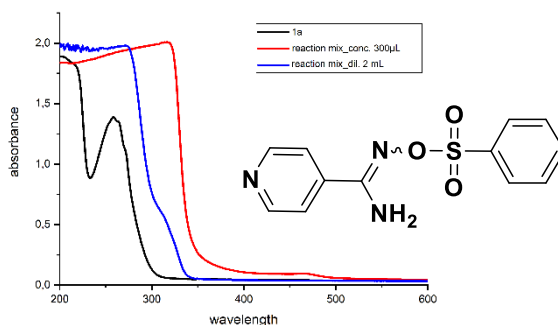
### 5.2.4 Towards the formation of EDA complexes

Electron donor-acceptor (EDA) complexes,<sup>[14]</sup> also called charge transfer (CT) complexes have been widely studied through decades, although their synthetic applications are somehow limited. However, in recent years, visible light photoredox catalysis using EDA complexes have been studied extensively. The sulfonyl amidoximes show absorbance in the UV region of the spectrum. As our starting materials are colored, we predicted that they could form EDA complexes with an electron donor. Hence, the use of a photocatalyst could be avoided. Upon addition of an electron donor (triethylamine), to the sulfonyl amidoximes, we observed a shift in the absorbance of the reaction mixture to the visible region. Furthermore, upon irradiation there was a significant change in color of the reaction mixture.

#### UV measurements for EDA complex formation



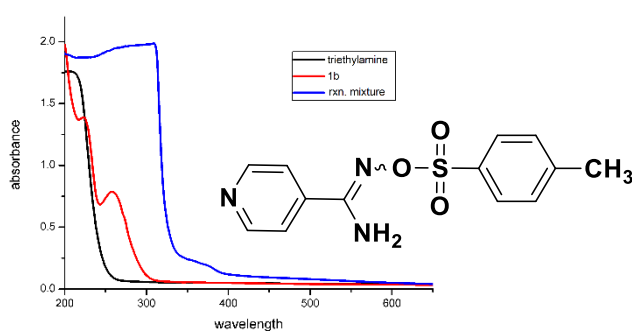
(a)



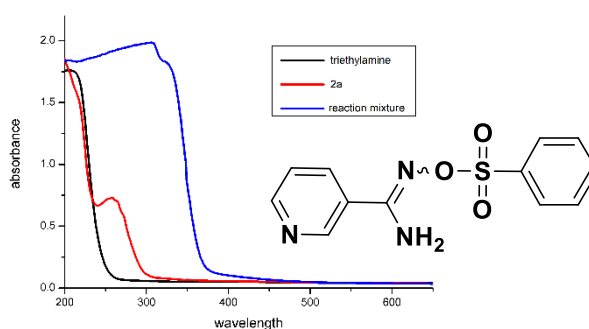
(b)

**Figure 3:** Comparison of UV-Vis spectra of **1a** at different concentrations. (a) 0.06 mmol amidoxime + Et<sub>3</sub>N (2 equiv.) + 300  $\mu$ L acetonitrile = reaction mixture and (b) 0.06 mmol amidoxime + Et<sub>3</sub>N (2 equiv.) + 2 mL acetonitrile = reaction mixture.

However, an absorbance in the visible region (blue line, **Figure 3a**) is observed at a very high concentrations of the substrate. Upon dilution, there was no absorbance in the visible region (see **Figure 3b**, blue line) showing that this change in spectra was due to higher concentration of the substrate, and not due to EDA complex formation. The same condition applies to the other two amidoximes under the same concentrations and same reaction conditions (**Figure 4a and 4b**). There was no significant change in the spectra at lower concentrations of the substrate.



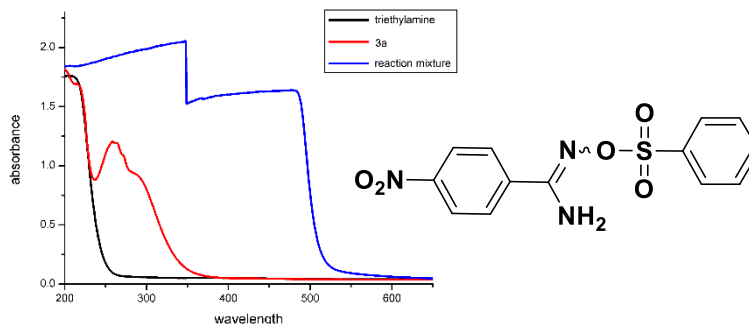
(a)



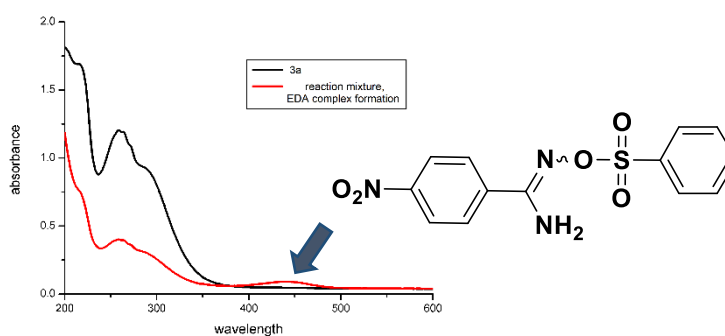
(b)

**Figure 4:** (a) UV-Vis spectra of **1b** at concentration 0.06 mmol amidoxime + Et<sub>3</sub>N (2 equiv.) + 300  $\mu$ L acetonitrile = reaction mixture. (b) UV-Vis spectra of **2a** at concentration 0.06 mmol amidoxime + Et<sub>3</sub>N (2 equiv.) + 300  $\mu$ L acetonitrile = reaction mixture.

However, we were able to observe electron donor-acceptor (EDA) complex formation with the nitro-sulfonyl amidoxime **3a** (**Figure 5b**). This has a distinct absorption in the visible region of the spectrum, so we used this substrate for the trial reaction.



**5 (a)**

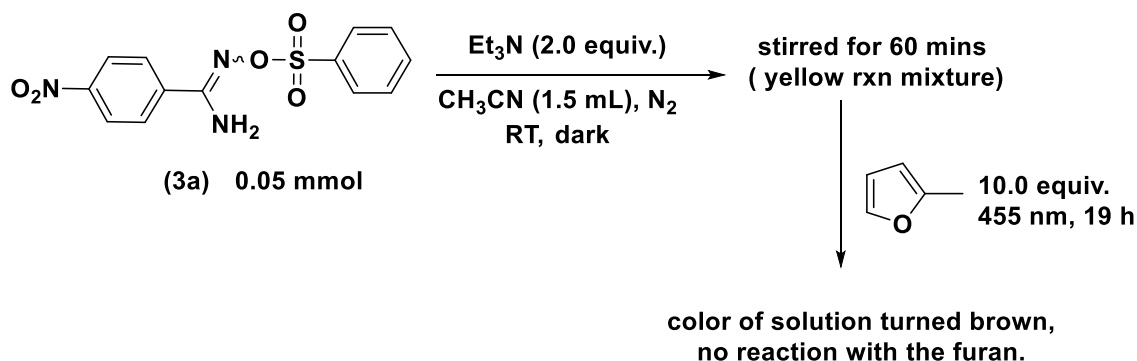


**5 (b)**

**Figure 5:** Comparison of UV-Vis spectra of **3a** at different concentrations. (a) 0.06 mmol amidoxime + Et<sub>3</sub>N (2 equiv.) + 300  $\mu$ L acetonitrile = reaction mixture. (b) 0.06 mmol amidoxime + Et<sub>3</sub>N (2 equiv.) + 2 mL acetonitrile = reaction mixture.

The amidoxime **3a** was stirred in the dark with trimethylamine as the electron donor and CH<sub>3</sub>CN as the solvent for 60 minutes under nitrogen at room temperature. The color of the solution turned dark yellow, which might be due to a charge transfer complex formation in the ground state. Then, 10 equivalents of 2-methylfuran were added to the reaction mixture, which was irradiated with 455 nm blue LED (**Scheme 7**). Unfortunately, the color of the reaction mixture turned brown after some time, and no product formation was observed. Upon irradiation at the wavelength of its charge transfer (CT) band, the [D,A]<sub>EDA</sub> complex

can evolve, via a reactive excited complex ( $[D, A]^*$ ), and produce an electron-transfer event, thus generating a radical ion pair trapped in the solvent cage  $[D^{\cdot+}, A^{\cdot-}]_{\text{SOLV}}$ . This radical ion pair can undergo different reactions. In our case, it is possible that the back electron transfer from the radical ion pair is the key event, which would regenerate the starting materials, rather than the fragmentation.



**Scheme 7:** Attempts to generate amidinyl radicals via EDA complex formation.

With these observations, we did not proceed further to explore the reactivity of the pyridyl amidoximes. We realized that, the amidinyl radical is nucleophilic, therefore, it is necessary to have an electrophilic partner as a trapping agent.

### 5.2.5 Generation of amidinyl radicals from *N*-phenylsulfonyl benzimidamide

From the previous **section 5.2.4**, the attempt to alkylate/arylate the free NH<sub>2</sub> group was unsuccessful. Therefore, we changed our synthetic strategy and synthesized the following two phenylsulfonyl benzimidamides as test substrate (**Figure 6**).

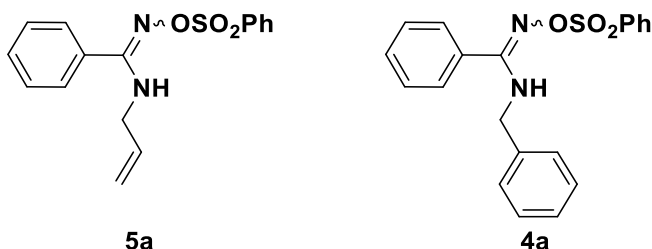


**Figure 6:** Structures of *N*-phenylsulfonyl-oxy benzimidamide.

Our idea was to trap the amidinyl radical intramolecularly with these alkene/ arene. A few trial reactions that were performed are shown in **Table 4**.

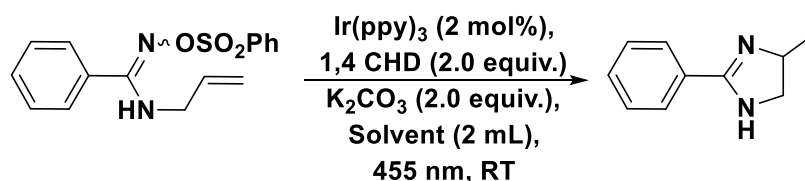
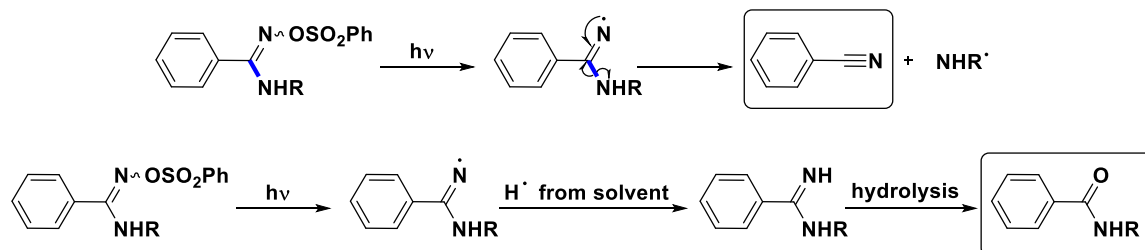


**Table 4:**

| Entry | Starting materials | Reaction conditions  | Observations   |
|-------|--------------------|--|--|
| 1.    |                    | Ir(ppy) <sub>3</sub> (2 mol%), 1, 4 CHD (2 equiv.), K <sub>2</sub> CO <sub>3</sub> (2 equiv.), CH <sub>3</sub> CN (2 mL), 455 nm, RT, N <sub>2</sub> | PhCN and Ph(CO)NHR were formed mostly, along with other hydrolyzed product from the amidoxime. |
| 2.    |                    | Ir(ppy) <sub>3</sub> (2 mol%), 1, 4 CHD (2 equiv.), K <sub>2</sub> CO <sub>3</sub> (2 equiv.), DMF (2 mL), 455 nm, RT, N <sub>2</sub>                | Same as above.   |
| 3.    |                    | Ir(ppy) <sub>3</sub> (2 mol%), K <sub>2</sub> CO <sub>3</sub> (2 equiv.), CH <sub>3</sub> CN (2 mL), 455 nm, RT, N <sub>2</sub>                      | Same as above.   |
| 4.    |                    | Ir(ppy) <sub>3</sub> (2 mol%), K <sub>2</sub> CO <sub>3</sub> (2 equiv.), DMF (2 mL), 455 nm, RT, N <sub>2</sub>                                     | Same as above.   |

Apart from the formation of the corresponding amidines, the formation of the side products PhCN and Ph(CO)NHR could be explained as follows (**Scheme 8**), although the detailed mechanisms are not clear. The benzimidamide can generate the benzamidinyl radical upon photocleavage of the N-O bond, which can undergo a radical fragmentation to form the benzonitrile. Again, this amidinyl radical can abstract a hydrogen atom from the solvent to

form the amidine, which can subsequently hydrolyze to the corresponding carbonyl compound. We tried to perform our photocatalytic reaction under moisture free and oxygen free conditions, but in any case the formation of the ketone was not suppressed.



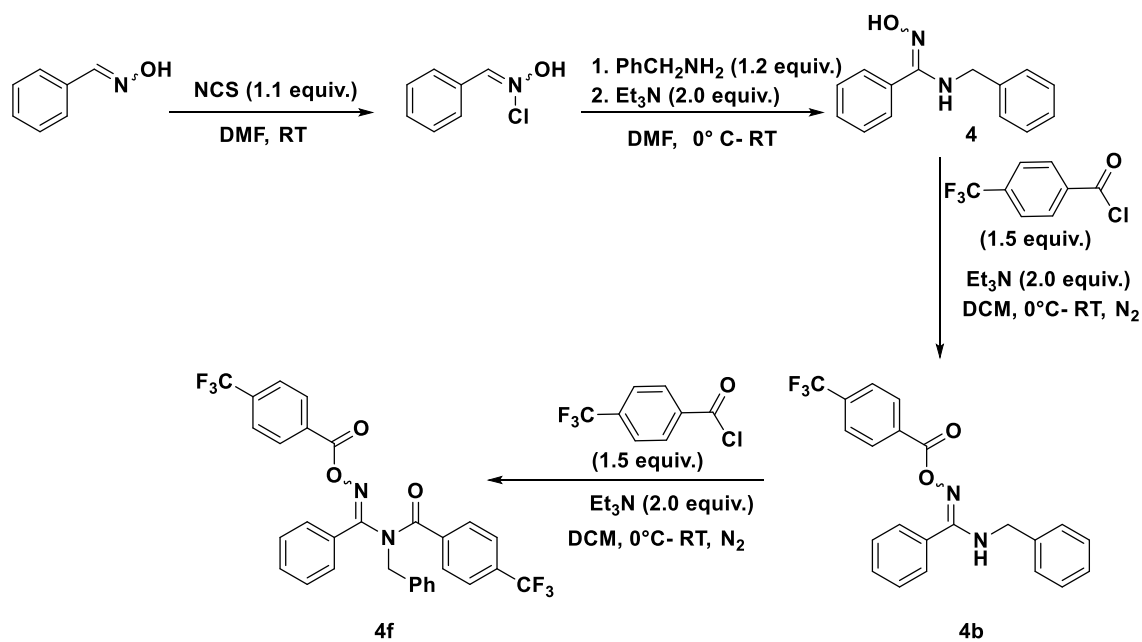
**Scheme 8:** Probable mechanism for the formation of side products.

We tried to go one step back and investigated the reason for the rapid hydrolysis of the amidine; the observed results will be discussed in **Section 5.4.2.1**.

### 5.2.6 Generation of amidinyl radicals from a different class of benzamides and synthesis of quinazolinone derivatives

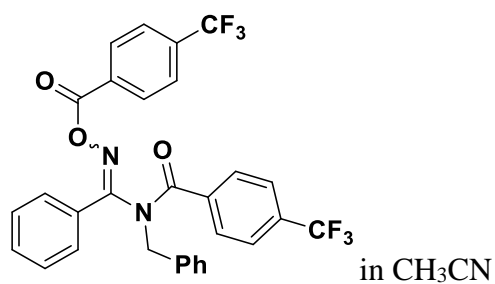
In further studies, we modified our starting materials, synthesized a new class of benzamides (**Scheme 9**), and attempted to generate amidinyl radicals followed by subsequent cyclization (**Scheme 10**). The reduction potential of the starting material **4f** is calculated to be  $-1.43\text{ V vs SCE}$  (**Figure 7**). We screened different photocatalysts and solvents, and  $\text{Ir(ppy)}_3$  was found to be the best photocatalyst in this case.  $\text{Ir(ppy)}_3$  has an excited state reduction potential of  $-1.73\text{ V vs SCE}$ . A few of the optimization reactions are summarized in **Table 5**. The side products formed in this reaction were the amidine, the corresponding ketone from the hydrolysis of the amidine and surprisingly a product

obtained from the dimerization of two aminidyl subunits. The addition of an external electron donor *e.g.*, DIPEA, resulted in the degradation of the starting materials. Control experiments without light and without photocatalyst showed no product formation. However, in these cases, all starting material was converted to its corresponding benzamidine.



**Scheme 9:** Synthetic route for synthesis of compound **4f**.

Cyclic voltammogram of compound **4f**:



$E^0 = -1.43 \text{ V vs SCE.}$

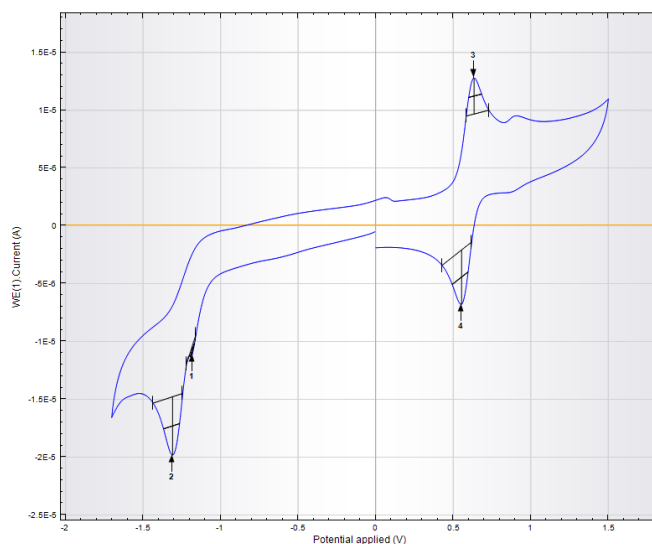
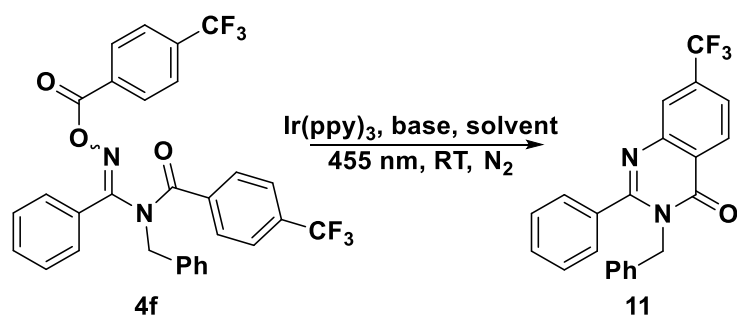


**Figure 7:** Cyclic voltammogram of compound **4f**.



**Scheme 10:** Synthesis of 3-benzyl-2-phenyl-7-(trifluoromethyl)quinazolin-4(3*H*)-one.

**Table 5:**

| Entry | Base (2.0 equiv.)              | Solvent (1.5 mL)  | Yield (%) |
|-------|--------------------------------|-------------------|-----------|
| 1     | CH <sub>3</sub> COONa          | DMF               | 9         |
| 2     | CH <sub>3</sub> COONa          | Toluene           | 12        |
| 3     | K <sub>3</sub> PO <sub>4</sub> | Toluene           | 40        |
| 4     | K <sub>3</sub> PO <sub>4</sub> | <i>m</i> -xylene  | 40        |
| 5     | K <sub>3</sub> PO <sub>4</sub> | 1,2 DCE           | 20        |
| 6     | K <sub>3</sub> PO <sub>4</sub> | MTBE              | <10       |
| 7     | K <sub>3</sub> PO <sub>4</sub> | PhCF <sub>3</sub> | <10       |



|   |                                |         |   |
|---|--------------------------------|---------|---|
| 8 | K <sub>3</sub> PO <sub>4</sub> | Diglyme | 0 |
|---|--------------------------------|---------|---|

Toluene and *m*-xylene were found to be the best solvents for the reaction and the desired product was obtained in 40% isolated yield. Polar solvents, such as DMF, DMSO and CH<sub>3</sub>CN led to the formation of more N-N coupling product. The use of non-polar solvents in this reaction suppressed the formation of the hydrolyzed product to some extent, but, not completely. Further optimization of the reaction conditions did not improve the yields of the reaction. Recently, a strongly reducing organic photoredox catalyst has been developed by the group of Miyake (**Figure 8**).<sup>[15]</sup> The phenoxazine and dihydrophenazine moieties contain electron rich chromophores that can form a stable radical cation upon oxidation, thereby making them strong reductants in their excited state. These photocatalysts have a similar reduction potential in the excited state like that of Ir(ppy)<sub>3</sub>, therefore, can serve as an alternative for precious metal photocatalysts like Ir(ppy)<sub>3</sub> or Ru(bpy)<sub>3</sub>Cl<sub>2</sub>. We used these photocatalysts for our trial reactions (**Table 6**). Photocatalyst **A** and **B** have absorption maxima at 343 and 388 nm respectively. Therefore, we used a light source of 400 nm for our photoreactions. Although the conversion to the desired product was around 70% (determined by NMR), we were able to isolate only 40% of the product, due to difficulties in column separation. The addition of an external electron donor resulted in the degradation of the starting material in this case.

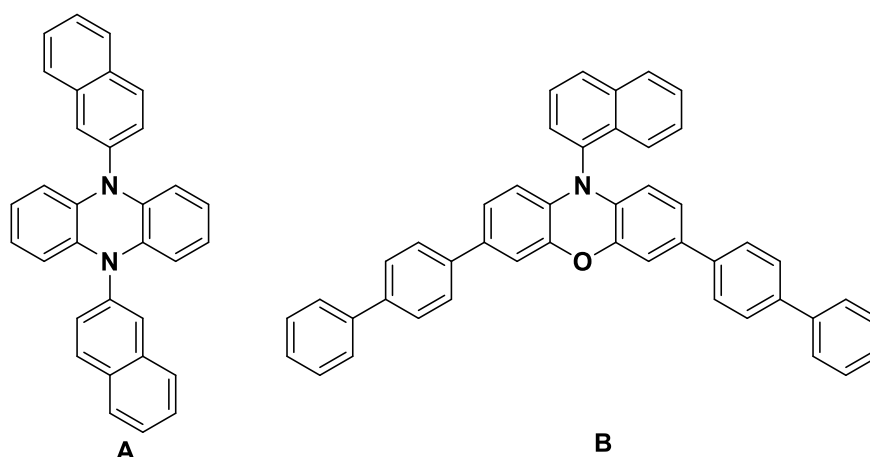


**Figure 8:** Phenazine and phenoxazine based organic dye.

| Photophysical and electrochemical properties | Photocatalyst A        | Photocatalyst B        |
|--|------------------------|------------------------|
| $E^0$  | - 1.69 V <i>vs</i> SCE | - 1.80 V <i>vs</i> SCE |
| $\lambda_{\text{max, abs}}$ (nm)             | 343                    | 388                    |
| $\tau_{\text{triplet}}$ ( $\mu\text{s}$ )    | $4.3 \pm 0.5$          | $480 \pm 50$           |

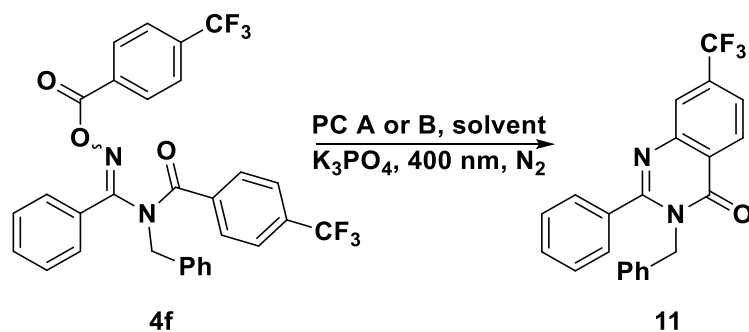
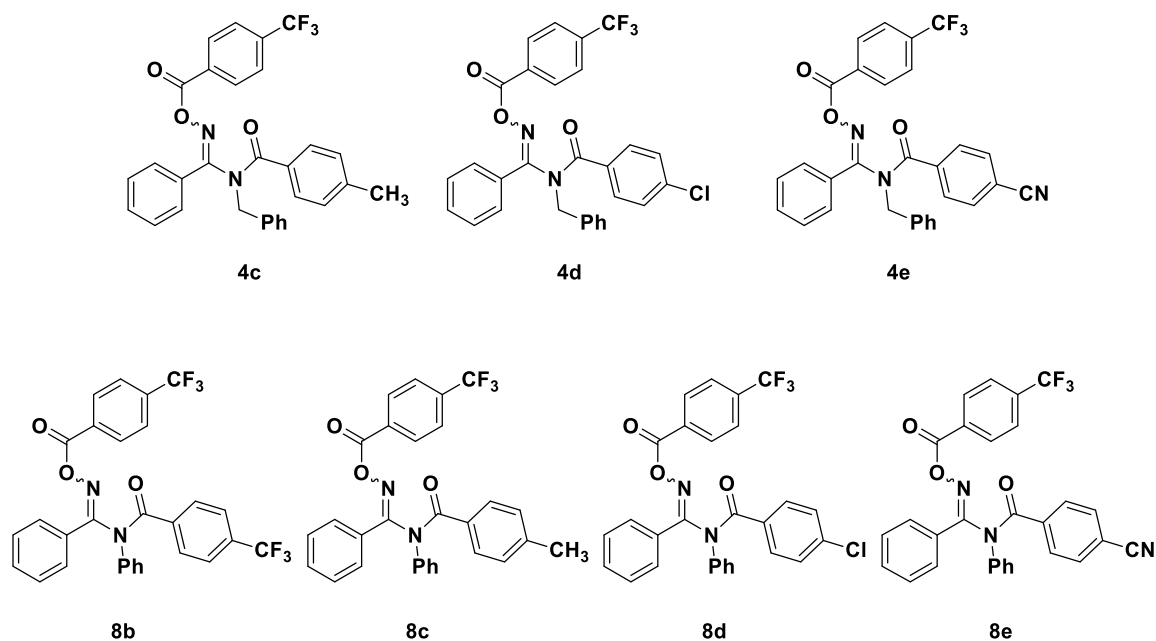


Table 6:

| Entry | Photocatalyst                              | Solvent (1.5 mL) | Conversion to product by NMR (%) | Observations                 |
|-------|--|------------------|----------------------------------|------------------------------|
| 1     | A  | Toluene          |                                  | N-N coupling<br>Dimer forms. |
| 2     | B  | Toluene          | <40                              | SM, dimer                    |
| 3     | A, no base, 455 nm                         | Toluene          | <40                              | More side reactions          |
| 4     | A, K <sub>3</sub> PO <sub>4</sub> , 455 nm | Toluene          | --                               | More side reactions          |
| 5     | B, no base, 455 nm                         | Toluene          | --                               | Side reactions               |
| 6     | B, K <sub>3</sub> PO <sub>4</sub> , 455 nm | Toluene          | <40                              | More side reactions          |
| 7     | A  | Toluene          | ~70                              |                              |
| 8     | A  | 1,2 DCE          | ~60                              |                              |
| 9     | A  | MTBE             | ~50                              |                              |
| 10    | A  | NMP              | ~35                              |                              |
| 11    | A, no base                                 | Toluene          | ~50                              |                              |

|    |                |         |     |                  |
|----|----------------|---------|-----|------------------|
| 12 | No PC, no Base | Toluene | --- | Unknown compound |
|----|----------------|---------|-----|------------------|

We have synthesized a series of differently substituted benzamides to explore the substrate scope (**Figure 9**).



**Figure 9:** Structures of synthesized benzamides.

Compound **11** was isolated in 22%. Unfortunately, we were not able to increase the yield further after optimization of the reaction conditions. To our surprise, the reaction did not proceed with compounds **8b-8e**, where a benzyl group is replaced by phenyl group and the starting materials were recovered.

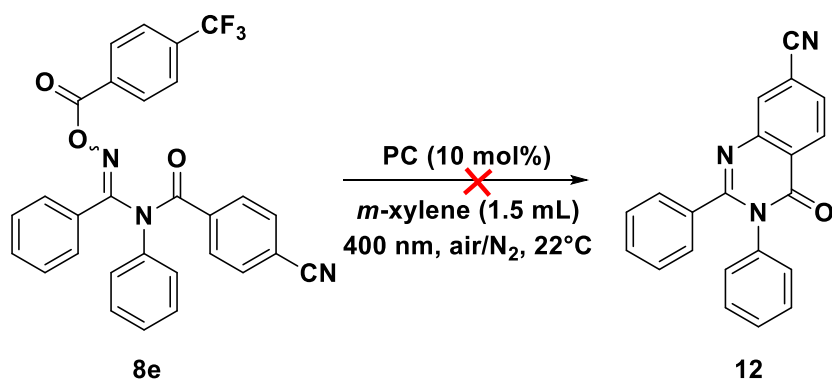
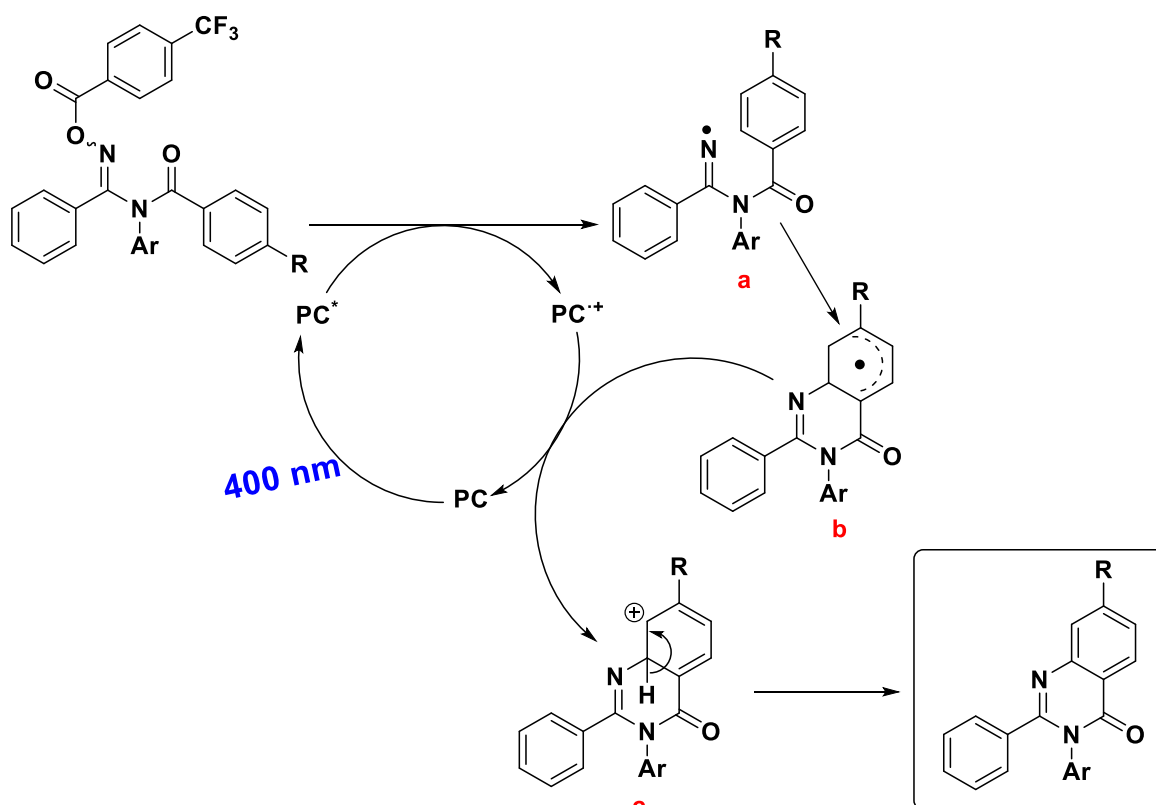


Table 7:

| Entry | Photocatalyst | Light source | Air/N <sub>2</sub> | base                           | Observation   |
|-------|---------------|--------------|--------------------|--------------------------------|---|
| 1     | --            | 400 nm       | air                | --                             | Degradation, no SM  |
| 2     | A             | 400 nm       | N <sub>2</sub>     | --                             | No product, side reactions along with SM                          |
| 3     | A             | 400 nm       | air                | --                             | No product, a lot of side reactions along with SM                 |
| 4     | A             | --           | air                | --                             | No product, side reactions along with SM                          |
| 5     | A             | 400 nm       | N <sub>2</sub>     | K <sub>3</sub> PO <sub>4</sub> | No product, side reactions along with SM                          |
| 6     | B             | 400 nm       | N <sub>2</sub>     | K <sub>3</sub> PO <sub>4</sub> | No product, side reactions along with SM                          |
| 7     | --            | 400 nm       | air                | --                             | Trace product, SM, side products<br>(Toluene was used as solvent) |
| 8     | A             | 400 nm       | N <sub>2</sub>     | K <sub>3</sub> PO <sub>4</sub> | No product formation<br>(toluene as solvent)                      |

### 5.2.7 Plausible mechanism for the formation of quinazolinone derivative

The plausible mechanism for this reaction is given in **Scheme 11**. The excited photocatalyst can donate one electron to the substrate, which can undergo N-O bond cleavage to form the amidinyl radical (**a**), while the photocatalyst is oxidized to its radical cation. The amidinyl radical can undergo an intramolecular addition to the electron deficient arene to form an intermediate (**b**), which reduces the photocatalyst back to its ground state. The intermediate (**c**) gives the desired product upon rearomatization.



**Scheme 11:** Plausible mechanism for the formation of quinazolinone derivatives.

## 5.3 Conclusion

In conclusion, we could develop a photocatalytic method for the generation of amidinyl radicals. Quinazolinone derivatives were synthesized under mild reaction conditions at room temperature. However, the photochemical conversion was successful for only two substrates, and the product yields were poor. Although we were able to generate the

amidinyl radical by our photocatalytic method, we believe, the cyclization is interrupted due to the conformational complexity in the molecule.

## 5.4 Attempts towards the syntheses of oxadiazoles using visible light photoredox catalysis

### 5.4.1 Introduction

Nitrogen containing heterocycles have always been the center of research mainly because of their broad biological activity and wide range of pharmaceutical applications. Among various classes of nitrogen heterocycles, oxadiazoles are of great importance. They are a class of aromatic compounds of the azole family. In view of this, substituted 1,2,4-oxadiazoles are an important class of compounds which occur in various natural products. These compounds are highly bioactive, possessing a large spectrum of biological activities, including antitumor, antiviral and antibacterial activity.<sup>[16]</sup> Precisely, due to these interesting properties of oxadiazoles, much interest was focused on effective synthetic pathways. **Figure 10** shows some commercially available drugs containing 1,2,4-oxadiazoles.

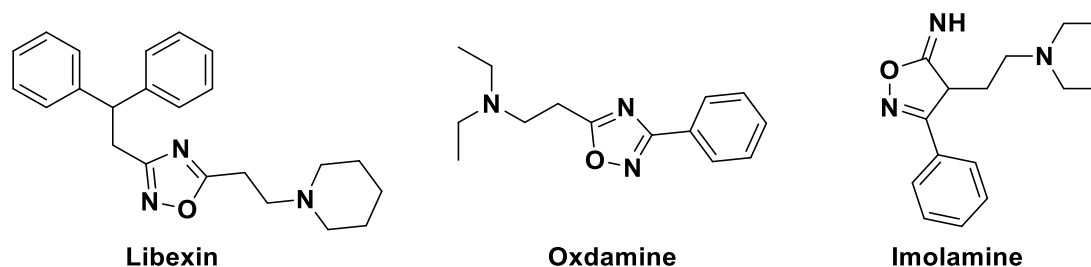


**Figure 10:** Drugs containing 1,2,4-oxadiazole moiety.

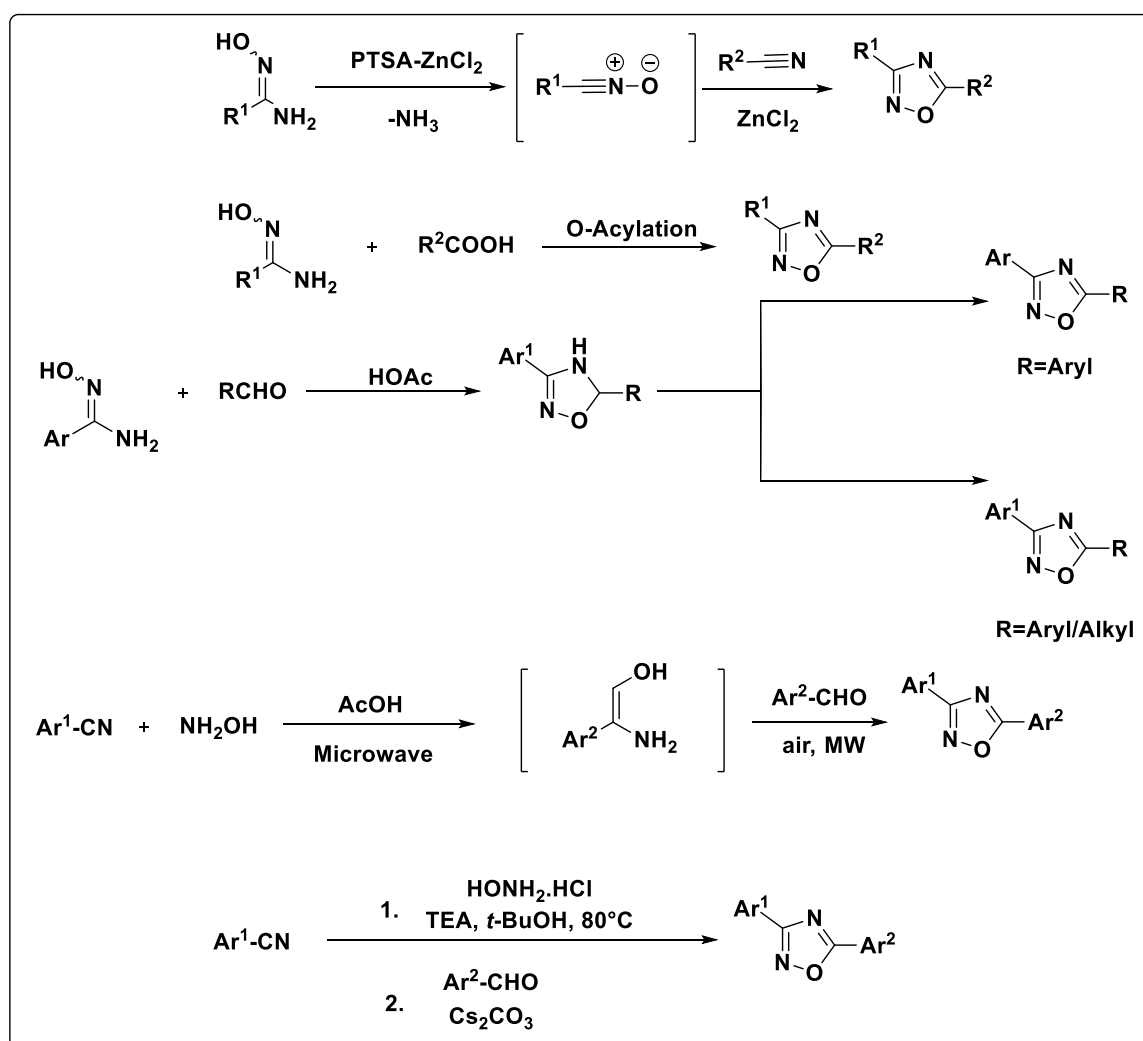
The most common synthetic pathways are shown in **Scheme 12**.<sup>[17-19]</sup>

1. 1, 3-Dipolar cycloaddition of nitrile oxides to nitriles.
2. O-acylation of amidoximes using carboxylic acids.
3. Intermolecular cyclodehydration of amidoximes with aldehydes yielding 4, 5-dihydro-1,2,4-oxadiazole, which is followed by oxidative dehydrogenation.

4. When employed as intermediates, amidoximes react with aldehydes and hydroxylamine giving 4,5-dihydro-1,2,4-oxadiazole, which is then followed by oxidative dehydrogenation in which air is used as an oxidant, under microwave conditions.

5. Base mediated one pot synthesis of substituted-1,2,4-oxadiazole, in which aldehyde plays a dual role of substrate and oxidant.

Though all these methods are efficient, they suffer from severe disadvantages. Some need microwave conditions, elevated temperatures, use of metals or acids and pre-functionalization of the starting materials.

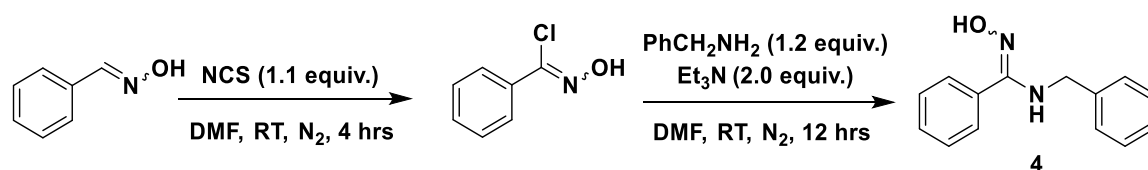


**Scheme 12:** General synthetic strategy towards oxadiazole syntheses.

## 5.4.2 Results and discussions

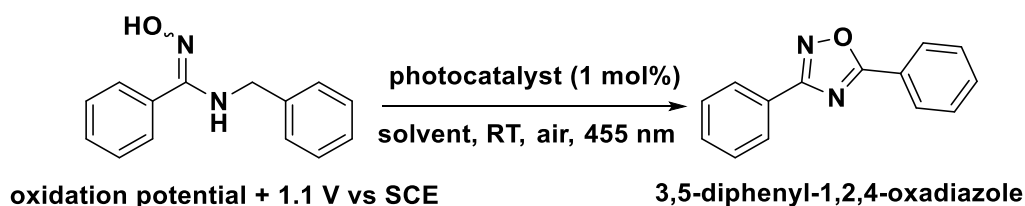
### 5.4.2.1 Synthesis of 1,2,4-oxadiazole and optimization of reaction conditions

As we have discussed in **Section 5.2.5**, benzimidamides undergo rapid hydrolysis to the corresponding carbonyl compounds. Therefore, we went one step backward and investigated the amidoxime (which is the precursor for the benzimidamide synthesis). The amidoxime **4** was synthesized following the general procedure<sup>[20]</sup> (**Scheme 13**).



**Scheme 13:** General procedure for the synthesis of amidoxime **4**.

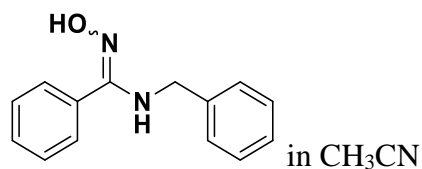
The oxidation potential of **4** was measured to be +1.1 V vs SCE. This means that the substrate could be oxidized by a photocatalyst whose oxidation potential is higher than or similar to +1.1 V. When subjected to our photocatalytic condition, this amidoxime reacted to the 1,2,4-oxadiazole (**Scheme 14**).



**Scheme 14:** Our photocatalytic approach for oxadiazole syntheses.

Based on the oxidation potential of this amidoxime, we have screened few different photocatalysts like 4-CzIPN, Eosin Y, Na-salt of Eosin Y, Fukuzumi catalyst, [Ru(bpy)<sub>3</sub>]Cl<sub>2</sub> under different conditions. Different solvents were used (**Table 8**), which was then followed by absence or presence of molecular sieves, O<sub>2</sub> balloon and light. Later, reactions with a spectrum of terminal oxidants were also investigated, which will be discussed in the later sections.





$E^0 = +1.1 \text{ V vs SCE}$

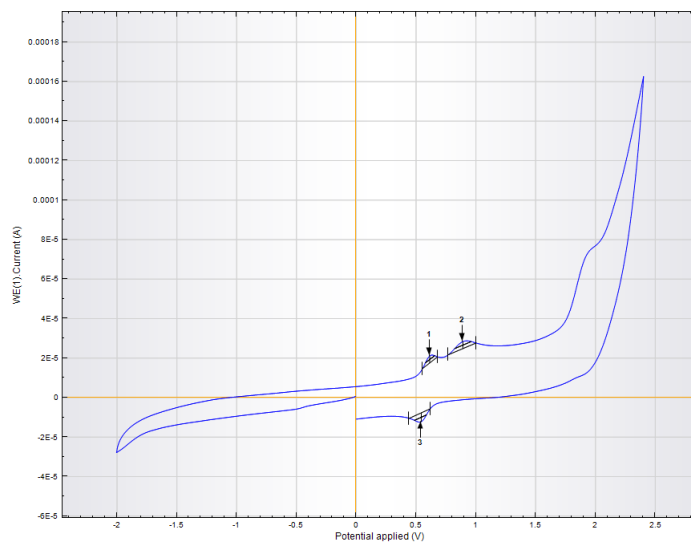


**Figure 11:** Cyclic voltammogram of compound **4**.

**Table 8:**

[Ir(dF(CF<sub>3</sub>)-ppy)<sub>2</sub>(dtbpy)]PF<sub>6</sub> (1 mol%) was added to the amidoxime **4** and the reaction mixture was irradiated in the presence of blue light 455 nm and air for 24 hrs.

| Entry | Solvent                           | Light source | Observation   |
|-------|-----------------------------------|--------------|---|
| 1     | CD <sub>3</sub> CN                | 455 nm       | 20% product was formed within 1 hour, the corresponding amide formation and the starting material was observed. |
| 2     | CD <sub>3</sub> COCD <sub>3</sub> | 455 nm       | Same as above   |
| 3     | (NMP) <i>N</i> -methylpyrrolidone | 455 nm       | Same as above   |
| 4     | <i>Tert</i> -butyl methyl ether   | 455 nm       | Same as before  |

|   |  |    |  |
|---|--|----|--|
| 5 | CD <sub>3</sub> CN/ CH <sub>3</sub> CN | -- | Only starting material was observed, after 8 hrs product started forming. Background reaction was faster in deuterated acetonitrile. |
|---|--|----|--|

In each case, 20% of the oxadiazole was isolated along with the corresponding amide and starting material. There was no further conversion to the desired product on irradiating for longer time, rather more amide formation was observed. Therefore, to find out if the reaction was faster in the presence of an oxygen balloon, and if molecular sieves help, we performed the following conditions using the above mentioned photocatalyst [Ir(dF(CF<sub>3</sub>)-ppy)<sub>2</sub>(dtbpy)]PF<sub>6</sub> (1 mol%) (**Table 9**).

**Table 9:**

| Entry | Photocatalyst | Solvent                           | Molecular sieves | O <sub>2</sub> balloon | Light |
|-------|---------------|-----------------------------------|------------------|------------------------|-------|
| 1     | yes           | CH <sub>3</sub> CN                | no               | no                     | no    |
| 2     | no            | CH <sub>3</sub> CN                | yes              | no                     | yes   |
| 3     | no            | CD <sub>3</sub> CN                | no               | no                     | yes   |
| 4     | yes           | CD <sub>3</sub> CN                | yes              | no                     | yes   |
| 5     | yes           | CD <sub>3</sub> CN                | yes              | yes                    | yes   |
| 6     | yes           | CD <sub>3</sub> CN                | no               | no                     | yes   |
| 7     | yes           | CD <sub>3</sub> CN                | no               | yes                    | yes   |
| 8     | yes           | CH <sub>3</sub> CN                | yes              | yes                    | yes   |
| 9     | yes           | CD <sub>3</sub> COCD <sub>3</sub> | yes              | yes                    | yes   |

In all of the above cases, the formation of the product was observed within 1 hour of photo-irradiation. However, the side reaction was faster than the product formation, *i.e.*, the formation of amide is observed. The reaction was performed in the presence and absence of oxygen balloon and molecular sieves. Presence or absence of molecular sieves did not make any significant difference. We also screened other photocatalysts like Eosin Y, Ru(bpy)<sub>3</sub>Cl<sub>2</sub>, Mes-Acr, Ir(ppy)<sub>3</sub>, 4-CzIPN. The product formation was observed with all photocatalysts within 1 hour in presence of oxygen, but the reaction was not clean, a lot of

side reactions were observed. The consumption of the starting material was faster when there was large quantity of oxygen, which resulted in the formation of amide instead of the desired product, oxadiazole.

Thereafter, we went on to investigate the reason for the formation of the amide as side product. We synthesized compound **8** as a test substrate and subjected it to our photocatalytic conditions to test the formation of *N*-phenylbenzamide (**Table 10**), and will eliminate the possibility of the oxadiazole formation.

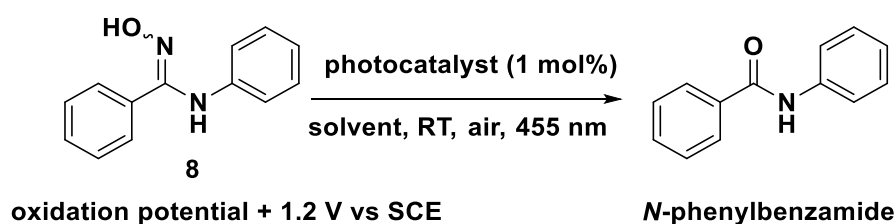
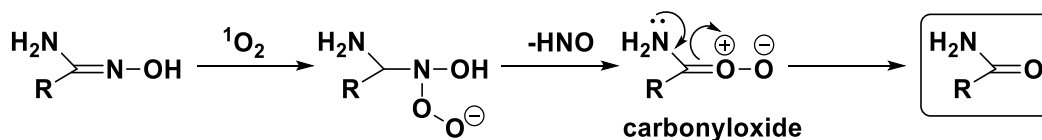


**Table 10:**

| Entry | [Ir(dF(CF <sub>3</sub> )-ppy) <sub>2</sub> (dtbpy)]PF <sub>6</sub> | Solvent                           | Oxygen | Observations                      |
|-------|--|-----------------------------------|--------|-----------------------------------|
| 1     | yes  | CH <sub>3</sub> CN                | yes    | Amide formation in 1.5 h, SM      |
| 2     | yes  | CD <sub>3</sub> CN                | no     | Amide formation in 1.5 h, SM      |
| 3     | yes  | CH <sub>3</sub> COCH <sub>3</sub> | yes    | Full conversion to amide in 1.5 h |
| 4     | yes  | CD <sub>3</sub> COCD <sub>3</sub> | no     | Full conversion to amide in 2.5 h |

From the above observations, we conclude the direct conversion of this substrate into the corresponding amide in almost 100% within 1.5 hours of irradiation in the presence of oxygen balloon. Furthermore, this transformation was slower when there was no externally added oxygen, *i.e.*, under atmospheric pressure. This implies that oxygen promotes the oxidation of the amidoxime to the amide. Amidoximes could be converted into amides in the presence of singlet oxygen under UV irradiation.<sup>[21]</sup> In our case, an option for this transformation could be the generation of singlet oxygen in the system by energy transfer

from the excited photocatalyst to the ground state triplet oxygen that promoted the oxidation of the amidoxime to the amide. The mechanism of oxidation of amidoximes to amides can be proposed as follows:



Therefore, to prevent this side product formation, it is necessary to add an external oxidant to carry out a facile transformation to the oxadiazole. We have screened several oxidants with different photocatalysts which are shown in Table (11-14).

However, in our previous model system (Section 5.2.5), we carried out the photochemical reactions under nitrogen. We believe that very trace amounts of oxygen present in the system can facilitate the formation of the amide as a side product.

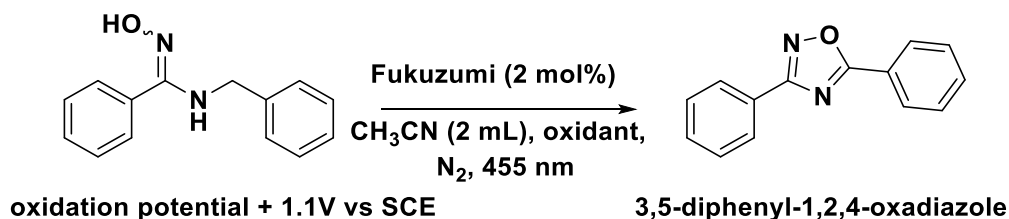


**Table 11:**

| Entry | Terminal oxidant (3 equiv.)                                   | Observations  |
|-------|---|---|
| 1     | (NH <sub>4</sub> ) <sub>2</sub> S <sub>2</sub> O <sub>8</sub> | Along with product, many side products were observed              |
| 2     | K <sub>2</sub> S <sub>2</sub> O <sub>8</sub>                  | Along with product, many side products were observed              |
| 3     | Ph-S-S-Ph   | Along with product, many side products were observed              |
| 4     | PhNO <sub>2</sub>   | More side reactions was observed along with the starting material |

***Attempts Towards the Photochemical Generation of Amidinyl Radicals and Syntheses of Oxadiazole and Quinazolinone Derivatives***

|   |                     |  |
|---|---------------------|--|
| 5 | CBr <sub>4</sub>    | Along with product, many side products were observed |
| 6 | CCl <sub>3</sub> Br | Along with product, many side products were observed |
| 7 | TEMPO               | Along with product, many side products were observed |

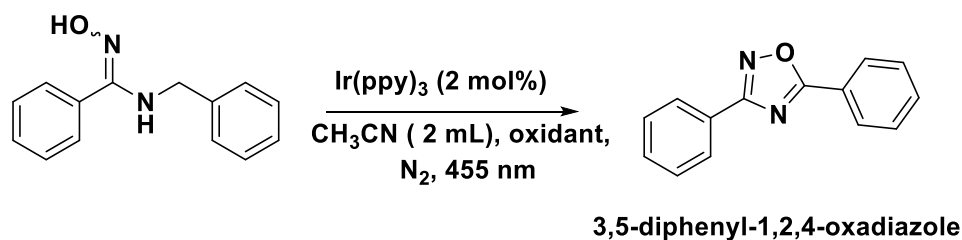


**Table 12:**

| Entry | Terminal oxidant (3 equiv.)                                   | Observations   |
|-------|---|--|
| 1     | (NH <sub>4</sub> ) <sub>2</sub> S <sub>2</sub> O <sub>8</sub> | The reaction was not clean, many side reactions were observed. |
| 2     | Ph-S-S-Ph   | Same observation as above                                      |
| 3     | PhNO <sub>2</sub>   | Same observation as above                                      |
| 4     | CBr <sub>4</sub>  | Same observation as above                                      |
| 5     | CCl <sub>3</sub> Br   | Same observation as above                                      |

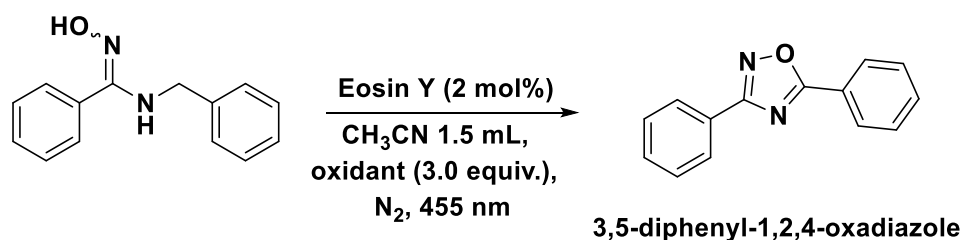


Table 13:

| Entry | Terminal oxidant (3 equiv.)                   | Observations                                    |
|-------|---|---|
| 1     | Na <sub>2</sub> S <sub>2</sub> O <sub>8</sub> | After 30 mins photocatalyst degraded completely |
| 2     | Ph-S-S-Ph                                     | Photocatalyst was bleached                      |
| 3     | PhNO <sub>2</sub>                             | After 60 mins photocatalyst degraded completely |
| 4     | CBr <sub>4</sub>                              | Degradation of photocatalyst                    |
| 5     | CCl <sub>3</sub> Br                           | Degradation of photocatalyst                    |

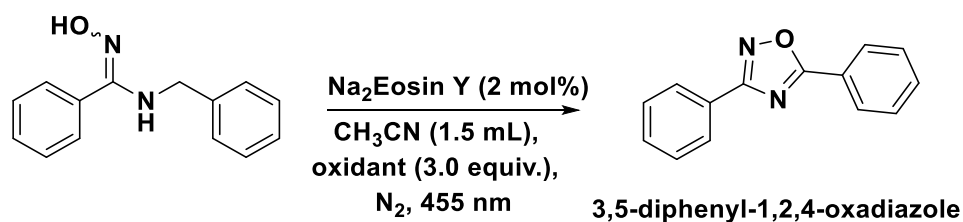


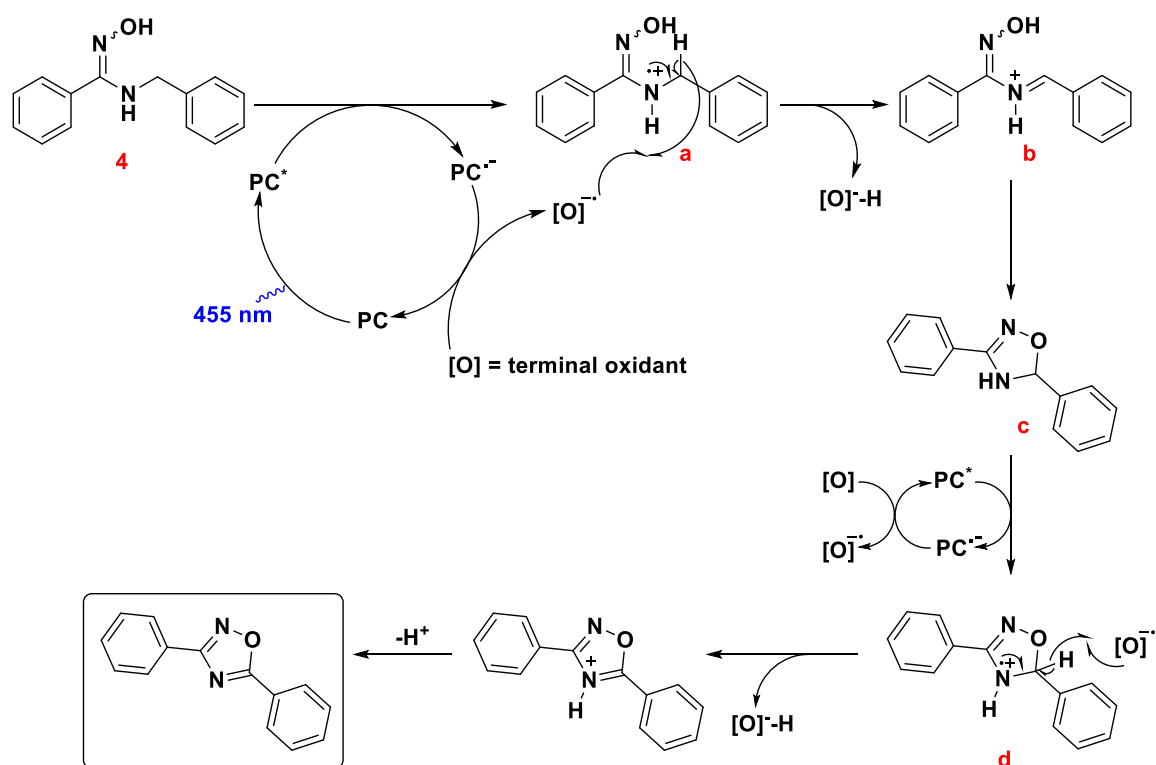
Table 14:

| Entry | Terminal oxidant (3.0 equiv.)                 | Observations                        |
|-------|---|-------------------------------------|
| 1     | Na <sub>2</sub> S <sub>2</sub> O <sub>8</sub> | 20% conversion to product in 1 hour |
| 2     | Ph-S-S-Ph                                     | 20% conversion to product in 1 hour |
| 3     | PhNO <sub>2</sub>                             | The reaction was not clean          |
| 4     | CBr <sub>4</sub>                              | Degradation of the reaction mixture |
| 5     | CCl <sub>3</sub> Br                           | The catalyst was bleached           |

In all the above cases, the desired product could not be isolated in more than 10 - 20% yield. On irradiation for longer times, the side reactions predominated. The starting materials were recovered in quantitative yield.

#### 5.4.2.2 Plausible mechanism for the formation of oxadiazole

The proposed mechanism of oxadiazole formation is as follows (**Scheme 15**). This mechanism is based on the pathway involving abstraction of the hydrogen atom from the amine radical cation. The photocatalyst is excited in the first step, the excited photocatalyst abstracts one electron from the nitrogen to form the amine radical cation (**a**). The terminal oxidant then abstracts the  $\alpha$ -hydrogen atom to form the iminium ion (**b**). Addition of the oxygen atom to the iminium ion, results in the formation of the intermediate (**c**). The photocatalyst can again oxidize the intermediate (**c**) to form the amine radical cationic intermediate (**d**). The terminal oxidant can again abstract the  $\alpha$ -hydrogen atom to form the iminium ion, which after the loss of a proton results in the formation of the desired oxadiazole.



**Scheme 15:** Plausible mechanism for the formation of 1,2,4-oxadiazole

## 5.4.2.3 Synthesis and reaction with phenyl methanone oximes

We synthesized two different model substrates to check the further applicability of the reaction (**Figure 12**).

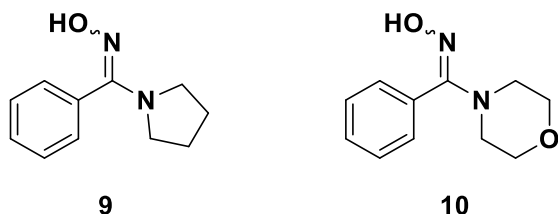
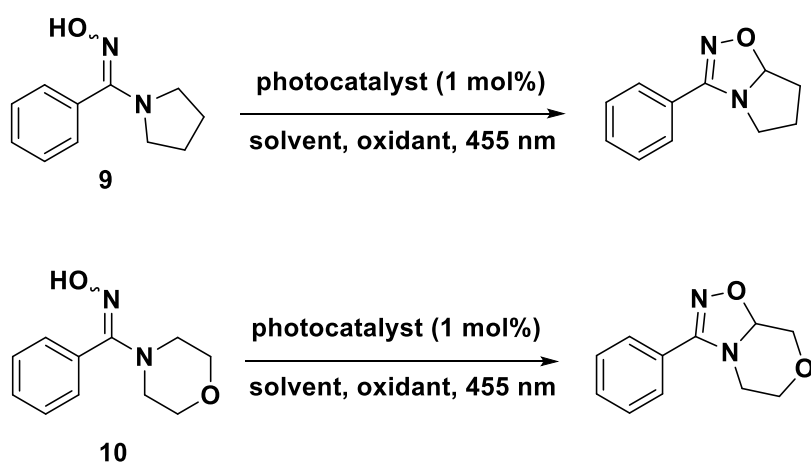


**Figure 12:** Synthesis of phenyl methanone oximes.

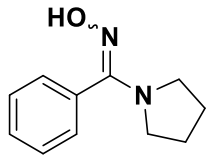
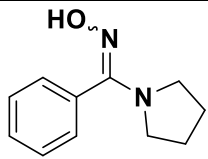
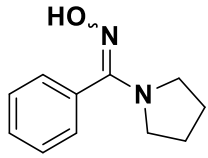
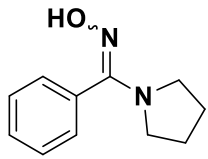
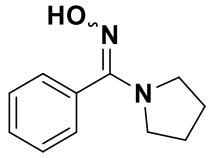
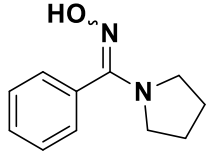
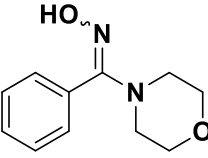
We expected similar kinds of transformation (**Scheme 16**) of these oximes to oxadiazole as above. However, subjecting these amidoximes to different reaction conditions did not yield any product (**Table 15**). In most of the cases, the starting materials remained unreacted. From these observations and based on the reaction mechanism, we could conclude that, prior to cyclization, a benzylic position is mandatory to generate the iminium ion, which is the key step in the overall mechanism.

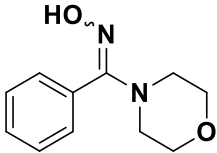
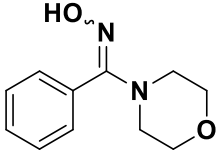
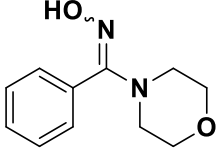
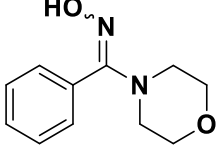


**Scheme 16:** Expected transformation of the amidoximes to their corresponding oxadiazole.



**Table 15:**

| Entry | Substrate (0.1 mmol)  | Catalyst (2 mol%)         | Oxidant (3 equiv.)                                    | Solvent (1.5 mL)   | N <sub>2</sub> /air | Observations   |
|-------|---|---------------------------|---|--------------------|---------------------|--|
| 1     |    | -                         | -   | CH <sub>3</sub> CN | air                 | No conversion of the starting material                             |
| 2     |    | EosinY<br>Na <sub>2</sub> | Ph-S-S-Ph<br>K <sub>2</sub> CO <sub>3</sub> (as base) | CH <sub>3</sub> CN | air                 | After 1 hour, PC started to bleach, reaction was stopped after 2 h |
| 3     |   | EosinY<br>Na <sub>2</sub> | Ph-S-S-Ph   | CH <sub>3</sub> CN | N <sub>2</sub>      | No reaction after 16 hours   |
| 4     |  | EosinY<br>Na <sub>2</sub> | Ph-S-S-Ph   | CH <sub>3</sub> CN | air                 | After 1 hour, PC started to bleach, No reaction after 16 hours     |
| 5     |  | EosinY<br>Na <sub>2</sub> | Ph-S-S-Ph<br>K <sub>2</sub> CO <sub>3</sub> (as base) | CH <sub>3</sub> CN | N <sub>2</sub>      | Catalyst bleached, no conversion of the starting material          |
| 6     |  | Ir(ppy) <sub>3</sub>      | -   | CH <sub>3</sub> CN | air                 | No conversion of starting material after 3 days                    |
| 7     |  | EosinY<br>Na <sub>2</sub> | Ph-S-S-Ph<br>K <sub>2</sub> CO <sub>3</sub> (as base) | CH <sub>3</sub> CN | air                 | No reaction after 16 hours   |

|    |  |                           |   |                    |                |  |
|----|--|---------------------------|---|--------------------|----------------|--|
| 8  |   | EosinY<br>Na <sub>2</sub> | Ph-S-S-Ph   | CH <sub>3</sub> CN | N <sub>2</sub> | After 2 hours, PC started to bleach,<br>No reaction after 16 hours |
| 9  |   | EosinY<br>Na <sub>2</sub> | Ph-S-S-Ph   | CH <sub>3</sub> CN | air            | After 1 hour, PC started to bleach,<br>No reaction after 16 hours  |
| 10 |   | EosinY<br>Na <sub>2</sub> | Ph-S-S-Ph<br>K <sub>2</sub> CO <sub>3</sub> (as base) | CH <sub>3</sub> CN | N <sub>2</sub> | Catalyst bleached,<br>no conversion of the starting material       |
| 11 |  | Ir(ppy) <sub>3</sub>      | -   | CH <sub>3</sub> CN | air            | No conversion of starting material after 3 days                    |

## 5.5 Conclusion

In conclusion, we could develop a visible light mediated photocatalytic method to synthesize substituted 1,2,4-oxadiazoles. The proposed synthetic approach establishes the formation of the desired product through the formation of an amine radical cation. This radical cation intermediate can be formed conveniently by oxidation of the corresponding amine. The yields of the oxadiazoles could not be increased above 20-30%, even by using different external oxidants and photocatalyst. From our reaction mechanism, we have realized that the net reaction would generate two hydrogen atoms. Therefore, along with a photosensitizer, we could use an earth-abundant molecular complex Co(dmgh)<sub>2</sub>pyCl (dmgh = dimethylglyoximate) as a co-catalyst to capture the electrons and protons eliminated from the C–H bonds of substrates. This cobalt complex allows liberation of dihydrogen from the substrate without the need of any sacrificial oxidants. As no sacrificial oxidants would be necessary, this method might be attractive for systems, which are sensitive to the presence of oxidants. However, unfortunately, screening of different cobalt based catalysts along with different photocatalysts did not produce any satisfactory results.

## 5.6 Experimental section

### 5.6.1 Materials and methods

Solvents and reagents were obtained from commercial sources and used without further purification. Proton NMR spectra were recorded on a Bruker Avance 300 MHz spectrometer and 600 MHz spectrometer in CDCl<sub>3</sub> solution and DMSO-*d*<sub>6</sub> solution with internal solvent signal peak at 7.26 ppm and 2.50 ppm respectively. Carbon NMR were recorded at 75 MHz spectrometer and 151 MHz spectrometer in CDCl<sub>3</sub> solution and DMSO-*d*<sub>6</sub> solution and referenced to the internal solvent signal at 77.26 ppm and 39.5 ppm respectively. Proton NMR data are reported as follows: chemical shift (ppm), multiplicity (s = singlet, d = doublet, t = triplet, q = quartet, quint = quintet, dd = doublet of doublets, ddd = doublet of doublet of doublets, td = triplet of doublets, qd = quartet of doublets, m = multiplet, br. s. = broad singlet), and coupling constants (Hz). High resolution mass spectra (HRMS) were obtained from the central analytic mass spectrometry facilities of the Faculty of Chemistry and Pharmacy, Regensburg University and are reported according to the IUPAC recommendations 2013. Melting points of solids were determined by MPA100 OptiMelt Automated Melting Point Apparatus with the temperature range from 30°C to 250°C and the temperature increment of 5°C per minute. All reactions were monitored by thin-layer chromatography using Merck silica gel plates 60 F254; visualization was accomplished with short wave length UV light (254 nm). UV–Vis and fluorescence measurements were performed with Varian Cary 50 UV/Vis spectrophotometer and FluoroMax-4 spectrofluorometer, respectively. Electrochemical studies were performed in acetonitrile (CH<sub>3</sub>CN) containing 0.1 M tetra-*n*-butylammonium tetrafluoroborate using ferrocene/ferrocenium (Fc/Fc<sup>+</sup>) as an internal reference. A glassy carbon electrode (working electrode), platinum wire (counter electrode), and silver wire (quasi-reference electrode) were employed. Spectroelectrochemical studies were carried out in an optically transparent thin layer electrochemical cell (OTTLE). Standard flash chromatography was performed using silica gel of particle size 40–63 μm. Photo reductions were performed with 400 nm and 455 nm LEDs.

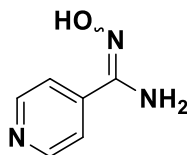
## 5.6.2 General procedures

### Synthesis of starting materials

#### 5.6.2.1 Procedure for the synthesis of amidoxmies (GP1)

A solution of hydroxylamine (6.0 equiv.) in H<sub>2</sub>O (30 mL) was slowly added to a stirred solution of the nitrile (1.0 equiv.) in EtOH (20 mL), then NaHCO<sub>3</sub> (3.0 equiv.) was added. The resulting mixture was refluxed for 3 hours. The solvent was evaporated under reduced pressure and the resulting residue was poured into cold water. The formed precipitate was filtered off, washed in water and lyophilized.

#### Synthesis of *N'*-hydroxyisonicotinimidamide (1)



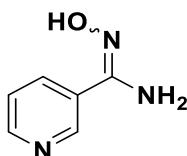
Synthesized according to **GP1**. White solid. Yield 52%.

<sup>1</sup>H NMR (DMSO-*d*<sub>6</sub>, 300 MHz, ppm): δ 9.59 (s, 1H), 8.06 (dd, *J* = 4.5 Hz, 1.5 Hz, 2H), 7.14 (dd, *J* = 4.5 Hz, 1.5 Hz, 2H), 5.52 (s, 2H).

<sup>13</sup>C NMR (DMSO-*d*<sub>6</sub>, 75 MHz, ppm): δ 149.7, 149.0, 140.6, 119.7.

HRMS [M+H]<sup>+</sup> C<sub>6</sub>H<sub>7</sub>N<sub>3</sub>O calculated 138.0662 found 138.0663.

#### Synthesis of *N'*-hydroxynicotinimidamide (2)<sup>[22]</sup>



Synthesized according to **GP1**. White solid. Yield 51%.

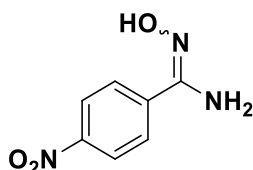
<sup>1</sup>H NMR (DMSO-*d*<sub>6</sub>, 300 MHz, ppm): δ 9.83 (s, 1H), 8.84 (d, *J* = 1.2 Hz, 1H), 8.54 (dd, *J* = 4.7 Hz, 1.6 Hz, 1H), 8.00 (dt, *J* = 8.04 Hz, 2.01 Hz, 1H), 7.41-7.37 (m, 1H), 5.97 (s, 2H).

<sup>13</sup>C NMR (DMSO-*d*<sub>6</sub>, 75 MHz, ppm): δ 149.7, 148.9, 146.5, 132.8, 129.0, 123.2.

HRMS [M+H]<sup>+</sup> C<sub>6</sub>H<sub>7</sub>N<sub>3</sub>O calculated 138.0662 found 138.0659.

The values are in accordance with the literature.

**Synthesis of *N'*-hydroxy-4-nitrobenzimidamide (3)**<sup>[23]</sup>



Synthesized according to **GP1**. Yellow solid. Yield 92%.

**<sup>1</sup>H NMR** (DMSO-*d*<sub>6</sub>, 300 MHz, ppm): δ 10.1 (s, 1H), 8.2 (d, *J* = 8.9 Hz, 2H), 7.9 (d, *J* = 8.9 Hz, 2H), 6.0 (s, 2H).

**<sup>13</sup>C NMR** (DMSO-*d*<sub>6</sub>, 75 MHz, ppm): δ 149.3, 147.4, 139.4, 126.3, 123.3.

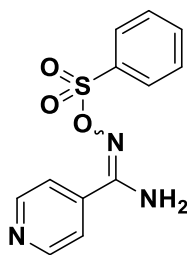
**HRMS** [**M+H**]<sup>+</sup> C<sub>7</sub>H<sub>7</sub>N<sub>3</sub>O<sub>3</sub> calculated 182.0560 found 182.0561.

The values are in accordance with the literature.

**5.6.2.2 Procedure for the synthesis of sulfonyl-amidoxmies (GP2)**

To a solution of amidoxime (1.0 equiv.) in [CHCl<sub>3</sub>/DMF (8/1) (0.15M)] at 0°C was added Et<sub>3</sub>N (1.0 equiv.), followed by the corresponding sulfonyl chloride (1.0 equiv.). The mixture was stirred overnight allowing the temperature to rise to room temperature. After the reaction, the mixture was extracted with DCM and either recrystallized from MeOH or purified by column chromatography on silica gel using PE/EA as the eluent.

**Synthesis of *N'*-((phenylsulfonyl)oxy)isonicotinimidamide (1a)**<sup>[13]</sup>



Synthesized according to **GP2**. The product was recrystallized from MeOH to obtain a yellow solid (51%).

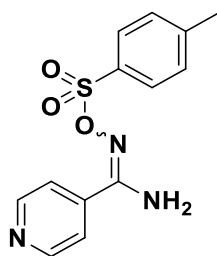
**<sup>1</sup>H NMR** (DMSO-*d*<sub>6</sub>, 300 MHz, ppm): δ 8.55 (d, *J* = 5.6 Hz, 2H), 7.93 (d, *J* = 7.8 Hz, 2H), 7.59 (t, *J* = 7.7 Hz, 1H), 7.46-7.53 (m, 4H), 6.60 (s, 2H).

**<sup>13</sup>C NMR** (DMSO-*d*<sub>6</sub>, 75 MHz, ppm): δ 155.0, 148.8, 137.8, 135.0, 132.9, 128.0, 127.7, 120.3.

**HRMS** [**M+H**]<sup>+</sup> C<sub>12</sub>H<sub>11</sub>N<sub>3</sub>O<sub>3</sub>S calculated 278.0594 found 278.0596.

The values are in accordance with the literature.

### Synthesis of *N'*-(tosyloxy)isonicotinimidamide (**1b**)<sup>[13]</sup>



Synthesized according to **GP2**. The crude was purified by column chromatography using 40:60 PE/EA to obtain a pink solid (64%).

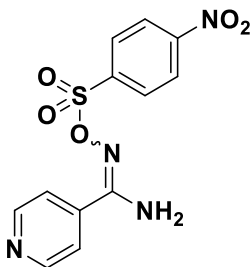
**<sup>1</sup>H NMR** (DMSO-*d*<sub>6</sub>, 300 MHz, ppm): δ 8.64 (d, *J* = 7.3 Hz, 2H), 7.86 (d, *J* = 8.3 Hz, 2H), 7.50 (d, *J* = 7.3 Hz, 2H), 7.44 (d, *J* = 8.3 Hz, 2H), 7.36 (s, 2H), 2.39 (s, 3H).

**<sup>13</sup>C NMR** (DMSO-*d*<sub>6</sub>, 75 MHz, ppm): δ 155.9, 150.2, 144.7, 138.0, 132.6, 129.7, 128.3, 121.0, 21.1.

**HRMS** [**M**+**H**]<sup>+</sup> C<sub>13</sub>H<sub>13</sub>N<sub>3</sub>O<sub>3</sub>S calculated 292.0750 found 292.0753.

The values are in accordance with the literature.

### Synthesis of *N'*-(((4-nitrophenyl)sulfonyl)oxy)isonicotinimidamide (**1c**)<sup>[13]</sup>



Synthesized according to **GP2**. The crude was recrystallized from MeOH to obtain a pale yellow solid (64%).

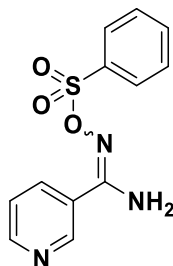
**<sup>1</sup>H NMR** (DMSO-*d*<sub>6</sub>, 300 MHz, ppm): δ 8.54 (d, *J* = 5.7 Hz, 2H), 8.54 (d, *J* = 5.7 Hz, 2H), 8.34 (d, *J* = 8.7 Hz, 2H), 8.18 (d, *J* = 8.9 Hz, 2H), 7.44 (d, *J* = 5.9 Hz, 2H), 6.98 (s, 2H).

**<sup>13</sup>C NMR** (DMSO-*d*<sub>6</sub>, 75 MHz, ppm): δ 155.5, 149.4, 148.8, 140.2, 136.6, 128.8, 122.7, 119.8.

**HRMS** [**M**+**H**]<sup>+</sup> C<sub>12</sub>H<sub>10</sub>N<sub>4</sub>O<sub>5</sub>S calculated 323.0445 found 323.0447.

The values are in accordance with the literature.

**Synthesis of N'-((phenylsulfonyl)oxy)nicotinimidamide (2a)<sup>[13]</sup>**



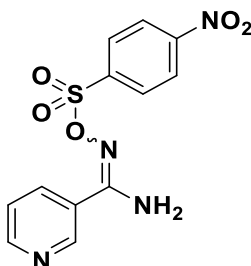
Synthesized according to **GP2**. The crude was recrystallized from MeOH to obtain a pale yellow solid (90%).

**<sup>1</sup>H NMR** (DMSO-*d*<sub>6</sub>, 300 MHz, ppm): δ 8.67 (d, *J* = 1.4 Hz, 1H), 8.59 (d, *J* = 3.6 Hz, 1H), 7.94 (d, *J* = 7.6 Hz, 2H), 7.79 (d, *J* = 7.9 Hz, 1H), 7.60 (t, *J* = 7.9 Hz, 1H), 7.50 (t, *J* = 7.5 Hz, 2H), 7.26 (dd, *J* = 7.9 Hz, 4.8 Hz, 1H), 6.60 (bs, 2H).

**<sup>13</sup>C NMR** (DMSO-*d*<sub>6</sub>, 75 MHz, ppm): δ 155.2, 150.5, 146.9, 135.0, 133.7, 132.7, 127.8, 127.5, 125.7, 122.2.

The values are in accordance with the literature.

**Synthesis of N'-(((4-nitrophenyl)sulfonyl)oxy)nicotinimidamide (2b)<sup>[13]</sup>**



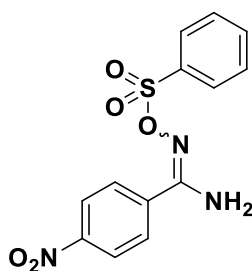
Synthesized according to **GP2**. The crude was recrystallized from MeOH to obtain a greenish solid (64%).

**<sup>1</sup>H NMR** (DMSO-*d*<sub>6</sub>, 300 MHz, ppm): δ 8.70 (d, *J* = 1.7 Hz, 1H), 8.57 (dd, *J* = 4.8, 1.5 Hz, 1H), 8.33 (d, *J* = 8.9 Hz, 2H), 8.17 (d, *J* = 8.9 Hz, 2H), 7.83 (dt, *J* = 8.1, 1.7 Hz, 1H), 7.27 (dd, *J* = 7.8, 4.8 Hz, 1H), 6.82 (s, 2H).

**<sup>13</sup>C NMR** (DMSO-*d*<sub>6</sub>, 75 MHz, ppm): δ 155.8, 150.7, 149.5, 146.7, 140.7, 133.8, 129.0, 125.5, 123.1, 122.3.

The values are in accordance with the literature.

### Synthesis of 4-nitro-*N'*-((phenylsulfonyl)oxy)benzimidamide (3a)<sup>[13]</sup>



Synthesized according to **GP2**. The crude was recrystallized from MeOH to obtain a yellowish white solid (40%).

<sup>1</sup>H NMR (DMSO-*d*<sub>6</sub>, 300 MHz, ppm): δ 8.11 (d, *J* = 8.5 Hz, 2H), 7.93 (d, *J* = 8.3 Hz, 2H), 7.72 (d, *J* = 8.8 Hz, 2H), 7.59 (t, *J* = 7.5 Hz, 1H), 7.50 (t, *J* = 7.8 Hz, 2H), 6.62 (s, 2H).

<sup>13</sup>C NMR (DMSO-*d*<sub>6</sub>, 75 MHz, ppm): δ 155.4, 148.2, 135.8, 134.7, 133.0, 128.0, 127.8, 127.1, 122.7.

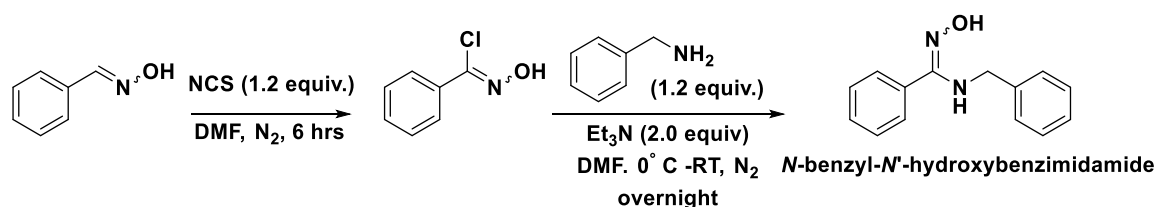
HRMS [*M*+*H*]<sup>+</sup> C<sub>13</sub>H<sub>11</sub>N<sub>3</sub>O<sub>5</sub>S calculated 322.0492 found 322.0495.

The values are in accordance with the literature.

#### 5.6.2.3 Procedure for the synthesis of benzimidamides (GP3)

To the solution of oxime in *N,N*-dimethylformamide at room temperature was added *N*-chloro succinimide in three portions. During each addition, the reaction mixture became yellow and then gradually returned to colourless. After the addition was complete, the reaction mixture was stirred at room temperature for 6 hours. The chloro-oxime was generated in situ. Aryl amine and triethylamine were added dropwise to the reaction mixture at 0°C and the reaction mixture was stirred overnight and allowed to come to room temperature. The reaction mixture was then extracted with DCM/ water and the crude was purified by column chromatography using hexane/ethyl acetate as eluent.

### Synthesis of *N*-benzyl-*N'*-hydroxybenzimidamide (4)<sup>[24]</sup>



Synthesized according to **GP3**. To a solution of oxime (1.0 equiv.) in DMF at room temperature was added NCS (1.1 equiv.) in two portions and was stirred for 6 hours. Et<sub>3</sub>N (2 equiv) was added dropwise at 0°C, followed by the benzyl amine (1.2 equiv.) and the



reaction mixture was stirred overnight. Column chromatography with 30:70 EA/PE yielded the desired product as a white crystalline solid (71%).

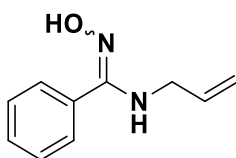
**<sup>1</sup>H NMR** (CDCl<sub>3</sub>, 300 MHz, ppm): δ 7.51–7.48 (m, 2 H), 7.43–7.35 (m, 3 H), 7.34–7.30 (m, 2 H), 7.27–7.20 (m, 3 H), 5.76 (s, 1 H), 4.25 (s, 2 H).

**<sup>13</sup>C NMR** (CDCl<sub>3</sub>, 75 MHz, ppm): δ = 156.5, 139.7, 131.3, 129.7, 128.7, 128.7, 128.5, 127.3, 126.9, 47.5.

**HRMS** [M+H]<sup>+</sup> C<sub>14</sub>H<sub>14</sub>N<sub>2</sub>O calculated 227.1179 found 227.1180.

The values are in accordance with the literature.

#### Synthesis of *N*-allyl-*N'*-hydroxybenzimidamide (5)<sup>[24]</sup>



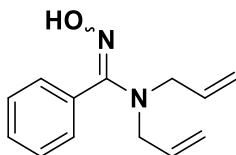
Synthesized according to **GP3**. To a solution of oxime (1.0 equiv.) in DMF at room temperature was added NCS (1.1 equiv.) in two portions and was stirred for 6 hours. Et<sub>3</sub>N (2 equiv) was added dropwise at 0°C, followed by the allyl amine (1.2 equiv.) and the reaction mixture was stirred overnight. Column chromatography with 15:85 EA/PE yielded the desired product as a white solid (54%).

**<sup>1</sup>H NMR** (CDCl<sub>3</sub>, 300 MHz, ppm): δ 8.59 (bs, 1H), 7.47-7.44 (m, 2H), 7.40-7.36 (m, 3H), 5.81-5.69 (m, 1H), 5.75 (dddd, *J* = 17.0 Hz, 15.2 Hz, 10.0 Hz, 4.8 Hz, 1H), 5.50(bs, 1H), 5.22-5.05 (m 2H), 3.62 (s, 1H).

**<sup>13</sup>C NMR** (CDCl<sub>3</sub>, 75 MHz, ppm): δ 156.7, 135.9, 131.1, 129.8, 128.6, 128.5, 115.6, 46.0.

**HRMS** [M+H]<sup>+</sup> C<sub>10</sub>H<sub>12</sub>N<sub>2</sub>O calculated 177.1022 found 177.1020.

#### Synthesis of *N,N*-diallyl-*N'*-hydroxybenzimidamide (6)



Synthesized according to **GP3**. To a solution of oxime (1.0 equiv.) in DMF at room temperature was added NCS (1.1 equiv.) in two portions and was stirred for 6 hours. Et<sub>3</sub>N (2 equiv) was added dropwise at 0°C, followed by the diallyl amine (1.2 equiv.) and the reaction mixture was stirred overnight. Column chromatography with 7:93 EA/PE yielded the desired product as a white solid (70%).

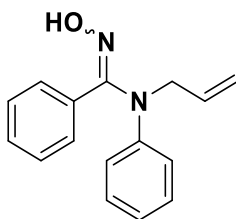
**$^1\text{H}$  NMR** ( $\text{CDCl}_3$ , 400 MHz, ppm):  $\delta$  7.43-7.35 (m, 5H), 7.25-7.24 (m, 1H), 5.74 (dddd,  $J$  = 16.4 Hz, 11.6 Hz, 10.8 Hz, 6.0 Hz, 2H), 5.20-5.08 (m, 4H), 4.99-4.93 (m, 4H), 3.65 (d,  $J$  = 5.8 Hz, 4H).

**$^{13}\text{C}$  NMR** ( $\text{CDCl}_3$ , 100 MHz, ppm):  $\delta$  159.9, 133.9, 131.6, 129.3, 128.8, 128.4, 117.5, 50.0.

**HRMS**  $[\text{M}+\text{H}]^+$   $\text{C}_{13}\text{H}_{16}\text{N}_2\text{O}$  calculated 217.1335 found 217.1336.

**Melting point:** 68°C.

#### Synthesis of *N*-allyl-*N'*-hydroxy-*N*-phenylbenzimidamide (7)



Synthesized according to **GP3**. To a solution of oxime (1.0 equiv.) in DMF at room temperature was added NCS (1.1 equiv.) in two portions and was stirred for 6 hours.  $\text{Et}_3\text{N}$  (2 equiv) was added dropwise at 0°C, followed by the *N*-allyl aniline (1.2 equiv.) and the reaction mixture was stirred overnight. Column chromatography with 10:90 EA/PE yielded the desired product as a white solid (60%).

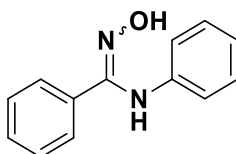
**$^1\text{H}$  NMR** ( $\text{CDCl}_3$ , 400 MHz, ppm):  $\delta$  7.66 (d,  $J$  = 3.2 Hz, 2H), 7.42 (d,  $J$  = 3.2 Hz, 3H), 7.41-7.17 (m, 2H), 6.72-6.77 (m, 1H), 6.65-6.68 (m, 2H), 5.03 (dddd,  $J$  = 16.4 Hz, 11.6 Hz, 10.8 Hz, 6.0 Hz, 1H), 4.98-3.19 (m, 4H).

**$^{13}\text{C}$  NMR** ( $\text{CDCl}_3$ , 100 MHz, ppm):  $\delta$  157.2, 147.9, 130.4, 129.5, 128.9, 126.9, 118.3, 113.4, 79.7, 47.3, 38.2.

**HRMS**  $[\text{M}+\text{H}]^+$   $\text{C}_{16}\text{H}_{16}\text{N}_2\text{O}$  calculated 253.1335 found 253.1336.

**Melting point:** 116.3°C.

#### Synthesis of *N'*-hydroxy-*N*-phenylbenzimidamide (8)<sup>[25]</sup>



Synthesized according to **GP3**. To a solution of oxime (1.0 equiv.) in DMF at room temperature was added NCS (1.1 equiv.) in two portions and was stirred for 6 hours.  $\text{Et}_3\text{N}$

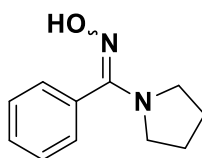
(2 equiv) was added dropwise at 0°C, followed by the aniline (1.2 equiv.) and the reaction mixture was stirred overnight. Column chromatography with 20:80 EA/PE yielded the desired product as a white solid (75%).

**<sup>1</sup>H NMR** (DMSO-*d*<sub>6</sub>, 300 MHz, ppm): δ 10.54 (s, 1 H, OH), 8.28 (s, 1 H, NH), 7.38-7.31 (m, 5 H), 7.04 (t, *J* = 7.9 Hz, 2H), 6.77 (t, *J* = 7.3 Hz, 1H), 6.63 (d, *J* = 7.8 Hz, 2H).

**<sup>13</sup>C NMR** (DMSO-*d*<sub>6</sub>, 175 MHz, ppm) δ 149.2, 141.4, 132.8, 128.9, 128.34, 128.25, 127.7, 120.7, 119.8.

The values are in accordance with the literature.

### Synthesis of phenyl(pyrrolidin-1-yl)methanone oxime (9)



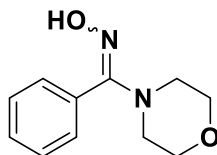
Synthesized according to **GP3**. To a solution of oxime (1.0 equiv.) in DMF at room temperature was added NCS (1.1 equiv.) in two portions and was stirred for 6 hours. Et<sub>3</sub>N (2 equiv) was added dropwise at 0°C, followed by the pyrrolidine (1.2 equiv.) and the reaction mixture was stirred overnight. Column chromatography with 15:85 EA/PE yielded the desired product as a white solid (95%).

**<sup>1</sup>H NMR** (CDCl<sub>3</sub>, 300 MHz, ppm): δ 7.45-7.35 (m, 5H), 3.10 (t, *J* = 6.9 Hz, 4H), 1.81 (t, *J* = 6.6 Hz, 4H).

**<sup>13</sup>C NMR** (CDCl<sub>3</sub>, 75 MHz, ppm): δ 158.9, 132.5, 129.1, 128.5, 128.3, 51.1, 48.0, 25.6, 25.1.

**HRMS** [**M**+**H**]<sup>+</sup> C<sub>11</sub>H<sub>14</sub>N<sub>2</sub>O calculated 191.1179 found 191.1180.

### Synthesis of morpholino(phenyl)methanone oxime (10)



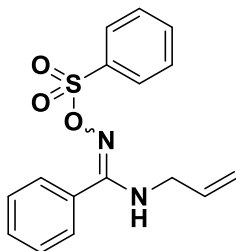
Synthesized according to **GP3**. To a solution of oxime (1.0 equiv.) in DMF at room temperature was added NCS (1.1 equiv.) in two portions and was stirred for 6 hours. Et<sub>3</sub>N (2 equiv) was added dropwise at 0°C, followed by the morpholine (1.2 equiv.) and the reaction mixture was stirred overnight. Column chromatography with 15:85 EA/PE yielded the desired product as a white solid (86%).

**$^1\text{H}$  NMR** ( $\text{CDCl}_3$ , 300 MHz, ppm):  $\delta$  7.47-7.26 (m, 5H), 3.67 (t,  $J$  = 4.8 Hz, 4H), 2.99 (t,  $J$  = 4.8 Hz, 4H).

**$^{13}\text{C}$  NMR** ( $\text{CDCl}_3$ , 75 MHz, ppm):  $\delta$  160.1, 130.3, 129.7, 129.1, 128.6, 67.5, 66.6, 49.6, 47.7.

**HRMS**  $[\text{M}+\text{H}]^+$   $\text{C}_{11}\text{H}_{14}\text{N}_2\text{O}_2$  calculated 207.1128 found 207.1130.

#### Synthesis of *N*-allyl-*N'*-((phenylsulfonyl)oxy)benzimidamide (5a)



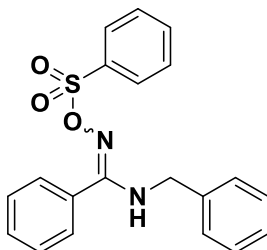
Synthesized according to **GP2**. The crude product was purified by column chromatography using 20:80 PE/EA to obtain a yellow liquid (45%).

**$^1\text{H}$  NMR** ( $\text{CDCl}_3$ , 300 MHz, ppm):  $\delta$  8.25 (s, 1H), 7.95-7.92 (m, 2H), 7.72-7.76 (m, 1H), 7.59-7.50 (m, 5H), 7.29-7.26 (m, 1H), 5.69 (dddd,  $J$  = 16.2 Hz, 11.8 Hz, 10.2 Hz, 5.9 Hz, 1H), 5.29 (s, 1H), 5.12-5.01 (m, 2H), 4.25 (d,  $J$  = 5.9 Hz, 2H).

**$^{13}\text{C}$  NMR** ( $\text{CDCl}_3$ , 75 MHz, ppm):  $\delta$  161.6, 161.0, 135.2, 134.4, 131.7, 130.8, 129.4, 129.2, 128.8, 126.4, 119.0, 44.6.

**HRMS**  $[\text{M}+\text{H}]^+$   $\text{C}_{16}\text{H}_{16}\text{N}_2\text{O}_3\text{S}$  calculated 317.0082 found 317.0085.

#### Synthesis of *N*-benzyl-*N'*-((phenylsulfonyl)oxy)benzimidamide (4a)

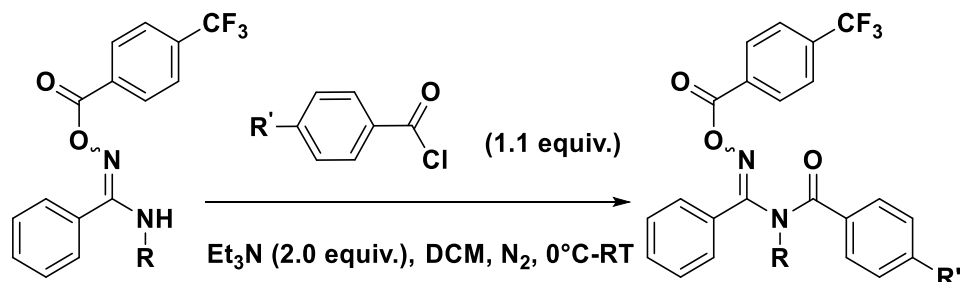


Synthesized according to **GP2**. The crude product was purified by column chromatography using 20:80 PE/EA to obtain a yellow liquid (40%).

**$^1\text{H}$  NMR** ( $\text{CDCl}_3$ , 300 MHz, ppm):  $\delta$  8.32 (s, 1H), 7.83-7.80 (m, 2H), 7.70-7.65 (m, 1H), 7.53-7.46 (m, 5H), 7.27-7.23 (m, 3H), 7.18-7.10 (m, 3H), 4.89 (s, 2H).

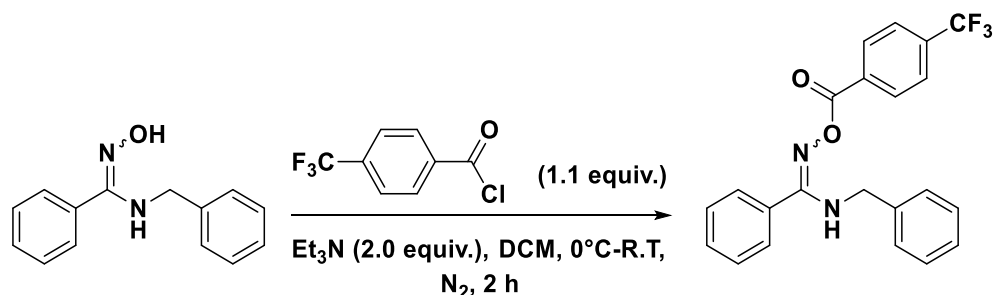
**$^{13}\text{C}$  NMR** ( $\text{CDCl}_3$ , 75 MHz, ppm):  $\delta$  162.0, 161.3, 135.8, 135.2, 134.2, 131.6, 129.4, 129.2, 129.0, 128.7, 128.6, 127.9, 126.5, 45.5.

#### 5.6.2.4 Typical procedure for synthesis of *N*-benzyl amidoxime and *N*-benzoyl amidoxime (GP4)



To a solution of the benzimidamide in dry DCM was added Et<sub>3</sub>N (2 equiv.) dropwise at 0°C. The corresponding benzoyl chloride (1.5 equiv.) was added and the reaction mixture was stirred for indicated time allowing it to come to room temperature. After the reaction, the solvent was evaporated and the crude product was purified by column chromatography using PE/EA as eluent.

#### Synthesis of *N*-benzyl-*N*'-((4-(trifluoromethyl)benzoyl)oxy)benzimidamide (4b)



Amidoxime (1.5 g, 6.6 mmol) was dissolved in dry DCM (50 mL). Et<sub>3</sub>N (1.8 mL, 13.2 mmol) was added dropwise at 0°C, followed by the addition of the acid chloride (1.5 mL, 9.9 mmol). The reaction mixture was stirred at room temperature for 2 hrs. After the reaction, the solvent was evaporated and the crude product was purified by column chromatography using 10:90 EA/PE to obtain a white solid (1.6 g, 62%).

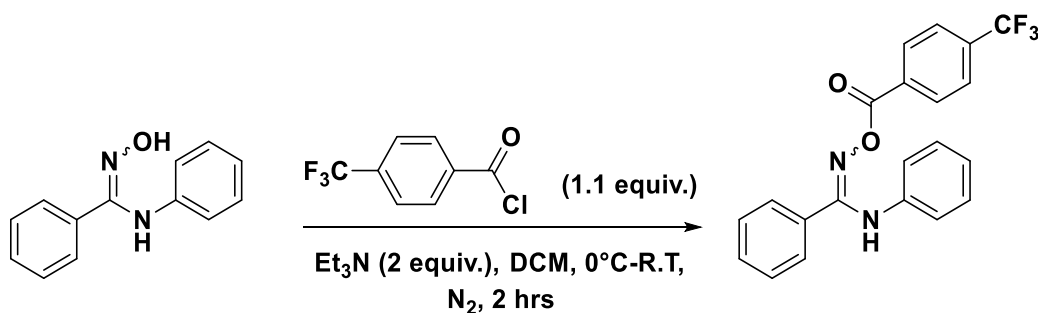
<sup>1</sup>H NMR (CDCl<sub>3</sub>, 300 MHz, ppm): δ 8.14 (d, *J* = 9.3 Hz, 2H), 7.73 (d, *J* = 8.1 Hz, 2H), 7.56-7.20 (m, 9H), 5.86 (s, 1H), 4.34 (d, *J* = 5.1 Hz, 2H).

<sup>13</sup>C NMR (CDCl<sub>3</sub>, 75 MHz, ppm): δ 163.1, 161.1, 138.5, 133.0, 130.9, 130.1, 129.2, 129.1, 128.9, 128.0, 126.9, 125.7, 125.7, 48.1.

HRMS [*M*+*H*]<sup>+</sup> C<sub>22</sub>H<sub>17</sub>F<sub>3</sub>N<sub>2</sub>O<sub>3</sub> calculated 399.1315 found 399.1331.

Melting point: 100.4°C.

### Synthesis of *N*-phenyl-*N'*-((4-(trifluoromethyl)benzoyl)oxy)benzimidamide (8a)



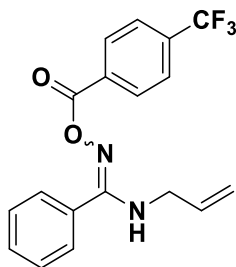
Amidoxime (1.2 g, 5.9 mmol) was dissolved in dry DCM (40 mL). Et<sub>3</sub>N (1.25 mL, 1.5 mmol) was added dropwise at 0°C, followed by the addition of the acid chloride (0.9 mL, 1.4 mmol). The reaction mixture was stirred at room temperature for 2 hrs. After the reaction, the solvent was evaporated and the crude product was purified by column chromatography using 5:95 EA/PE to obtain a white solid (2.6 g, 90%).

<sup>1</sup>H NMR (CDCl<sub>3</sub>, 300 MHz, ppm): δ 8.15 (d, *J* = 6 Hz, 2H), 7.71 (d, *J* = 6 Hz, 2H), 7.53 (d, *J* = 5.4 Hz, 2H), 7.43-7.30 (m, 3H), 7.17 (t, *J* = 5.7 Hz, 2H), 7.04 (t, *J* = 6 Hz, 1H), 6.83 (d, *J* = 5.7 Hz, 2H).

<sup>13</sup>C NMR (CDCl<sub>3</sub>, 75 MHz, ppm): δ 162.9, 157.2, 138.6, 132.8, 131.0, 130.1, 129.6, 129.2, 128.7, 125.8, 125.7, 124.8, 123.2, 122.8.

HRMS [*M*+*H*]<sup>+</sup> C<sub>21</sub>H<sub>15</sub>F<sub>3</sub>N<sub>2</sub>O<sub>2</sub> calculated 385.1158 found 385.1164.

### Synthesis of *N*-allyl-*N'*-((4-(trifluoromethyl)benzoyl)oxy)benzimidamide (5b)



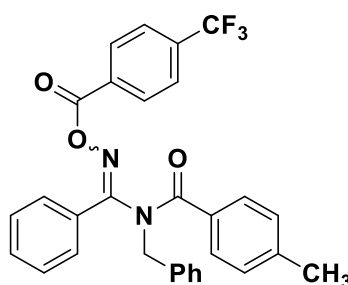
Amidoxime (1.2 g, 5.9 mmol) was dissolved in dry DCM (40 mL). Et<sub>3</sub>N (1.25 mL, 1.5 mmol) was added dropwise at 0°C, followed by the addition of the acid chloride (0.9 mL, 1.4 mmol). The reaction mixture was stirred at room temperature for 2 hrs. After the reaction, the solvent was evaporated and the crude product was purified by column chromatography using 5:95 EA/PE to obtain a pink solid (2.1 g, 61%).

**<sup>1</sup>H NMR** (DMSO-*d*<sub>6</sub>, 300 MHz, ppm): δ 8.36 (d, *J* = 8.1 Hz, 2H), 7.92 (d, *J* = 8.1 Hz, 2H), 7.78 (s, 1H), 7.53-7.50 (m, 5H), 5.75 (dddd, *J* = 16.4 Hz, 11.6 Hz, 10.8 Hz, 6.0 Hz, 1H), 5.09-5.03 (m, 2H), 3.63-3.60 (m, 2H).

**<sup>13</sup>C NMR** (DMSO-*d*<sub>6</sub>, 300 MHz, ppm): δ 162.2, 160.3, 136.5, 130.4, 130.2, 129.3, 128.7, 128.4, 127.8, 125.5, 125.5, 115.0, 45.4.

**HRMS** [**M+H**]<sup>+</sup> C<sub>18</sub>H<sub>15</sub>F<sub>3</sub>N<sub>2</sub>O<sub>2</sub> calculated 349.1158 found 349.1165.

**Synthesis of *N*-benzyl-4-methyl-*N*-(phenyl(((4-(trifluoromethyl)benzoyl)oxy)imino)methyl)benzamide (4c)**



Synthesized according to **GP4**. Reaction time 25 hrs.

61% yield as white solid.

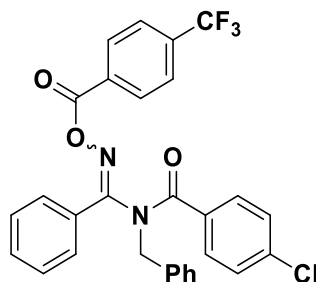
**<sup>1</sup>H NMR** (CDCl<sub>3</sub>, 300 MHz, ppm): δ 7.99 (d, *J* = 6.3 Hz, 1H), 7.88 (d, *J* = 5.4 Hz, 2H), 7.58 (d, *J* = 5.7 Hz, 1H), 7.53-7.51 (m, 6H), 7.39 (t, *J* = 6.3 Hz, 4H), 7.25-7.20 (m, 5H), 5.44 (d, *J* = 9.9 Hz, 1H), 4.45 (d, *J* = 10.8 Hz, 1H), 2.44 (s, 3H).

**<sup>13</sup>C NMR** (CDCl<sub>3</sub>, 75 MHz, ppm): δ 170.0, 162.3, 155.7, 144.8, 135.8, 132.6, 130.4, 130.0, 129.9, 129.8, 129.6, 129.5, 129.4, 128.8, 128.7, 128.5, 127.9, 125.4, 125.3, 125.0, 50.7, 22.0.

**HRMS** [**M+H**]<sup>+</sup> C<sub>30</sub>H<sub>23</sub>F<sub>3</sub>N<sub>2</sub>O<sub>3</sub> calculated 517.1734 found 517.1741.

**Melting point:** 165.4°C.

**Synthesis of *N*-benzyl-4-chloro-*N*-(phenyl(((4-(trifluoromethyl)benzoyl)oxy)imino)methyl)benzamide (4d)**



Synthesized according to **GP4**. Reaction time 25 hrs.

54% yield as yellowish white solid.

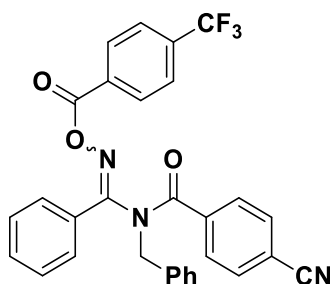
**<sup>1</sup>H NMR** (CDCl<sub>3</sub>, 300 MHz, ppm): δ 7.91 (dd, *J* = 6.3 Hz, 13.5 Hz, 1H), 7.79 (d, *J* = 5.7 Hz, 2H), 7.52-7.05 (m, 15H), 5.32 (d, *J* = 9.6 Hz, 1H), 4.32 (d, *J* = 9.6 Hz, 1H).

**<sup>13</sup>C NMR** (CDCl<sub>3</sub>, 75 MHz, ppm): δ 169.9, 161.4, 156.3, 140.5, 137.8, 135.8, 132.8, 131.7, 131.0, 129.9, 129.7, 129.7, 129.2, 129.1, 128.9, 128.7, 128.6, 127.8, 126.2, 125.4, 125.4, 50.8.

**HRMS [M+H]<sup>+</sup>** C<sub>29</sub>H<sub>20</sub>ClF<sub>3</sub>N<sub>2</sub>O<sub>3</sub> calculated 537.1187 found 537.1191.

**Melting point:** 167.6°C.

**Synthesis of *N*-benzyl-4-cyano-*N*-(phenyl(((4-(trifluoromethyl)benzoyl)oxy)imino)methyl)benzamide (4e)**



Synthesized according to **GP4**. Reaction time 25 hrs.

15% yield as white solid.

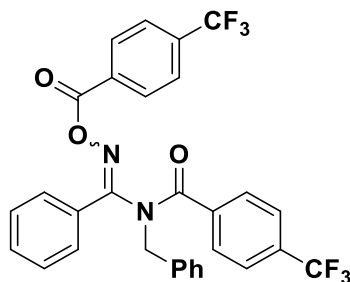
**<sup>1</sup>H NMR** (CDCl<sub>3</sub>, 300 MHz, ppm): δ 7.97-7.95 (m, 2H), 7.70-7.20 (m, 16H), 5.47 (d, *J* = 9.9 Hz, 1H), 4.34 (d, *J* = 10.2 Hz, 1H).

**<sup>13</sup>C NMR** (CDCl<sub>3</sub>, 75 MHz, ppm): δ 169.8, 190.7, 157.0, 135.8, 133.1, 132.5, 131.7, 130.1, 129.9, 129.9, 129.3, 129.0, 128.8, 128.6, 127.8, 125.5, 117.8, 117.3, 51.0.

**HRMS [M+H]<sup>+</sup>** C<sub>30</sub>H<sub>20</sub>F<sub>3</sub>N<sub>3</sub>O<sub>3</sub> calculated 528.1530 found 528.1537.



**Synthesis of *N*-benzyl-*N*-(phenyl(((4-(trifluoromethyl)benzoyl)oxy)imino)methyl)-4-(trifluoromethyl)benzamide (4f)**



Synthesized according to **GP4**. Reaction time 25 hrs.

82% yield as white solid.

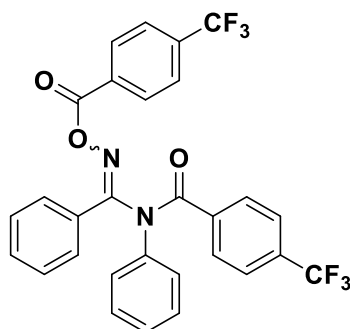
**<sup>1</sup>H NMR** (CDCl<sub>3</sub>, 300 MHz, ppm): δ 8.22 (d, *J* = 8.4 Hz, 2H), 7.97-7.94 (m, 2H), 7.86 (d, *J* = 8.1 Hz, 2H), 7.75 (d, *J* = 8.4 Hz, 2H), 7.63-7.40 (m, 25H), 7.15 (t, *J* = 7.8 Hz, 2H), 6.92-6.90 (m, 2H), 5.48 (d, *J* = 13.5 Hz, 1H), 5.35 (s, 1H), 4.36 (d, *J* = 13.5 Hz, 1H).

**<sup>13</sup>C NMR** (CDCl<sub>3</sub>, 75 MHz, ppm): δ 162.2, 161.1, 156.7, 140.3, 137.7, 136.6, 135.8, 135.4, 135.2, 135.2, 135.0, 133.6, 133.4, 133.0, 132.5, 132.3, 131.6, 131.2, 131.1, 131.1, 130.8, 130.2, 130.0, 130.0, 129.9, 129.8, 129.5, 129.0, 129.0, 128.9, 128.8, 128.6, 128.5, 128.4, 128.1, 127.8, 125.8, 125.8, 125.8, 125.7, 125.5, 125.5, 125.3, 125.3, 124.5, 124.5, 122.7, 52.9, 50.9.

**HRMS** [M+H]<sup>+</sup> C<sub>30</sub>H<sub>20</sub>F<sub>6</sub>N<sub>2</sub>O<sub>3</sub> calculated 571.1451 found 571.1459.

**Melting point:** 167.0°C.

**Synthesis of *N*-phenyl-*N*-(phenyl(((4-(trifluoromethyl)benzoyl)oxy)imino)methyl)-4-(trifluoromethyl)benzamide (8b)**



Synthesized according to **GP4**. Reaction time 18 hrs.

90% yield as white solid.

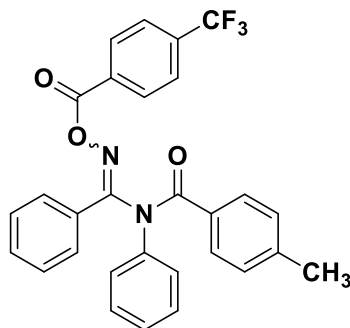
**$^1\text{H}$  NMR** ( $\text{CDCl}_3$ , 300 MHz, ppm):  $\delta$  8.27 (d,  $J$  = 6.3 Hz), 7.96 (d,  $J$  = 6 Hz), 7.89 (d,  $J$  = 5.4 Hz), 7.82 (d,  $J$  = 6 Hz), 7.69-7.64 (m, 3H), 7.50-7.45 (m, 2H), 7.41-7.37 (m, 3H), 7.36-7.27 (m, 2H).

**$^{13}\text{C}$  NMR** ( $\text{CDCl}_3$ , 75 MHz, ppm):  $\delta$  161.4, 160.7, 156.1, 139.0, 137.7, 133.8, 132.1, 131.7, 131.1, 130.9, 130.5, 130.4, 130.0, 129.7, 129.1, 128.6, 127.4, 126.0, 126.0, 125.7, 125.7, 125.4, 125.4, 125.3

**HRMS** [ $\text{M}+\text{H}$ ] $^+$   $\text{C}_{29}\text{H}_{18}\text{F}_6\text{N}_2\text{O}_3$  calculated 557.1294 found 557.1287

**Melting point:** 150.0°C.

**Synthesis of 4-methyl-*N*-phenyl-*N*-(phenyl(((4-(trifluoromethyl)benzoyl)oxy)imino)methyl)benzamide (8c)**



Synthesized according to **GP4**. Reaction time 22 hrs.

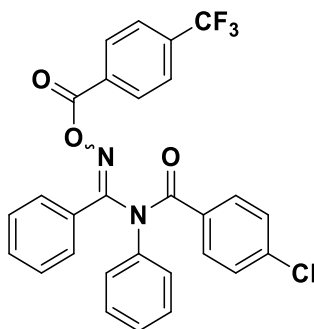
**$^1\text{H}$  NMR** ( $\text{CDCl}_3$ , 300 MHz, ppm):  $\delta$  7.93-7.89 (m, 2H), 7.79 (d,  $J$  = 8.4 Hz, 2H), 7.66 (d,  $J$  = 8.1 Hz, 2H), 7.48-7.20 (m, 12H), 2.41 (s, 3H).

**$^{13}\text{C}$  NMR** ( $\text{CDCl}_3$ , 75 MHz, ppm):  $\delta$  169.8, 162.7, 155.3, 145.0, 139.0, 138.1, 133.8, 133.4, 132.1, 130.7, 129.9, 129.8, 129.6, 129.2, 128.7, 128.7, 127.5, 125.7, 125.5, 125.5, 125.1, 22.0.

**HRMS** [ $\text{M}+\text{H}$ ] $^+$   $\text{C}_{29}\text{H}_{21}\text{F}_3\text{N}_2\text{O}_3$  calculated 503.1580 found 503.1581.

**Melting point:** 150.1°C.

**Synthesis of 4-chloro-N-phenyl-N-(phenyl(((4-(trifluoromethyl)benzoyl)oxy)imino)methyl)benzamide (8d)**



Synthesized according to **GP4**. Reaction time 16 hrs.

58% yield as white solid.

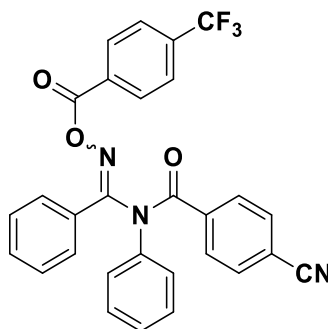
**<sup>1</sup>H NMR** (CDCl<sub>3</sub>, 300 MHz, ppm): δ 7.91-7.88 (m, 2H), 7.83-7.78 (m, 2H), 7.65 (d, *J* = 9 Hz, 2H), 7.53-7.22 (m, 12H).

**<sup>13</sup>C NMR** (CDCl<sub>3</sub>, 75 MHz, ppm): δ 140.6, 139.1, 137.9, 133.9, 133.5, 132.2, 132.0, 131.2, 130.5, 129.8, 129.3, 129.2, 128.7, 127.6, 126.3, 125.6, 125.3, 121.7.

**HRMS** [**M+H**]<sup>+</sup> C<sub>28</sub>H<sub>18</sub>F<sub>3</sub>ClN<sub>2</sub>O<sub>3</sub> calculated 523.1031 found 523.1034.

**Melting point:** 144.1°C.

**Synthesis of 4-cyano-N-phenyl-N-(phenyl(((4-(trifluoromethyl)benzoyl)oxy)imino)methyl)benzamide (8e)**



Synthesized according to **GP4**. Reaction time 16 hrs.

87% yield as white solid.

**<sup>1</sup>H NMR** (CDCl<sub>3</sub>, 300 MHz, ppm): δ 7.69 (d, *J* = 6.3 Hz, 2H), 7.64 (d, *J* = 3 Hz, 2H), 7.43 (dd, *J* = 6.3 Hz, 8 Hz, 4H), 7.25-6.97 (m, 10H).

**<sup>13</sup>C NMR** (CDCl<sub>3</sub>, 75 MHz, ppm): δ 169.5, 161.1, 156.5, 139.1, 137.7, 133.9, 133.6, 132.6, 132.3, 131.8, 130.4, 130.2, 129.8, 129.2, 128.7, 128.7, 127.6, 125.6, 125.5, 125.5, 124.7, 117.7, 117.3.

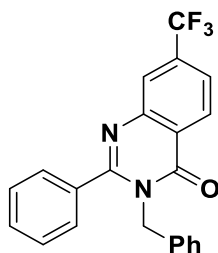
**HRMS**  $[M+H]^+$   $C_{29}H_{18}F_3N_3O_3$  calculated 514.1373 found 514.1380.

**Melting point:** 159.0°C.

#### 5.6.2.5 Photocatalytic procedure for the synthesis of quinazolinone derivative (GP5)

In a 5 mL snap vial with magnetic stirring bar the benzamide (0.02 mmol, 1.0 equiv.),  $K_3PO_4$  (2 equiv.) and photocatalyst A (0.01 mmol, 0.2 equiv.) were added and the mixture was degassed by “pump-freeze-thaw” cycles ( $\times 3$ ) via a syringe needle. Dry toluene (total volume of the solution 1.5 mL), were added under  $N_2$  and the resulting mixture was again degassed twice by syringe needle and irradiated with 400 nm LED under nitrogen at 22° C. The reaction progress was monitored by TLC. After irradiation, the reaction mixture was filtered to remove the base and washed with ethyl acetate and was concentrated in vacuum. Purification of the crude product was achieved by flash column chromatography using petrol ether/ethyl acetate as eluent.

#### Synthesis of 3-benzyl-2-phenyl-7-(trifluoromethyl)quinazolin-4(3H)-one (11)



Synthesized according to **GP5**.

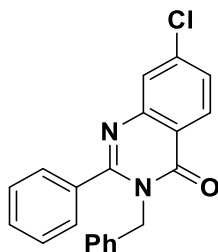
Isolated yield: 40%, colorless liquid.

**$^1H$  NMR** ( $CDCl_3$ , 300 MHz, ppm):  $\delta$  8.48 (d,  $J$  = 8.4 Hz, 1H), 8.09 (s, 1H), 7.73 (d,  $J$  = 8.4 Hz), 7.53-7.34 (m, 5H), 7.22 (t,  $J$  = 3 Hz, 3H), 6.93-6.90 (m, 2H), 5.29 (s, 2H).

**$^{13}C$  NMR** ( $CDCl_3$ , 300 MHz, ppm):  $\delta$  161.8, 158.1, 147.0, 136.2, 134.6, 130.6, 128.9, 128.8, 128.5, 128.1, 127.9, 127.1, 125.2, 123.4, 49.3.

**HRMS**  $[M+H]^+$   $C_{22}H_{15}F_3N_2O$  calculated 381.1209 found 381.1217.

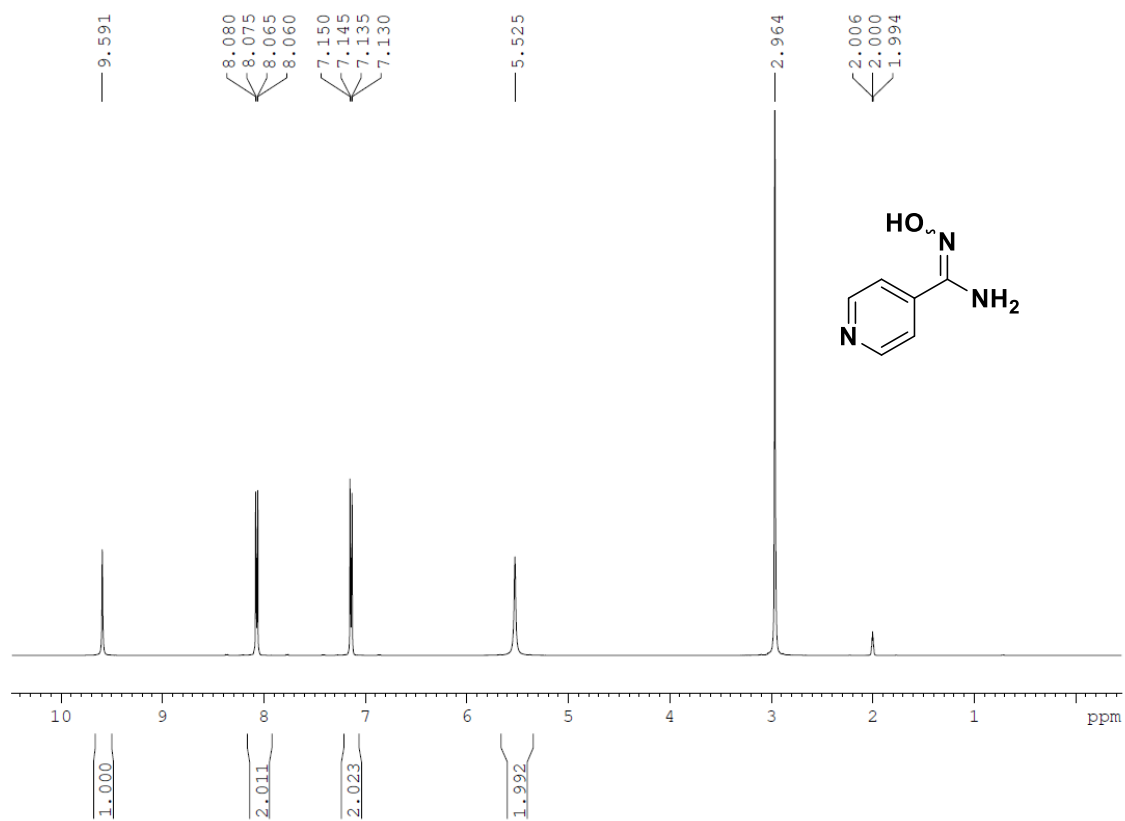
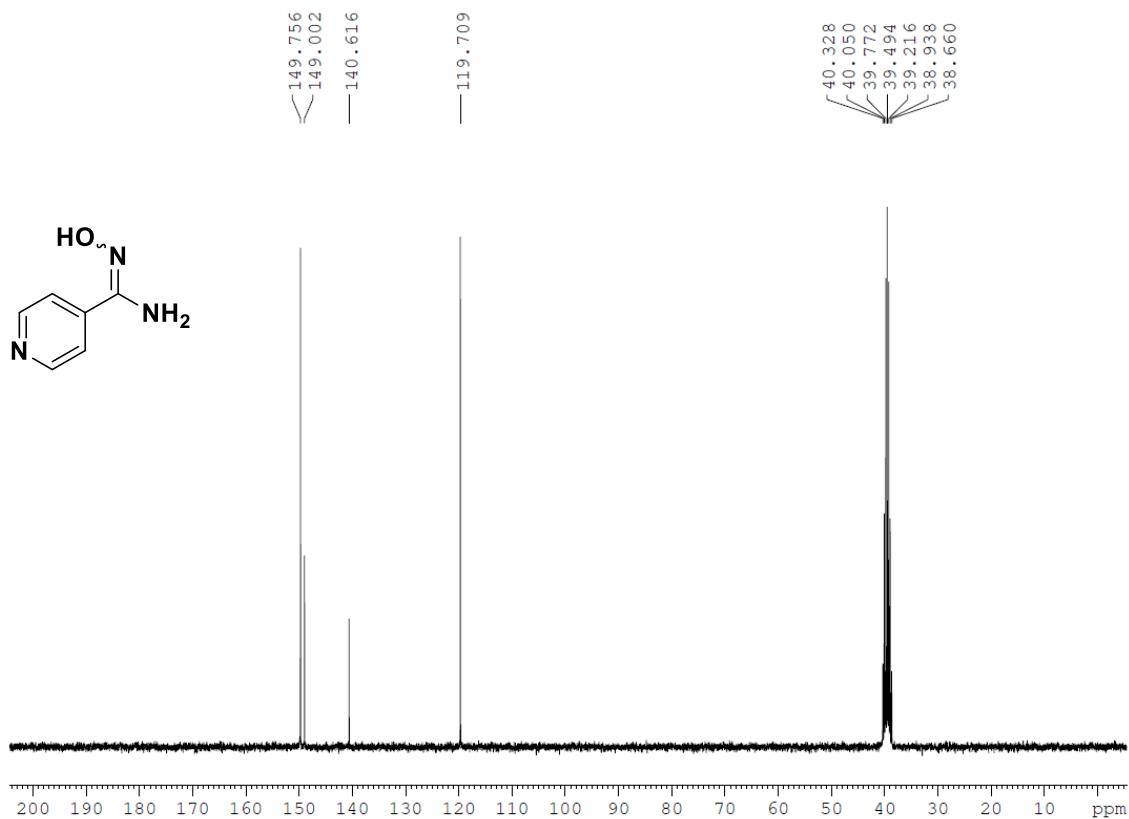
**Synthesis of 3-benzyl-7-chloro-2-phenylquinazolin-4(3H)-one (12):**



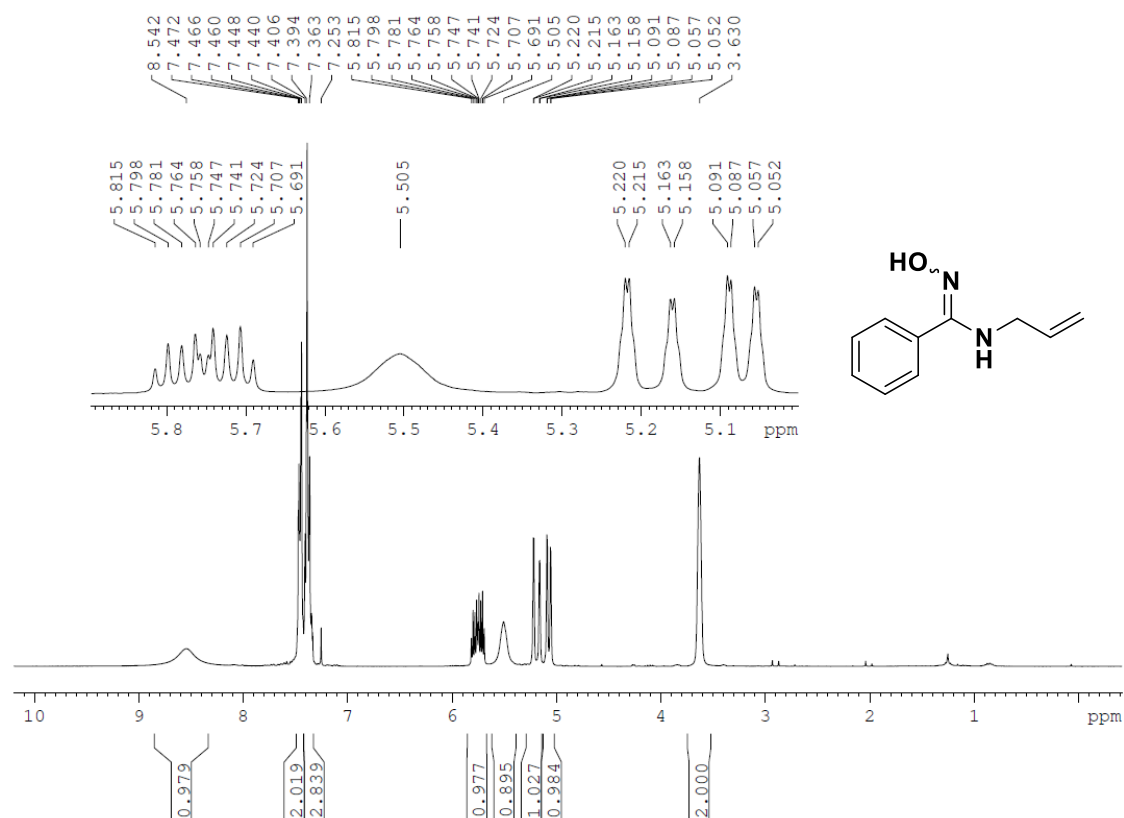
Synthesized according to **GP5**.

Isolated yield: 22%

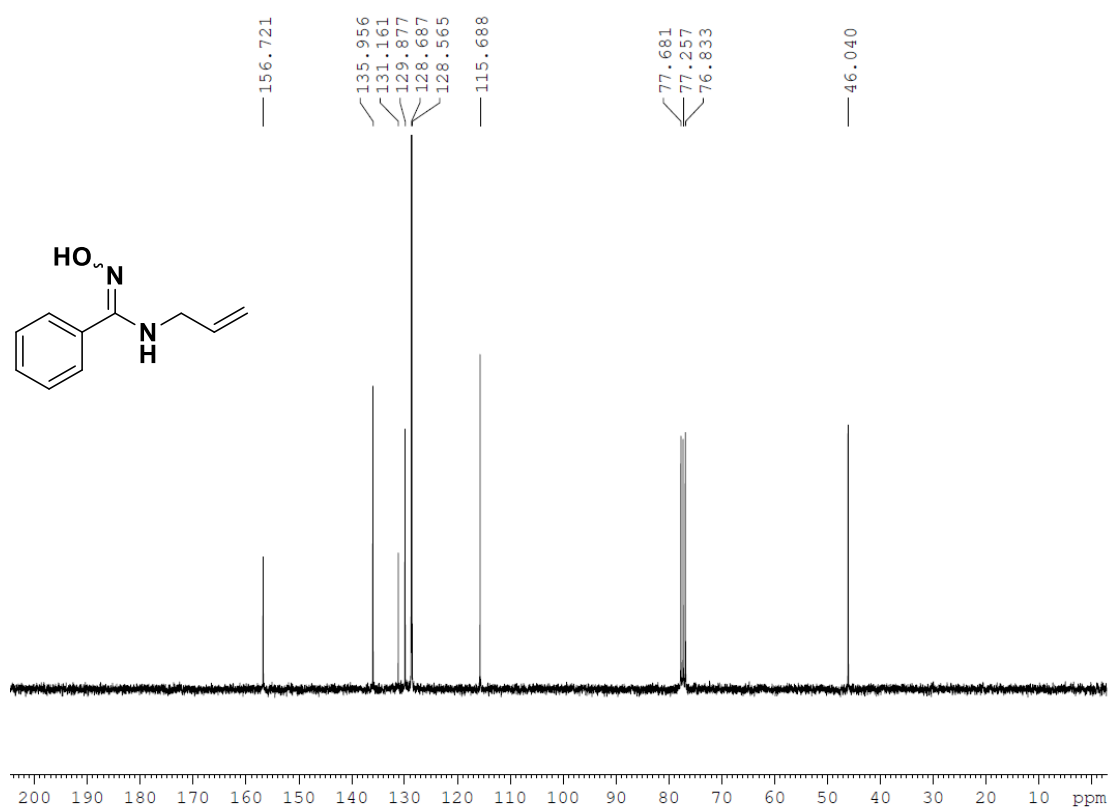
**<sup>1</sup>H NMR** (CDCl<sub>3</sub>, 300 MHz, ppm): δ 8.48 (d, J = 8.4 Hz, 1H), 8.07 (s, 1H), 7.72 (dd, J = 1.5 Hz, 8.4 Hz, 1H), 7.48-7.33 (m, 5H), 7.21 (t, J = 3 Hz, 3H), 5.29 (s, 1H).

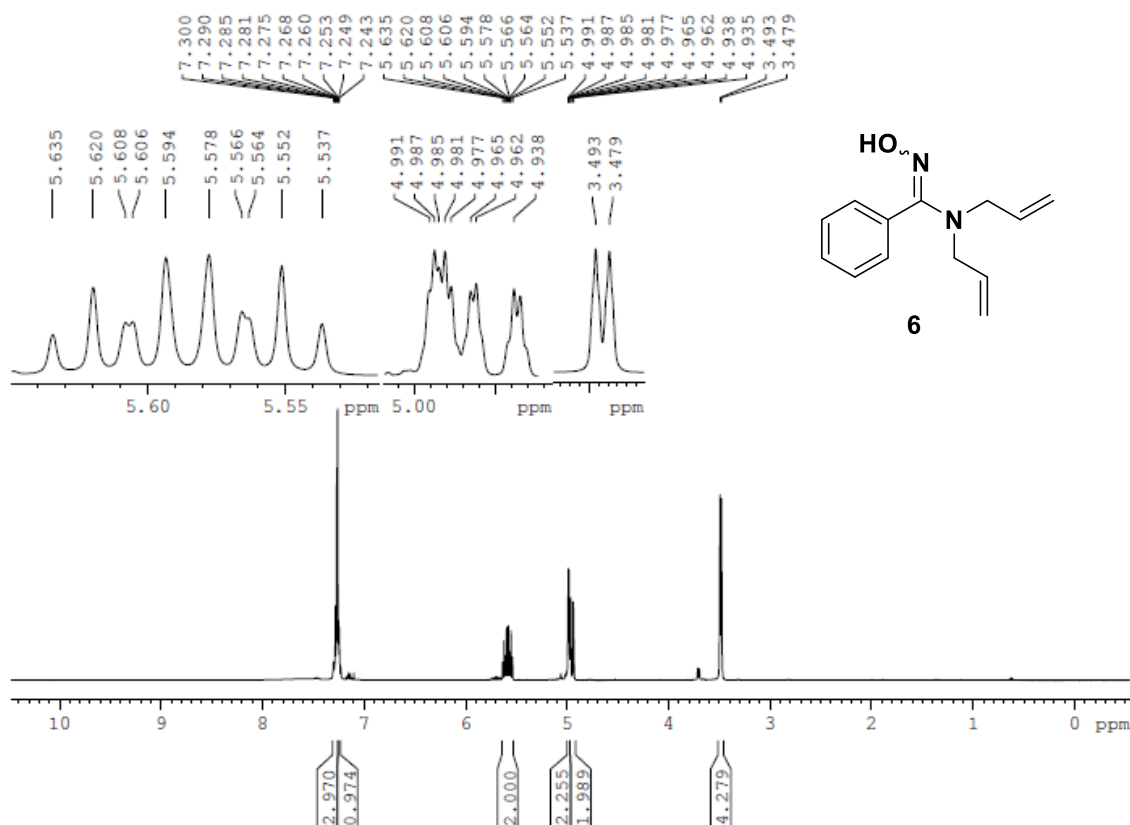
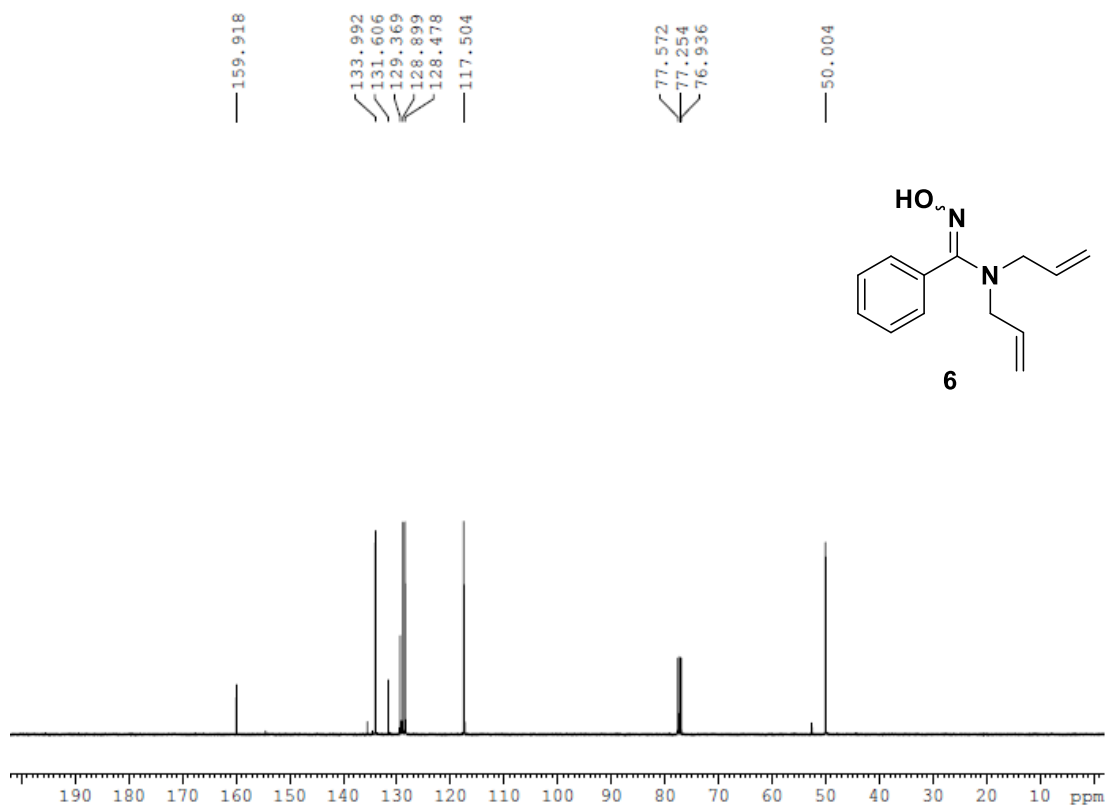
5.6.3  $^1\text{H}$ - and  $^{13}\text{C}$  NMR spectra of synthesized compounds $^1\text{H}$  NMR of compound 1 ( $\text{DMSO}-d_6$ , 300 MHz) $^{13}\text{C}$  NMR of compound 1 ( $\text{DMSO}-d_6$ , 300 MHz)

**<sup>1</sup>H NMR of compound 5 (CDCl<sub>3</sub>, 300 MHz)**



**<sup>13</sup>C NMR of compound 5 (CDCl<sub>3</sub>, 75 MHz)**

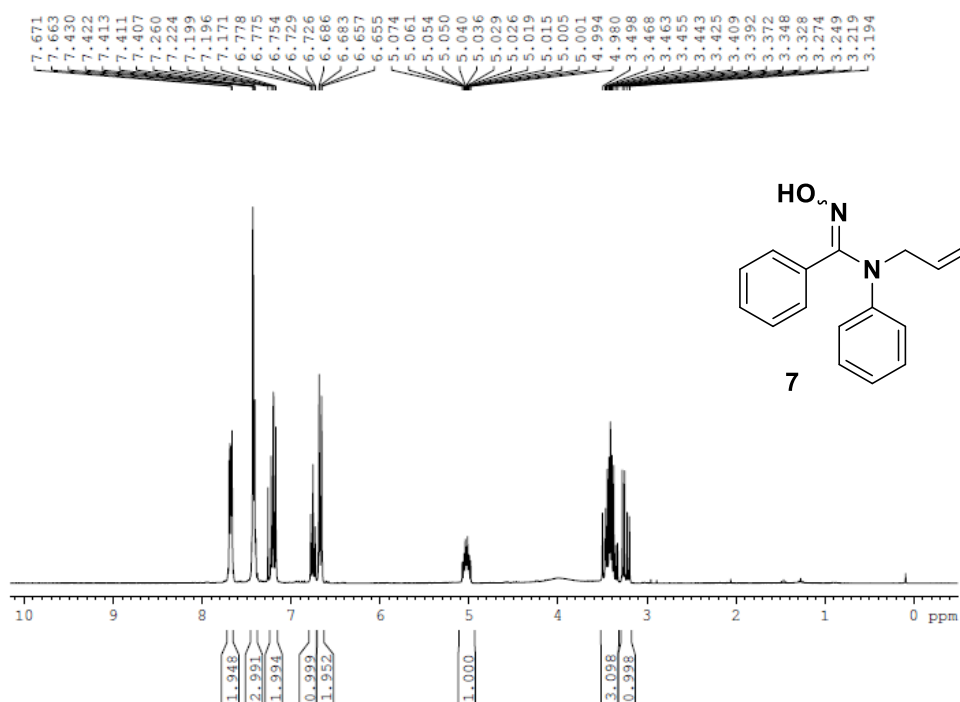


**$^1\text{H}$  NMR of compound 6 ( $\text{CDCl}_3$ , 400 MHz)** **$^{13}\text{C}$  NMR of compound 6 ( $\text{CDCl}_3$ , 100 MHz)**

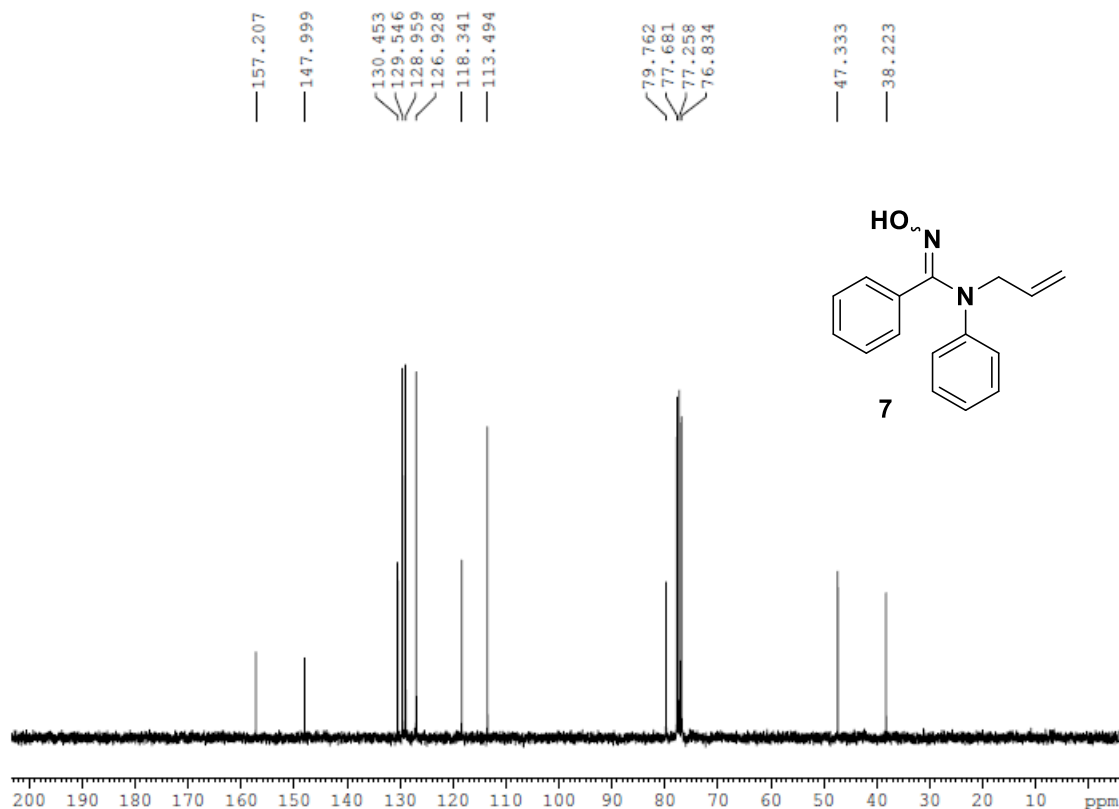


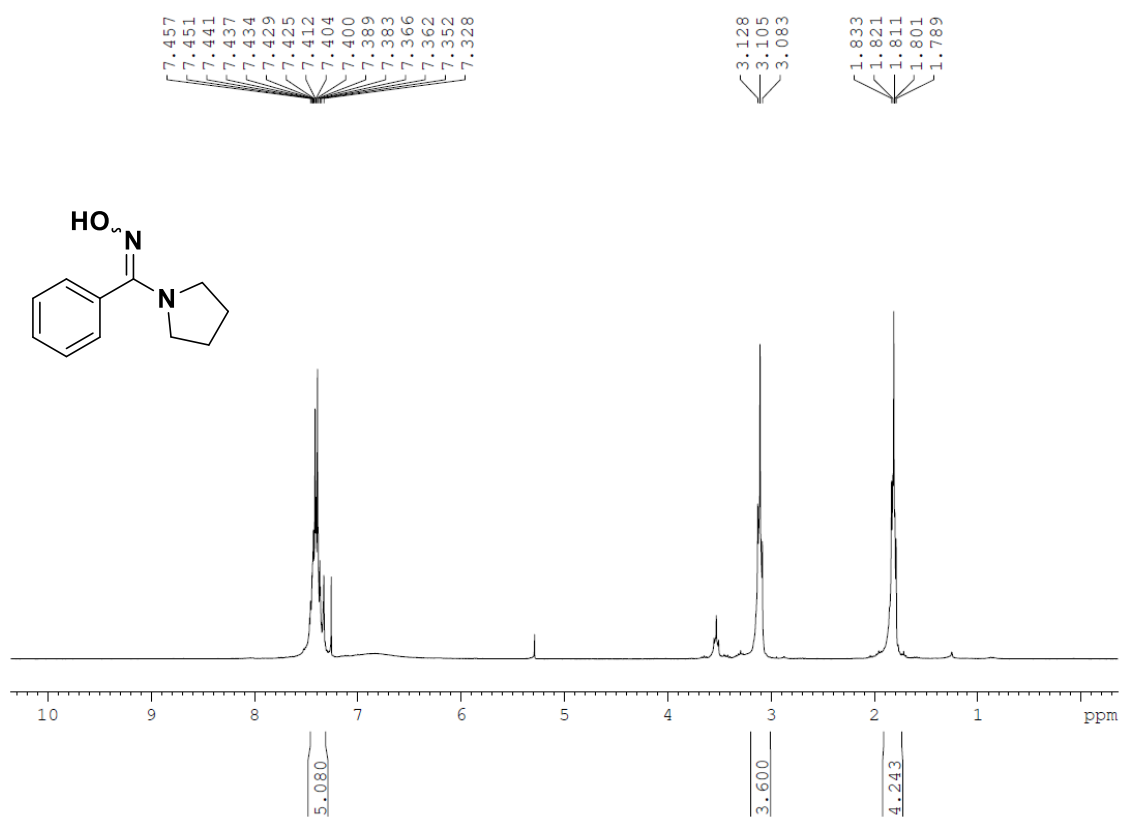
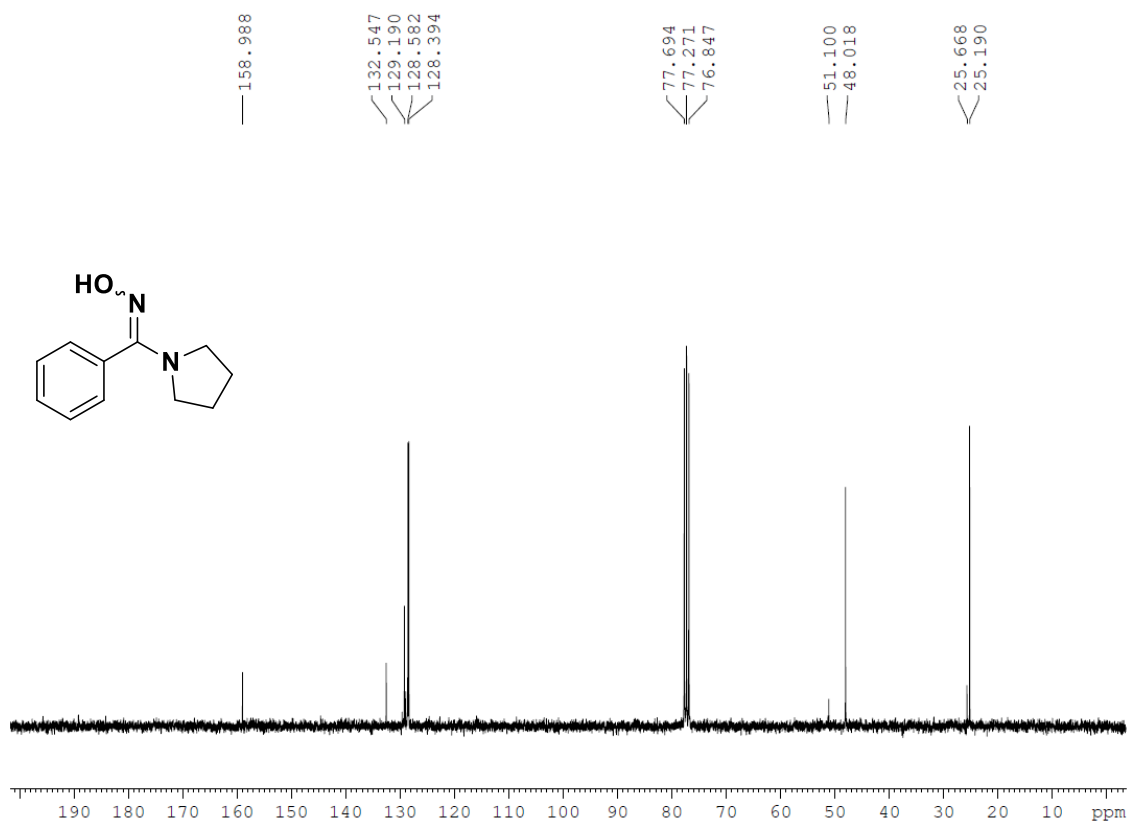
*Attempts Towards the Photochemical Generation of Amidinyl Radicals and Syntheses of Oxadiazole and Quinazolinone Derivatives*

**$^1\text{H}$  NMR of compound 7 ( $\text{CDCl}_3$ , 400 MHz)**

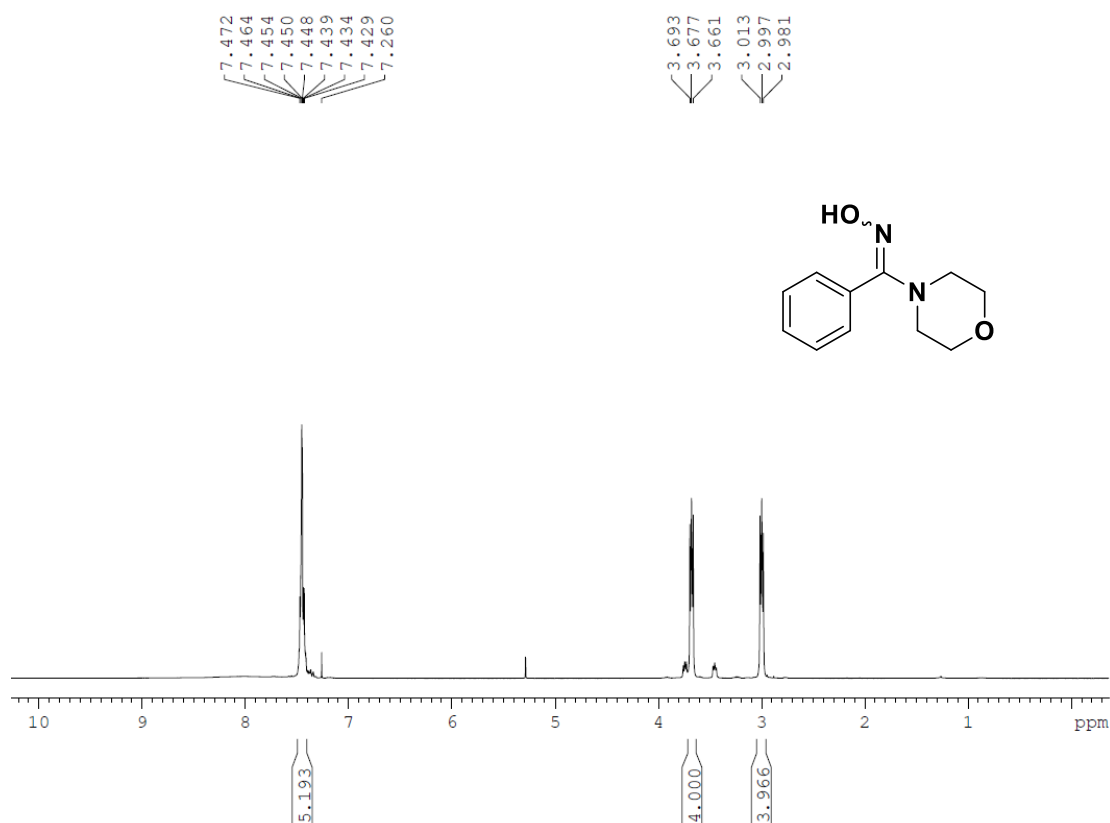


**$^{13}\text{C}$  NMR of compound 7 ( $\text{CDCl}_3$ , 100 MHz)**

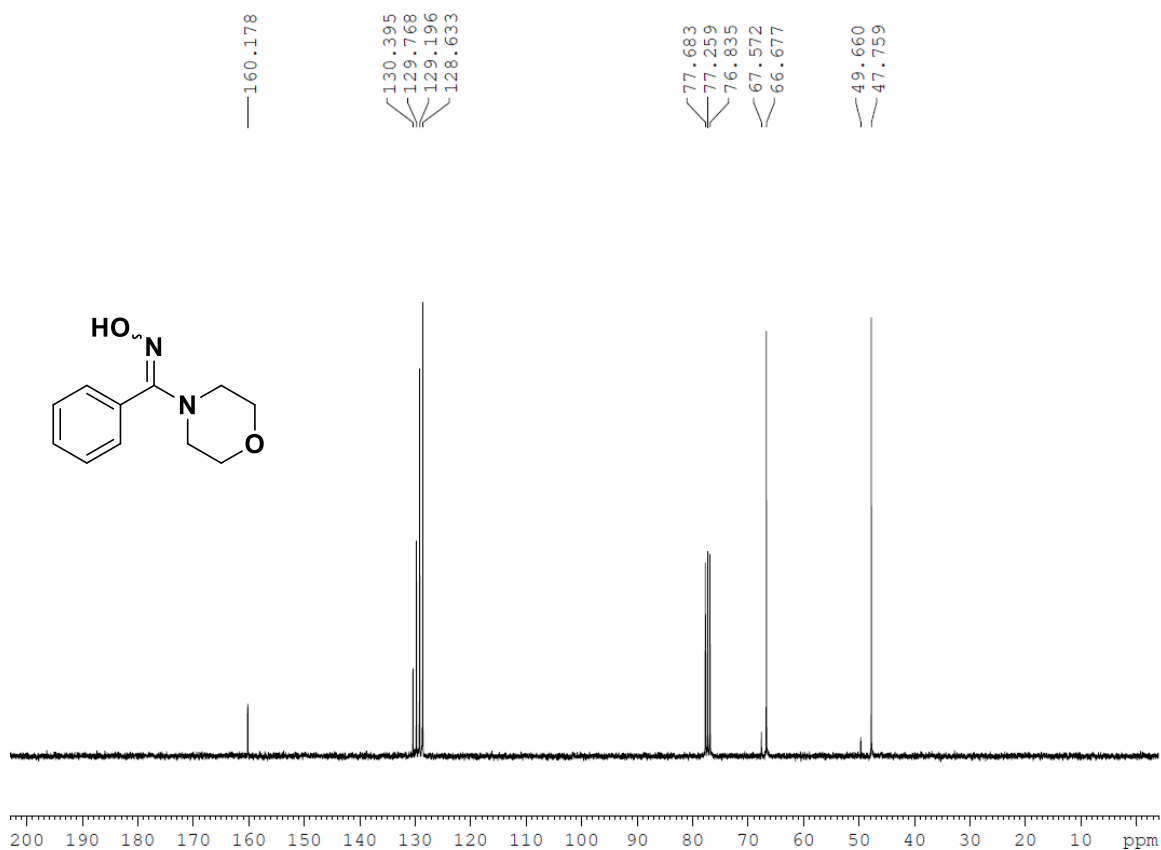


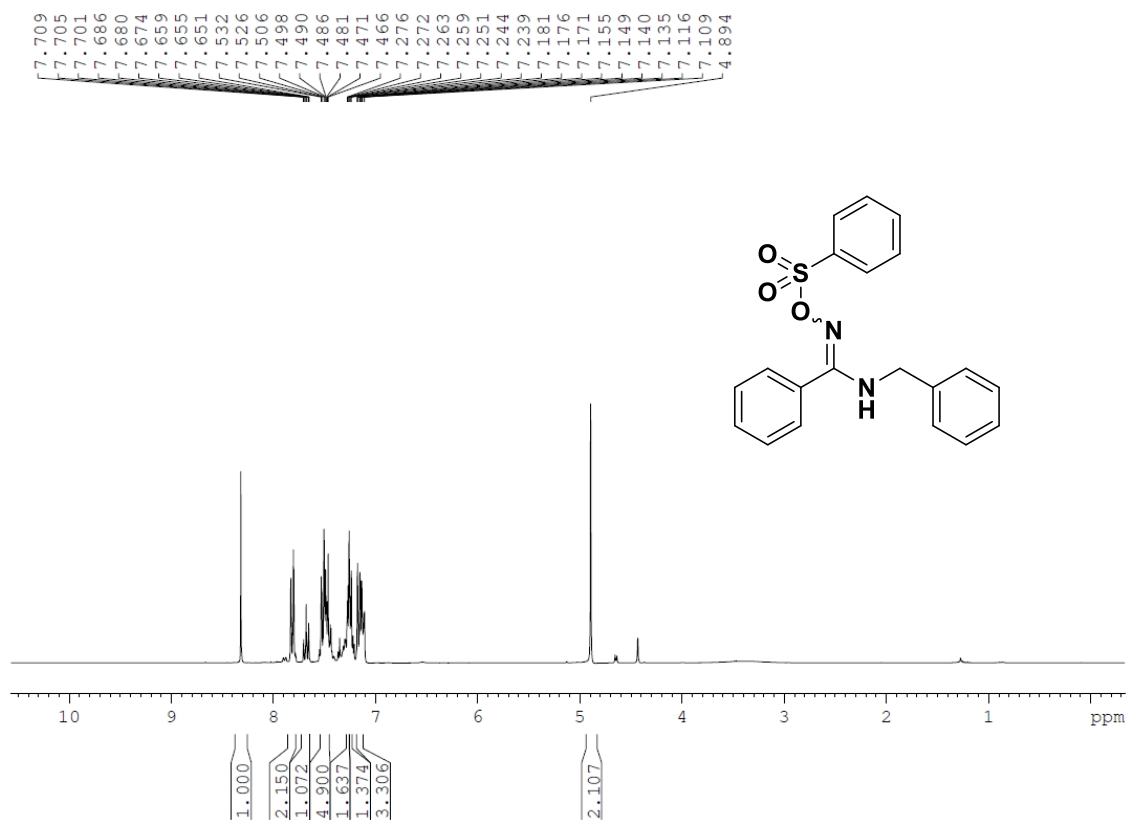
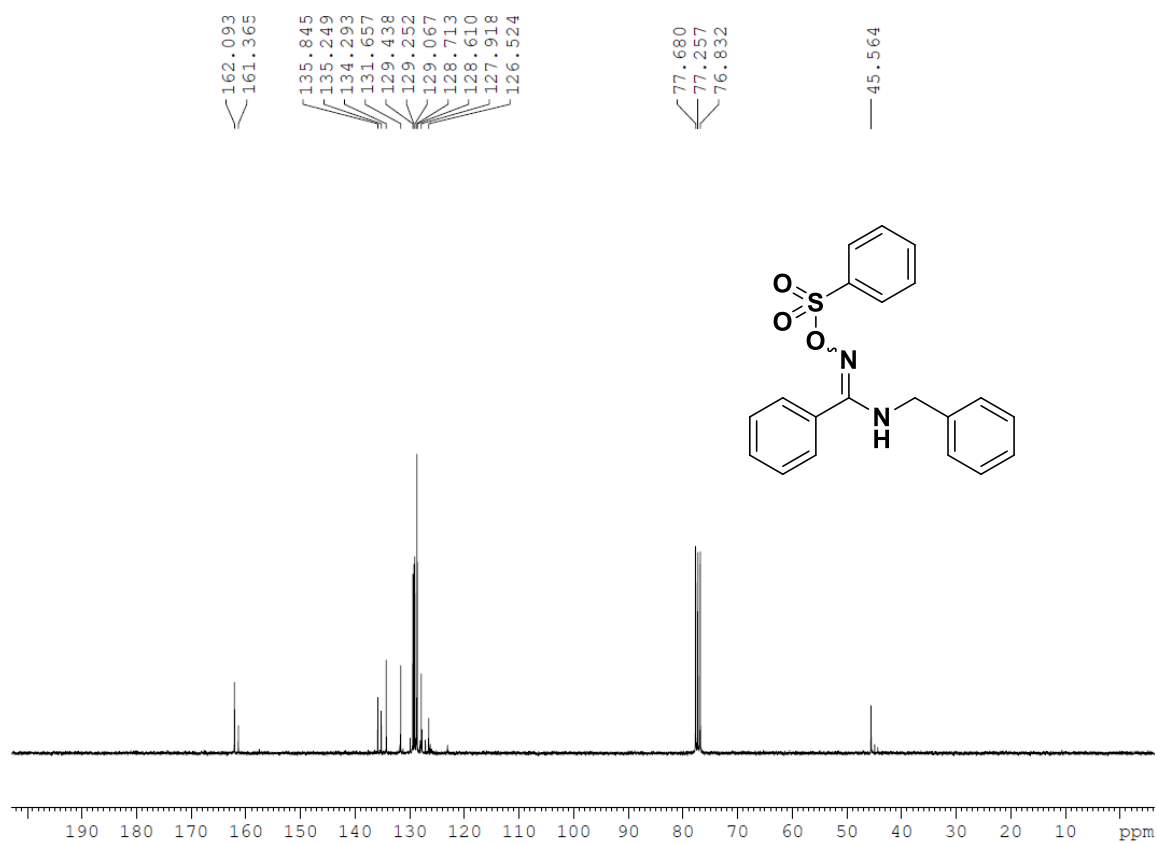
**$^1\text{H}$  NMR of compound 9 ( $\text{CDCl}_3$ , 300 MHz)** **$^{13}\text{C}$  NMR of compound 9 ( $\text{CDCl}_3$ , 75 MHz)**

**<sup>1</sup>H NMR of compound 10 (CDCl<sub>3</sub>, 300 MHz)**

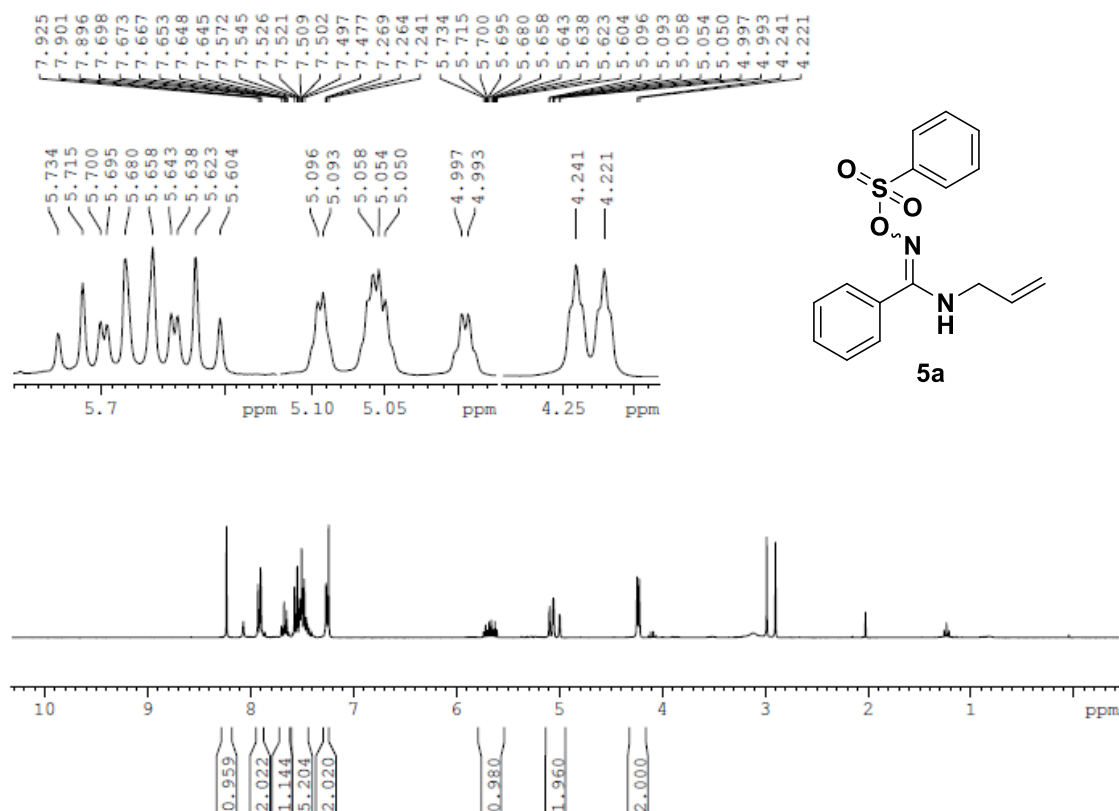


**<sup>13</sup>C NMR of compound 10 (CDCl<sub>3</sub>, 75 MHz)**

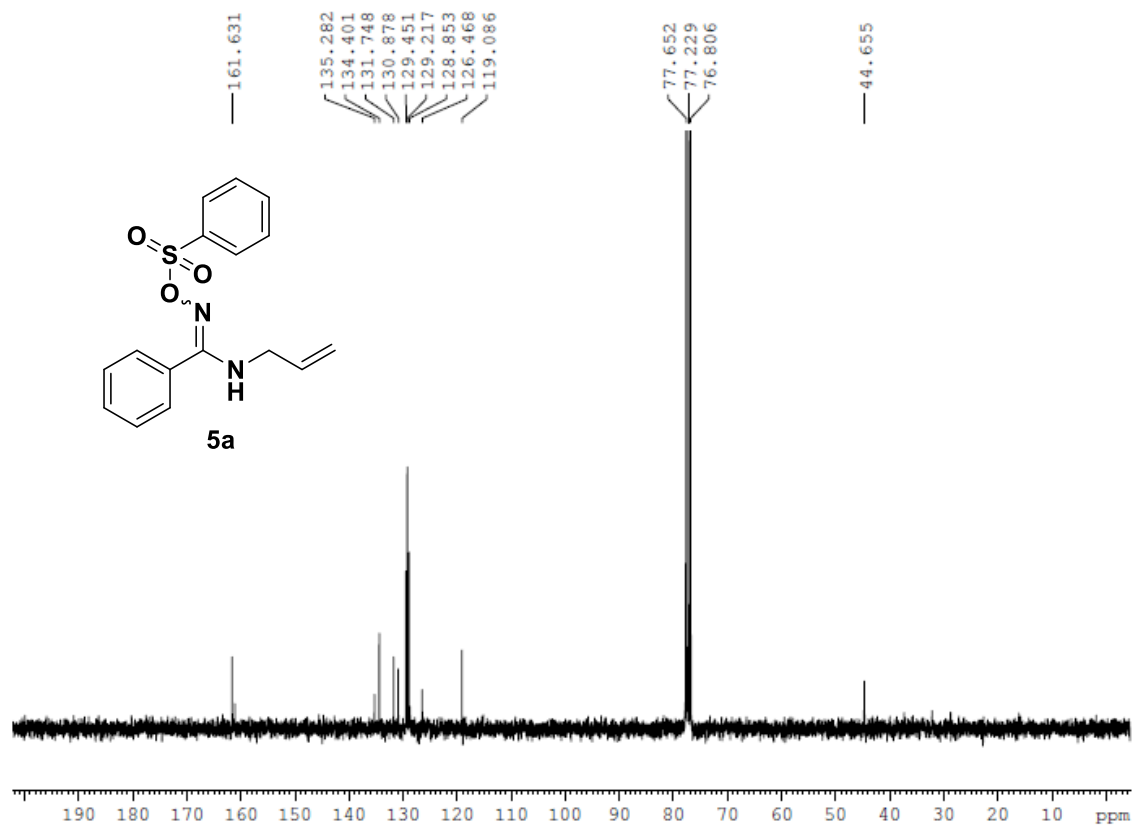


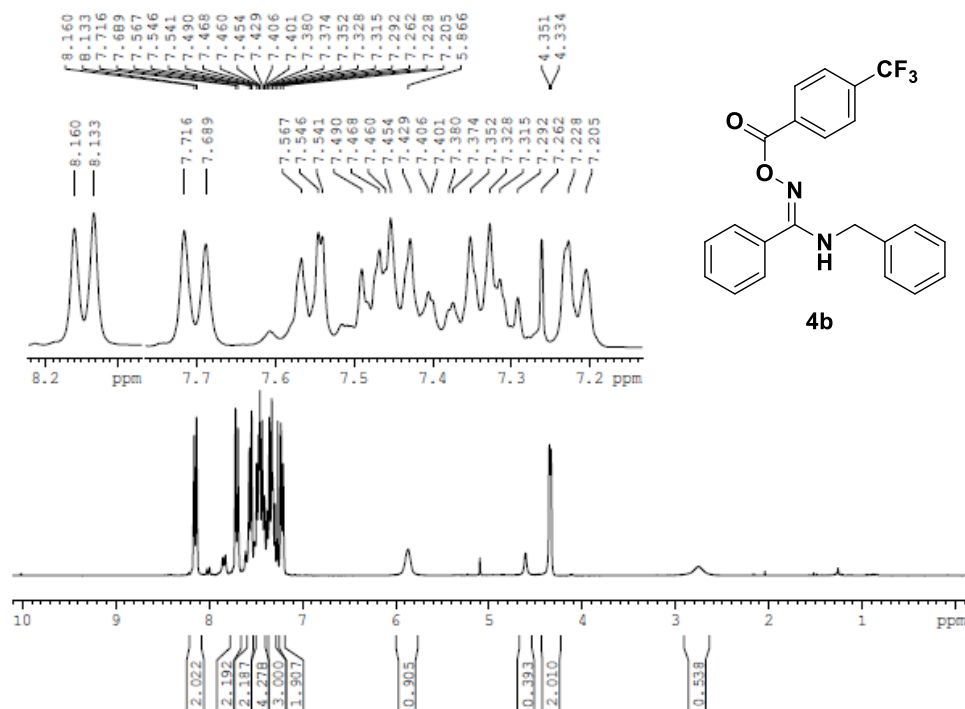
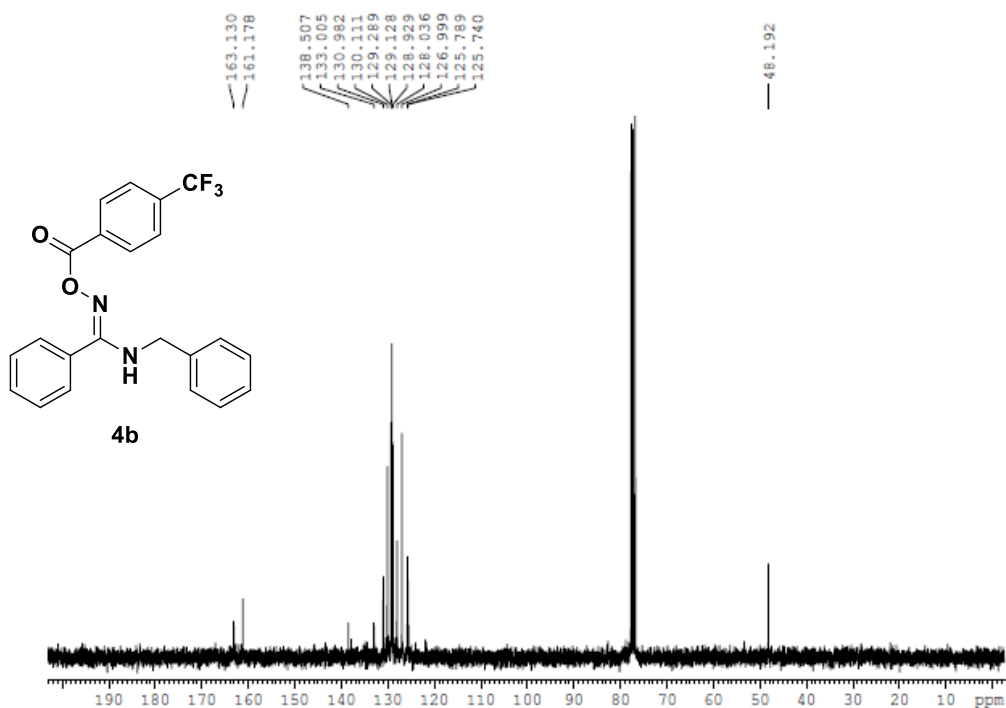
**$^1\text{H}$  NMR of compound 4a ( $\text{CDCl}_3$ , 300 MHz)** **$^{13}\text{C}$  NMR of compound 4a ( $\text{CDCl}_3$ , 75 MHz)**

**<sup>1</sup>H spectra of compound 5a (CDCl<sub>3</sub>, 300 MHz)**



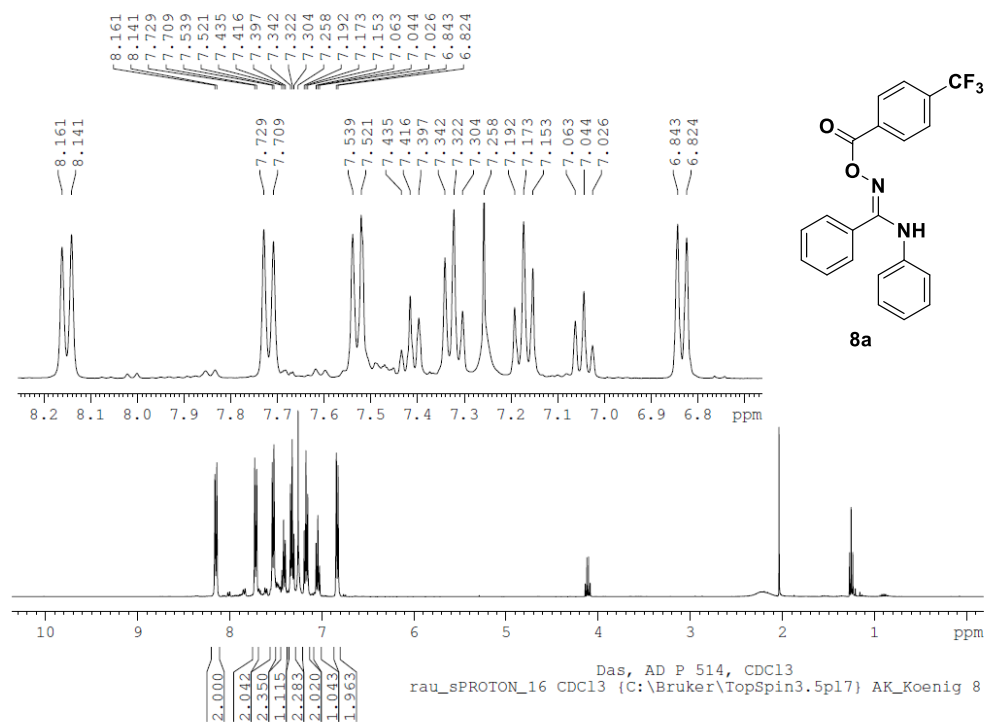
**<sup>13</sup>C NMR of compound 5a (CDCl<sub>3</sub>, 75 MHz)**



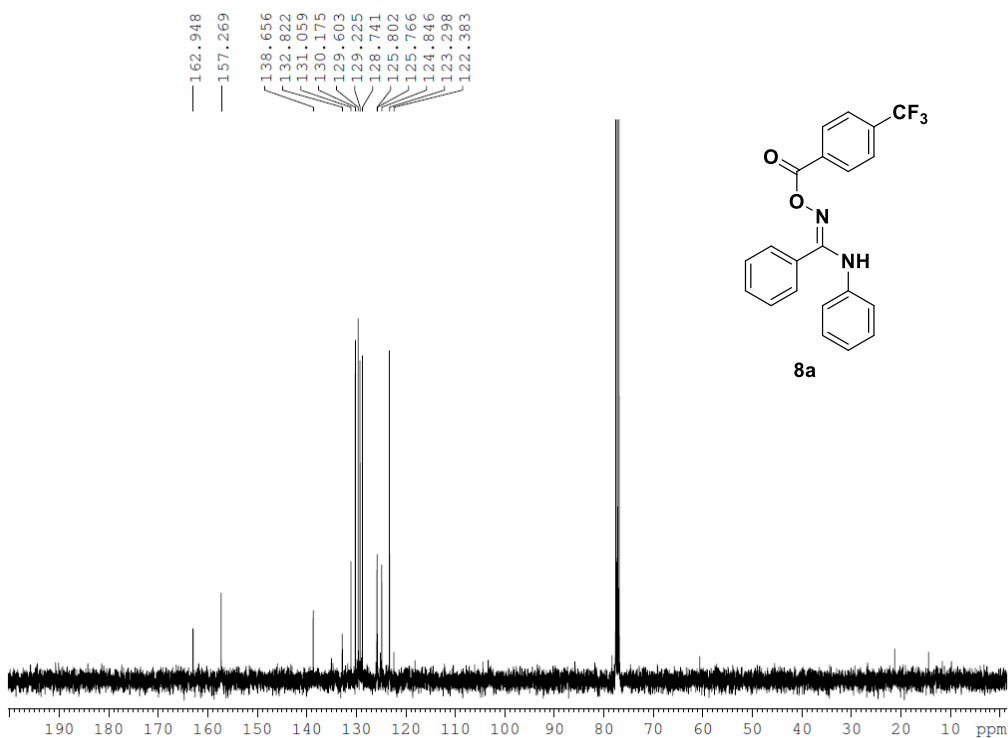
<sup>1</sup>H spectra of compound 4b (CDCl<sub>3</sub>, 300 MHz)<sup>13</sup>C NMR of compound 4b (CDCl<sub>3</sub>, 75 MHz)

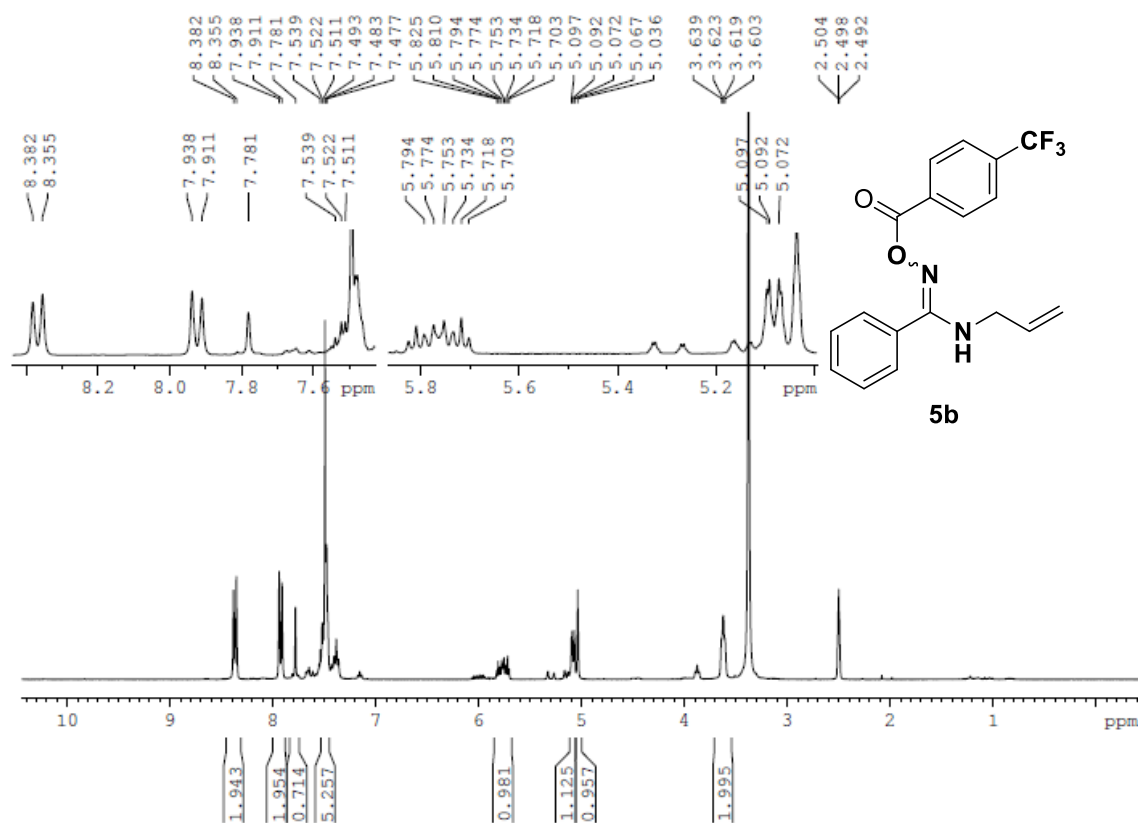
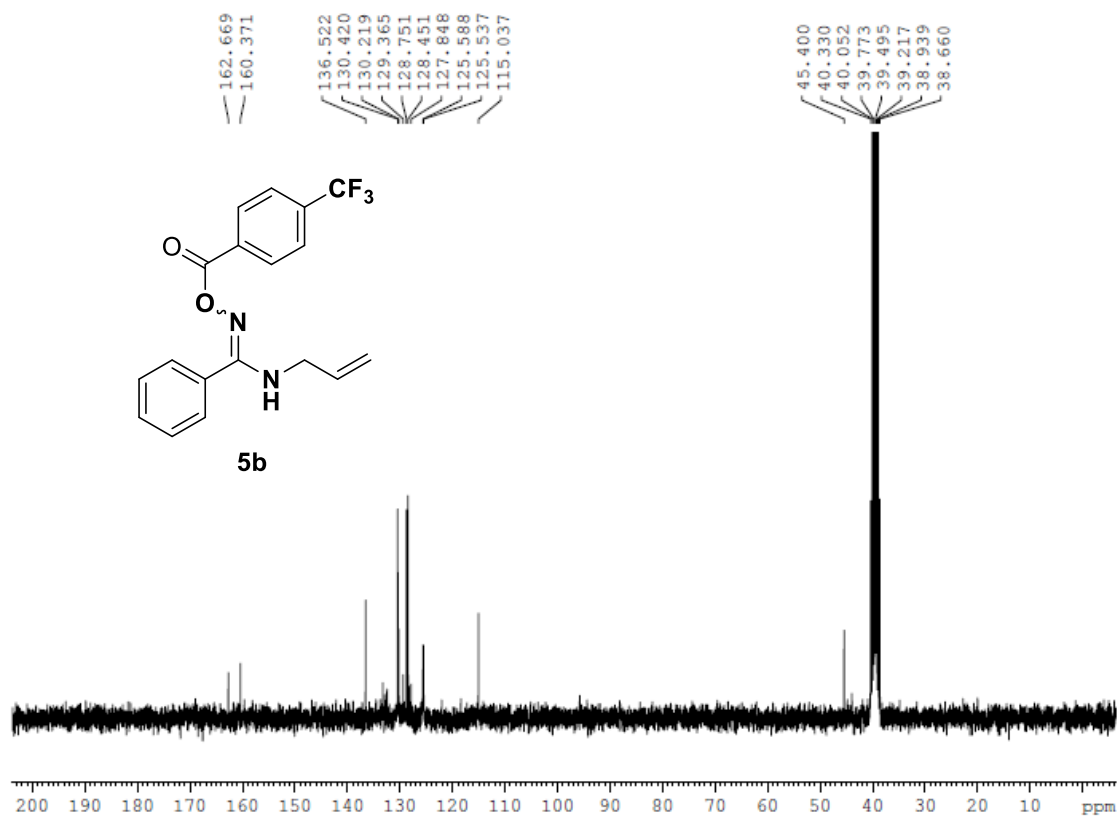
**Attempts Towards the Photochemical Generation of Amidinyl Radicals and Syntheses of Oxadiazole and Quinazolinone Derivatives**

**<sup>1</sup>H NMR of compound 8a (CDCl<sub>3</sub>, 300 MHz)**



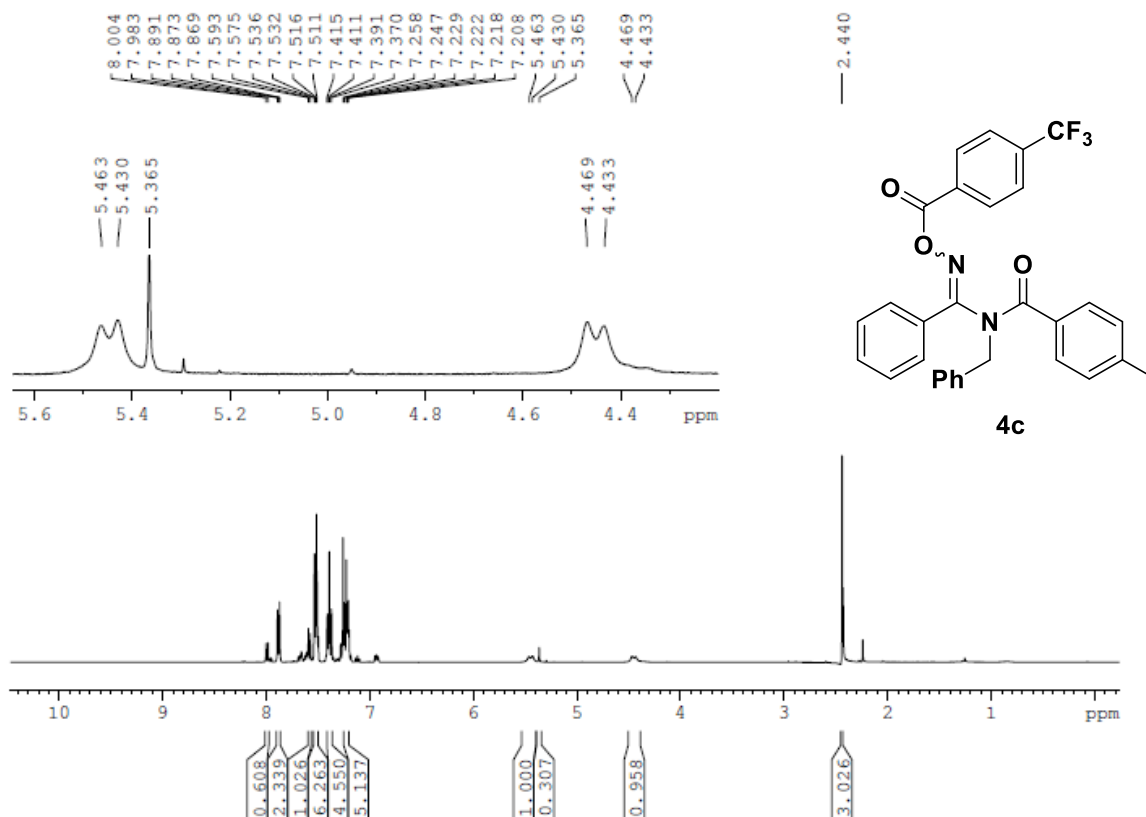
**<sup>13</sup>C NMR of compound 8a (CDCl<sub>3</sub>, 75 MHz)**



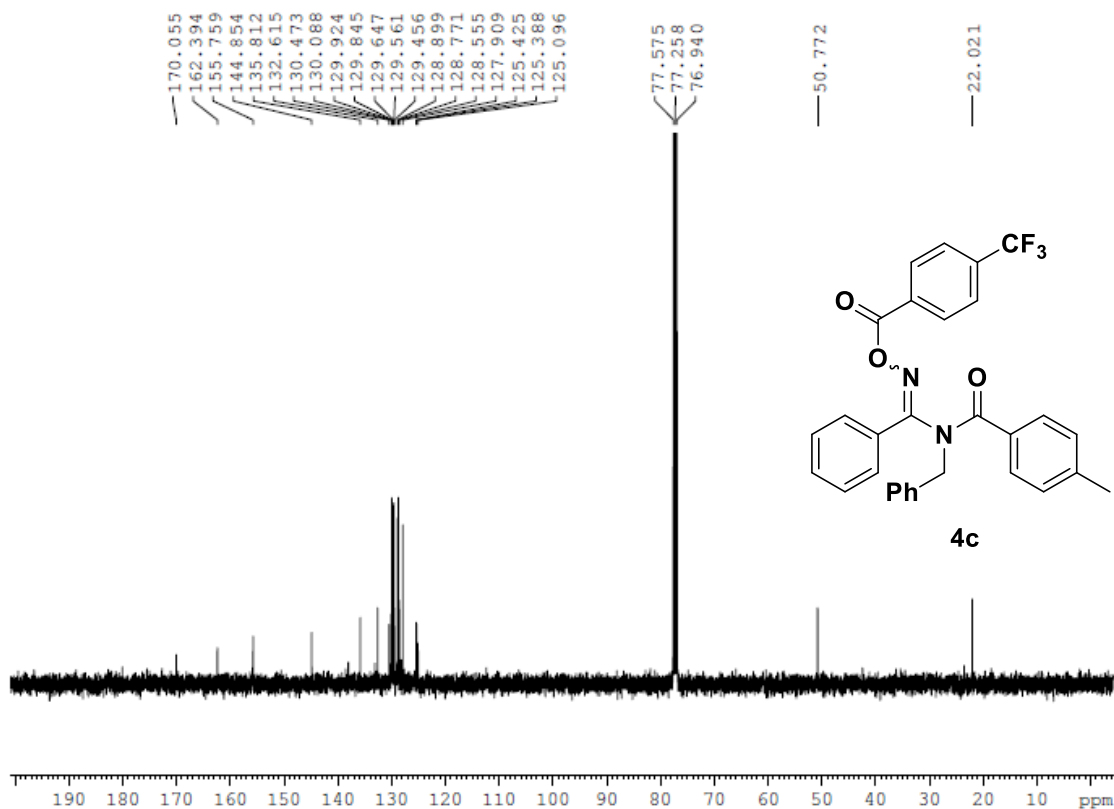
**<sup>1</sup>H NMR of compound 5b (DMSO-*d*<sub>6</sub>, 300 MHz)****<sup>13</sup>C NMR of compound 5b (DMSO-*d*<sub>6</sub>, 75 MHz)**

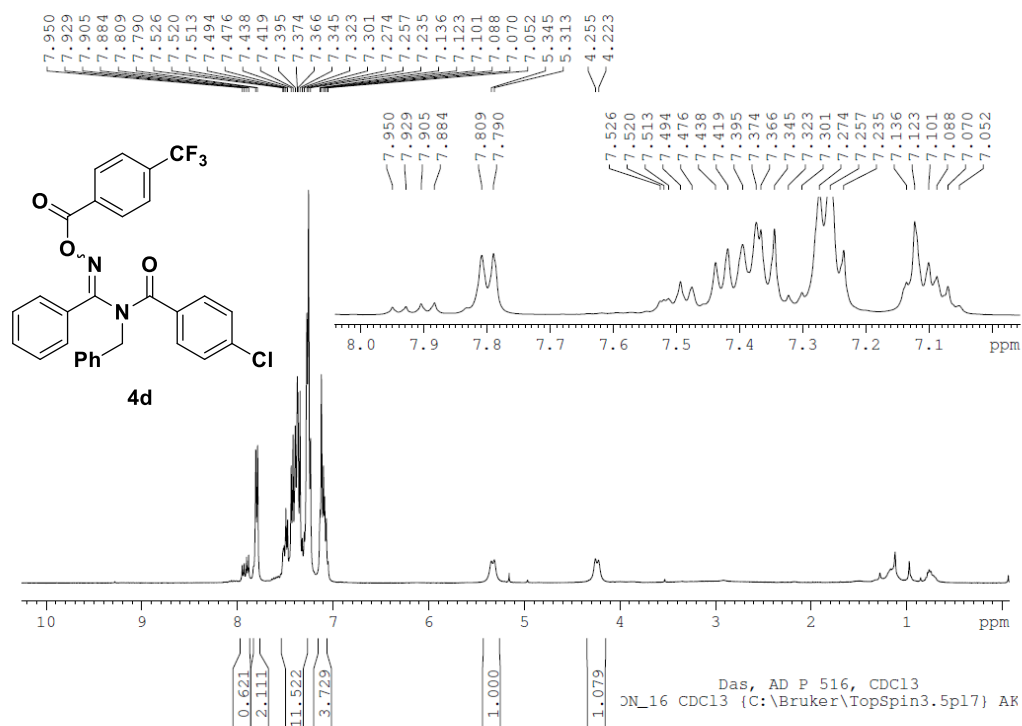
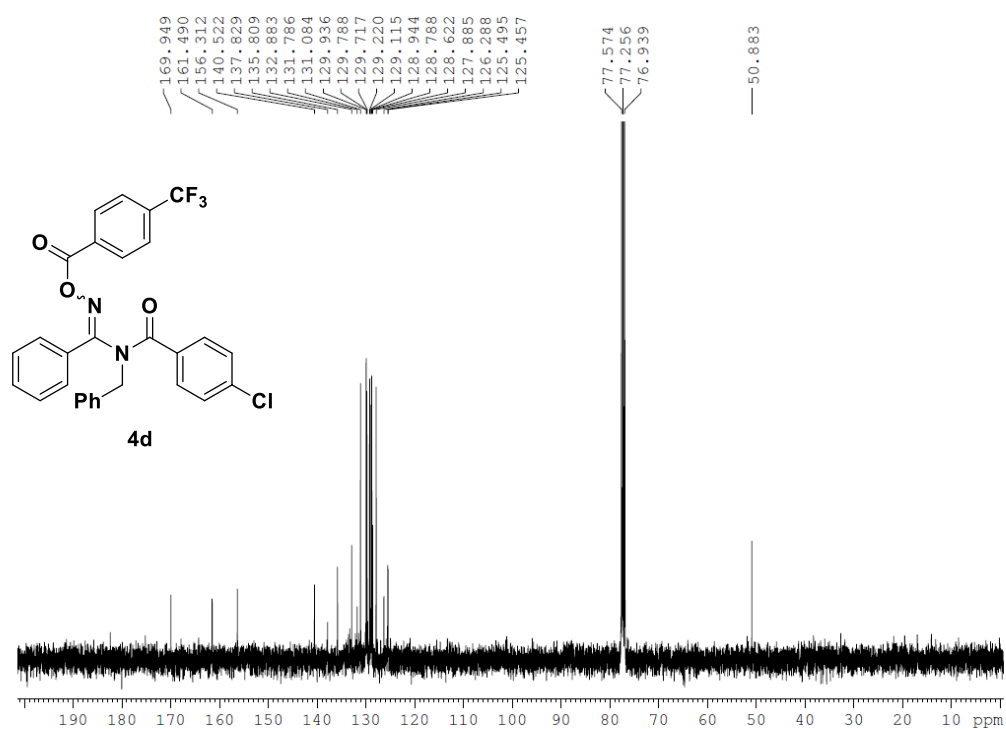


**$^1\text{H}$  NMR of compound 4c ( $\text{CDCl}_3$ , 300 MHz)**



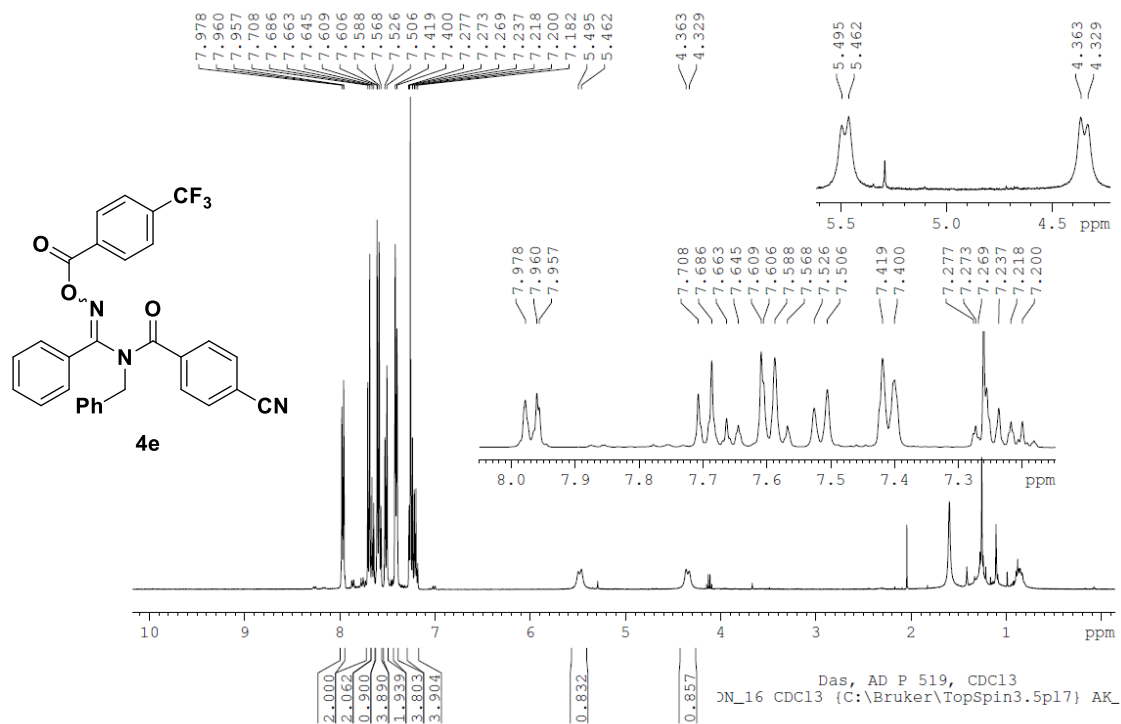
**$^{13}\text{C}$  NMR of compound 4c ( $\text{CDCl}_3$ , 75 MHz)**



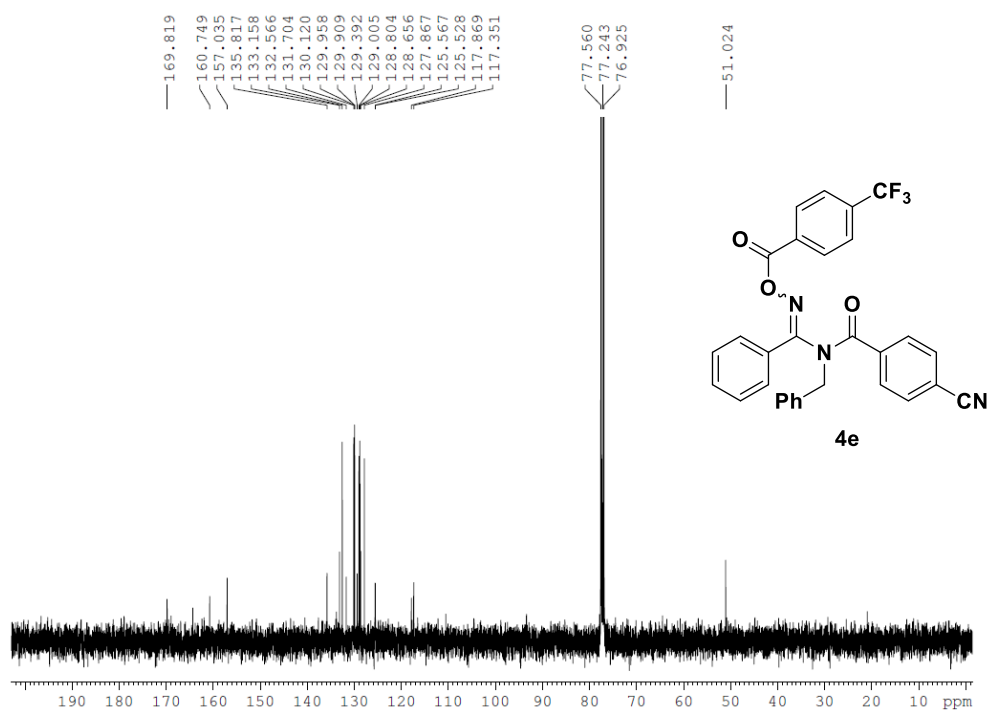
**$^1\text{H}$  NMR of compound 4d ( $\text{CDCl}_3$ , 300 MHz)** **$^{13}\text{C}$  NMR of compound 4d ( $\text{CDCl}_3$ , 75 MHz)**

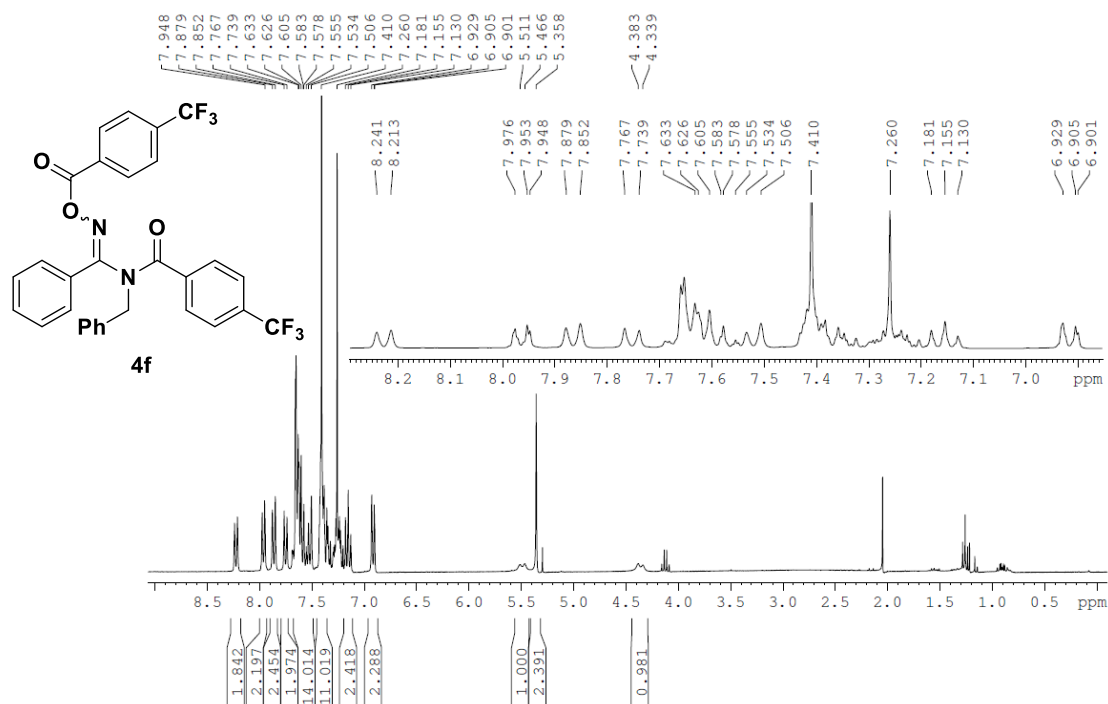
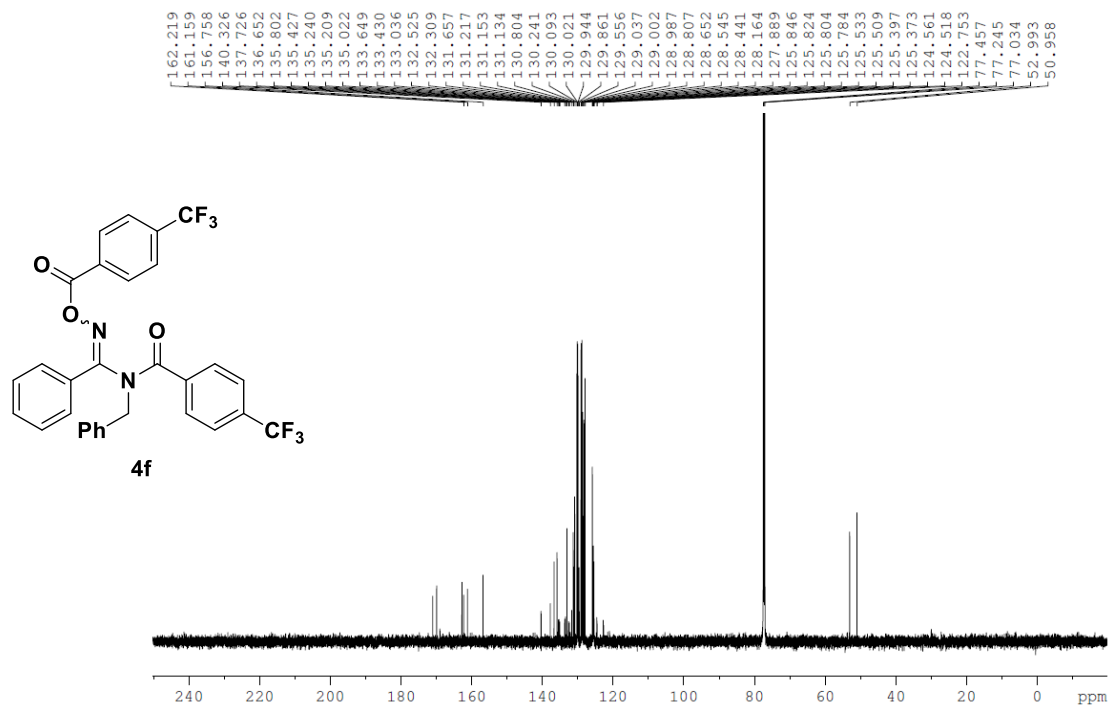
**Attempts Towards the Photochemical Generation of Amidinyl Radicals and Syntheses of Oxadiazole and Quinazolinone Derivatives**

**<sup>1</sup>H NMR of compound 4e (CDCl<sub>3</sub>, 300 MHz)**

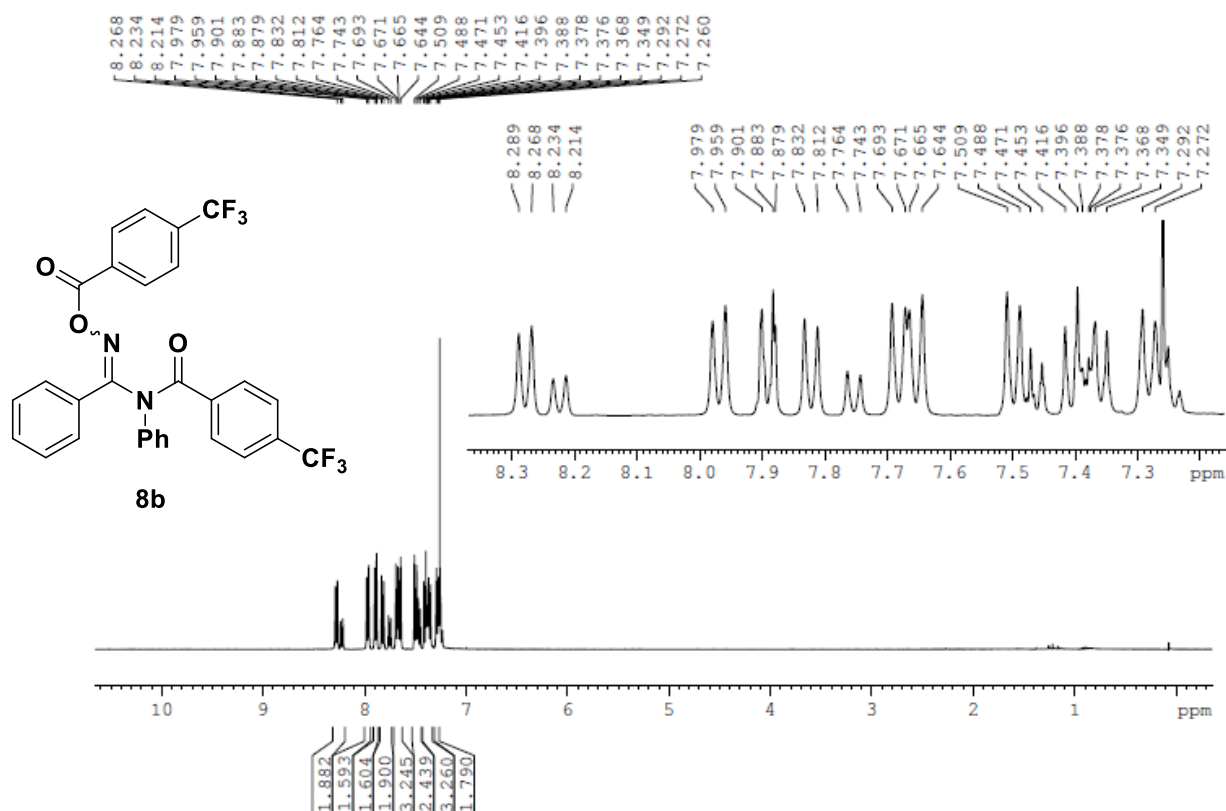


**<sup>13</sup>C NMR of compound 4e (CDCl<sub>3</sub>, 75 MHz)**

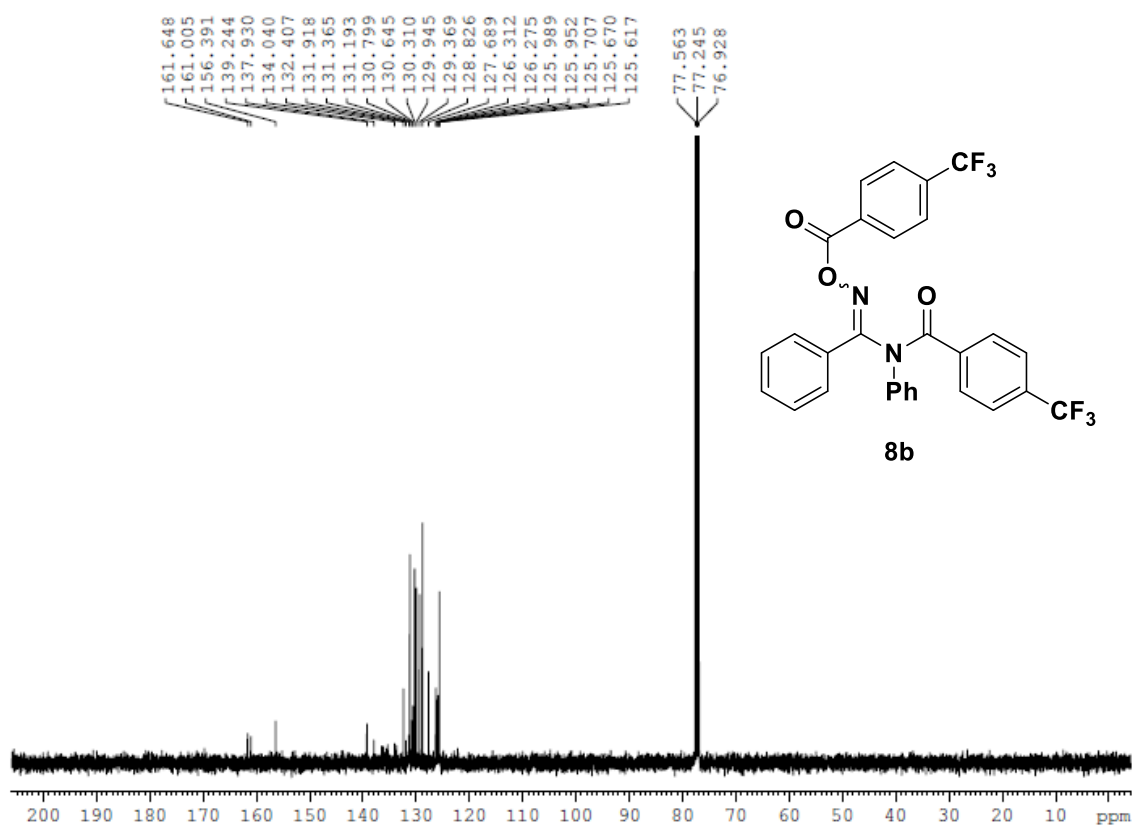


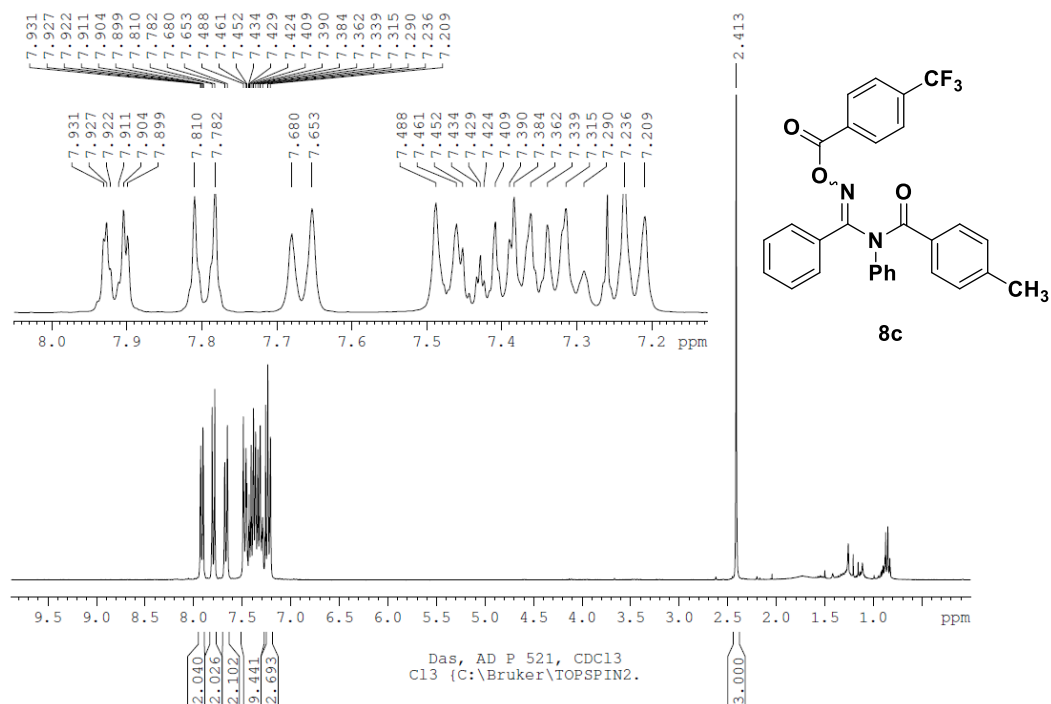
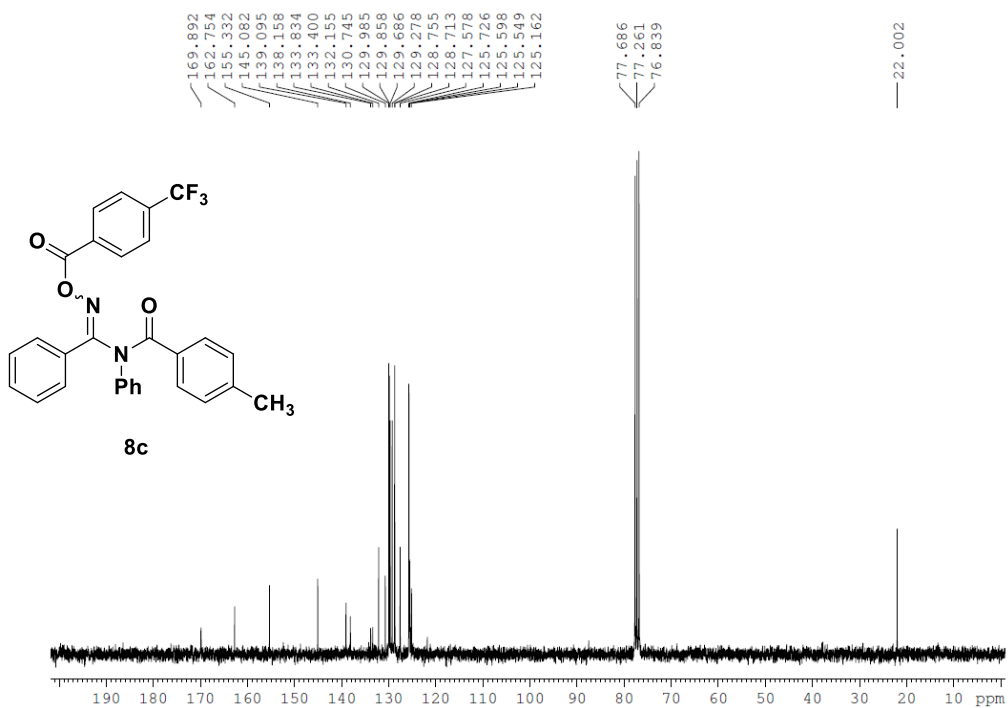
**$^1\text{H}$  NMR of compound 4f ( $\text{CDCl}_3$ , 300 MHz)** **$^{13}\text{C}$  NMR of compound 4f ( $\text{CDCl}_3$ , 75 MHz)**

**<sup>1</sup>H NMR of compound 8b (CDCl<sub>3</sub>, 300 MHz)**



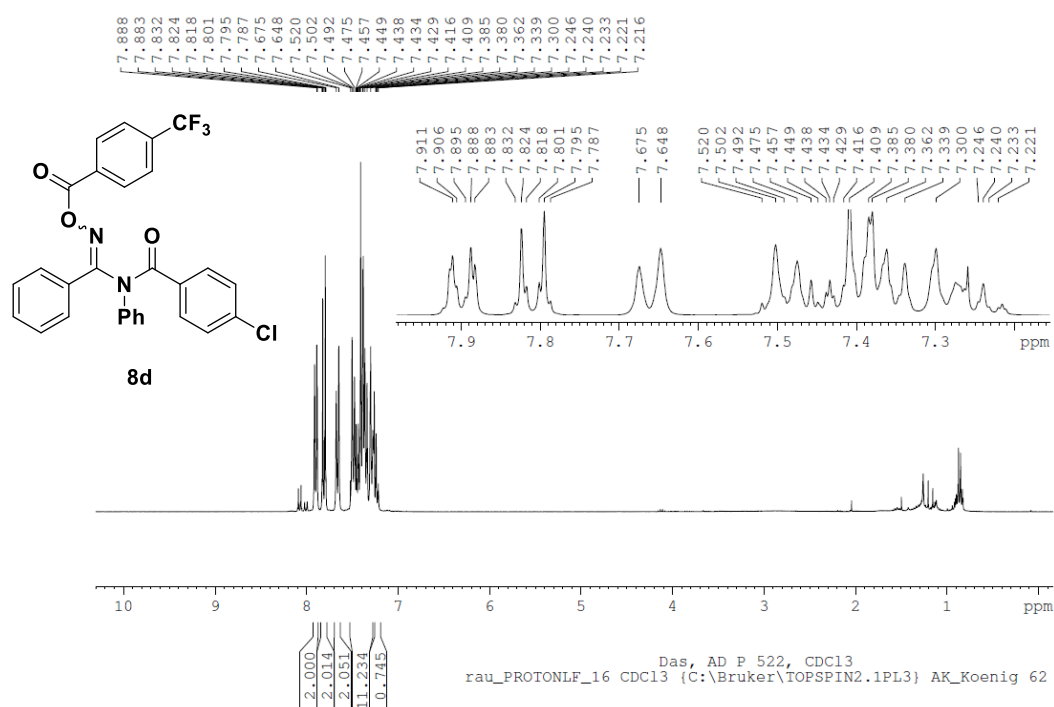
**<sup>13</sup>C NMR of compound 8b (CDCl<sub>3</sub>, 75 MHz)**



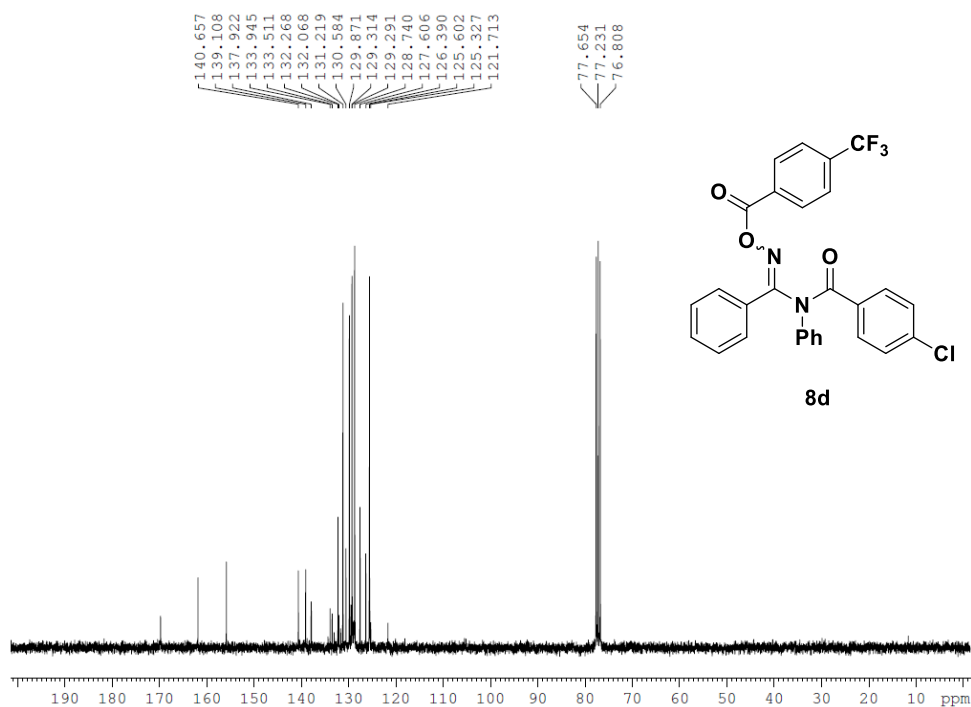
**$^1\text{H}$  NMR of compound 8c ( $\text{CDCl}_3$ , 300 MHz)** **$^{13}\text{C}$  NMR of compound 8c ( $\text{CDCl}_3$ , 75 MHz)**

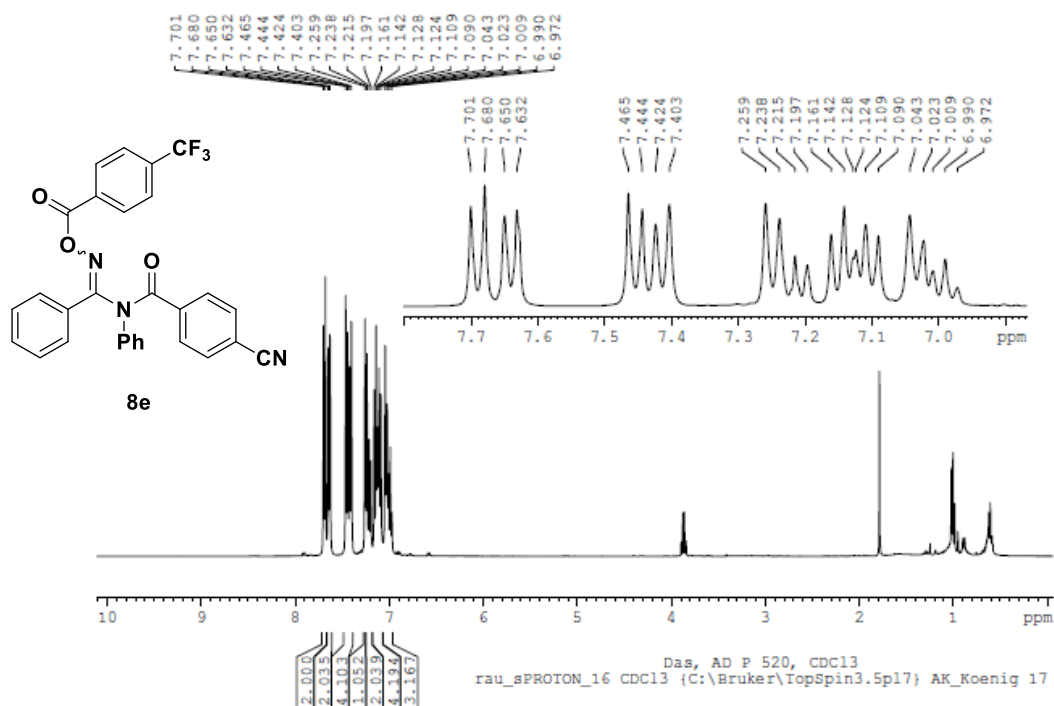
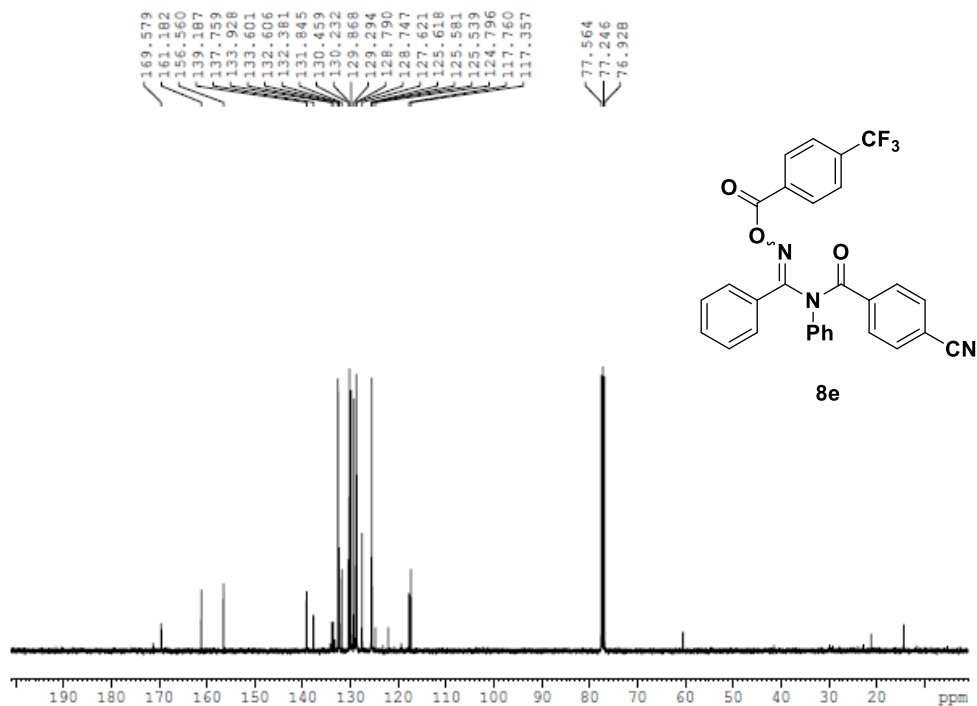
**Attempts Towards the Photochemical Generation of Amidinyl Radicals and Syntheses of Oxadiazole and Quinazolinone Derivatives**

**<sup>1</sup>H NMR of compound 8d (CDCl<sub>3</sub>, 300 MHz)**



**<sup>13</sup>C NMR of compound 8d (CDCl<sub>3</sub>, 75 MHz)**

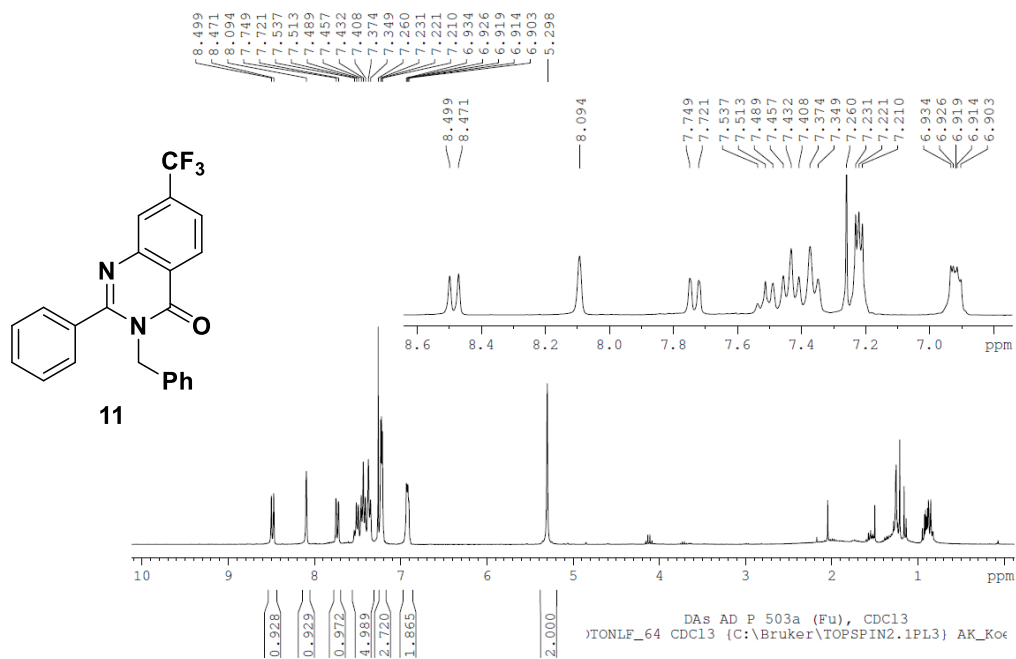


**$^1\text{H}$  NMR of compound 8e ( $\text{CDCl}_3$ , 300 MHz)** **$^{13}\text{C}$  NMR of compound 8e ( $\text{CDCl}_3$ , 75 MHz)**

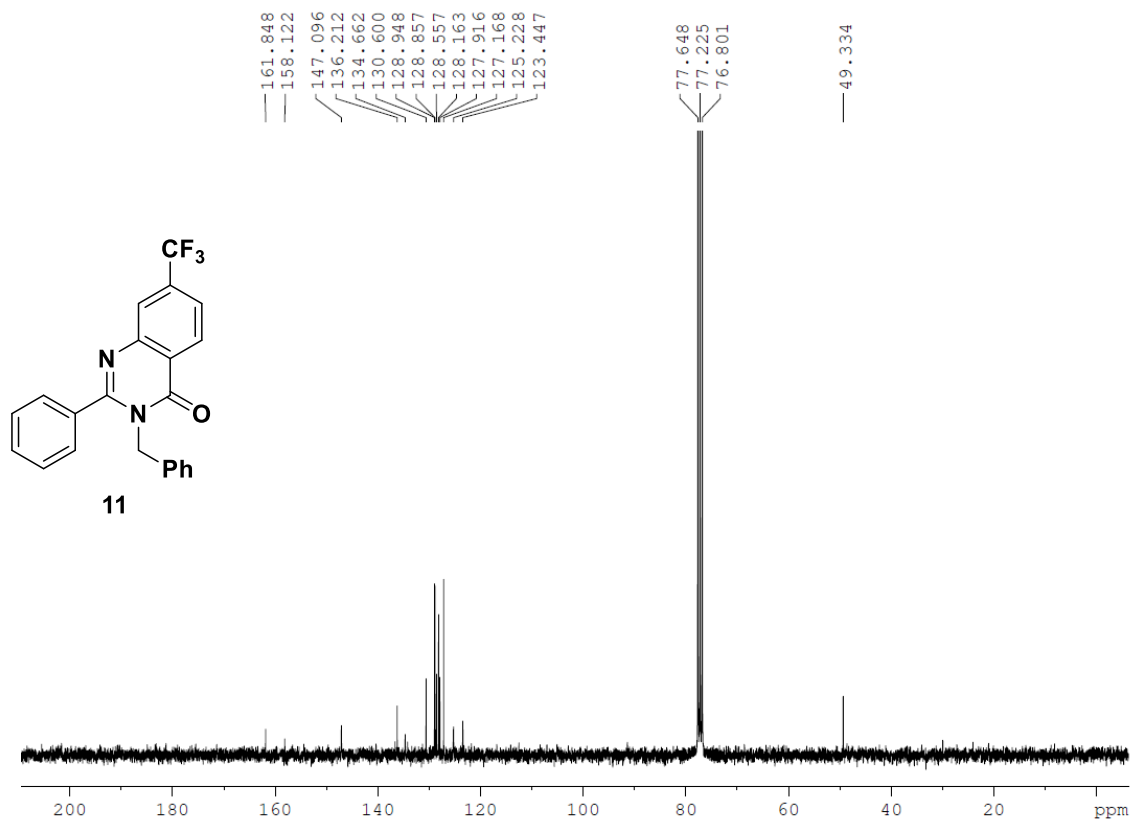


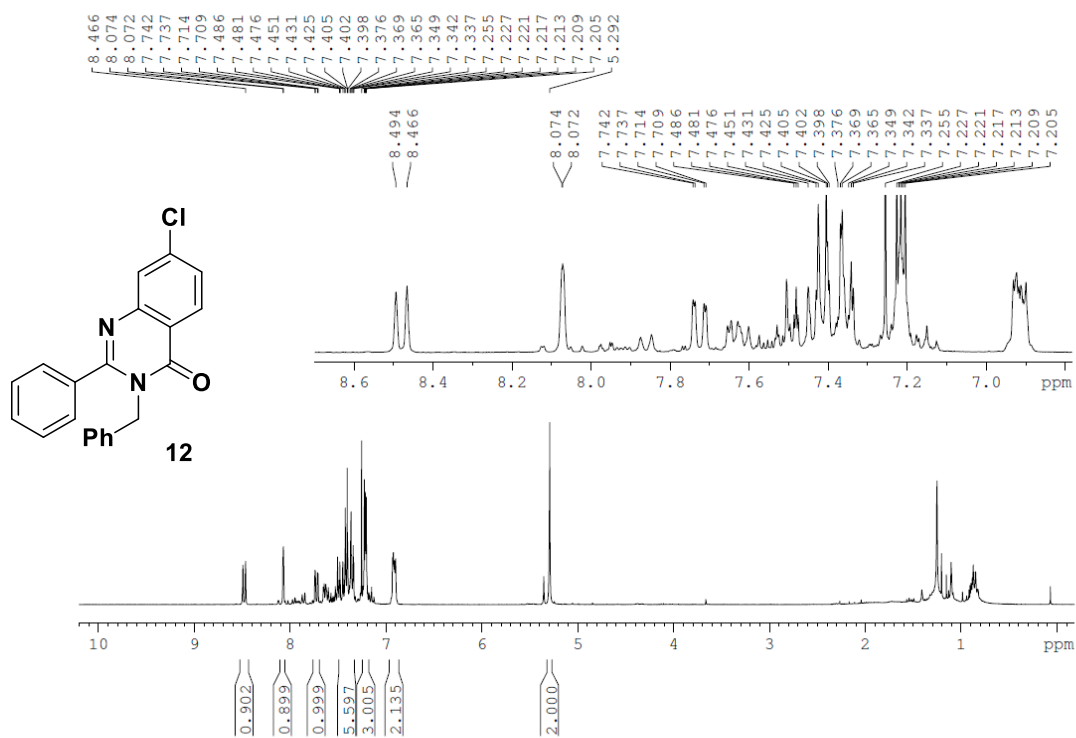
*Attempts Towards the Photochemical Generation of Amidinyl Radicals and Syntheses of Oxadiazole and Quinazolinone Derivatives*

**<sup>1</sup>H NMR of compound 11 (CDCl<sub>3</sub>, 300 MHz)**



**<sup>13</sup>C NMR of compound 11 (CDCl<sub>3</sub>, 75 MHz)**



$^1\text{H}$  NMR of compound 12 ( $\text{CDCl}_3$ , 300 MHz)

## 5.7 References

1. G. Evano, N. Blanchard, M. Toumi, *Chem. Rev.* **2008**, *108*, 3054-3131.
2. P. R. Castillo, S. L. Buchwald, *Chem. Rev.* **2016**, *116*, 12564-12649.
3. S. Z. Zard, *Chem. Soc. Rev.* **2008**, *37*, 1603-1618.
4. M. E. Wolff, *Chem. Rev.* **1963**, *63*, 55-64.
5. H. Wieland, *Liebigs Ann. Chem.* **1911**, *381*, 200-216.
6. J. R. Chen, X. Q. Hu, L. Q. Lu, W. J. Xiao, *Chem. Soc. Rev.* **2016**, *45*, 2044-2056.
7. D. Gennet, S. Z. Zard, H. Zhang, *Chem. Commun.* **2003**, 1870-1871.
8. D. Gennet, S. Z. Zard, H. Zhang, *Chem. Commun.* **2003**, 1870-1871.
9. H. Chen, S. Sanjaya, Y. F. Wang, S. Chiba, *Org. Lett.* **2013**, *15*, 215-217.
10. H. Chen, S. Chiba, *Org. Biomol. Chem.* **2014**, *12*, 42-46.
11. H. B. Zhao, Z. W. Hou, Z. J. Liu, Z. F. Zhou, J. Song, H. C. Xu, *Angew. Chem. Int. Ed.* **2017**, *56*, 587-590.
12. J. R. B. Gomes, M. D. M. C. Ribeiro da Silva, M. A. V. Ribeiro da Silva, *J. Phys. Chem. A* **2004**, *108*, 2119-2130.
13. I. Doulou, C. Kontogiorgis, A. E. Koumbis, E. Evgenidou, D. H. –Litina, K. C. Fylaktakidou, *Eur. J. Med. Chem.* **2014**, *80*, 145-153.
14. C. G. S. Lima, T. M. Lima, M. Duarte, I. D. Jurberg, M. W. Paixao, *ACS. Catal.* **2016**, *6*, 1389-1407.
15. Y. Du, R. M. Pearson, C. H. Lim, S. M. Sartor, M. D. Ryan, H. Yang, N. H. Damrauer, G. M. Miyake, *Chem. Eur. J.* **2017**, *23*, 10962-10968.
16. R. Saha, O. Tanwar, A. Marella, M. M. Alam, M. Akhter, *Mini-Rev. Med. Chem.* **2013**, *13*, 1027-1046.
17. W. Wang, H. Xu, Y. Xu, T. Ding, W. Zhang, Y. Ren, H. Chang, *Org. Biomol. Chem.* **2016**, *14*, 9814-9822.
18. M. Okimoto, Y. Takahashi, *Bull. Chem. Soc. Jpn.* **2003**, *76*, 427-428.
19. S. Kandre, P. R. Bhagat, R. Sharma, A. Gupte, *Tetrahedron. Lett.* **2013**, *54*, 3526-3529.
20. P. D. Parker, J. G. Pierce, *Synthesis.* **2016**, *48*, 1902-1909.
21. N. Öcal, I. Erden, *Tetrahedron Lett.* **2001**, *42*, 4765-4767.
22. P. Wang, H. Li, H. Zeng, S. Kang, H. Wang, *Acta. Cryst.* **2007**, *E63*, o4151.
23. X. Yu, K. Chen, F. Yang, S. Zha, J. Zhu, *Org. Lett.* **2016**, *18*, 5412-5415.
24. P. D. Parker, J. G. Pierce, *Synthesis.* **2016**, *48*, 1902-1909.

25. C. C. Lin, T. H. Hsieh, P. Y. Liao, Z. Y. Liao, C. W. Chang, Y. C. Shih, W. H. Yeh, T. C. Chien, *Org. Lett.* **2014**, *16*, 892-895.

# 6

## *6. Summary*



This thesis reports new methods using both reductive and oxidative quenching cycles in photoredox catalysis for organic synthesis aiming at the synthesis of quinoline and ullazine derivatives, the synthesis of aryl thiols and the oxidation of lignin model compounds.

In **Chapter 1**, we have compared reported approaches of transition metal catalyzed and photoredox catalyzed valorization of lignin subunits and discussed the advantages and disadvantages of the methods. We have also discussed the results of our photocatalytic approach on the oxidation of lignin model compounds.

In **Chapter 2**, we have developed a novel method for the synthesis of quinoline and ullazine derivatives. The organic dye Rhodamine 6G (Rh-6G) can undergo a consecutive photo-induced electron transfer (con-PET) and can achieve a reduction potential of  $\sim -2.4$  V vs SCE. Therefore, the electron rich aryl halides that are difficult to reduce, could be reduced by Rh-6G. Photo excited Rh-6G is reduced by DIPEA to form the corresponding radical anion (Rh-6G $\bullet^-$ ) which is again excited by 455 nm light. The excited radical anion of Rh-6G donates an electron to the aryl bromide giving an aryl radical that is trapped by aromatic alkynes. The intermediate vinyl radical cyclizes intramolecularly and yield the product after rearomatization.

In **Chapter 3**, we have developed a photocatalytic method for the synthesis of aryl thiols via a radical-radical cross coupling of electron rich arenes with aryl and alkyl disulfides. They react in the presence of catalytic amounts of Ir[dF(CF<sub>3</sub>)ppy]<sub>2</sub>(dtbpy))PF<sub>6</sub> and (NH<sub>4</sub>)<sub>2</sub>S<sub>2</sub>O<sub>8</sub> under blue light irradiation to form aryl thiols. The reaction goes via the formation of the radical cation of the arene, which is the trapped by the sulfide radical to form the aryl thiol. The reaction proceeds at room temperature and avoids the use of pre-functionalized arenes.

In **Chapter 4**, we have compared a photochemical versus photocatalyzed oxidation of benzyl alcohols. We have used a high power UV LED for the direct photochemical oxidation of 4-methoxy benzyl alcohol to 4-methoxy benzaldehyde. We could find out that the photocatalyzed oxidation of this alcohol is much faster than the direct photochemical oxidation with UV light. We have also studies the rate of oxidation of few differently methoxy substituted benzylic 1,3 diols. The oxidation rate decreases with the increase in substitution. Transient absorption spectroscopic results indicated that, with increase of the

alkoxy groups, i.e. with the increase in the stability of the radical cation, the unproductive recombination pathway of the radical pair back to the starting materials also increases, hence the rate of oxidation decreases.

In **Chapter 5**, we have summarized several attempts towards the generation of amidinyl radicals using visible light photoredox catalysis. We have synthesized several classes of amidoximes, benzimidamides and benzamides containing an easily cleavable N-O bond for the generation of nitrogen centered radicals. We attempted to trap these amidinyl radicals either intramolecularly or intermolecularly. We succeeded in generation of an amidinyl radical, which yields in an intramolecular cyclization quinazolinone derivatives. However, conformational complexity of the molecule limited the scope of the reaction. We could also develop a visible light mediated photocatalytic method to synthesize substituted 1,2,4-oxadiazoles.



# 7

## *7. Zusammenfassung*



Diese Arbeit berichtet über neue Methoden der Photoredoxkatalyse und ihre Anwendung in der organischen Synthese, einschließlich der Synthese von Chinolin- und Ullazinderivaten, Aryl thiolen und der Oxidation von Lignin-Modellverbindungen.

In **Kapitel 1** vergleichen wir literaturbekannte Ansätze zur übergangsmetallkatalysierten und photokatalytischen Umwandlung von Lignin-Untereinheiten und diskutieren die Vor- und Nachteile dieser Methoden. Außerdem diskutieren wir die Ergebnisse unseres photokatalytischen Ansatzes zur Oxidation von Lignin-Modellverbindungen.

In **Kapitel 2** wird eine neue Methode für die Synthese von Chinolin- und Ullazinderivaten vorgestellt. Der organische Farbstoff Rhodamine 6G (Rh-6G) kann einen konsekutiven photo-induzierten Elektronentransfer durchführen (con-PET) und ein Reduktionspotential von  $\sim -2.4$  V vs SCE erreichen. Daher konnten elektronenreiche Arylhalogenide, deren Reduktion schwierig ist, mit Rh-6G reduziert werden. Das angeregte Rh-6G wird von DIPEA reduziert und bildet das entsprechende Radikalanion (Rh-6G $^{\bullet-}$ ), welches nochmals durch blaues Licht angeregt wird. Das angeregte Radikalanion überträgt ein Elektron auf das Arylhalogenid, wodurch ein Arylradikal gebildet wird, welches durch aromatische Alkine abgefangen wird. Das intermediäre Vinylradikal zyklisiert intermolekular und anschließende Rearomatisierung führt zum Produkt.

In **Kapitel 3** beschreiben wir eine photokatalytische Methode für die Synthese von Arylthiolen über eine Radikal-Radikal-Kreuzkupplung von elektronenreichen Arenen mit Aryl- und Alkyl-Disulfiden. Diese reagieren in Gegenwart katalytischer Mengen von  $\text{Ir}[\text{dF}(\text{CF}_3)\text{ppy}]_2(\text{dtbpy})\text{PF}_6$  und  $(\text{NH}_4)_2\text{S}_2\text{O}_8$  bei Bestrahlung mit blauem Licht zu Arylthiolen. Die Reaktion läuft über die Bildung des Radikalkations des Arens ab, welches durch das Sulfid-Radikal abgefangen wird, wobei das Arylthiol gebildet wird. Die Reaktion läuft bei Raumtemperatur ab und vermeidet die Anwendung präfunktionalisierter Arene.

In **Kapitel 4** verglichen wir die photochemische und die photokatalytische Oxidation von Benzylalkoholen. Wir verwendeten eine UV-LED für die direkte photochemische Oxidation von 4-Methoxybenzylalkohol zu 4-Methoxybenzaldehyd. Wir fanden, dass die photokatalytische Oxidation wesentlich schneller abläuft als die direkte photochemische Oxidation mit UV-Licht. Außerdem untersuchten wir die Geschwindigkeit der Oxidation einiger verschieden methoxy- substituierten benzyli-scher 1,3-Diole. Die Oxidation wird mit

zunehmender Substitution verlangsamt. Ergebnisse der transienten Absorptionsspektroskopie weisen auf eine Zunahme des unproduktiven Rekombinationsweges des Radikalpaares zu den Ausgangsstoffen mit zunehmender Zahl der Methoxygruppen, also mit einer Zunahme der Stabilität des Radikalkations hin, wodurch die Geschwindigkeit der Oxidation abnimmt.

In **Kapitel 5** fassten wir mehrere Ansätze zur photokatalytischen Erzeugung von Amidinyl-Radikalen zusammen. Wir synthetisierten mehrere Klassen von Amidoximen, Benzimidamiden und Benzamiden, welche eine leicht zu spaltende N-O-Bindung für die Erzeugung Stickstoff-basierter Radikale besitzen. Wir versuchten, diese Amidinyl-Radikale intra- und intermolekular abzufangen. Uns gelang die Erzeugung des Amidinyl-Radikals und die intramolekulare Cyclisierung zu Chinazolinin-Derivaten. Allerdings verhindern die konformelle Komplexität des Moleküls und die limitierte Substratbreite der Reaktion eine breitere Anwendung der Transformation. Wir konnten eine photokatalytische Synthese für substituierte 1,2,4-oxadiazole entwickeln, vermittelt durch sichtbares Licht.

# 8

## ***8. Abbreviations***



|                                 |   |
|---------------------------------|---|
| AIBN                            | Azobisisobutyronitrile                              |
| Ar                              | aryl  |
| atm                             | atmosphere  |
| Bpy                             | 2,2'-bipyridine                                     |
| C                               | carbon  |
| °C                              | degree Celsius                                      |
| CDCl <sub>3</sub>               | deuterated chloroform                               |
| CD <sub>3</sub> OD              | deuterated methanol                                 |
| CHD                             | cyclohexadiene                                      |
| Cl                              | chlorine  |
| cm                              | centimeter  |
| COD                             | 1,5-cyclooctadiene                                  |
| ConPET                          | consecutive photo-induced electron transfer         |
| Cs <sub>2</sub> CO <sub>3</sub> | cesium carbonate                                    |
| CT                              | charge transfer                                     |
| CV                              | cyclic voltammetry                                  |
| CzCp                            | carbazolic copolymer                                |
| 4CzIPN                          | 1,2,3,5-Tetrakis(carbazol-9-yl)-4,6-dicyano-benzene |
| [D, A]                          | [Donor, acceptor]                                   |
| DCM                             | dichloromethane                                     |
| DDQ                             | 2,3-Dichloro-5,6-dicyano-1,4-benzoquinone           |
| DFT                             | density functional theory                           |
| DIPEA                           | <i>N,N</i> -diisopropylethylamine                   |
| DMF                             | dimethyl formamide                                  |
| DMSO                            | dimethyl sulfoxide                                  |
| DMSO-d <sub>6</sub>             | deuterated dimethyl sulfoxide                       |
| Dtbbpy                          | 4,4'-Di-tert-butyl-2,2'-dipyridyl                   |
| EDA                             | electron donor acceptor                             |
| eT                              | electron transfer                                   |
| EtOAc                           | ethylacetate  |
| EI                              | electron impact (MS)                                |
| Equiv.                          | equivalents   |
| Et <sub>3</sub> N               | trimethylamine                                      |
| ESI                             | electron spray ionization (MS)                      |
| EtOH                            | ethanol   |
| Et                              | ethyl   |
| eV                              | electron volts                                      |
| Fc                              | ferrocene   |
| Fc <sup>+</sup>                 | ferrocenium   |
| FID                             | flame ionization detector                           |
| GC                              | gas chromatography                                  |
| H <sub>2</sub>                  | hydrogen  |
| h                               | hour (s)  |

|   |                                   |
|---|-----------------------------------|
| HRMS  | high resolution mass spectrometry |
| ISC   | inter system crossing             |
| K <sub>2</sub> CO <sub>3</sub>                  | potassium carbonate               |
| K <sub>q</sub>                                  | quenching rate constant           |
| LED   | light emitting diode              |
| M   | molar                             |
| <i>m</i> -                                      | meta                              |
| MBA   | 4-methoxy benzylalcohol           |
| MBAld   | 4-methoxybenzaldehyde             |
| Me  | methyl                            |
| MeCN  | acetonitrile                      |
| MeOH  | methanol                          |
| mg  | milligram                         |
| MHz   | mega hertz                        |
| min   | minutes                           |
| mL  | milliliter                        |
| mmol  | millimole                         |
| mol%  | mole percent                      |
| MS  | mass spectroscopy                 |
| MTBE  | methyl tert-butyl ether           |
| NaOH  | sodium hydroxide                  |
| NCS   | N-chlorosuccinimide               |
| NHPI  | N-hydroxyphthalimide              |
| (NH) <sub>2</sub> S <sub>2</sub> O <sub>8</sub> | ammonium persulfate               |
| nm  | nanometer                         |
| NMR   | nuclear magnetic resonance        |
| <i>o</i> -                                      | <i>ortho</i>                      |
| OAc   | acetate                           |
| OD  | optical density                   |
| <i>p</i> -                                      | <i>para</i>                       |
| PC  | photocatalyst                     |
| P(Cy) <sub>3</sub>                              | tricyclohexylphosphine            |
| PE  | petroleum ether                   |
| Ph  | phenyl                            |
| Ppm   | parts per million                 |
| Ppy   | phenylpyridine                    |
| PQY   | product quantum yield             |
| QYDS  | quantum yield determination setup |
| RFTA  | riboflavin tetraacetate           |
| Rh-6G   | rhodamine 6G                      |
| R.T.  | room temperature                  |
| S <sub>1</sub>                                  | singlet state                     |
| SCE   | saturated calomel electrode       |
| SET   | single electron transfer          |



|                 |   |
|-----------------|---|
| SM              | starting material                       |
| T <sub>1</sub>  | triplet state                           |
| TA              | transient absorption                    |
| <sup>t</sup> Bu | <i>tert</i> -butyl                      |
| TEMPO           | (2,2,6,6-Tetramethylpiperidin-1-yl)oxyl |
| TLC             | thin layer chromatography               |
| TMEDA           | tetramethylethylenediamine              |
| TMDSO           | tetramethyldisiloxane                   |
| TMS             | trimethylsilyl                          |
| UV              | ultraviolet                             |
| V               | volt                                    |
| Vis             | visible                                 |
| W               | watt                                    |
| X               | arbitrary anion                         |





## ***9. Acknowledgements***



Firstly, I would like to express my deep respect and sincere gratitude to my research supervisor Prof. Dr. Burkhard König for giving me an opportunity to work in his research group and expand my scientific research career. His supervision, enthusiasm, constant encouragement and valuable discussions has inspired me throughout my research period. Moreover, his freedom to work and his problem solving approach has helped me to explore different directions in research and has also helped me to work independently.

I am very much grateful to Prof. Dr. Julia Rehbein and Prof. Dr. Frank-Michael Matysik for being the doctoral committee members and examining my thesis. I am also thankful to Prof. Dr. Hubert Motschmann for being the chair person in my Ph.D defence.

I am highly obliged to Prof. Sundarababu Baskaran, Department of Organic Chemistry, Indian Institute of Technology, Madras (IITM), India who gave me an opportunity to carry out my first research in his laboratory during my M.Sc studies. His lectures in total synthesis of natural products has helped me to learn a lot about synthetic organic chemistry.

I would like to thank Dr. Rudolf Vasold and Simone Strauß for the GC and GC-MS measurements, Ernst Lautenschlager for all kinds of technical supports, Britta Badziura for ordering chemicals, Julia Zach for taking care of all the instruments, specially helping me with the Quantum Yield Determination Setup (QYDS) and Regina Hoheisel for CV measurements.

I sincerely thank all my past and present lab members of our working group ‘AK König’ who always kept a very friendly and happy environment in the group. It was a great time to share the moments together in....Ph.D parties, short group trips especially, skiing, barbeque parties in summer, Dult, international evenings and many more....

I am glad to share my lab (32.1.22) with my two awesome lab mates Nadja and Anna who was always there in my good and bad times and always made me feel at home.

I thank Dr. Tamal Ghosh for helping me with everything in and outside the lab, fruitful discussions in chemistry, especially, teaching me how to cook food. :P

I thank my closest friends Manjusha, Swarupa, Dr. Rohit Menon Dr. Zbigniew T. Czyz, Martin, Dr. Mitasree Maity and Dr. Somnath Das for being with me all along this

journey...cooking and eating together, our hangouts, our late night discussions on the bank of Donau....and so on...

Thank you Regina and Max for taking care of me like a parent all throughout the time. I really enjoyed cooking and baking the Christmas cookies together.

My special thanks go to Manjusha and Swarupa for being a very important part of my life. Thank you Manjusha for being a very good listener. I will miss each and every moment we spent together chatting, giggling and gossiping (haha!) and specially our crazy discussions over tea on Sunday evenings!

For the thorough proofreading of parts of my thesis and valuable suggestions I would like to thank Regina Hoheisel and Dr. Namrata Rastogi. I thank Martin for translating the summary in German.

I am very much grateful to Deutsche Forschungsgemeinschaft (GRK 1626) for the financial support during my doctoral research.

Last but not the least I pay deep respect and love to my parents, my grandma whose unconditional love, support and blessings have helped me to accomplish my dreams so far. I express my sincere gratitude to my teacher Dr. Chandan Saha who has introduced me to organic chemistry and took me step by step through the basics and beauties of organic chemistry. Just words are really difficult to explain what I owe to them. A basket of thanks to all of you.

Finally, to anyone who has supported me on this journey, I would like to thank all of you. There have been too many names and faces that have passed through my life in the last years and all of you have helped me to grow not only as a chemist but also as a good human being.

*Thank you*

*Danke Schön*

*ধন্যবাদ*

# 10

## *10. Curriculum Vitae*





## CURRICULUM VITAE

**AMRITA DAS**

**Ph.D student**

**Institute of Organic Chemistry**

**Universität Regensburg**

**93040- Regensburg**

**Germany**

**Email:** [Amrita.Das@chemie.uni-regensburg.de](mailto:Amrita.Das@chemie.uni-regensburg.de)

[amritadas1991@gmail.com](mailto:amritadas1991@gmail.com)

**Phone no.** [+4917627530105](tel:+4917627530105)



### ***Objective:***

Seeking postdoctoral position in the area of medicinal chemistry, synthetic biology, asymmetric synthesis and development of novel strategies.

### ***Education:***

**2014 - present:** Ph.D in Chemistry

Universität Regensburg, Regensburg, Germany.

**2012 - 2014:** M.Sc in Chemistry (GPA 8.48)

Indian Institute of Technology, Madras (IITM), India

**2009 - 2012:** B.Sc in Chemistry (71%)

Scottish Church College, Kolkata, India

### ***Research experience:***

**2014 - Present:** Ph.D in Organic Chemistry

Research area: **“Development Of Novel Strategies And Synthesis Of Heterocycles Using Visible light Photoredox Catalysis**

Supervisor: **Prof. Dr. Burkhard König**

Universität Regensburg, Germany.

- Developed a photocatalytic method for the generation of aryl radicals and trap them intramolecularly to form pyrrolo[1,2-*a*] quinolones and ullazines in a single step.

- Developed a method for C-S bond formation via photocatalytic C-H bond activation of arenes.
- Contributed to the development of a photocatalytic method for the *N*-formylation of amines.
- Currently working on generation of amidinyl radicals by visible light photoredox catalysis and their application in medicinally useful heterocycles.
- Working on the investigation and photophysical studies on the substitution effect in the lignin model compounds and their photocatalytic oxidation and degradation.

**2012 - 2014:** M.Sc in Organic Chemistry

Dissertation title: “**Ring Closing Metathesis Based Strategy Towards The Synthesis Of Novel Bicyclic Iminosugar**”.

- Development of a novel strategy towards the stereoselective synthesis of structurally diverse novel iminosugar C-alkynylglycosides.

Supervisor: **Prof. Sundarababu Baskaran**

Indian Institute of Technology Madras (IITM), India.

### ***Academic Achievements:***

- Qualified in JAM (Joint admission to M.Sc. IIT) Test 2012 with all India rank 119.
- Qualified in national level Graduate Aptitude Test for Engineering (GATE), 2014 in Chemistry, India.
- Qualified in Council of Science and Industrial Research (CSIR) – University Grants Commission (UGC) (June-2014) national level exam LS, India.

### ***Competence:***

- Skilled in multistep synthesis.
- Experienced in handling of moisture and air sensitive organic reagents and chemicals.

- Structural elucidation of complex organic compounds using IR, HRMS, 1D & 2D NMR spectroscopy.
- Experienced in handling analytical tools such as GC, HPLC (Perkin Elmer), FT NMR spectroscopy (ADVANCE 400 MHz & 600 MHz BRUKER), IR, Cyclovoltametry, UV-Vis spectrophotometry, Fluorometer, Infra-Red spectroscopy (JASCO 4100 FT-IR), Quantum yield determination setup (QYDS).

### ***List of Publications:***

1. Ghosh, T.; [Das, A.](#) and König, B. *Photocatalytic N-Formylation of Amines via a Reductive Quenching Cycle in The Presence of Air.* *Org. Biomol. Chem.*, **2017**, *15*, 2536.
2. Ghosh, I.; Marzo, L.; [Das, A.](#); Shaikh, R. and König, B. *Visible Light Mediated Photoredox Catalytic Arylation Reactions.* *Acc. Chem. Res.*, **2016**, *49*, 1566.
3. [Das, A.](#); Ghosh, I. and König, B. *Selective Synthesis of Pyrrolo[1,2-a]quinolines and Ullazines by Visible Light Mediated One- and Twofold Annulation of N-Arylpyrroles with Arylalkynes.* *Chem. Commun.*, **2016**, *52*, 8695.
4. Senthilkumar, S.; Prasad, S. S.; [Das, A.](#) and Baskaran, S. *One-pot Synthesis of Hydrophobically Modified Iminosugar C-Alkynylglycoside: Facile Synthesis of Polyhydroxy Tetrahydroindolizines.* *Chem. Eur. J.*, **2015**, *21*, 15914.

### ***Manuscripts in preparation:***

1. [Das, A.](#) and König, B, *Transition Metal and Photoredox- catalyzed Valorization of Lignin Subunits.*
2. [Das, A.](#), Maity, M and König, *Synthesis of Aryl Sulfides via Radical-Radical Cross Coupling of Electron Rich Arenes using Visible Light Photoredox Catalysis.*

### ***Conferences:***

- Actively participated in “Green Chemistry Horizon”, Kármán Conference at RWTH Aachen University, February 2-3, **2017**, Aachen, Germany.

- **Das, A.**; and König, B. *poster presentation* on “Metal free aerobic oxidation of lignin using visible light photocatalysis” in *ICOS 21, 21<sup>st</sup> International Conference on Organic Synthesis*, December 11-16, **2016**, IIT Bombay, Mumbai, India.
- **Das, A.**; Ghosh, I. and König, B. *Oral presentation* on “Selective Synthesis of Pyrrolo[1,2-*a*]quinolines and Ullazines by Visible Light mediated one- and twofold Annulation of *N*-Arylpyrroles with Arylalkynes” in *25. Lecture conference on Photochemistry*, September 26-28, **2016**, Jena, Germany.
- **Das, A.**; Ghosh, I. and König, B. *poster presentation* on “Selective Synthesis of Pyrrolo[1,2-*a*]quinolines and Ullazines by Visible Light mediated one- and twofold Annulation of *N*-Arylpyrroles with Arylalkynes” in *ORCHEM 2016, 20. Lecture Conference*, September 5-7, **2016**, Weimar, Germany.
- **Das, A.**; Ghosh, I. and König, B. *poster presentation* on “Selective Synthesis of Pyrrolo[1,2-*a*]quinolines and Ullazines by Visible Light mediated one- and twofold Annulation of *N*-Arylpyrroles with Arylalkynes” In *Gordon Research Conference (GRC)*, June 19-24, **2016**, Salve Regina University, Newport RI, United States.
- Kolb, A.; **Das, A.** and König, B. *poster presentation* on “Deep Eutectic Solvents as Green Metal- Extraction Media” In *DECHEMA Infoday “Switchable Solvent Systems”* September 28, **2015**, DECHEMA-Haus, Frankfurt am Main, Germany.
- Actively participated in the *Chemistry in- House Symposium*, August 21-22, **2012** and **2013**, Department of Chemistry, IIT Madras, India.
- Actively participated in *Medicinal Chemistry Conference* (MED CHEM), October, **2013**, IIT Madras, India.
- Actively participated in a UGC sponsored “*National Seminar on Modern trends in Biology*” organized jointly by Indian Association for Cultivation of Science (IACS) & Maulana Azad College, Kolkata, October, **2010**.

## References:

**Prof. Dr. Burkhard König.** (Ph.D supervisor)

Institut für Organische Chemie

Universität Regensburg

D- 93040 Regensburg

Germany

Email: [Burkhard.Koenig@chemie.uni-regensburg.de](mailto:Burkhard.Koenig@chemie.uni-regensburg.de)

**Prof. Sundarababu Baskaran.** (M.Sc supervisor)

Department of Chemistry

Indian Institute of Technology Madras

Chennai - 600036

Tamil Nadu, INDIA

*Email: [sbhaskar@iitm.ac.in](mailto:sbhaskar@iitm.ac.in)*



